Non-invasive diagnosis and follow-up of right ventricular overload

Henkens, I.R.

Non-invasive diagnosis and follow-up of right ventricular overload

I.R. Henkens

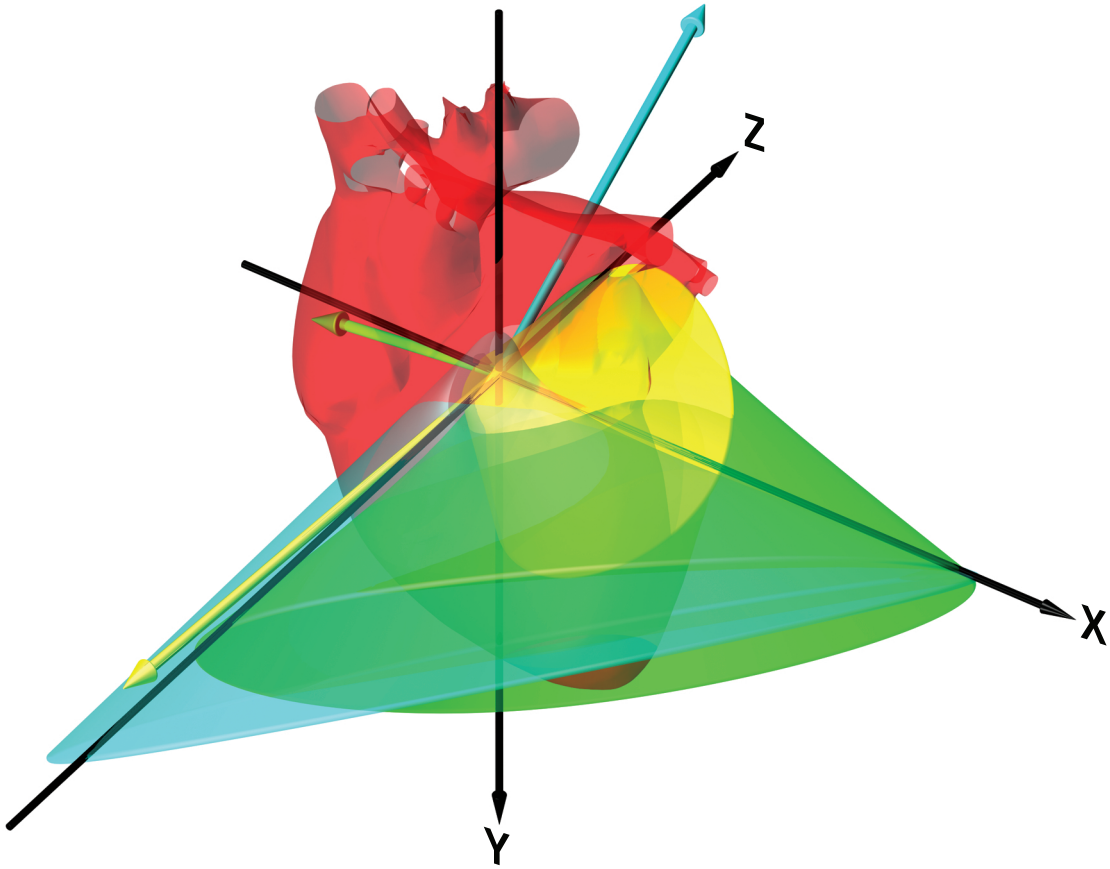

Non-invasive diagnosis and follow-up of right ventricular overload

Cover

A three-dimensional representation of the resultant electrical vectors of the myocardium of a patient with pulmonary arterial hypertension, and the normal range of resultant myocardial vectors. The resultant QRS vector is depicted in yellow, the resultant T vector in blue, and the resultant Ventricular Gradient in green. Right ventricular pressure load strongly changes myocardial electrical characteristics, detectable with electrocardiography.

Colophon

The studies described in this thesis were performed at the department of Cardiology, Leiden University Medical Center, Leiden, the Netherlands, and at the departments of Pulmonology and Physiology of the VU University Medical Center, Amsterdam, the Netherlands.

Cover design

Jurgen Kuivenhoven, industrial designer at Skottkarra, Amsterdam, The Netherlands.

Layout

Annette Heijn, Delft, The Netherlands

Printing

Gildeprint, Enschede, The Netherlands

ISBN 978-90-7138-266-6

Non-invasive diagnosis and follow-up of right ventricular overload

Ter verkrijging van
de graad van Doctor aan de Universiteit Leiden,
op gezag van de Rector Magnificus prof.mr. P.F. van der Heijden,
volgens besluit van het College voor Promoties
te verdedigen op donderdag 20 november 2008
klokke 13:45 uur

door

Ivo Henkens
geboren te Leiderdorp
in 1977

Promotiecommissie

Promotores	Prof. Dr. E.E. van der Wall Prof. Dr. M.J. Schalij
Co-promotor	Dr. H.W. Vliegen
Referent	Prof. Dr. B.J.M. Mulder (Academisch Medisch Centrum, Amsterdam)
Leden	Prof. Dr. A. van der Laarse (Leids Universitair Medisch Centrum, Leiden) Dr. A. Vonk Noordegraaf (VU Medisch Centrum, Amsterdam) Dr. A. Boonstra (VU Medisch Centrum, Amsterdam) Dr. C.A. Swenne (Leids Universitair Medisch Centrum, Leiden)

Table of contents

I

Introduction

Introduction

Right ventricular overload can be described as a situation in which the normal limits of right ventricular dimensions or stroke work are exceeded. Such a condition can be of sudden onset, leading to acute overload (e.g. in pulmonary embolism) or of gradual onset, leading to subacute or chronic right ventricular overload. Theoretically, right ventricular overload can be limited to volume or pressure overload alone, but in general these conditions accompany one another to a certain extent. To understand the effect of the dominant mechanism of overload, i.e. pressure or volume overload, one must be familiar with the normal anatomy and function of the right ventricle. Suspecting right ventricular overload is the first step towards its diagnosis. Using the correct tools will assure adequate diagnosis, and will allow for unambiguous follow-up of the observed abnormalities. It is important to be familiar with the natural history of right ventricular overload. This introduction will focus on normal and pathological right ventricular anatomy before and after surgery, prenatal and postnatal physiology, pathophysiology, functional assessment, and the consequences of right ventricular failure.

General anatomy of the right ventricle

The right ventricle, positioned in the thoracic cavity directly behind the sternum, lies to the front and to the right of the left ventricle. In series with the left ventricle, the right ventricle generates the same output directed towards the lungs, aimed at blood re-oxygenation. Blood enters the right ventricular cavity once it passes the tricuspid annulus, and leaves the right ventricular cavity through the pulmonary valve. The three cusps of the tricuspid valve are connected to the septum, and the anterolateral and posterolateral walls of the right ventricle by their chordae tendinae and papillary muscles [1]. The semilunar cusps of the pulmonary valve resemble the cusps of the aortic valve, closing passively as blood pressure in the pulmonary artery exceeds right ventricular pressure. The right ventricle has three characteristic properties, which allow it to be distinguished morphologically from the left ventricle. Firstly, the right ventricle is identified by its tricuspid atrio-ventricular valve with one septal insertion, whereas the left ventricle with its bicuspid mitral valve has two opposing groups of papillary muscles inserted in the free wall. Secondly, the right ventricle has a trabeculated myocardium, especially towards the apex. The left ventricular myocardium, in contrast, is more solid. Finally, the right ventricle contains a muscular band of heart tissue running from the base of the anterior papillary muscle to the interventricular septum, called the septomarginal trabeculae or moderator band [1]. These characteristics often help identify

the right ventricle in echocardiography or magnetic resonance imaging in situations where both ventricles are comparable in size due to right ventricular overload. The right ventricle, by many physicians overlooked or seen as a separate entity, in fact shares many features with the left ventricle. Contained by the pericardial sac, the ventricles contract virtually at the same time, activated by their common conductance system and individual bundle branches and Purkinje fibers. The sole right ventricular bundle branch is often affected in right heart disease. However, in the general population too, depending on the age group observed, a right bundle branch block can be found in otherwise healthy subjects [2-4]. The interventricular septum is an essential part of both ventricles' contractile system [5]. Under physiological conditions, however, the left ventricle intracavitary pressure exceeds that of the right ventricle by far during systole (and by little during diastole), generating a globular shape of the left ventricular, with the right ventricle almost wrapped around it [6]. The fibrous skeleton of the heart, lying mainly around the heart valves, not only functions as an electrically inert barrier between atria and ventricles, but also forms a solid base when ventricular contraction brings the apex inward [7]. The muscle array of the heart, aligned for optimal conduction times and contraction efficiency, is such that during contraction the heart shortens along its longitudinal axis, and twists at the same time, effectively wringing most of the blood out of the ventricular cavities [8]. Since the pulmonary circulation is a low-resistance system, right ventricular oxygen consumption per gram of myocardium is normally only approximately half of left ventricular oxygen consumption per gram of myocardium [9-11]. Generally speaking, the left ventricle is predominantly supplied by the left coronary artery, while the right coronary artery generally supplies the right atrium and sinus node, the right ventricle, and the left ventricular wall and part of the apex [9, 11].

Anatomy in tetralogy of Fallot

Patients with a tetralogy of Fallot have four explicit coinciding features of the heart, first reported by Etienne-Louis Arthur Fallot in 1888. Dr. Fallot was able to understand the clinical consequences of the observed four cardiac abnormalities: a ventricular septum defect under the aortic root, a right ventricular outflow tract obstruction (with a generally abnormal pulmonary valve and underdeveloped pulmonary vasculature), an 'overriding' aorta (the aorta is positioned more rightward, receiving blood from both ventricles), and right ventricular hypertrophy (Figure 1). Consequently, blood can travel freely between both ventricles in favor of the pulmonary or systemic circulation, depending on vascular resistance, and the right ventricular outflow tract pressure gradient [12, 13]. The fact that there is relatively uninhibited flow between the ventricles signifies that there is a pressure equilibrium between

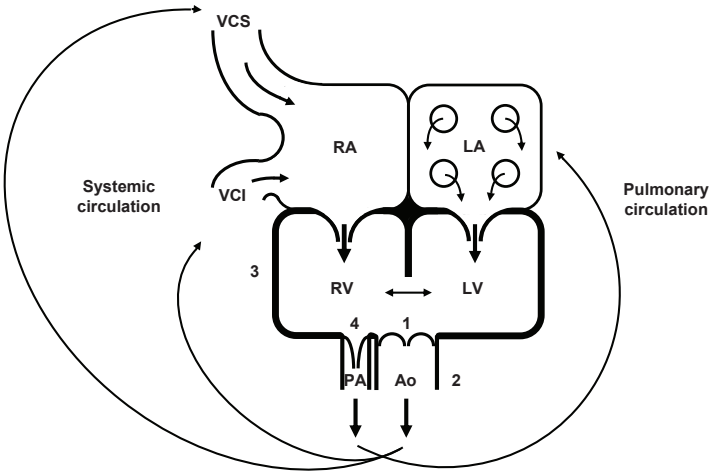

Figure 1

Schematic outline of the Fallot anatomy and circulation: there is a ventricular septal defect (1) located under the aorta (2), which 'overrides' the septum and hence there is a pressure equilibrium between the right and left ventricle, preventing loss of prenatal right ventricular hypertrophy (3: right ventricular wall thickness equals left ventricular wall thickness). The degree of right ventricular outflow tract stenosis (4: infundibular and pulmonary valve stenosis) then determines the balance between the pulmonary and systemic circulation. RA=right atrium, LA=left atrium, RV=right ventricle, LV=left ventricle, PA=pulmonary artery, Ao=aorta, VCI=inferior vena cava, VCS=superior vena cava. Shortly after birth Fallot patients may present as 'blue babies' in cases where (sub)pulmonary stenosis is severe, and desaturated blood will flow towards the systemic circulation more easily. In patients with a less severe (sub)pulmonary stenosis, pulmonary blood flow may exceed systemic blood flow, but there may also be a more or less 'balanced circulation'. In the latter situation, the pressure gradient over the right ventricular outflow tract - i.e. the pressure drop, - is such that equal volumes of blood flow through the pulmonary and systemic circulation. Only in situations where pulmonary vascular resistance increases, will pink babies present with cyanosis. This is typically the case during feeding, or when a baby is crying. In the case of feeding, heart rate increases and systemic vascular resistance decreases, allowing desaturated blood to flow more easily towards the systemic circulation. A similar phenomenon occurs during crying, when a rise in intrathoracic pressures increases pulmonary vascular resistance even more.

the ventricles, which inhibits postnatal decline of relative right ventricular muscle mass [14]. This explains the right ventricular hypertrophy in Fallot patients. Due to the septal defect and an incomplete or malalignment of the endocardial cushions, the aorta is said to override the septum. The aorta therefore directly receives a mix of blood from the right and left ventricle (Figure 1).

Early surgical correction in tetralogy of Fallot

The objective of early surgical correction is to separate the pulmonary and systemic circulation, and to relieve right ventricular outflow tract stenosis, in order to prevent right ventricular failure [12]. There has been considerable progress in surgical techniques over the years. Initially, Fallot patients would often receive a systemic-to-pulmonary-artery shunt [15]. These shunts were designed to increase pulmonary blood flow, allowing the pulmonary vasculature to mature in anticipation of final correction at a later age [16]. Several shunts have been used (Figure 2), but the modified Blalock shunt (a side-tot side artificial shunt between the subclavian artery and the pulmonary artery) is probably the most practical shunt. The modified Blalock shunt does not require sacrifice of the subclavian artery, since it does not directly compromise the original vasculature. Furthermore, blood flow can be controlled better, and the shunt can be occluded more easily at a later stage, either by percutaneous intervention or by surgical intervention [12, 13, 17].

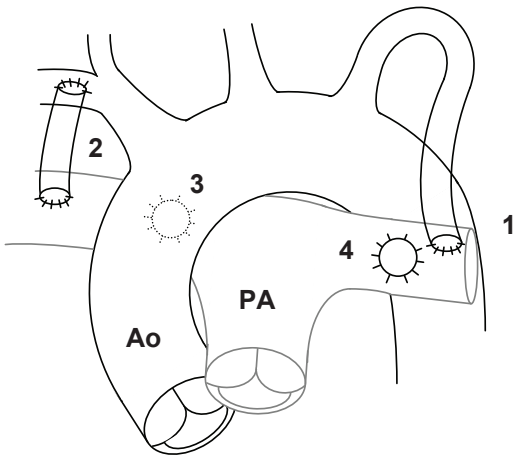

Figure 2

Schematic representation of the surgical palliative shunts used early in life for augmentation of pulmonary blood flow. The classic Blalock-Taussig shunt (1) requires sacrifice of the distal subclavian artery with an end-to-side anastomosis on the pulmonary artery (left or right). The upper limb supplied by the subclavian artery will receive blood from collateral vessels. The modified Blalock-Taussig shunt (2) is an artificial graft implanted end-to-side between the subcavian and pulmonary artery. There are several advantages over the classis Blalock-Taussig shunt: flow is easier to control by choice of the graft diameter, there is no need to sacrifice the vessel supporting the upper limb, and it is more easily occluded or resected at a later stage. The aorto-pulmonary Waterston (3) and Potts (4) shunts are no longer in use due to the often massive flow over a difficult-to-control shunt.

Subsequent corrective surgery then consisted of relieving (sub)pulmonary stenosis, ventricular septal defect closure, and closure of the artificial shunt [17]. Historically, the infundibulum was approached transventricularly, allowing the surgeon a clear view of the muscular subpulmonary obstruction [18, 19]. Often, the incision over the right ventricle was extended over the pulmonary valve, and subsequently closed with a patch. This patch relieved right ventricular outflow tract stenosis, and hence decreased right ventricular afterload. At the same time though, pulmonary regurgitation was created, inducing long-term volume-loading of the right ventricle [20].

Nowadays, complete surgical correction is often performed without prior palliative surgery, and the right ventricular outflow tract is approached through the right atrium [21], without the need for a patch in the right ventricular outflow tract [12, 13, 22]. The one-step surgical correction of tetralogy of Fallot patients is expected to result in a better long-term outcome in these patients, but definite results are still awaited, since this approach did not really catch on until approximately twenty-five years ago.

Late surgical correction in tetralogy of Fallot

After total correction in early childhood, patients are left with an incompetent pulmonary valve which becomes progressively insufficient, inducing volume loading of the right ventricle [20, 23, 24]. As a consequence, the right ventricle dilates, and the tricuspid valve often becomes insufficient. Even in the absence of right ventricular outflow tract stenosis, and with normal pulmonary vascular resistance, right ventricular stroke work is necessarily much higher than normal. Hence, adult patients with tetralogy of Fallot generally present with right ventricular dilatation and hypertrophy. Especially dilatation is thought to be detrimental to right ventricular function, characterized by poor right ventricular ejection fraction, and limited exercise capacity [25]. Furthermore, dilated right ventricles, associated with prolonged QRS duration, predispose to fatal arrhythmias [24, 26-28]. Surgical reintervention aimed at preservation and possibly restoration of right ventricular function has received much attention in the past ten to fifteen years [29-32]. After the initial success of pulmonary valve replacement with respect to positive right ventricular remodeling [32], well-being [33, 34], and exercise capacity [25, 35], there has been much debate regarding the optimal timing of pulmonary valve replacement [15, 30, 36, 37].

Although surgical pulmonary valve replacement is an intervention with low mortality [29], there is considerable associated morbidity. Since the use of a homograft is preferred over the use of a mechanical pulmonary valve with the need for long-term anticoagulant therapy [38], (surgical) reintervention for pulmonary valve replacement is anticipated in all of these

patients [39-41]. Apart from pulmonary valve replacement, patients often require resection of the aneurysm in the region of the right ventricular outflow tract, possibly dilatation or resection of a persistent peripheral pulmonary artery stenosis (either congenital or as a consequence of a prior palliative shunt), closure of a residual ventricular septal defect, and/or tricuspid annuloplasty or valvuloplasty [36, 42]. Although reports of repeated pulmonary valve replacement are encouraging [43, 44], available long-term follow-up of cryopreserved homograft in adult Fallot patients indicate that these patients will likely require multiple reinterventions [40].
For patients meeting the criteria, there is currently also the possibility of percutaneous pulmonary valve replacement, a minimally invasive procedure with good short-term results in expert centres [39, 45-50].

Anatomy in pulmonary arterial hypertension
Patients with pulmonary arterial hypertension can roughly be divided in those with congenital heart disease related pulmonary arterial hypertension, and those with post-natal onset of pulmonary arterial hypertension, without congenital heart disease [51-54]. The latter group of patients has a normal anatomy at birth and will not be discussed here. Pulmonary arterial hypertension associated with congenital heart disease is a consequence of an incompletely separated pulmonary and systemic circulation, allowing volume and/or pressure overload of the pulmonary circulation [6, 55, 56]. So-called pre-tricuspid shunts (i.e. atrial septal defect, aberrant pulmonary venous return) generally cause volume loading of pulmonary circulation, whereas post-tricuspid shunts (ventricular septal defect, persistent ductus arteriosus, and oversized palliative shunts) may cause both volume and pressure loading of the pulmonary circulation, depending on associated congenital abnormalities or surgical interventions (Figure 2 and 3) [57]. There is a strong association between excessive volume loading of the pulmonary circulation (Qp:Qs > 1.5) and the prevalence of late pulmonary arterial hypertension. However, there is by no means a cause-effect relationship, and even in the presence of pulmonary arterial hypertension late shunt closure may be beneficial in patients [58, 59]. The right ventricle is often dilated, and hypertrophied in volume loading of the pulmonary circulation, due to an increased right ventricular stroke volume [12]. Increased pulmonary artery pressures may reflect an increased pulmonary vascular resistance in the presence of a near-normal right-sided cardiac output, but may also reflect the necessarily increased driving pressure in the setting of a supra-normal right-sided cardiac output [60]. A careful measurement of Qp:Qs is therefore essential before increased pulmonary artery pressures are explained as a consequence of increased pulmonary vascular resistance.

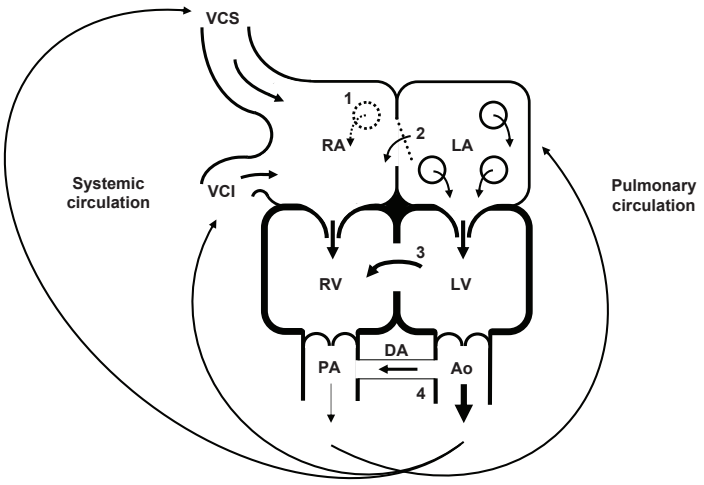

Figure 3

Schematic representation of the foetal situation in which pre-tricuspid and post-tricuspid shunts are not yet harmful to the right ventricle or the pulmonary circulation.

RA=right atrium, LA=left atrium, RV=right ventricle, LV=left ventricle, PA=pulmonary artery, Ao=aorta, VCI=inferior vena cava, VCS=superior vena cava.

Pre-tricuspid shunts primarily induce right ventricular volume loading. Anomalous pulmonary venous return (1) to the right atrium is of no consequence before birth. However, once the patent oval foramen (dotted line between RA and LA) closes after birth, the right ventricle undergoes volume loading, since much of the blood that is pumped into the pulmonary circulation, directly returns to the right atrium. There is therefore a discrepancy in pulmonary flow (Qp) and systemic flow (Qs): Qp>Qs. The same is true when there is an atrial septal defect (2). The higher left atrial pressure will allow blood to flow into the right atrium, again causing volume loading of the right ventricle. A small atrial septal defect with a Qp:Qs < 1.5:1 will rarely cause any symptoms, yet larger shunts are associated with long-term right ventricular dysfunction. Interestingly, when left ventricular diastolic function decreases with age, the atrial shunt may increase due to increased filling pressures. Patients may therefore only present in their forties or fifties.

Post-tricuspid shunts directly induce right ventricular pressure loading. The degree of additional volume loading is inversely related to the resistance of the right ventricular outflow tract and pulmonary circulation. Apart from the surgically created shunts (Figure 2) the ventricular septal defect (3) and persistent ductus arteriosus (4) are the most common congenital causes of right ventricular pressure load and pulmonary arterial hypertension. Initially, the pulmonary blood flow may be many times that of the systemic circulation (Qp>>Qs). As pulmonary vascular resistance rises due to vasoconstriction and progressive pulmonary vascular damage, blood flow becomes more balanced. As long as the fixed pulmonary vascular resistance is substantially lower than systemic vascular resistance, patients may still effectively increase oxygen delivery by increasing cardiac output. Eventually, however, pulmonary vascular resistance may supersede systemic vascular resistance, and an increase in cardiac output will not necessarily lead to an increase in oxygen uptake, and therefore not to an increase in oxygen delivery either.

In contrast, in post-tricuspid shunting without a significant pressure-drop between systemic and pulmonary circulation, there is direct pressure overload of the pulmonary vasculature, which may lead to irreversible changes in the pulmonary arterioles within months to years [57, 61, 62].

In the face of congenital heart disease associated pulmonary arterial hypertension, surgical correction is often considered impossible, with the exception of patients who qualify for heart transplantation [54, 63-65].

Prenatal physiology

Early in intrauterine life, the right ventricle is essentially the left ventricle's equal (Figure 4). The presence of an open oval foramen and ductus arteriosus allow the separated chambers to function more or less as one, propulsing approximately 90% of the placenta-oxygenated blood into the systemic circulation, bypassing the non-ventilated lungs. Shortly after birth, the circulation is changed dramatically in response to the presence of intra-alveolar oxygen

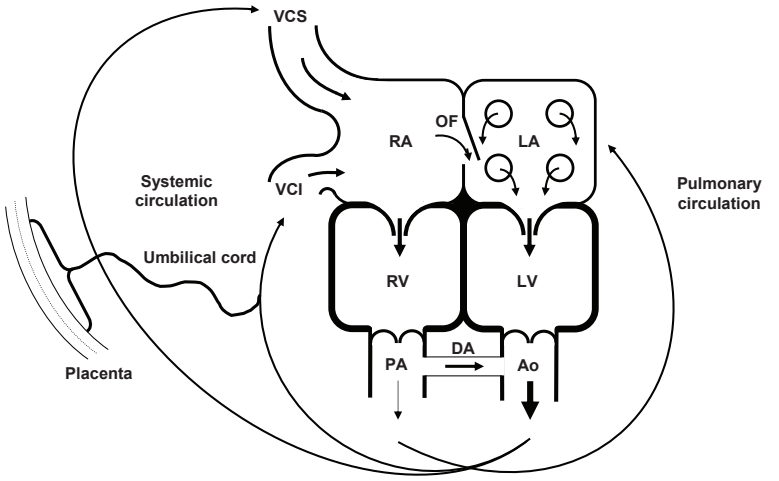

Figure 4

Schematic representation of the intra-uterine circulation. Pulmonary and systemic circulation are not yet independent entities, but function in parallel. Blood oxygenated by the placenta enters the heart through the right atrium, and then flows either into the right ventricle, or passes through the oval foramen into the left atrium and then into the left ventricle. Over 90% of the blood leaving the ventricles subsequently flows towards the systemic circulation, either directly through the left ventricle, or through the ductus arteriosus. The right and left ventricle are essentially performing as one, and as such are equally thick-walled, and perform similar stroke work.

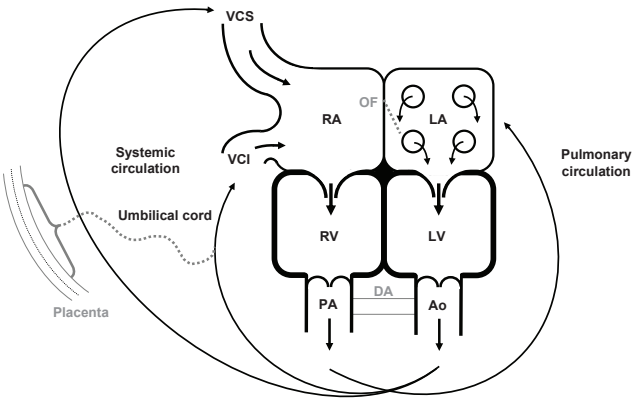

Figure 5
Schematic representation of the postnatal circulation. Pulmonary and systemic circulation are now independent entities, and function in sequence. Oxygenation of the lungs decreases pulmonary vascular resistance, and induces vasoconstriction, and subsequent obliteration of the ductus arteriosus. The subsequent rise in left atrial pressure due to pulmonary blood flow closes the oval foramen, effectively separating the pulmonary and systemic circulation.

[66, 67]. The latter decreases pulmonary vascular resistance almost instantly, allowing blood to flow through the lungs, which increases pulmonary venous pressure by enough to close the oval foramen, preventing oxygen-poor systemic venous blood entering the left ventricle. At the same time, the smooth muscle cells in the ductus arteriosus contract, preventing further flow between the systemic and pulmonary circulation (Figure 5).

Postnatal physiology

After approximately 6-12 weeks, the pulmonary circulation will have reduced its resistance from several times that of the systemic circulation before birth to a fraction of the vascular resistance of the systemic circulation [68]. The reduction in afterload is believed to induce both atrophy and a certain degree of apoptosis of the right ventricle [14, 68]. The persistent right ventricular hypertrophy after birth is one of the explanations for the observed better survival in patients with pulmonary arterial hypertension related to congenital heart disease [14]. As discussed above, both ventricles roughly perform similarly in the antenatal period when systemic and pulmonary circulations are situated in parallel. Once the circulations are separated after birth, the right heart soon delivers no more than a fraction of the work the left ventricle delivers [11, 69, 70]. Under normal conditions the right ventricle is therefore

thin-walled, and exercise will be limited by left ventricular performance. The self-regulatory nature of the coronary arteries is such that coronary venous blood is virtually always oxygen-depleted [11]. Nevertheless, in contrast to left coronary artery flow - which is predominantly diastolic due to systemic pressures in the left ventricular cavity during systole - right coronary flow is both systolic and diastolic, since systemic pressures in the right ventricular cavity do not exceed systemic pressures under physiologic conditions [71].

Pathophysiology

Although patients with a Fontan circulation prove that a right ventricle is not paramount for adequate systemic oxygen delivery in patients with a univentricular heart, the latter is only true for Fontan patients with a physiological pulmonary vascular resistance [13, 56, 72]. Furthermore, exercise capacity is markedly impaired in patients without an adequate right ventricle supporting the pulmonary circulation [25]. When pulmonary vascular resistance increases, pulmonary driving pressure needs to increase in order to maintain pulmonary flow [71]. This situation demands increased right ventricular performance, and induces right ventricular hypertrophy [73]. Resting cardiac output is generally maintained at rest until end-stage pulmonary arterial hypertension is present [60]. However, the fixed pulmonary vascular resistance in pulmonary arterial hypertension patients generally precludes an increase in cardiac output to normal physiological limits, because the right ventricle is unable to increase pulse pressure enough [74, 75]. Unable to adequately increase stroke volume [75], patients with pulmonary arterial hypertension will not reach normal exercise levels due to inadequate oxygen delivery, and virtually always present with excessive exertional dyspnea [76]. Furthermore, mean right coronary artery driving pressure decreases with an increasing right ventricular systolic pressure, since right coronary artery perfusion mimics left coronary artery perfusion, which is predominantly diastolic [71]. Impaired stroke volume may therefore paradoxically decrease right ventricular myocardial oxygen supply in the face of an already increased right ventricular oxygen demand [71]. Diastole therefore becomes even more important as right ventricular pressure overload progresses. However, the compromised cardiac output induces reflex noradrenergic activation [77], effectively decreasing net diastolic duration per heart beat. Patients with right ventricular pressure overload are therefore at risk of ischemia at higher heart rates. Even without macrovascular right coronary artery flow impairment, ischemia may therefore present as a result of a mismatch between oxygen supply and demand [78]. Patients with pulmonary arterial hypertension due to congenital heart disease have a few important differences in the heart, exercise hemodynamics, and blood, that explain their overall better survival compared to patients with other forms of pulmonary

arterial hypertension [79-81]. Firstly, the fact that pulmonary arterial hypertension is present from birth, prevents right ventricular atrophy to normal wall-size limits. Theoretically, muscles fibers that do not atrophy or go into apoptosis are better suited for the job than right ventricular muscle fibers that have to undergo compensatory hypertrophy later in life [14]. Patients with a post-tricuspid shunt related pulmonary arterial hypertension often have a much higher pulmonary vascular resistance than patients with pulmonary arterial hypertension of different etiology [54, 82-84]. Nevertheless, right ventricular peak pressure may be higher in pulmonary arterial hypertension patients without congenital heart disease [60], since the ventricles function in sequence, rather than partially in parallel (Figure 3 and 5). This is easily understood when considering what the right ventricle is required to do in order to increase output twofold. At a given fixed pulmonary vascular resistance of 800 dynes·s·cm^{-5} with pulmonary artery pressures of 84/40 mmHg (mean 55 mmHg), and a pulmonary venous pressure of 5 mmHg, cardiac output is 5 L/min. To increase cardiac output to 10 L/min, the right ventricle needs to double the transpulmonary gradient (=mean pulmonary artery pressure – pulmonary venous pressure). To achieve a mean pulmonary artery pressure of 105 mmHg, pulmonary artery pressures would need to be in the order of 160/80 mmHg. In contrast, a patient with congenital heart disease associated pulmonary arterial hypertension would not be able to achieve such an increase in pulmonary perfusion pressure, since the post-tricuspid shunt serves as a pop-off valve, effectively shunting right ventricular blood into the systemic circulation, proportionate to the pressure difference between the right and left ventricle. In the face of a systemic circulation that is still able to decrease its vascular resistance with exercise, the shunt may be quite large. This explains the deep hypoxemia that can be observed in patients with pulmonary arterial hypertension related to uncorrected congenital heart disease [35, 51, 54-56, 72, 83]. An important hematological disorder is present in all patients with congenital heart disease associated pulmonary arterial hypertension and normal renal function: erythrocytosis due to an increased erythropoietin drive. This enables these patients to secure oxygen delivery despite lower arterial oxygenation [56, 85, 86]. Furthermore, erythropoietin enhances exercise capacity [86] not only by increasing hemoglobin levels, but likely also by inducing neovascularization through its anti-apoptotic, mitogenic, and angiogenic effects [87-90]. Importantly, an “anti-pulmonary hypertensive” effect is also attributed to erythropoietin, given the observed beneficial effect on the pulmonary vasculature as well [91]. The atrioseptostomy procedure, regarded as a rescue-procedure or a bridge to transplantation renders a similar situation [92]. Hence, it is understandable that patients surviving the procedure, tend to live longer, despite lower arterial oxygenation [93].

Functional assessment of right ventricular function

A patient will almost always present with complaints of dyspnea associated with inadequate oxygen delivery as a result of right ventricular overload. Patients often complain of fatigue, and approximately one in two patients experiences chest pain on exertion, likely related to right ventricular ischemia [6, 71, 78]. Furthermore, patients with right ventricular overload may complain of palpitations or recurrent (pre-)syncope due to supraventricular or ventricular arrhythmias [76]. Also, patients may experience peripheral edema and ascites. Once there is considerable right ventricular diastolic dysfunction and/or tricuspid regurgitation, right atrial pressure tends to rise [60]. Furthermore, once the right ventricle fails to secure left ventricular preload, systemic blood pressure falls [94, 95], and renal perfusion becomes suboptimal. Hence, the renin-angiotensin-aldosterone system is activated, which leads to sodium and water retention [52, 76]. As in left-sided heart failure, patients with end-stage right ventricular failure may experience spectacular weight gain in just a few days as a result of fluid retention. In patients with congenital heart disease related pulmonary arterial hypertension, cyanosis may be observed, as well as hour-glass like fingernails [55, 85]. In patients with systemic sclerosis, sclerodactyly and even digital ulcers may be observed [52, 76]. Raynaud's phenomenon is also common in these patients, although rare in pulmonary arterial hypertension patients without connective tissue disease [76, 96, 97]. In other pulmonary arterial hypertension patients there may be no abnormalities at all, apart from peripheral edema. On chest examination a right ventricular 'heave' may be felt in the left 3rd and 4th intercostal space; although not very sensitive, this is a highly specific sign of right ventricular hypertrophy [97]. On auscultation, with increased right ventricular pressure load, tricuspid regurgitation is heard more easily, since the gradient over the tricuspid valve increases likewise [98]. There is often a loud second heart sound, and in case of right ventricular volume loading, there is often a split second heart sound due to the increased time necessary for propulsing a larger stroke volume than the left ventricle. In case of a right bundle branch block, the splitting of the second heart sound may be even more prolonged, since activation of the right ventricular myocardium then depends on cell-to-cell activation instead of diffuse activation by the Purkinje fibers [99]. In adult Fallot patients, a pulmonary regurgitation murmur is almost always present due to the incompetent pulmonary valve. A louder regurgitation murmur generally denotes a larger pressure gradient, but more important is the duration of the regurgitation murmur: the shorter the duration, the sooner a pressure equilibrium is reached between the pulmonary artery and right ventricle. A regurgitation murmur of a short duration is therefore more serious than a regurgitation murmur that lasts throughout the diastole [100].

The electrocardiogram is no less important in evaluation of patients with suspected right

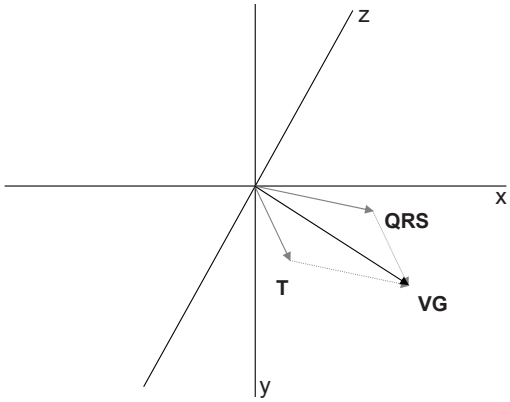

Figure 6
Schematic depiction of the ventricular gradient (VG) as a summation of net QRS and net T electrical activity. QRS and T vectors each depict net electrical activity, measured three-dimensionally, with a magnitude and direction. Summation of these vectors renders the ventricular gradient, i.e. the net electrical force of the whole myocardium. Depending on both individual magnitude and orientation of QRS and T vectors, the resultant vector depicting the ventricular gradient will be larger or smaller.

heart overload than it is in evaluation of patients with suspected left heart overload [26, 68, 101-107]. There is an increased incidence and prevalence of atrial fibrillation and atrial flutter in patients with right heart overload [26, 108-110]. Especially in Fallot patients with post-surgical scars in the right atrium and/or in the right ventricle, a range of arrhythmias may be observed [111, 112]. The majority of patients with right heart overload will present in sinus rhythm, however. Established markers of compromised cardiac function in left heart disease, resting heart rate [113], heart rate variability [114], and heart rate response with exercise [115-119], are likely just as important in right heart disease. Important markers of right heart disease are the heart rate at rest, since this likely reflects reflex noradrenergic activation in response to cardiac output [120]; i.e. heart rate will be higher in patients with poor stroke volume (*Chapter IX)*. In severe right heart overload, a rightward deviation of the electrical axis of the heart is almost always present, with the exception of patients with a large ventricular septal defect, who mostly have a leftward oriented heart axis. That the standard 12-lead ECG contains more information than meets the eye, is explained in *Chapter V, Chapter VI,* and *Chapter VII*. In short, ventricular depolarization is characterized on the ECG by the QRS complex, whereas ventricular repolarization is characterized by the T wave. Both QRS complex and T wave have amplitudes during a certain amount of time (mV·ms). The ECG is therefore a simple representation of three-dimensionally moving electrical wave fronts. Both QRS complex and

T wave can be represented by a vector, reflecting the orientation and magnitude of these wave fronts (Figure 6). The *ventricular gradient*, i.e. the resultant vector of the individual QRS and T vectors, defines the net magnitude and orientation of the electrical wave fronts of the ventricles during one cardiac cycle. Interestingly, the *ventricular gradient* is highly stable, and to a large extent independent of activation order [121]. Nevertheless, there are considerable gender differences in the *ventricular gradient*, and heart rate also influences the *ventricular gradient* within individuals [122]. An increased PR-interval, and/or QRS duration may be observed in right heart overload, as a consequence of increased fibrosis [123, 124]. Typically, a right bundle branch block may be a sign of right ventricular overload, although there is a relatively high prevalence of right bundle branch block in the general population without right heart disease [2-4]. Conventionally, voltage criteria for right atrial enlargement are based on a 'P pulmonale', a P wave ≥ 0.25 mV in lead II, or a P wave with an amplitude of

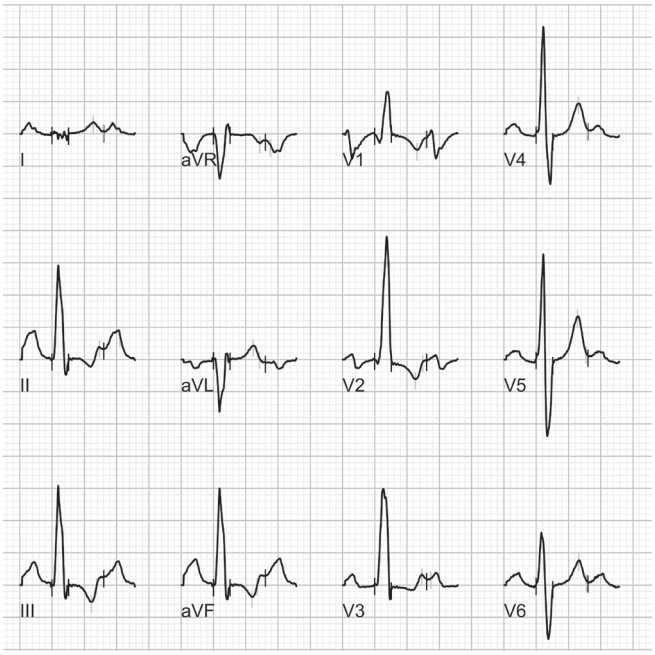

Figure 7

Typical ECG observed in right ventricular pressure load: there is a sinustachycardia of approximately 115 bpm, a rightward oriented heart axis, a borderline first degree AV-block, an increased QRS duration with a right bundle branch block configuration, and inverted T-waves – a 'strain pattern', most prominent in the right ventricular leads (V1, V2) and the inferior wall leads (II, III, aVF).

≥ 0.1 mV or a duration of ≥ 40 ms in lead V1. Voltage criteria for right ventricular hypertrophy are based on an R wave > 5mm with R:S > 1 in lead V1, overlying the right ventricle, and an R:S < 1 in lead V5, overlying the left ventricle [103, 125]. Repolarization disorders are often seen in right ventricular overload, most likely as a consequence of right ventricular hypertrophy, fibrosis and recurrent ischemia. A typical 'strain'-pattern may be observed in leads V1 and V2: the J-point is normal, but there is a down-sloping ST-T segment, discordant with the QRS complex (Figure 7).

A chest X-ray may indicate whether there is severe pulmonary disease, left heart disease (Kerley-B lines) or long-standing pulmonary hypertension (prominent proximal pulmonary arteries) [6, 51, 76]. Standard blood tests may clarify whether there is concomitant thyroid disease [126, 127], increased wall stress (elevated (NT-pro)BNP), or ischemia (elevated Troponin I or T) [128-130]. Every patient deserves adequate assessment of pulmonary function, including an arterial blood sample analysis, and spirometric analysis. In specific cases where alveolar hypoventilation is suspected, one should perform overnight oximetry. Similarly, when hypoxia is observed, alveolar diffusion capacity should be measured, corrected for alveolar volume [51, 52]. Exercise capacity is an important marker of disease burden, and can distinguish pulmonary impairment from cardiac impairment [131]. Although not as thorough as for instance bicycle ergometry, the 6-minute walk test is an adequate reflection of exercise capacity, oxygen consumption, and daily functioning [25, 33, 35, 56, 72, 76, 131-135]. This test is especially useful in advanced right ventricular failure when more vigorous exercise tests, such as bicycle ergometry, are no longer feasible [132].

Right heart imaging is not as easy as left heart imaging due to the directly retrosternal position, and functional assessment is only reliable in experienced hands. In contrast to the globular-shaped left ventricle, the normal right ventricle is not easily reflected by a common mathematical three-dimensional figure [136]. This becomes evident when the heart is imaged in its orthogonal planes: at best it can be stated that after birth, under physiological conditions, the right ventricle is crescent-shaped, half wrapped around the left ventricle (Figure 8). This is easily understood considering the higher systolic and diastolic left ventricular filling pressures, rendering the left ventricle globular-shaped in a physiological situation.

The use of Simpson's rule has allowed radiologists to accurately calculate right ventricular volumes in diastole and systole, as well as ejection fraction [136]. Cardiac MRI has helped greatly to understand the contraction pattern of the right ventricle, and is nowadays considered the gold standard for measurement of volume and ejection fraction [32, 75, 104, 137-139]. Nevertheless, echocardiography - which revolutionized cardiology by producing straightforward moving images of the heart - is easier to perform, less expensive, more

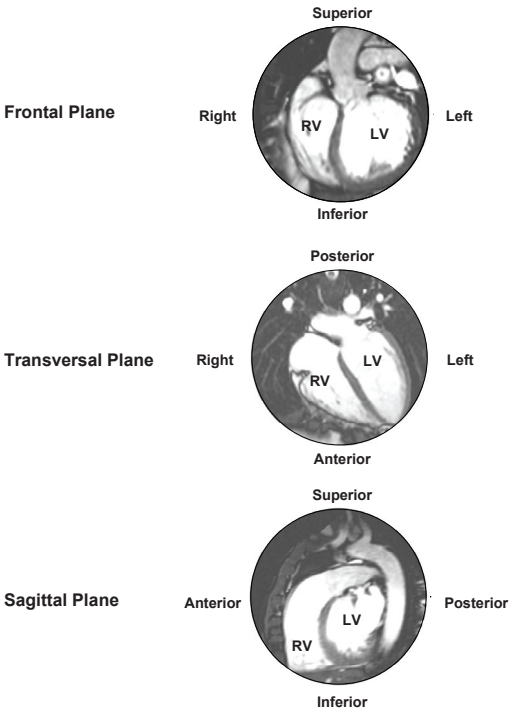

Figure 8
Cardiac magnetic resonance imaging of the normal heart in orthogonal slices.
Top: depiction of the left and right ventricle in the frontal plane. There is clear bulging of the septum towards the right ventricular cavity, which seems smaller in this section.
Middle: depiction of the left and right ventricle in the transversal plane. It is clear that the right ventricle is thin-walled with a trabeculated aspect.
Bottom: depiction of the left and right ventricle in the sagittal plane. The right ventricle lies retrosternally on the diaphragm, within the pericardial sac. Although the left ventricle has a consistent globular-shape, the right ventricle may at best be appreciated as crescent-shaped.

readily available, and allows a fairly reliable estimation of right atrial, right ventricular, and pulmonary pressures, the latter by application of the simplified Bernoulli equation [24, 60, 97, 100, 140, 141]. Although echocardiography is beyond the scope of this thesis, it should be considered an essential part of evaluation of patients with suspected right heart disease [51, 52, 76]. In patients with suspected pulmonary embolism the use of a computed tomography (CT) angiogram may help diagnose both large and small vessel thrombosis [62, 142]. So far, CT imaging is not yet of much help for assessment of right ventricular function, although a

rough idea of right-to-left ventricular volume ratios is also rendered by CT imaging.
In general, right ventricular overload is often diagnosed with considerable delay, except for in patients with congenital heart disease, who are generally recognized before or shortly after birth [51, 76]. Due to successful research there is an increasing awareness for the entity of right ventricular overload in the setting of pulmonary arterial hypertension. However, good screening methods are lacking [143]. Since right ventricular overload is generally already moderate-to-severe when patients become symptomatic, there is a theoretical benefit of case-finding and/or screening. Whether indeed earlier treatment initiation secures a better long-term outcome is unknown. The current concept of pulmonary arterial hypertension, however, is that of a progressive disease that should best be treated earlier, rather than later [144].

The significance of right ventricular overload

A chain is as strong as its weakest link. An otherwise perfectly healthy person with a good left atrium and ventricle may therefore be highly symptomatic when faced with right ventricular overload. Of course, right ventricular pressure overload is ultimately more limiting than right ventricular volume overload, since the Fontan circulation proves that with normal pulmonary vascular resistance a reasonable cardiac output is feasible [13, 25, 55]. Nevertheless, right ventricular overload is generally associated with poor exercise capacity, arrhythmias, and poor survival. The reason why pulmonary arterial hypertension is defined as a mean pulmonary artery pressure of >25 mmHg, is that this is approximately double of what is normally found in healthy subjects [60]. At less than systemic pulmonary artery pressures still, e.g. 78/36 mmHg (mean 50 mmHg), the right ventricle would therefore have to produce approximately four times the normal work [60, 84]. Despite the misleading right ventricular hypertrophy and impressive stroke work, the right ventricle likely passes a point of compensated adaptation early on in the process of overload. This view is supported by the reports regarding the poor right ventricular remodeling after pulmonary valve replacement in adult tetralogy of Fallot patients with severely dilated right ventricles [30, 31, 36]. Similarly, the right ventricle appears to be physiologically limited in its hypertrophy [84, 145], most likely due to maximum myocardial oxygen delivery. This then leads to an increase in heart rate once stroke work - and hence stroke volume - can no longer be increased [75]. A decrease in stroke volume and a compensatory increase in heart rate should therefore be regarded as relatively late symptoms of compromised cardiac output [113].
Early detection of right ventricular overload therefore remains a clinical challenge [146]. A challenge we best face with non-invasive diagnostic modalities.

Aim and outline of the thesis

The main aim of this thesis was to improve non-invasive diagnosis and follow-up of right ventricular function in the setting of right ventricular volume and/or pressure overload. The thesis focused on right ventricular volume overload in the setting of adult Fallot patients who underwent pulmonary valve replacement, and on right ventricular pressure overload in the setting of pulmonary arterial hypertension.

Part I focuses on right ventricular volume overload in adults with Fallot's tetralogy after correction in early childhood. The innate pulmonary valve abnormality precludes long-term surgical correction, and many adult Fallot patients will require repeated pulmonary valve replacement. In *Chapter II* we attempt to elucidate which patient characteristics were associated with a more prompt recovery time after surgical replacement, describing a small, yet well-documented cohort of adult Fallot patients who underwent elective pulmonary valve replacement. In *Chapter III* we analyze what may be expected from pulmonary valve replacement with respect to right ventricular reverse remodeling: i.e. what post-operative results may be expected based on the degree of pulmonary regurgitation and right ventricular function. In *Chapter IV w*e determine what effect pulmonary valve replacement has on cardiac repolarization characteristics in adult Fallot patients, since many adult Fallot patients have a high arrhythmia propensity as a consequence of long-standing right ventricular volume overload.

Part II concentrates on right ventricular pressure overload due to pulmonary arterial hypertension. In *Chapter V*, using an animal experimental setup, we document the evolutionary changes in right ventricular morphology and function during the development of pulmonary arterial hypertension. We compare electrocardiography, echocardiography, heart catheterization and right ventricular histology to monitor this chain of events. Documentation of evolutionary electrocardiographic changes due to right ventricular pressure overload helps to understand especially the early right ventricular changes in developing pulmonary arterial hypertension. In *Chapter VI* we subsequently study the additional value of three dimensional vectorcardiography for diagnosis of increased right ventricular pressure load, compared to conventional 12-lead ECG diagnosis. In *Chapter VII* we report on a particular patient whose ECG recordings changed markedly after developing idiopathic pulmonary arterial hypertension, and briefly review the available literature on this subject. In *Chapter VIII*, based on the hemodynamic abnormalities associated with electrocardiographically detectable

abnormalities, we define electrocardiographic cut-off points for determination of treatment response in pulmonary arterial hypertension patients. In *Chapter IX* we determine that resting heart rate, reflecting hemodynamics and neurohumoral activation, is a very important marker of prognosis in pulmonary arterial hypertension. Finally, in *Chapter X* we discuss the individual chapters, the conclusions we may draw from this research, and we reflect on future research and what this should address with respect to right ventricular failure.

References

1. Farb A, Burke AP and Virmani R. Anatomy and pathology of the right ventricle (including acquired tricuspid and pulmonic valve disease). Cardiol Clin 1992;10:1-21.

2. Liao YL, Emidy LA, Dyer A, Hewitt JS, Shekelle RB, Paul O, Prineas R and Stamler J. Characteristics and prognosis of incomplete right bundle branch block: an epidemiologic study. J Am Coll Cardiol 1986;7:492-499.

3. Rabkin SW, Mathewson FA and Tate RB. The natural history of right bundle branch block and frontal plane QRS axis in apparently healthy men. Chest 1981;80:191-196.

4. Fleg JL, Das DN and Lakatta EG. Right bundle branch block: long-term prognosis in apparently healthy men. J Am Coll Cardiol 1983;1:887-892.

5. Ho SY and Nihoyannopoulos P. Anatomy, echocardiography, and normal right ventricular dimensions. Heart 2006;92 Suppl 1:i2-13.

6. Chin KM, Kim NH and Rubin LJ. The right ventricle in pulmonary hypertension. Coron Artery Dis 2005;16:13-18.

7. Dell'Italia LJ. The right ventricle: anatomy, physiology, and clinical importance. Curr Probl Cardiol 1991;16:653-720.

8. Pettersen E, Helle-Valle T, Edvardsen T, Lindberg H, Smith HJ, Smevik B, Smiseth OA and Andersen K. Contraction pattern of the systemic right ventricle shift from longitudinal to circumferential shortening and absent global ventricular torsion. J Am Coll Cardiol 2007;49:2450-2456.

9. Duncker DJ and Bache RJ. Regulation of coronary blood flow during exercise. Physiol Rev 2008;88:1009-1086.

10. Zong P, Tune JD and Downey HF. Mechanisms of oxygen demand/supply balance in the right ventricle. Exp Biol Med (Maywood) 2005;230:507-519.

11. Westerhof N, Boer C, Lamberts RR and Sipkema P. Cross-talk between cardiac muscle and coronary vasculature. Physiol Rev 2006;86:1263-1308.

12. Bashore TM. Adult congenital heart disease: right ventricular outflow tract lesions. Circulation 2007;115:1933-1947.

13. Sommer RJ, Hijazi ZM and Rhodes JF. Pathophysiology of congenital heart disease in the adult: part III: Complex congenital heart disease. Circulation 2008;117:1340-1350.

14. Hopkins WE and Waggoner AD. Severe pulmonary hypertension without right ventricular failure: the unique hearts of patients with Eisenmenger syndrome. Am J Cardiol 2002;89:34-38.

15. Shrivastava S. Timing of surgery/catheter intervention in common congenital cardiac defects. Indian J Pediatr 2000;67:S2-S6.

16. Agnoletti G, Boudjemline Y, Bonnet D, Sidi D and Vouhe P. Surgical reconstruction of occluded pulmonary arteries in patients with congenital heart disease: effects on pulmonary artery growth. Circulation 2004;109:2314-2318.

17. Sivakumar K, Krishnan P, Pieris R and Francis E. Hybrid approach to surgical correction of tetralogy of Fallot in all patients with functioning Blalock Taussig shunts. Catheter Cardiovasc Interv 2007;70:256-264.

18. Brock RC. The surgery of pulmonary stenosis. Br Med J 1949;2:399-406.

19. Campbell M, Deuchar DC and Brock R. Results of pulmonary valvotomy and infundibular resection in 100 cases of Fallot's tetralogy. Br Med J 1954;2:111-122.

20. Giannopoulos NM, Chatzis AC, Bobos DP, Kirvassilis GV, Tsoutsinos A and Sarris GE. Tetralogy of Fallot: influence of right ventricular outflow tract reconstruction on late outcome. Int J Cardiol 2004;97 Suppl 1:87-90.

21. Hoohenkerk GJ, Schoof PH, Bruggemans EF, Rijlaarsdam M and Hazekamp MG. 28 years' experience with transatrial-transpulmonary repair of atrioventricular septal defect with tetralogy of Fallot. Ann Thorac Surg 2008;85:1686-1689.

22. Billig DM. Current considerations in the surgical management of tetralogy of Fallot. Chest 1973;64:79-83.

23. Oosterhof T, Tulevski II, Vliegen HW, Spijkerboer AM and Mulder BJ. Effects of volume and/or pressure overload secondary to congenital heart disease (tetralogy of fallot or pulmonary stenosis) on right ventricular function using cardiovascular magnetic resonance and B-type natriuretic peptide levels. Am J Cardiol 2006;97:1051-1055.

24. Gatzoulis MA, Clark AL, Cullen S, Newman CG and Redington AN. Right ventricular diastolic function 15 to 35 years after repair of tetralogy of Fallot. Restrictive physiology predicts superior exercise performance. Circulation 1995;91:1775-1781.

25. Diller GP, Dimopoulos K, Okonko D, Li W, Babu-Narayan SV, Broberg CS, Johansson B, Bouzas B, Mullen MJ, Poole-Wilson PA, Francis DP and Gatzoulis MA. Exercise intolerance in adult congenital heart disease: comparative severity, correlates, and prognostic implication. Circulation 2005;112:828-835.

26. Gatzoulis MA, Till JA, Somerville J and Redington AN. Mechanoelectrical interaction in tetralogy of Fallot. QRS prolongation relates to right ventricular size and predicts malignant ventricular arrhythmias and sudden death. Circulation 1995;92:231-237.

27. Abd El Rahman MY, Abdul-Khaliq H, Vogel M, Alexi-Meskishvili V, Gutberlet M and Lange PE. Relation between right ventricular enlargement, QRS duration, and right ventricular function in patients with tetralogy of Fallot and pulmonary regurgitation after surgical repair. Heart 2000;84:416-420.

28. Gatzoulis MA, Balaji S, Webber SA, Siu SC, Hokanson JS, Poile C, Rosenthal M, Nakazawa M, Moller JH, Gillette PC, Webb GD and Redington AN. Risk factors for arrhythmia and sudden cardiac death late after repair of tetralogy of Fallot: a multicentre study. Lancet 2000;356:975-981.

29. Hazekamp MG, Kurvers MM, Schoof PH, Vliegen HW, Mulder BM, Roest AA, Ottenkamp J and Dion RA. Pulmonary valve insertion late after repair of Fallot's tetralogy. Eur J Cardiothorac Surg 2001;19:667-670.

30. Therrien J, Provost Y, Merchant N, Williams W, Colman J and Webb G. Optimal timing for pulmonary valve replacement in adults after tetralogy of Fallot repair. Am J Cardiol 2005;95:779-782.

31. Therrien J, Siu SC, McLaughlin PR, Liu PP, Williams WG and Webb GD. Pulmonary valve replacement in adults late after repair of tetralogy of fallot: are we operating too late? J Am Coll Cardiol 2000;36:1670-1675.

32. Vliegen HW, van Straten A, de Roos A, Roest AA, Schoof PH, Zwinderman AH, Ottenkamp J, van der Wall EE and Hazekamp MG. Magnetic resonance imaging to assess the hemodynamic effects of pulmonary valve replacement in adults late after repair of tetralogy of fallot. Circulation 2002;106:1703-1707.

33. Fredriksen PM, Therrien J, Veldtman G, Ali WM, Liu P, Thaulow E and Webb G. Aerobic capacity in adults with tetralogy of Fallot. Cardiol Young 2002;12:554-559.

34. Roest AA, Helbing WA, Kunz P, van den Aardweg JG, Lamb HJ, Vliegen HW, van der Wall EE and de Roos A. Exercise MR imaging in the assessment of pulmonary regurgitation and biventricular function in patients after tetralogy of fallot repair. Radiology 2002;223:204-211.

35. Diller GP, Dimopoulos K, Okonko D, Uebing A, Broberg CS, Babu-Narayan S, Bayne S, Poole-Wilson PA, Sutton R, Francis DP and Gatzoulis MA. Heart rate response during exercise predicts survival in adults with congenital heart disease. J Am Coll Cardiol 2006;48:1250-1256.

36. Henkens IR, van Straten A, Schalij MJ, Hazekamp MG, de Roos A, van der Wall EE and Vliegen HW. Predicting outcome of pulmonary valve replacement in adult tetralogy of Fallot patients. Ann Thorac Surg 2007;83:907-911.

37. Oosterhof T, van Straten A, Vliegen HW, Meijboom FJ, van Dijk AP, Spijkerboer AM, Bouma BJ, Zwinderman AH, Hazekamp MG, de Roos A and Mulder BJ. Preoperative thresholds for pulmonary valve replacement in patients with corrected tetralogy of Fallot using cardiovascular magnetic resonance. Circulation 2007;116:545-551.

38. Waterbolk TW, Hoendermis ES, den Hamer IJ and Ebels T. Pulmonary valve replacement with a mechanical prosthesis. Promising results of 28 procedures in patients with congenital heart disease. Eur J Cardiothorac Surg 2006;30:28-32.

39. Frigiola A, Tsang V, Nordmeyer J, Lurz P, van Doorn C, Taylor AM, Bonhoeffer P and de Leval M. Current approaches to pulmonary regurgitation. Eur J Cardiothorac Surg 2008;34:576-581.

40. Oosterhof T, Meijboom FJ, Vliegen HW, Hazekamp MG, Zwinderman AH, Bouma BJ, van Dijk AP and Mulder BJ. Long-term follow-up of homograft function after pulmonary valve replacement in patients with tetralogy of Fallot. Eur Heart J 2006;27:1478-1484.

41. Quintessenza JA, Jacobs JP, Chai PJ, Morell VO, Giroud JM and Boucek RJ. Late replacement of the pulmonary valve: when and what type of valve? Cardiol Young 2005;15 Suppl 1:58-63.

42. Karamlou T, McCrindle BW and Williams WG. Surgery insight: late complications following repair of tetralogy of Fallot and related surgical strategies for management. Nat Clin Pract Cardiovasc Med 2006;3:611-622.

43. Erez E, Tam VK, Doublin NA and Stakes J. Repeat right ventricular outflow tract reconstruction using the Medtronic Freestyle porcine aortic root. J Heart Valve Dis 2006;15:92-96.

44. Meyns B, Jashari R, Gewillig M, Mertens L, Komarek A, Lesaffre E, Budts W and Daenen W. Factors influencing the survival of cryopreserved homografts. The second homograft performs as well as the first. Eur J Cardiothorac Surg 2005;28:211-216.

45. Ghez O, Tsang VT, Frigiola A, Coats L, Taylor A, van DC, Bonhoeffer P and de LM. Right ventricular outflow tract reconstruction for pulmonary regurgitation after repair of tetralogy of Fallot. Preliminary results. Eur J Cardiothorac Surg 2007;31:654-658.

46. Khambadkone S and Bonhoeffer P. Percutaneous implantation of pulmonary valves. Expert Rev Cardiovasc Ther 2003;1:541-548.

47. Khambadkone S, Coats L, Taylor A, Boudjemline Y, Derrick G, Tsang V, Cooper J, Muthurangu V, Hegde SR, Razavi RS, Pellerin D, Deanfield J and Bonhoeffer P. Percutaneous pulmonary valve implantation in humans: results in 59 consecutive patients. Circulation 2005;112:1189-1197.

48. Lurz P, Coats L, Khambadkone S, Nordmeyer J, Boudjemline Y, Schievano S, Muthurangu V, Lee TY, Parenzan G, Derrick G, Cullen S, Walker F, Tsang V, Deanfield J, Taylor AM and Bonhoeffer P. Percutaneous pulmonary valve implantation: impact of evolving technology and learning curve on clinical outcome. Circulation 2008;117:1964-1972.

49. Schievano S, Coats L, Migliavacca F, Norman W, Frigiola A, Deanfield J, Bonhoeffer P and Taylor AM. Variations in right ventricular outflow tract morphology following repair of congenital heart disease: implications for percutaneous pulmonary valve implantation. J Cardiovasc Magn Reson 2007;9:687-695.

50. Schievano S, Migliavacca F, Coats L, Khambadkone S, Carminati M, Wilson N, Deanfield JE, Bonhoeffer P and Taylor AM. Percutaneous pulmonary valve implantation based on rapid prototyping of right ventricular outflow tract and pulmonary trunk from MR data. Radiology 2007;242:490-497.

51. Galie N, Torbicki A, Barst R, Dartevelle P, Haworth S, Higenbottam T, Olschewski H, Peacock A, Pietra G, Rubin LJ, Simonneau G, Priori SG, Garcia MA, Blanc JJ, Budaj A, Cowie M, Dean V, Deckers J, Burgos EF, Lekakis J, Lindahl B, Mazzotta G, McGregor K, Morais J, Oto A, Smiseth OA, Barbera JA, Gibbs S, Hoeper M, Humbert M, Naeije R and Pepke-Zaba J. Guidelines on diagnosis and treatment of pulmonary arterial hypertension. The Task Force on Diagnosis and Treatment of Pulmonary Arterial Hypertension of the European Society of Cardiology. Eur Heart J 2004;25:2243-2278.

52. Simonneau G, Galie N, Rubin LJ, Langleben D, Seeger W, Domenighetti G, Gibbs S, Lebrec D, Speich R, Beghetti M, Rich S and Fishman A. Clinical classification of pulmonary hypertension. J Am Coll Cardiol 2004;43:5S-12S.

53. Schulze-Neick I and Beghetti M. Classifying pulmonary hypertension in the setting of the congenitally malformed heart--cleaning up a dog's dinner. Cardiol Young 2008;18:22-25.

54. Galie N, Manes A, Palazzini M, Negro L, Marinelli A, Gambetti S, Mariucci E, Donti A, Branzi A and Picchio FM. Management of pulmonary arterial hypertension associated with congenital systemic-to-pulmonary shunts and Eisenmenger's syndrome. Drugs 2008;68:1049-1066.

55. Diller GP and Gatzoulis MA. Pulmonary vascular disease in adults with congenital heart disease. Circulation 2007;115:1039-1050.

56. Dimopoulos K, Diller GP, Piepoli MF and Gatzoulis MA. Exercise intolerance in adults with congenital heart disease. Cardiol Clin 2006;24:641-60, vii.

57. Sommer RJ, Hijazi ZM and Rhodes JF, Jr. Pathophysiology of congenital heart disease in the adult: part I: Shunt lesions. Circulation 2008;117:1090-1099.

58. Viswanathan S and Kumar RK. Assessment of operability of congenital cardiac shunts with increased pulmonary vascular resistance. Catheter Cardiovasc Interv 2008;71:665-670.

59. Ussia GP, Mule M, Caruso E, Aiello R and Tamburino C. Combined endothelin receptor antagonist and transcatheter interventional therapy of patent ductus arteriosus with severe pulmonary artery hypertension. Int J Cardiol 2007;116:427-429.

60. Chemla D, Castelain V, Herve P, Lecarpentier Y and Brimioulle S. Haemodynamic evaluation of pulmonary hypertension. Eur Respir J 2002;20:1314-1331.

61. Diller GP, Dimopoulos K, Broberg CS, Kaya MG, Naghotra US, Uebing A, Harries C, Goktekin O, Gibbs JS and Gatzoulis MA. Presentation, survival prospects, and predictors of death in Eisenmenger syndrome: a combined retrospective and case-control study. Eur Heart J 2006;27:1737-1742.

62. Silversides CK, Granton JT, Konen E, Hart MA, Webb GD and Therrien J. Pulmonary thrombosis in adults with Eisenmenger syndrome. J Am Coll Cardiol 2003;42:1982-1987.

63. Goerler H, Simon A, Gohrbandt B, Hagl C, Oppelt P, Weidemann J, Haverich A and Strueber M. Heart-lung and lung transplantation in grown-up congenital heart disease: long-term single centre experience. Eur J Cardiothorac Surg 2007;32:926-931.

64. Choong CK, Sweet SC, Guthrie TJ, Mendeloff EN, Haddad FJ, Schuler P, De La MM and Huddleston CB. Repair of congenital heart lesions combined with lung transplantation for the treatment of severe pulmonary hypertension: a 13-year experience. J Thorac Cardiovasc Surg 2005;129:661-669.

65. Hosseinpour AR, Cullen S and Tsang VT. Transplantation for adults with congenital heart disease. Eur J Cardiothorac Surg 2006;30:508-514.

66. Michelakis ED, Rebeyka I, Wu X, Nsair A, Thebaud B, Hashimoto K, Dyck JR, Haromy A, Harry G, Barr A and Archer SL. O2 sensing in the human ductus arteriosus: regulation of voltage-gated K+ channels in smooth muscle cells by a mitochondrial redox sensor. Circ Res 2002;91:478-486.

67. Therrien J, Connelly MS and Webb GD. Patent Ductus Arteriosus. Curr Treat Options Cardiovasc Med 1999;1:341-346.

68. Penaloza D and Arias-Stella J. The heart and pulmonary circulation at high altitudes: healthy highlanders and chronic mountain sickness. Circulation 2007;115:1132-1146.

69. Jones DP, Damiano R, Cox JL and Wolfe WG. The effect of altitude-induced hypoxia on regional myocardial blood flow. J Thorac Cardiovasc Surg 1981;82:216-220.

70. Murray PA, Baig H, Fishbein MC and Vatner SF. Effects of experimental right ventricular hypertrophy on myocardial blood flow in conscious dogs. J Clin Invest 1979;64:421-427.

71. van Wolferen SA, Marcus JT, Westerhof N, Spreeuwenberg MD, Marques KM, Bronzwaer JG, Henkens IR, Gan CT, Boonstra A, Postmus PE and Vonk-Noordegraaf A. Right coronary artery flow impairment in patients with pulmonary hypertension. Eur Heart J 2008;29:120-127.

72. Diller GP, Okonko DO, Uebing A, Dimopoulos K, Bayne S, Sutton R, Francis DP and Gatzoulis MA. Impaired heart rate response to exercise in adult patients with a systemic right ventricle or univentricular circulation: Prevalence, relation to exercise, and potential therapeutic implications. Int J Cardiol 2008;

73. Henkens IR, Mouchaers KT, Vliegen HW, van der Laarse WJ, Swenne CA, Maan AC, Draisma HH, Schalij I, van der Wall EE, Schalij MJ and Vonk-Noordegraaf A. Early changes in rat hearts with developing pulmonary arterial hypertension can be detected with three-dimensional electrocardiography. Am J Physiol Heart Circ Physiol 2007;293:H1300-H1307.

74. Castelain V, Chemla D, Humbert M, Sitbon O, Simonneau G, Lecarpentier Y and Herve P. Pulmonary artery pressure-flow relations after prostacyclin in primary pulmonary hypertension. Am J Respir Crit Care Med 2002;165:338-340.

75. Holverda S, Gan CT, Marcus JT, Postmus PE, Boonstra A and Vonk-Noordegraaf A. Impaired stroke volume response to exercise in pulmonary arterial hypertension. J Am Coll Cardiol 2006;47:1732-1733.

76. Barst RJ, McGoon M, Torbicki A, Sitbon O, Krowka MJ, Olschewski H and Gaine S. Diagnosis and differential assessment of pulmonary arterial hypertension. J Am Coll Cardiol 2004;43:40S-47S.

77. Velez-Roa S, Ciarka A, Najem B, Vachiery JL, Naeije R and Van de Borne P. Increased sympathetic nerve activity in pulmonary artery hypertension. Circulation 2004;110:1308-1312.

78. Gomez A, Bialostozky D, Zajarias A, Santos E, Palomar A, Martinez ML and Sandoval J. Right ventricular ischemia in patients with primary pulmonary hypertension. J Am Coll Cardiol 2001;38:1137-1142.

79. Badesch DB, Tapson VF, McGoon MD, Brundage BH, Rubin LJ, Wigley FM, Rich S, Barst RJ, Barrett PS, Kral KM, Jobsis MM, Loyd JE, Murali S, Frost A, Girgis R, Bourge RC, Ralph DD, Elliott CG, Hill NS, Langleben D, Schilz RJ, McLaughlin VV, Robbins IM, Groves BM, Shapiro S and Medsger TA, Jr. Continuous intravenous epoprostenol for pulmonary hypertension due to the scleroderma spectrum of disease. A randomized, controlled trial. Ann Intern Med 2000;132:425-434.

80. McLaughlin VV. 'Raising the bar' for the treatment of pulmonary arterial hypertension. Eur Heart J 2006;27:510-511.

81. McLaughlin VV, Shillington A and Rich S. Survival in primary pulmonary hypertension: the impact of epoprostenol therapy. Circulation 2002;106:1477-1482.

82. Galie N, Ghofrani HA, Torbicki A, Barst RJ, Rubin LJ, Badesch D, Fleming T, Parpia T, Burgess G, Branzi A, Grimminger F, Kurzyna M and Simonneau G. Sildenafil citrate therapy for pulmonary arterial hypertension. N Engl J Med 2005;353:2148-2157.

83. Galie N, Beghetti M, Gatzoulis MA, Granton J, Berger RM, Lauer A, Chiossi E and Landzberg M. Bosentan therapy in patients with Eisenmenger syndrome: a multicenter, double-blind, randomized, placebo-controlled study. Circulation 2006;114:48-54.

84. Lankhaar JW, Westerhof N, Faes TJ, Gan CT, Marques KM, Boonstra A, van den Berg FG, Postmus PE and Vonk-Noordegraaf A. Pulmonary vascular resistance and compliance stay inversely related during treatment of pulmonary hypertension. Eur Heart J 2008;

85. Dimopoulos K, Okonko DO, Diller GP, Broberg CS, Salukhe TV, Babu-Narayan SV, Li W, Uebing A, Bayne S, Wensel R, Piepoli MF, Poole-Wilson PA, Francis DP and Gatzoulis MA. Abnormal ventilatory response to exercise in adults with congenital heart disease relates to cyanosis and predicts survival. Circulation 2006;113:2796-2802.

86. Mancini DM, Katz SD, Lang CC, LaManca J, Hudaihed A and Androne AS. Effect of erythropoietin on exercise capacity in patients with moderate to severe chronic heart failure. Circulation 2003;107:294-299.

87. Smith KJ, Bleyer AJ, Little WC and Sane DC. The cardiovascular effects of erythropoietin. Cardiovasc Res 2003;59:538-548.

88. van der MP, Voors AA, Lipsic E, van Gilst WH and van Veldhuisen DJ. Erythropoietin in cardiovascular diseases. Eur Heart J 2004;25:285-291.

89. van der MP, Lipsic E, Henning RH, Boddeus K, van d, V, Voors AA, van Veldhuisen DJ, van Gilst WH and Schoemaker RG. Erythropoietin induces neovascularization and improves cardiac function in rats with heart failure after myocardial infarction. J Am Coll Cardiol 2005;46:125-133.

90. Bullard AJ, Govewalla P and Yellon DM. Erythropoietin protects the myocardium against reperfusion injury in vitro and in vivo. Basic Res Cardiol 2005;100:397-403.

91. Weissmann N, Manz D, Buchspies D, Keller S, Mehling T, Voswinckel R, Quanz K, Ghofrani HA, Schermuly RT, Fink L, Seeger W, Gassmann M and Grimminger F. Congenital erythropoietin over-expression causes “anti-pulmonary hypertensive” structural and functional changes in mice, both in normoxia and hypoxia. Thromb Haemost 2005;94:630-638.

92. Klepetko W, Mayer E, Sandoval J, Trulock EP, Vachiery JL, Dartevelle P, Pepke-Zaba J, Jamieson SW, Lang I and Corris P. Interventional and surgical modalities of treatment for pulmonary arterial hypertension. J Am Coll Cardiol 2004;43:73S-80S.

93. Sandoval J, Gaspar J, Pulido T, Bautista E, Martinez-Guerra ML, Zeballos M, Palomar A and Gomez A. Graded balloon dilation atrial septostomy in severe primary pulmonary hypertension. A therapeutic alternative for patients nonresponsive to vasodilator treatment. J Am Coll Cardiol 1998;32:297-304.

94. Chang SM, Lin CC, Hsiao SH, Lee CY, Yang SH, Lin SK and Huang WC. Pulmonary hypertension and left heart function: insights from tissue Doppler imaging and myocardial performance index. Echocardiography 2007;24:366-373.

95. Wensel R, Opitz CF, Anker SD, Winkler J, Hoffken G, Kleber FX, Sharma R, Hummel M, Hetzer R and Ewert R. Assessment of survival in patients with primary pulmonary hypertension: importance of cardiopulmonary exercise testing. Circulation 2002;106:319-324.

96. Kawut SM, Taichman DB, Ahya VN, Kaplan S, Archer-Chicko CL, Kimmel SE and Palevsky H. Hemodynamics and survival in patients with pulmonary arterial hypertension related to systemic sclerosis. Chest 2003;123:344-350.

97. McGoon M, Gutterman D, Steen V, Barst R, McCrory DC, Fortin TA and Loyd JE. Screening, early detection, and diagnosis of pulmonary arterial hypertension: ACCP evidence-based clinical practice guidelines. Chest 2004;126:14S-34S.

98. Perloff JK. Auscultatory and phonocardiographic manifestations of pulmonary hypertension. Prog Cardiovasc Dis 1967;9:303-340.

99. Perloff JK and Harvey WP. Mechanisms of fixed splitting of the second heart sound. Circulation 1958;18:998-1009.

100. Silversides CK, Veldtman GR, Crossin J, Merchant N, Webb GD, McCrindle BW, Siu SC and Therrien J. Pressure half-time predicts hemodynamically significant pulmonary regurgitation in adult patients with repaired tetralogy of fallot. J Am Soc Echocardiogr 2003;16:1057-1062.

101. Dhingra R, Ho NB, Benjamin EJ, Wang TJ, Larson MG, D'Agostino RB, Sr., Levy D and Vasan RS. Cross-sectional relations of electrocardiographic QRS duration to left ventricular dimensions: the Framingham Heart Study. J Am Coll Cardiol 2005;45:685-689.

102. Karliner JS, Sarnquist FF, Graber DJ, Peters RM, Jr. and West JB. The electrocardiogram at extreme altitude: experience on Mt. Everest. Am Heart J 1985;109:505-513.

103. Lehtonen J, Sutinen S, Ikaheimo M and Paakko P. Electrocardiographic criteria for the diagnosis of right ventricular hypertrophy verified at autopsy. Chest 1988;93:839-842.

104. Book WM, Parks WJ, Hopkins KL and Hurst JW. Electrocardiographic predictors of right ventricular volume measured by magnetic resonance imaging late after total repair of tetralogy of Fallot. Clin Cardiol 1999;22:740-746.

105. Ahearn GS, Tapson VF, Rebeiz A and Greenfield JC, Jr. Electrocardiography to define clinical status in primary pulmonary hypertension and pulmonary arterial hypertension secondary to collagen vascular disease. Chest 2002;122:524-527.

106. Kashani A and Barold SS. Significance of QRS complex duration in patients with heart failure. J Am Coll Cardiol 2005;46:2183-2192.

107. Henkens IR, Scherptong RW, van Kralingen KW, Said SA and Vliegen HW. Pulmonary hypertension: the role of the electrocardiogram. Neth Heart J 2008;16:250-254.

108. Luciani GB, Viscardi F, Pilati M, Crepaz R, Faggian G and Mazzucco A. Age at repair affects the very long-term outcome of sinus venosus defect. Ann Thorac Surg 2008;86:153-159.

109. Neffke JG, Tulevski II, van der Wall EE, Wilde AA, van Veldhuisen DJ, Dodge-Khatami A and Mulder BJ. ECG determinants in adult patients with chronic right ventricular pressure overload caused by congenital heart disease: relation with plasma neurohormones and MRI parameters. Heart 2002;88:266-270.

110. Tongers J, Schwerdtfeger B, Klein G, Kempf T, Schaefer A, Knapp JM, Niehaus M, Korte T and Hoeper MM. Incidence and clinical relevance of supraventricular tachyarrhythmias in pulmonary hypertension. Am Heart J 2007;153:127-132.

111. Zeppenfeld K, Schalij MJ, Bartelings MM, Tedrow UB, Koplan BA, Soejima K and Stevenson WG. Catheter ablation of ventricular tachycardia after repair of congenital heart disease: electroanatomic identification of the critical right ventricular isthmus. Circulation 2007;116:2241-2252.

112. Gatzoulis MA, Till JA and Redington AN. Depolarization-repolarization inhomogeneity after repair of tetralogy of Fallot. The substrate for malignant ventricular tachycardia? Circulation 1997;95:401-404.

113. Fox K, Borer JS, Camm AJ, Danchin N, Ferrari R, Lopez Sendon JL, Steg PG, Tardif JC, Tavazzi L and Tendera M. Resting heart rate in cardiovascular disease. J Am Coll Cardiol 2007;50:823-830.

114. Horner SM, Murphy CF, Coen B, Dick DJ, Harrison FG, Vespalcova Z and Lab MJ. Contribution to heart rate variability by mechanoelectric feedback. Stretch of the sinoatrial node reduces heart rate variability. Circulation 1996;94:1762-1767.

115. Gheorghiade M, Colucci WS and Swedberg K. Beta-blockers in chronic heart failure. Circulation 2003;107:1570-1575.

116. Colucci WS, Ribeiro JP, Rocco MB, Quigg RJ, Creager MA, Marsh JD, Gauthier DF and Hartley LH. Impaired chronotropic response to exercise in patients with congestive heart failure. Role of postsynaptic beta-adrenergic desensitization. Circulation 1989;80:314-323.

117. Colucci WS. In vivo studies of myocardial beta-adrenergic receptor pharmacology in patients with congestive heart failure. Circulation 1990;82:I44-I51.

118. Colucci WS, Kolias TJ, Adams KF, Armstrong WF, Ghali JK, Gottlieb SS, Greenberg B, Klibaner MI, Kukin ML and Sugg JE. Metoprolol reverses left ventricular remodeling in patients with asymptomatic systolic dysfunction: the REversal of VEntricular Remodeling with Toprol-XL (REVERT) trial. Circulation 2007;116:49-56.

119. Olshansky B, Sabbah HN, Hauptman PJ and Colucci WS. Parasympathetic nervous system and heart failure: pathophysiology and potential implications for therapy. Circulation 2008;118:863-871.

120. Daliento L, Folino AF, Menti L, Zanco P, Baratella MC and Dalla VS. Adrenergic nervous activity in patients after surgical correction of tetralogy of Fallot. J Am Coll Cardiol 2001;38:2043-2047.

121. Draisma HH, Schalij MJ, van der Wall EE and Swenne CA. Elucidation of the spatial ventricular gradient and its link with dispersion of repolarization. Heart Rhythm 2006;3:1092-1099.

122. Scherptong RW, Henkens IR, Man SC, Le Cessie S, Vliegen HW, Draisma HH, Maan AC, Schalij MJ and Swenne CA. Normal limits of the spatial QRS-T angle and ventricular gradient in 12-lead electrocardiograms of young adults: dependence on sex and heart rate. J Electrocardiol 2008;

123. Babu-Narayan SV, Kilner PJ, Li W, Moon JC, Goktekin O, Davlouros PA, Khan M, Ho SY, Pennell DJ and Gatzoulis MA. Ventricular fibrosis suggested by cardiovascular magnetic resonance in adults with repaired tetralogy of fallot and its relationship to adverse markers of clinical outcome. Circulation 2006;113:405-413.

124. McCann GP, Gan CT, Beek AM, Niessen HW, Vonk Noordegraaf A and van Rossum AC. Extent of MRI delayed enhancement of myocardial mass is related to right ventricular dysfunction in pulmonary artery hypertension. AJR Am J Roentgenol 2007;188:349-355.

125. Butler PM, Leggett SI, Howe CM, Freye CJ, Hindman NB and Wagner GS. Identification of electrocardiographic criteria for diagnosis of right ventricular hypertrophy due to mitral stenosis. Am J Cardiol 1986;57:639-643.

126. Chu JW, Kao PN, Faul JL and Doyle RL. High prevalence of autoimmune thyroid disease in pulmonary arterial hypertension. Chest 2002;122:1668-1673.

127. Lozano HF and Sharma CN. Reversible pulmonary hypertension, tricuspid regurgitation and right-sided heart failure associated with hyperthyroidism: case report and review of the literature. Cardiol Rev 2004;12:299-305.

128. Blyth KG, Groenning BA, Mark PB, Martin TN, Foster JE, Steedman T, Morton JJ, Dargie HJ and Peacock AJ. NT-proBNP can be used to detect right ventricular systolic dysfunction in pulmonary hypertension. Eur Respir J 2007;29:737-744.

129. Gan CT, McCann GP, Marcus JT, van Wolferen SA, Twisk JW, Boonstra A, Postmus PE and Vonk-Noordegraaf A. NT-proBNP reflects right ventricular structure and function in pulmonary hypertension. Eur Respir J 2006;28:1190-1194.

130. Torbicki A, Kurzyna M, Kuca P, Fijalkowska A, Sikora J, Florczyk M, Pruszczyk P, Burakowski J and Wawrzynska L. Detectable serum cardiac troponin T as a marker of poor prognosis among patients with chronic precapillary pulmonary hypertension. Circulation 2003;108:844-848.

131. Sun XG, Hansen JE, Oudiz RJ and Wasserman K. Exercise pathophysiology in patients with primary pulmonary hypertension. Circulation 2001;104:429-435.

132. ATS statement: guidelines for the six-minute walk test. Am J Respir Crit Care Med 2002;166:111-117.

133. Miyamoto S, Nagaya N, Satoh T, Kyotani S, Sakamaki F, Fujita M, Nakanishi N and Miyatake K. Clinical correlates and prognostic significance of six-minute walk test in patients with primary pulmonary hypertension. Comparison with cardiopulmonary exercise testing. Am J Respir Crit Care Med 2000;161:487-492.

134. Paciocco G, Martinez FJ, Bossone E, Pielsticker E, Gillespie B and Rubenfire M. Oxygen desaturation on the six-minute walk test and mortality in untreated primary pulmonary hypertension. Eur Respir J 2001;17:647-652.

135. Provencher S, Chemla D, Herve P, Sitbon O, Humbert M and Simonneau G. Heart rate responses during the 6-minute walk test in pulmonary arterial hypertension. Eur Respir J 2006;27:114-120.

136. Jauhiainen T, Jarvinen VM, Hekali PE, Poutanen VP, Penttila A and Kupari M. MR gradient echo volumetric analysis of human cardiac casts: focus on the right ventricle. J Comput Assist Tomogr 1998;22:899-903.

137. Babu-Narayan SV, Gatzoulis MA and Kilner PJ. Non-invasive imaging in adult congenital heart disease using cardiovascular magnetic resonance. J Cardiovasc Med (Hagerstown) 2007;8:23-29.

138. Oosterhof T, Mulder BJ, Vliegen HW and de Roos A. Cardiovascular magnetic resonance in the follow-up of patients with corrected tetralogy of Fallot: a review. Am Heart J 2006;151:265-272.

139. Vonk-Noordegraaf A, van Wolferen SA, Marcus JT, Boonstra A, Postmus PE, Peeters JW and Peacock AJ. Noninvasive assessment and monitoring of the pulmonary circulation. Eur Respir J 2005;25:758-766.

140. Raymond RJ, Hinderliter AL, Willis PW, Ralph D, Caldwell EJ, Williams W, Ettinger NA, Hill NS, Summer WR, de BB, Schwartz T, Koch G, Clayton LM, Jobsis MM, Crow JW and Long W. Echocardiographic predictors of adverse outcomes in primary pulmonary hypertension. J Am Coll Cardiol 2002;39:1214-1219.

141. Yeo TC, Dujardin KS, Tei C, Mahoney DW, McGoon MD and Seward JB. Value of a Doppler-derived index combining systolic and diastolic time intervals in predicting outcome in primary pulmonary hypertension. Am J Cardiol 1998;81:1157-1161.

142. Hoeper MM, Mayer E, Simonneau G and Rubin LJ. Chronic thromboembolic pulmonary hypertension. Circulation 2006;113:2011-2020.

143. Sitbon O, Lascoux-Combe C, Delfraissy JF, Yeni PG, Raffi F, De ZD, Gressin V, Clerson P, Sereni D and Simonneau G. Prevalence of HIV-related pulmonary arterial hypertension in the current antiretroviral therapy era. Am J Respir Crit Care Med 2008;177:108-113.

144. Hoeper MM, Markevych I, Spiekerkoetter E, Welte T and Niedermeyer J. Goal-oriented treatment and combination therapy for pulmonary arterial hypertension. Eur Respir J 2005;26:858-863.

145. Henkens IR, Gan CT, van Wolferen SA, Hew M, Boonstra A, Twisk JW, Kamp O, van der Wall EE, Schalij MJ, Vonk Noordegraaf A and Vliegen HW. Electrocardiographic monitoring of treatment response in pulmonary arterial hypertension patients. Chest 2008;

146. Provencher S, Jais X, Yaici A, Sitbon O, Humbert M and Simonneau G. Clinical challenges in pulmonary hypertension: Roger S. Mitchell lecture. Chest 2005;128:622S-628S

II

Preoperative determinants of recovery time in adult Fallot patients after late pulmonary valve replacement

Ivo R. Henkens

Alexander van Straten

Mark G. Hazekamp

Martin J. Schalij

Albert de Roos

Ernst E. van der Wall

Hubert W. Vliegen

Int J Cardiol 2007;121:123-4

Introduction

Tetralogy of Fallot is the most common type of cyanotic heart disease. Surgical correction at an early age offers good long-term results [1]. Pulmonary valve disease and right ventricular outflow tract size determine right ventricular function, and prognosis [2]. Success of pulmonary valve replacement has led to a debate regarding its optimal timing [3-5]. Recovery time, defined as time between pulmonary valve replacement and return to work or school, should be an important part of this discussion.

Methods

Patients

Records of 23 consecutively operated adult Fallot patients (15 male) of normal intelligence, working or in school before pulmonary valve replacement, were reviewed, and patients were interviewed regarding their recovery time. Concomitant interventions were necessary in 9 patients: right ventricular infundibulum resection (1), tricuspid valve annuloplasty (5), and residual ventricular septal defect closure (3).

Methods

Evaluated preoperative parameters were: gender, age, presence of symptoms (New York Heart Association functional class ≥2, n=14), necessity for concomitant surgical intervention(s), QRS duration, and right ventricular volumes and function (assessed by magnetic resonance imaging). Also assessed were: age at total correction (range 0.4 – 11.9 years), history of palliative intervention (n=8) and use of a transannular patch (n=10), and time since total correction (range 15.4 – 40.2 years). Cardiac magnetic resonance (CMR) was performed as previously described [4]. Right ventricular end-diastolic and end-systolic volume, pulmonary regurgitation severity, right ventricular ejection fraction, and restrictive right ventricular function (defined as end-diastolic pulmonary forward flow) were evaluated. Data evaluation was performed with SPSS (bivariate correlation analysis, Mann–Whitney test, and linear regression analysis). A value of $P<0.05$ was considered statistically significant.

Results

All patients fully recovered. Median recovery time was 14.1 weeks (range 5 – 43 weeks). After 3 and 6 months 15 (65%) and 21 (91%) patients, respectively, had fully recovered. In one patient with a protracted recovery time elective balloon dilatation was necessary to relieve a residual right pulmonary artery stenosis. Recovery time was not associated with gender, presence of symptoms, need for concomitant surgery, history of palliative surgery, use of a transannular patch, or restrictive right ventricular function. QRS duration, right ventricular end-diastolic and end-systolic volume, right ventricular ejection fraction, and severity of pulmonary regurgitation were not associated with recovery time either. Recovery time was only associated with age at total correction (r=0.49, $P<0.05$), time between total correction and pulmonary valve replacement (r=0.58, $P<0.01$), and patient age at the time of pulmonary valve replacement (r=0.64, $P<0.01$). Multivariate regression analysis was not allowed due to substantial collinearity, rendering age at pulmonary valve replacement the best predictor for recovery time (Fig. 1).

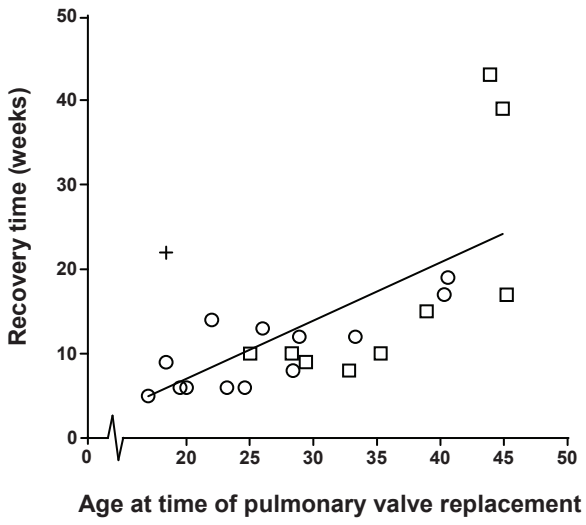

Figure 1
Recovery time after pulmonary valve replacement in patients according to New York Heart Association (NYHA) functional class. Open circles = NYHA class < II, open squares = NYHA class ≥ II (n=23, r=0.64, P<0.01), '+' = Patient with residual right pulmonary artery stenosis

Discussion

The fact that recovery time was not associated with presence of symptoms or decreased right ventricular function may come as a surprise. However, all patients were active in school or work, regardless of symptoms and, as reported before, right ventricular function improved in all patients [4]. Although it may be debated that comparing symptomatic and non-symptomatic patients is biased, correction for presence of symptoms did not change the age-effect. Given the excellent survival after pulmonary valve replacement, expected recovery time is the next most important parameter from a patient's point of view [6]. Since re-intervention indications were given careful consideration it was unexpected that two mildly symptomatic patients experienced a substantially protracted recovery time. Ideally, eligible patients would nowadays benefit from percutaneous valve implantation [7].

Conclusion

The majority of adult Fallot patients recover within reasonable time after pulmonary valve replacement. However, older adult Fallot patients should expect a more prolonged functional recovery time after pulmonary valve replacement, regardless of functional class or right ventricular function.

References

1. Daliento L, Mapelli D, Russo G, Scarso P, Limongi F, Iannizzi P, Melendugno A, Mazzotti E and Volpe B. Health related quality of life in adults with repaired tetralogy of Fallot: psychosocial and cognitive outcomes. *Heart* 2005;91:213-218.

2. Bouzas B, Kilner PJ and Gatzoulis MA. Pulmonary regurgitation: not a benign lesion. *Eur Heart J* 2005;26:433-439.

3. Therrien J, Provost Y, Merchant N, Williams W, Colman J and Webb G. Optimal timing for pulmonary valve replacement in adults after tetralogy of Fallot repair. *Am J Cardiol* 2005;95:779-782.

4. Vliegen HW, van Straten A, de Roos A, Roest AA, Schoof PH, Zwinderman AH, Ottenkamp J, van der Wall EE and Hazekamp MG. Magnetic resonance imaging to assess the hemodynamic effects of pulmonary valve replacement in adults late after repair of tetralogy of fallot. *Circulation* 2002;106:1703-1707.

5. Therrien J, Siu SC, McLaughlin PR, Liu PP, Williams WG and Webb GD. Pulmonary valve replacement in adults late after repair of tetralogy of fallot: are we operating too late? *J Am Coll Cardiol* 2000;36:1670-1675.

6. Yemets IM, Williams WG, Webb GD, Harrison DA, McLaughlin PR, Trusler GA, Coles JG, Rebeyka IM and Freedom RM. Pulmonary valve replacement late after repair of tetralogy of Fallot. *Ann Thorac Surg* 1997;64:526-530.

7. Khambadkone S, Coats L, Taylor A, Boudjemline Y, Derrick G, Tsang V, Cooper J, Muthurangu V, Hegde SR, Razavi RS, Pellerin D, Deanfield J and Bonhoeffer P. Percutaneous pulmonary valve implantation in humans: results in 59 consecutive patients. *Circulation* 2005;112:1189-1197.

III

Predicting outcome of pulmonary valve replacement in adult tetralogy of Fallot patients

Ivo R. Henkens

Alexander van Straten

Martin J. Schalij

Mark G. Hazekamp

Albert de Roos

Ernst E. van der Wall

Hubert W. Vliegen

Ann Thorac Surg 2007;83:907-11

Abstract

Background

Predicting changes in right ventricular (RV) size and function after pulmonary valve replacement (PVR) is important for timely reintervention in adult tetralogy of Fallot patients.

Methods

We analyzed the influence of pulmonary regurgitation severity and RV size and function before PVR on the outcome of RV size and function after PVR in 27 adult Fallot patients who had cardiac magnetic resonance imaging before and after PVR. RV dimensions were indexed for body surface area.

Results

Pulmonary regurgitation (48% ± 11% of RV stroke volume) was not related to RV dimensions and function before PVR. Moreover, severity of pulmonary regurgitation did not influence changes in RV dimensions after PVR. The indexed RV end-systolic volume before PVR (median, 98 $mL \cdot m^{-2}$; range, 52 - 235 $mL \cdot m^{-2}$) best predicted the indexed RV end-systolic volume after PVR (median, 59 $mL \cdot m^{-2}$; range, 24 - 132 $mL \cdot m^{-2}$, r=0.78, P<0.001) and the indexed RV end-diastolic volume after PVR (mean, 107 $mL \cdot m^{-2}$; range, 70 - 170 $mL \cdot m^{-2}$, r=0.73, P<0.001). Baseline RV ejection fraction corrected for valvular insufficiencies and shunting (21% ± 7%) best predicted the RV ejection fraction after PVR (43% ± 10%, r=0.77, P<0.001).

Conclusions

Timing of PVR should be based on indexed RV end-systolic volume and corrected RV ejection fraction rather than on severity of pulmonary regurgitation.

Introduction

Tetralogy of Fallot is a common form of cyanotic heart disease [1]. Correction in infancy offers good long-term results with minimal morbidity [2]. In most Fallot patients, however, residual pulmonary regurgitation, stenosis, or both, is present after total correction, the degree and duration of which determine size and function of the right ventricle (RV) [3-5]. Increased RV end-diastolic and end-systolic volumes are associated with diminished RV function and increased arrhythmia propensity [6, 7]. For patients with a dilated RV caused by significant pulmonary valve regurgitation, pulmonary valve replacement (PVR) has been proven to be beneficial with respect to reverse remodeling of the RV and a decrease in QRS duration [8, 9]. PVR is therefore the therapy of choice in patients with pulmonary regurgitation, a dilated RV, and risk factors for developing arrhythmias [10]. Although PVR is associated with low mortality, its intrinsic morbidity and the preferred use of non-mechanical valve substitutes in younger patients have led to an ongoing debate about the optimal timing of this intervention [11-17]. PVR is clearly indicated when patients become symptomatic or at risk for (fatal) arrhythmias [18]. Hence, PVR should preferably be performed before the right ventricle is dilated beyond a "point of no return," yet no sooner than necessary. Timing of PVR during this arbitrary time interval is therefore dependent both on patient features and the preference of the team of specialists involved. Because the shape of the RV cannot be described by a simple geometric model, adequate volumetric calculations of the RV have only become feasible in recent years with the advent of multiplanar magnetic resonance imaging [19]. Using Simpson's rule for analysis of serial tomographic slices acquired at the end of RV systole and diastole, RV volumes and function can be calculated reliably [20]. Considering the PVR-related reduction in RV volumes and improvement of ejection fraction, it would be of great interest to be able to predict the outcome of PVR for individual patients with respect to the degree of improvement in RV size and function [8, 13]. Despite overt evidence of benefit of PVR in groups of Fallot patients, lack of unequivocal data for individuals has led our group to analyze which cardiac magnetic resonance (CMR) imaging measurements of RV size and function best predict the degree of improvement in RV dimensions and function after PVR.

Methods

Patients

The CMR studies were part of a study protocol for preoperative and postoperative evaluation that had been previously approved by the Institutional Review Board. All data used were from patients who gave their informed consent.

Data on patients' surgical history are presented in Table 1. CMR imaging was available in 27 patients before and after PVR from a group of 31 consecutive adult Fallot patients who underwent operation. Total surgical correction of tetralogy of Fallot had been performed at a median age of 5.6 years (range, 1.3 - 13.2 years). At the time of the study, all patients had significant pulmonary regurgitation and a dilated right ventricle. All patients received an orthotopically implanted cryopreserved pulmonary homograft using normothermic or moderately hypothermic cardiopulmonary bypass. Residual RV outflow tract obstruction was relieved by resection of infundibular muscular tissue in two patients or augmentation with the implanted homograft itself in two other patients. An aneurysmatic RV outflow tract was corrected during the same operation in two patients. Other associated procedures were closure of a residual atrial defect in one patient and ventricular septal defects in three (one had been closed before), tricuspid valve repair in one, or annuloplasty or both in six others, if necessary. Residual pulmonary artery stenosis was relieved in one patient. All interventions were performed by a team of surgeons specialized in congenital heart disease. All patients were assessed for validity according to New York Heart Association (NYHA) class by the principal cardiologist both before and after PVR (within 1–4 weeks of the CMR studies) during outpatient visits. CMR studies were conducted at a median of 4.8 months (range, 0.7 - 15.4 months) before PVR. A similar CMR study was made for follow-up at a median of 7.3 months (range, 4.4 - 19.7 months).

Table 1: Patients' historical surgical data

n = 27, 17 (63%) male	n	%
History of palliative surgery	12	44.4
Use of RV patch	1	3.7
Use of transannular patch	13	48.1
APC patch only	6	22.2
No patch	7	25.9
Transatrial VSD closure	4	14.8
Transventricular VSD closure	21	77.8
VSD not closed	2	3.7

RV = right ventricle, APC = common pulmonary artery, VSD = ventricular septal defect

CMR Imaging

CMR imaging was performed as previously described [8]. In brief, these studies were performed on a 1.5 Tesla scanner (NT15 Gyroscan, Philips, Best, The Netherlands). Short-axis images of the heart were acquired with a multiphase, electrocardiogram-triggered, multi-shot echoplanar gradient echo technique during breath holds. We used a slice thickness of 10 mm and a 0.8 mm - 1.0 mm section gap. The flip angle was 30 degrees, and echo time was 5 to 10 ms. Between 18 and 25 frames per cycle resulted in a temporal resolution of 22 to 35 ms. Volumetric and functional RV measurements were derived from these studies, and differences between measurements over time were calculated. Variables were indexed for body surface area. Variables selected as end points of interest after PVR were indexed RV end-diastolic volume ($mL \cdot m^{-2}$), indexed RV end-systolic volume ($mL \cdot m^{-2}$), and RV ejection fraction (%). Also calculated was the so-called corrected RV ejection fraction (%), which corrects for pulmonary regurgitation, tricuspid regurgitation, and residual shunting (which equals net pulmonary forward flow/RV end-diastolic volume). Because surgery corrects such regurgitation and shunting, RV ejection fraction no longer needs correction after PVR. We tested the relationship between each of these variables before and after PVR. We also assessed the influence of severity of pulmonary regurgitation (as a percentage of RV stroke volume) on RV dimensions and function. We further evaluated consequences of postoperative pulmonary valve gradients (maximum and mean as seen with transthoracic echocardiography) as well as RV pressures (tricuspid regurgitation gradient estimated right atrial pressure).

Statistical Analysis

The SPSS 12.0.1 (SPSS Inc, Chicago, IL) software for Windows (Microsoft Inc, Redmond, WA) was used for data analysis. Assessment of the association between two continuous variables was performed with a correlation analysis. When two groups of patients were compared for differences in a factor described by a continuous variable, use was made of a two-tailed independent t-test or a Mann-Whitney test. Correlations are shown in parentheses. Values of $P<0.05$ were considered to be statistically significant. Baseline indexed RV end-systolic volume, baseline RV end-diastolic volume, baseline uncorrected RV ejection fraction, baseline corrected RV ejection fraction, and pulmonary regurgitation severity were entered in a multiple linear regression model, and a backward selection procedure (removed if $P>0.10$) was performed to determine the most significant predictor(s) of RV size and function after PVR. Additional logistic regression analysis was performed, incorporating the same baseline variables of pulmonary regurgitation and RV size and function, to construct a model for prediction of outcome below a cutoff value of RV end-systolic volume.

Results

CMR images were assessable for indexed RV end-diastolic volume, indexed RV end-systolic volume, and RV ejection fraction in all 27 patients. Measurements of corrected RV ejection fraction and pulmonary regurgitation severity were obtained in 26 patients because one CMR study showed artifacts. Mean patient age at the time of PVR was 30.8 ± 8.2 years. Median patient age at the time of palliation (n=12) was 2.0 years (range, 0.2 - 6.4 years), and mean patient age at the time of total correction was 5.6 ± 2.8 years. Pulmonary valve replacement had a clinically relevant result, reflected by mean patient NYHA class change from 2.0 ± 0.6 before PVR to 1.3 ± 0.3 after PVR (P<0.001).

Pulmonary Regurgitation

As summarized in Table 2, baseline pulmonary regurgitation as percentage of RV stroke volume (48% ± 11%) was not correlated with baseline indexed RV end-systolic volume (median, 98 mL·m^{-2}; range, 52 - 235 mL·m^{-2}), baseline indexed RV end-diastolic volume (median, 166 mL·m^{-2}; range, 113 - 290 mL·m^{-2}), or baseline RV ejection fraction (42% ± 11%). Moreover, pulmonary regurgitation severity was not related to the significant postoperative decrease in indexed RV end-diastolic volume (66 ± 30 mL·m^{-2}) or the decrease in indexed RV end-systolic volume (40 ± 26 mL·m^{-2}).

Right Ventricular Volumes

Indexed RV end-systolic volume and indexed RV end-diastolic volume were closely related before PVR (r=0.91, P<0.001). After PVR, indexed RV end-systolic volume (median, 59 mL·m^{-2}; range, 24 - 132 mL·m^{-2}) remained closely associated (r =0.77, P<0.001) with indexed RV end-diastolic volume (109 ± 26 mL·m^{-2}). Linear regression analysis defined baseline indexed RV end-systolic volume as the best predictor of both indexed RV end-systolic and indexed RV end-diastolic volume after PVR (Figure 1). Prediction of outcome of indexed RV end-systolic volume (mL·m^{-2}) was defined by 17.3 + [0.45·baseline indexed RV end-systolic

Table 2: Baseline RV size and function in relation to PR severity (n=26)

	PR as % of RV stroke volume	
Indexed RV end-systolic volume	r=0.14	P=0.50
Indexed RV end-diastolic volume	r=0.16	P=0.42
RV ejection fraction	r=-0.04	P=0.84

RV = right ventricular, PR = pulmonary regurgitation

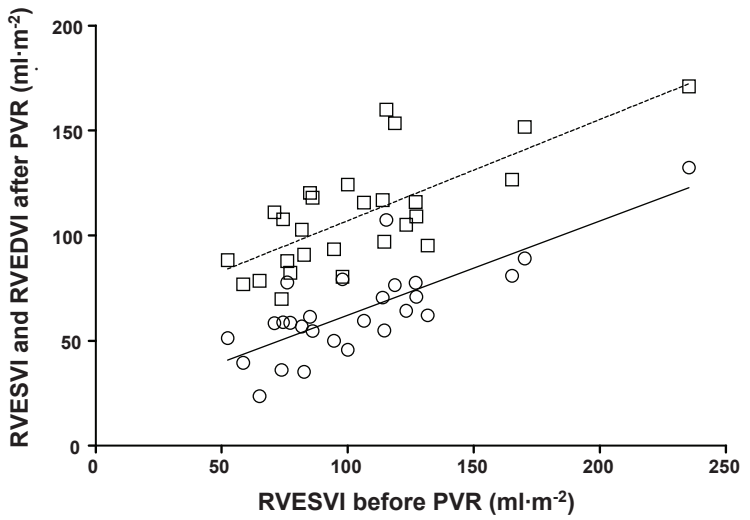

Figure 1
Baseline indexed right ventricular end-systolic volume (RVESVI) is an excellent predictor of indexed RV end-systolic volume and end-diastolic volume (RVEDVI) after pulmonary valve replacement (PVR). Open circles=postoperative RVESVI plotted against baseline RVESVI. Predicted postoperative RVESVI=17.3 + [0.45·baseline RVESVI] (n=27, r=0.78, P<0.001). Open squares=postoperative RVEDVI plotted against baseline RVESVI.
Predicted postoperative RVEDVI=58.8 + [0.49·baseline RVESVI] (n=27, r=0.73, P<0.001).

volume] (r=0.78, *P*<0.001). Prediction of outcome of indexed RV end-diastolic volume (mL·m^{-2}) was defined by 58.8 + [0.49·baseline indexed RV end-systolic volume] (r=0.73, *P*<0.001). An indexed RV end-systolic volume of less than 60 mL·m^{-2} was reached in 14 patients. Binary logistic regression analysis correctly identified patients who did or did not reach an indexed RV end-systolic volume of 60 mL·m^{-2} in 92.3% of cases with the following formula: predicted indexed RV end-systolic volume after PVR = -3.3 + [0.3·baseline indexed RV end-systolic volume] - [0.16·baseline indexed RV end-diastolic volume]. Patients with an outcome of indexed RV end-systolic volume of less than 60 mL·m^{-2} after PVR also had a lower mean indexed RV end-diastolic volume after PVR (97 ± 17 mL·m^{-2} versus 123 ± 29 mL·m^{-2}, *P*<0.01) and better mean RV ejection fraction after PVR (0.50 ± 0.07, versus 0.36 ± 0.06, *P*<0.001) than patients with an outcome of indexed RV end-systolic volume exceeding 60 mL·m^{-2} (n=13). Preoperative characteristics of patients with an indexed RV end-systolic volume after PVR above or below 60 mL·m^{-2} are summarized in Table 3.

Table 3: Baseline right ventricular volume and corrected right ventricular ejection fraction determine right ventricular end-systolic volume after pulmonary valve replacement

	RVESVI < 60 mL·m^{-2} (n=14)	RVESVI > 60 mL·m^{-2} (n=13)	
	Mean ± SD	Mean ± SD	*P*
RVESVI	81 ± 18	130 ± 41	0.001
RVEDVI	157 ± 24	196 ± 50	0.020
Corrected RVEF	25 ± 5	17 ± 7	0.002

RV = right ventricular, PVR = pulmonary valve replacement, RVESVI = indexed right ventricular end-systolic volume, RVEDVI = indexed right ventricular end-diastolic volume, RVEF = right ventricular ejection fraction

Right Ventricular Function Before and After Pulmonary Valve Replacement

RV ejection fraction did not change significantly after PVR, increasing from a 42% ± 10% to 43% ± 10% (P=0.30). The change from baseline mean corrected RV ejection fraction to uncorrected RV ejection fraction after PVR was considerable with 22% ± 6% (P<0.001). According to regression analysis, RV ejection fraction after PVR was best predicted by 21.6 + [1.02 · baseline corrected RV ejection fraction] (r = 0.77, P<0.001). Results are illustrated in Figure 2. After PVR, uncorrected RV ejection fraction was no longer different from corrected RV ejection fraction (0.43 ± 0.10 versus 0.42 ± 0.10, P=0.65).

Right Ventricular Pressure Load After Pulmonary Valve Replacement

Echocardiography was available in 26 patients within a median of 3 months (range, 0.3 - 8 months) after PVR. Tricuspid regurgitation in 23 patients was grade I or lower, and three patients had grade II residual tricuspid regurgitation. The median peak pulmonary valve gradient was 16.5 mmHg (range, 4.0 - 43.0 mmHg), and the median of the mean pulmonary valve gradient was 8.3 mmHg (range, 2.0 - 23.0 mmHg). The median peak RV pressure (tricuspid valve gradient + estimated right atrial pressure) was 35.0 mmHg (range, 23.0 - 78.5 mmHg). The calculated median pulmonary artery systolic pressure, which was calculated as [tricuspid valve gradient + estimated right atrial pressure] - mean pulmonary valve gradient, was 27.0 mmHg (range, 9.0 - 71.5 mmHg). One patient needed percutaneous balloon dilatation of a residual pulmonary artery stenosis. Pulmonary arterial hypertension developed in one patient a few weeks after PVR through recanalization of an old Potts shunt. This shunt was closed with a percutaneous intervention. An effect of higher pulmonary valve gradients or estimated pulmonary artery systolic pressures toward increased RV size or decreased RV function after PVR could not be found.

Left Ventricular Size and Function

Indexed left ventricular end-systolic volume did not change after PVR, from 40 ± 18 mL·m^{-2} to 39 ± 11 mL·m^{-2} (P=0.71). Similarly, indexed left ventricular end-diastolic volume remained unchanged, from 89 ± 31 mL·m^{-2} to 87 ± 18 mL·m^{-2} (P=0.76). Hence, left ventricular ejection fraction remained essentially unchanged after PVR, from 56% ± 12% to 55% ± 9% (P=0.87).

Discussion

Our results show that the right ventricle improved in dimensions and function after PVR in all 27 Fallot patients. Although our group previously reported a similar outcome, we were now able to demonstrate that changes in RV size and function after PVR are proportionate to baseline status [8]. It is important to realize that after PVR, patients may thus experience a large decrease in both RV end-diastolic and end-systolic volume as well as an increase in corrected RV ejection fraction, whereas absolute RV measurements of size and function may not normalize. Similar results have been reported by Therrien and colleagues [13] and Dave

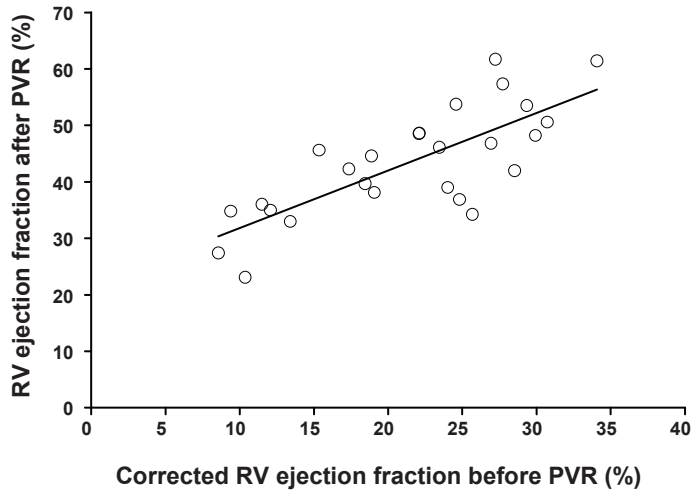

Figure 2

Baseline corrected right ventricular (RV) ejection fraction is the best predictor of RV ejection fraction after pulmonary valve replacement (PVR). Predicted RV ejection fraction after PVR=21.6 + [1.02·baseline corrected RV ejection fraction] (n=26, r=0.77, P<0.001).

and colleagues [17], suggesting that PVR should be performed before an indexed RV end-diastolic volume of 150 - 170 mL·m^{-2} is reached. Despite overt evidence of the importance of pulmonary regurgitation in adult Fallot patients, RV dimensions and function may vary greatly in patients with the same degree of pulmonary regurgitation [4]. And although pulmonary regurgitation is held responsible for RV dilatation and decrease of RV function over time, the absence of overt influence of pulmonary regurgitation severity on RV size or function before or after PVR strongly suggests that pulmonary regurgitation severity should not be the variable of primary consideration in deciding when to perform pulmonary valve replacement in adult Fallot patients [5, 10]. Rather, when pulmonary regurgitation is present, we should focus on variables of RV size and function that indicate how the individual's RV is coping with the burden of pulmonary regurgitation, and at the same time predict change in RV size and function if PVR were performed. Our results suggest that RV end-systolic volume and corrected RV ejection fraction are the most important measurements of RV size and function to assess. Baseline corrected RV ejection fraction had the closest relation with RV ejection fraction after PVR in our group. This can be explained by the fact that pulmonary regurgitation, tricuspid regurgitation, and shunting over a residual ventricular septal defect may all lead to a compensatory increase in RV stroke volume to maintain net pulmonary forward flow with each heartbeat. Hence, without correction for regurgitation and shunting, RV ejection fraction overestimates true RV performance. To evaluate the true RV performance and possible benefit of PVR for the patient, it has therefore been suggested that the corrected RV ejection fraction should be used in the preoperative situation [8]. Several reports have addressed changes in RV volumes after PVR, rendering different cut-off values for indexed RV end-systolic and end-diastolic volumes [13, 14, 17]. Indexed RV end-systolic volume is probably the most important preoperative measure of RV dimensions and function because it incorporates both RV volume overload and systolic function, variables strongly related to clinical status [5]. Five patients in our study returned to an indexed RV end-systolic volume within normal limits [21]. Ideally, lifelong optimal management of a Fallot patient would prevent important RV dilatation while preserving RV systolic function. That such management still requires repeated surgical intervention implies that the pursuit of optimal RV hemodynamics may not be successful in most patients [22]. Perhaps it is therefore more realistic to strive towards a near-normal RV size and function in adult Fallot patients that have not had the benefit of current surgical techniques and medical management. In our group, little over half of patients reached an indexed RV end-systolic volume of less than 60 mL·m^{-2}, which was associated with a better RV ejection fraction and a lower indexed RV end-diastolic volume. Preoperative cut-off values likely to result in a favorable outcome are therefore an

indexed RV end-systolic volume of 100 mL·m^{-2} and a corrected RV ejection fraction that exceeds 20%. The strong relation between indexed RV end-diastolic volume and indexed RV end-systolic volume, both before and after PVR, likely reflects ventricular adaptation in response to increased wall stress and volume loading. RV fibrosis might explain why in some patients RV dimensions regressed less, and RV ejection fraction remained impaired [23]. Although changes in surgical practice and techniques now allow for total correction much earlier in life, mostly with a transatrial approach, and with less need for prior palliation, we believe that our cohort of patients still represents an important part of adult Fallot patients who require long term management, and probably repeat PVR in time to come.

Conclusion

In patients with important pulmonary regurgitation, timing of pulmonary valve replacement should be based on indexed right ventricular end-systolic volume and corrected right ventricular ejection fraction rather than on severity of pulmonary regurgitation.

References

1. Gatzoulis MA. Diagnosis and management of adult congenital heart disease. London: Elsevier Limited, 2003.

2. Daliento L, Mapelli D, Russo G, Scarso P, Limongi F, Iannizzi P, Melendugno A, Mazzotti E and Volpe B. Health related quality of life in adults with repaired tetralogy of Fallot: psychosocial and cognitive outcomes. Heart 2005;91:213-218.

3. Silversides CK, Veldtman GR, Crossin J, Merchant N, Webb GD, McCrindle BW, Siu SC and Therrien J. Pressure half-time predicts hemodynamically significant pulmonary regurgitation in adult patients with repaired tetralogy of fallot. J Am Soc Echocardiogr 2003;16:1057-1062.

4. Frigiola A, Redington AN, Cullen S and Vogel M. Pulmonary regurgitation is an important determinant of right ventricular contractile dysfunction in patients with surgically repaired tetralogy of Fallot. Circulation 2004;110:II153-II157.

5. Geva T, Sandweiss BM, Gauvreau K, Lock JE and Powell AJ. Factors associated with impaired clinical status in long-term survivors of tetralogy of Fallot repair evaluated by magnetic resonance imaging. J Am Coll Cardiol 2004;43:1068-1074.

6. Carvalho JS, Shinebourne EA, Busst C, Rigby ML and Redington AN. Exercise capacity after complete repair of tetralogy of Fallot: deleterious effects of residual pulmonary regurgitation. Br Heart J 1992;67:470-473.

7. Gatzoulis MA, Balaji S, Webber SA, Siu SC, Hokanson JS, Poile C, Rosenthal M, Nakazawa M, Moller JH, Gillette PC, Webb GD and Redington AN. Risk factors for arrhythmia and sudden cardiac death late after repair of tetralogy of Fallot: a multicentre study. Lancet 2000;356:975-981.

8. Vliegen HW, van Straten A, de Roos A, Roest AA, Schoof PH, Zwinderman AH, Ottenkamp J, van der Wall EE and Hazekamp MG. Magnetic resonance imaging to assess the hemodynamic effects of pulmonary valve replacement in adults late after repair of tetralogy of fallot. Circulation 2002;106:1703-1707.

9. van Huysduynen BH, van Straten A, Swenne CA, Maan AC, van Eck HJ, Schalij MJ, van der Wall EE, de Roos A, Hazekamp MG and Vliegen HW. Reduction of QRS duration after pulmonary valve replacement in adult Fallot patients is related to reduction of right ventricular volume. Eur Heart J 2005;26:928-932.

10. Bouzas B, Kilner PJ and Gatzoulis MA. Pulmonary regurgitation: not a benign lesion. Eur Heart J 2005;26:433-439.

11. Yemets IM, Williams WG, Webb GD, Harrison DA, McLaughlin PR, Trusler GA, Coles JG, Rebeyka IM and Freedom RM. Pulmonary valve replacement late after repair of tetralogy of Fallot. Ann Thorac Surg 1997;64:526-530.

12. Hazekamp MG, Kurvers MM, Schoof PH, Vliegen HW, Mulder BM, Roest AA, Ottenkamp J and Dion RA. Pulmonary valve insertion late after repair of Fallot's tetralogy. Eur J Cardiothorac Surg 2001;19:667-670.

13. Therrien J, Provost Y, Merchant N, Williams W, Colman J and Webb G. Optimal timing for pulmonary valve replacement in adults after tetralogy of Fallot repair. Am J Cardiol 2005;95:779-782.

14. Therrien J, Siu SC, McLaughlin PR, Liu PP, Williams WG and Webb GD. Pulmonary valve replacement in adults late after repair of tetralogy of fallot: are we operating too late? J Am Coll Cardiol 2000;36:1670-1675.

15. Lim C, Lee JY, Kim WH, Kim SC, Song JY, Kim SJ, Choh JH and Kim CW. Early replacement of pulmonary valve after repair of tetralogy: is it really beneficial? Eur J Cardiothorac Surg 2004;25:728-734.

16. Davlouros PA, Karatza AA, Gatzoulis MA and Shore DF. Timing and type of surgery for severe pulmonary regurgitation after repair of tetralogy of Fallot. Int J Cardiol 2004;97 Suppl 1:91-101.

17. Dave HH, Buechel ER, Dodge-Khatami A, Kadner A, Rousson V, Bauersfeld U and Pretre R. Early insertion of a pulmonary valve for chronic regurgitation helps restoration of ventricular dimensions. Ann Thorac Surg 2005;80:1615-1620.

18. Therrien J, Siu SC, Harris L, Dore A, Niwa K, Janousek J, Williams WG, Webb G and Gatzoulis MA. Impact of pulmonary valve replacement on arrhythmia propensity late after repair of tetralogy of Fallot. Circulation 2001;103:2489-2494.

19. van Straten A, Vliegen HW, Hazekamp MG, Bax JJ, Schoof PH, Ottenkamp J, van der Wall EE and de Roos A. Right ventricular function after pulmonary valve replacement in patients with tetralogy of Fallot. Radiology 2004;233:824-829.

20. Jauhiainen T, Jarvinen VM, Hekali PE, Poutanen VP, Penttila A and Kupari M. MR gradient echo volumetric analysis of human cardiac casts: focus on the right ventricle. J Comput Assist Tomogr 1998;22:899-903.

21. Alfakih K, Plein S, Thiele H, Jones T, Ridgway JP and Sivananthan MU. Normal human left and right ventricular dimensions for MRI as assessed by turbo gradient echo and steady-state free precession imaging sequences. J Magn Reson Imaging 2003;17:323-329.

22. Oosterhof T, Meijboom FJ, Vliegen HW, Hazekamp MG, Zwinderman AH, Bouma BJ, van Dijk AP and Mulder BJ. Long-term follow-up of homograft function after pulmonary valve replacement in patients with tetralogy of Fallot. Eur Heart J 2006;27:1478-1484.

23. Babu-Narayan SV, Kilner PJ, Li W, Moon JC, Goktekin O, Davlouros PA, Khan M, Ho SY, Pennell DJ and Gatzoulis MA. Ventricular fibrosis suggested by cardiovascular magnetic resonance in adults with repaired tetralogy of fallot and its relationship to adverse markers of clinical outcome. Circulation 2006;113:405-413.

IV

Pulmonary valve replacement improves the repolarization in tetralogy of Fallot

Bart Hooft van Huysduynen

Ivo R. Henkens

Cees A. Swenne

Martin J. Schalij

Ernst E. van der Wall

Hubert W. Vliegen

Int J Cardiol 2008;124:301-6

Abstract

Background

Pulmonary valve regurgitation may cause right ventricular failure in adult patients with Fallot's tetralogy. In these patients, prolonged depolarization and disturbed repolarization are associated with ventricular arrhythmias and sudden cardiac death. We aimed to assess the effect of pulmonary valve replacement (PVR) on the repolarization of patients with tetralogy of Fallot.

Methods

Thirty Fallot patients (age 32 ± 9 years, 19 male) eligible for PVR were studied with cardiac magnetic resonance imaging (CMR) before and 6 months after PVR. Electrocardiograms obtained during initial and follow-up CMR were analyzed and occurrence of ventricular arrhythmias was studied.

Results

Right ventricular end-diastolic volume (RVEDV) decreased from 322 ± 87 mL to 215 ± 57 mL after PVR (P<0.001). The spatial QRS-T angle normalized from 117 ± 34° to 100 ± 35°, P<0.001 (normal angle <105°). QT dispersion and T-wave complexity did not change significantly. T-wave amplitude decreased from 376 ± 121 μV to 329 ± 100 μV (P=0.01). T-wave area decreased from 43 ± 15 μV·s to 38 ± 13 μV·s (P=0.02). Decreases in T-wave amplitude and area were most prominent in the right precordial leads overlying the RV. Three patients had sustained ventricular arrhythmias and one patient died suddenly. These patients had a QRS duration >160 ms. No severe ventricular arrhythmias were found in patients with a RVEDV <220 mL, QRS-T angle <100°, QT dispersion <60 ms or T-wave complexity <0.30.

Conclusion

Normal repolarization indices may be associated with the absence of severe ventricular arrhythmias. PVR in Fallot patients with dilated right ventricles has a beneficial effect on electrocardiographic indices of repolarization heterogeneity.

Introduction

The prognosis of patients with a tetralogy of Fallot has improved dramatically after the introduction of complete surgical repair at young age. However, in adult Fallot patients, residual pulmonary regurgitation may cause right ventricular failure [1, 2]. These patients are prone to develop ventricular arrhythmias and/or sudden cardiac death. This risk increases significantly when QRS duration is larger than 180 ms [3]. In addition to prolonged depolarization, disturbed repolarization may play a role in arrhythmogenesis. Repolarization disturbances are widely recognized as contributors to arrhythmias [4, 5]. QT dispersion has been shown to refine risk stratification for arrhythmias in Fallot patients [6], and several other electrocardiographic indices have been suggested to assess various characteristics of the repolarization. The spatial angle between the QRS and T axes is an electrocardiographic index that comprises both depolarization and repolarization and has prognostic value in normal subjects and selected patient groups [7-9]. T-wave complexity is related to repolarization heterogeneity, which is a pro-arrhythmogenic factor [10]. T-wave amplitude and T-wave area are also measures of repolarization heterogeneity [11, 12]. We have previously demonstrated that pulmonary valve replacement (PVR) reduces QRS duration and right ventricular end-diastolic volume [13]. In the present study we tested whether PVR has beneficial effects on the repolarization and whether electrocardiographic indices of the repolarization are related to ventricular arrhythmias.

Methods

Patients

Thirty Fallot patients (19 male/11 female) were evaluated. The age of the patients at the initial surgical procedure was 5.7 ± 3.1 years. In 15 patients a transannular patch had been applied during the initial procedure. Age at PVR was 31.8 ± 9.1 years. Indications for PVR were moderate to severe pulmonary regurgitation in combination with right ventricular dilatation. In addition to PVR, tricuspid regurgitation was corrected in 6 patients and residual ventricular septal defects were closed in 4 patients.

Cardiac Magnetic Resonance imaging

CMR was performed on a 1.5 Tesla scanner (NT15 Gyroscan, Philips, Best). Briefly, short axis images of the heart were acquired with a multiphase, ECG-triggered, multishot echoplanar gradient echo technique. Images were acquired during breath holds with a slice thickness of

10 mm and a 0.8 to 1.0 section gap. The flip angle was 30° and echo time was 5 to 10 ms. Eighteen to 25 frames/cycle resulted in a temporal resolution of 22 to 35 ms [14].

ECG analysis

ECGs were obtained before the initial CMR and during the follow-up procedure 6 months after surgery. The routinely made 10-s ECGs, digitally stored (sampling rate 500 Hz, resolution 5 μV/bit) in our hospital ECG database, were imported into LEADS, a MATLAB (The Math Works, Natick, USA) computer program that was developed for research oriented ECG analysis [15]. The ECGs were randomly renamed to assure blinded analysis. After QRS detection and fiducial point determination, the QRS-T complexes in the 10-s ECG were averaged in order to minimize noise. Besides the standard 12-lead ECG representation of the averaged beat, a vectorcardiographic X–Y–Z representation and the magnitude of the heart vector were computed using the inverse Dower matrix [16]. Onset and end of QRS were computed in the vector magnitude signal by a threshold procedure and by determining the minimal vector size in between the QRS complex and the T-wave, respectively. The default end-of-QRS instant was then manually adjusted to meet the Minnesota criteria [17] for end-of-QRS determination (being the last J point in any of the ECG leads, while in leads with two candidate J points the earliest J point is taken). End-of-T instant was set automatically in every lead at the intercept of the steepest tangent to the terminal limb of the T-wave with the baseline. QT dispersion was calculated as the longest minus the shortest QT interval in any lead. The spatial angle between the mean electrical axes of the QRS complex and the T-wave was computed from the vectorcardiogram [18]. T-wave complexity was derived by means of singular value decomposition of the 8 independent ECG leads I, II and V1–V6 [10, 19]. T-wave complexity was calculated by dividing the square root of the summed squared singular values 2–8 by the first singular value. Finally, the absolute T-wave amplitude and T-wave area were computed and averaged from the ECG leads.

Ventricular arrhythmias

The occurrence of ventricular arrhythmias and the relation to ECG and CMR measurements were studied. Sustained ventricular tachycardias (lasting >30 s or causing symptoms) and sudden cardiac death were categorized as severe ventricular arrhythmias. Postoperative data were used for this analysis, except in one patient that suffered from arrhythmias before PVR only, from whom the preoperative measurements were used.

Statistical analysis

All data are reported as mean ± standard deviation. Two-sided paired and unpaired Student's t-tests were used wherever appropriate. To correct for multiple testing, the significance level of the *P*-values was determined according to the false discovery rate method [20].

Results

Changes in right ventricular volume and QRS duration

Surgery had a positive effect on the right ventricular end-diastolic volume (RVEDV) which decreased from 322 ± 87 mL before surgery to 215 ± 57 mL after surgery ($P<0.001$). QRS duration decreased from 158 ± 34 ms to 153 ± 32 ms ($P<0.01$).

Changes in repolarization

The spatial angle between QRS and T axes decreased significantly from a preoperative value of 117 ± 34° to 100 ± 35° postoperatively ($P<0.001$). QT dispersion did not change significantly, with a preoperative value of 78 ± 27 ms and a postoperative value of 85 ± 30 ms ($P=0.19$). Pre- and postoperative values of T-wave complexity were 0.49 ± 0.22 and 0.44 ± 0.21, respectively ($P=0.16$). T-wave amplitude decreased significantly from 376 ± 121 μV to 329 ± 100 μV ($P=0.01$). T-wave area decreased significantly from 43 ± 15 μV·s to 38 ± 13 μV·s ($P=0.02$). These results and the cut-off values for significance

Table 1. Values of right ventricular end-diastolic volumes, QRS duration, and electrocardiographic repolarization indices, measured before and after pulmonary valve replacement

n=30	pre-PVR	post-PVR	*P*	significant cut-off value
RVEDV (mL)	322±87	215±57	<0.0001*	<0.007
QRS duration (ms)	158±34	153±32	0.002*	<0.021
QRS-T angle (º)	117±34	100±35	0.0004*	<0.014
QT dispersion (ms)	78±27	85±30	0.19	<0.05
T-wave complexity	0.49±0.22	0.44±0.21	0.16	<0.04
T-wave amplitude (μV)	376±121	329±100	0.01*	<0.029
T-wave area (μV·s)	43±15	38±13	0.02*	<0.036

*PVR = pulmonary valve replacement, RVEDV = right ventricular end-diastolic volume, *Significant P-values after false discovery rate correction, i.e. below the cut-off values provided in the last column*

according to the false discovery rate method [20] are summarized in Table 1. Changes in T-wave amplitude and area for all 12 leads are shown in Fig. 1. Note that changes are most pronounced in the leads overlying the right ventricle.

Relations between right ventricular volume and QRS duration

The average of the pre- and postoperative QRS duration related linearly to the average RVEDV (r=0.58, $P<0.01$). Changes in QRS duration correlated with changes in RVEDV (r=0.45, $P=0.03$).

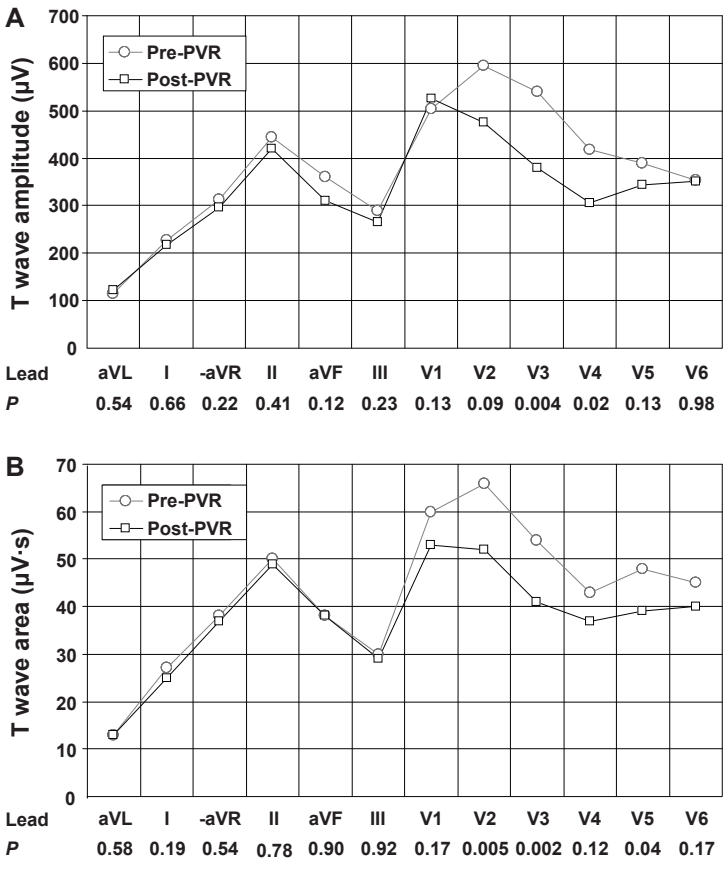

Figure 1

A. T-wave amplitude pre-PVR and post-PVR for all leads. Right precordial leads show the largest changes in T-wave amplitude.

B. T-wave area pre-PVR and post-PVR for all leads. The changes in T-wave area were most significant in leads V2 and V3, leads overlying the right ventricle.

Relations between QRS duration and repolarization indices

Average QRS durations correlated with the spatial angle (r=0.70, *P*<0.001), QT dispersion (r=0.62, *P*<0.001), T-wave complexity (r=0.52, *P*<0.01) and T-wave area (r=0.43, *P*=0.02).

Ventricular arrhythmias

Follow-up was available up to 5.5 ± 1.9 years after PVR. Three patients had sustained ventricular tachycardias and one patient died suddenly. This patient died 18 months post-PVR. The cause of death was uncertain, but the patient was hemodynamically stable and had no co-morbidity, making arrhythmia the most probable cause of death. Two of the patients had pre- as well as postoperative ventricular tachycardias and (pre)syncope, for which automatic internal cardiac defibrillators were implanted postoperatively. The last patient had preoperative repetitive sustained ventricular tachycardias, requiring cardioversion and hospitalization. After PVR this patient remained free of serious arrhythmias. All patients with severe ventricular arrhythmias had a QRS duration >160 ms. Among the 26 patients without severe ventricular tachycardias, 10 patients also had a postoperative QRS duration >160 ms. The group size was too small to analyze whether the combination of QRS duration and a repolarization measure or RVEDV could improve the specificity. However, no severe arrhythmias were found in patients with QRS-T angle <100°, QT dispersion <60 ms, T-wave complexity <0.30 or a RVEDV <220 mL.

Discussion

In this study we assessed the effects of pulmonary valve replacement in Fallot patients with dilated right ventricles on electrocardiographic indices of repolarization heterogeneity. We found that PVR alters the repolarization process. PVR results in normalization of the spatial QRS-T angle and reduction of T-wave amplitude and area. Furthermore, we analyzed the occurrence of ventricular arrhythmias in these patients. Although the findings are limited by the small number of patients with arrhythmias, the optimal discriminator of patients with severe arrhythmias was a QRS duration >160 ms. No severe arrhythmias were found in patients with RVEDV <220 mL, QRS-T angle <100°, QT dispersion <60 ms or T-wave complexity <0.30.

In previous studies in Fallot patients late after initial surgical correction, repolarization heterogeneity was implicated as a potential mechanism for arrhythmias [6, 21, 22]. In the current study, we used a dedicated computer program to enhance the reproducibility and accuracy of ECG analysis. This allowed concomitant calculation of electrocardiographic repolarization indices like the QRS-T angle, T-wave complexity, T-wave amplitude and T-wave area.

Spatial QRS-T angle

The spatial QRS-T angle comprises properties of both depolarization and repolarization and has prognostic capabilities. Kardys et al. showed that a wide QRS-T angle predicted cardiac death in a general population of more than 6000 men and women older than 55 years [7]. After adjustment for cardiovascular risk factors, hazard ratios of abnormal QRS-T angles for sudden death were 4.6 (CI 2.5 – 8.5). Zabel et al. showed that the QRS-T angle contributed to the risk stratification of patients after myocardial infarction, independent of classical risk factors [8]. Other studies underscored the prognostic value of the spatial QRS-T angle and the orientation of the T axis [9, 23, 24]. The large QRS-T spatial angle in our study is related to the right bundle branch block present in most Fallot patients. Subsequently, their right ventricles are mostly activated by the relatively slow myocardial cell-to-cell conduction instead of the specialized conduction system. Consequently, the order of repolarization is no longer predominated by primary factors (differences in action potential duration); instead, secondary factors (the depolarization order resulting from slow cell-to-cell conduction) predominate the repolarization order. The resultant similar order of de- and repolarization in combination with the opposed direction of the de- and repolarizing currents cause large differences in the orientation of the QRS and T vectors, i.e., a wide QRS-T angle. An increased QRS-T angle may also be caused by a disturbance in the distribution of myocardial action potential durations. Previous studies showed that increased wall stress and hypertrophy have a direct influence on action potential duration [25, 26]. In dogs, volume overload leading to eccentric hypertrophy caused interventricular differences in action potential durations and an increased sensitivity to arrhythmogenic medication [26]. Normal values for the QRS-T angle were defined as being smaller than 105° [7, 27]. The QRS-T angle in our Fallot patients decreased from 117 ± 34° to 100 ± 35°, denoting a transition from a value outside the normal range to a smaller value within the normal range after PVR. We observed no severe arrhythmias in patients with a QRS-T angle <100°.

QT dispersion

Previously, Gatzoulis et al. used QT dispersion to refine risk stratification of Fallot patients with a wide QRS complex [6]. All patients with clinically relevant arrhythmias appeared to have a QRS duration of more than 180 ms and a QT dispersion of more than 60 ms. In our patient group the combination of QRS duration and QT dispersion could not be assessed as only four patients had severe arrhythmias. However, we found no ventricular tachycardias in patients with QT dispersion <60 ms. Furthermore, our group of Fallot patients with large RVs had relatively high pre- and postoperative QT dispersion values. Surprisingly, we found

no change in QT dispersion after PVR, despite the relatively large right ventricular volume reduction in most patients. This finding is in agreement with the study of Helbing et al. [28], who did not find a correlation between right ventricular volume and QT dispersion in a group of Fallot patients and normal subjects. Initially, QT dispersion was proposed as a measure of local repolarization differences [29]. However, QT dispersion is strongly dependent on the orientation of the T vector, which represents the summed electromotive forces [30]. The QT interval is shortest in the ECG lead that is perpendicular to the orientation of the last part of the T vector. This shortest QT interval has a large influence on the magnitude of the QT dispersion, calculated as the longest minus the shortest QT interval in any lead. Thus, QT dispersion depends on projections of the global T vector on the different lead vectors and does not necessarily represent local repolarization differences [30].

T-wave complexity

T-wave complexity has been shown to yield independent prognostic information in patients with cardiovascular disease [31]. In patients with arrhythmogenic right ventricular dysplasia, higher T-wave complexity is associated with ventricular arrhythmias [32]. Additionally, T-wave complexity is increased in patients with primary repolarization disturbances and can be used to discriminate these patients from healthy individuals [10]. We calculated T-wave complexity by means of singular value decomposition, which is an algebraic algorithm used to characterize the T-waves of the eight independent ECG leads I, II and V1–V6. If the eight T-waves can be described by only the first few singular values, these T-waves are relatively simple as they can be composed from a limited set of basic patterns. The more singular values are needed to accurately describe the T-waves, the more complex the T-waves. We observed a non-significant reduction in T-wave complexity in our relatively small study, which can be interpreted as a trend in the direction of a more normal repolarization. Additionally, patients with a T-wave complexity <0.30 had no severe arrhythmias.

T-wave amplitude and area

T-wave amplitude and area were related to repolarization heterogeneity in previous studies. In rabbit hearts, T-wave area was strongly correlated to repolarization heterogeneity as measured by 7 monophasic action potential electrodes [33]. T-wave amplitude and area were also related to repolarization heterogeneity, measured as the difference in repolarization time between the left and right ventricle in canine hearts [12]. Experiments in preparations of the left ventricular wall mimicked Long QT-1 syndrome and increased repolarization heterogeneity, which was reflected by an increased T-wave amplitude and area [34]. Mathematical simulation studies

confirmed these experimental findings [11, 35]. In our Fallot patients we measured a decrease in T-wave amplitude and T-wave area after PVR, suggesting decreased repolarization heterogeneity. The changes in T-wave area and amplitude were more explicit in leads V2 and V3 than in the other ECG leads (Fig. 1). Leads V2 and V3 may display more electrical activity from the right ventricle than the other standard ECG leads due to their proximity to the right ventricle [36, 37], underscoring that the observed changes in T-wave amplitude and area were indeed related to changes in the right ventricle. The observed changes in T-wave amplitude and T-wave area suggest decreased repolarization heterogeneity in the right ventricle due to PVR.

Arrhythmias

The patients with severe arrhythmias had a QRS duration longer than 160 ms. Gatzoulis et al. found that every Fallot patient with symptomatic ventricular arrhythmias had a QRS duration longer than 180 ms [3]. Our study suggests that this criterion should be lowered to ascertain identification of patients with ventricular arrhythmias. The patient who died suddenly had a QRS duration of 164 ms. Our study was too small to combine electrocardiographic indices of the repolarization with the QRS duration to improve specificity. However, patients with either a QRS-T angle lower than 100°, a QT dispersion lower than 60 ms, a T-wave complexity lower than 0.30 or a RVEDV lower than 220 mL had no severe arrhythmias.

Limitations

The number of patients with arrhythmias is obviously too small to draw solid conclusions regarding the predictive value of arrhythmias. However, the observed association between normal repolarization indices and the absence of severe ventricular arrhythmias in this relatively small group has a physiological basis. Repolarization heterogeneity may form the substrate for ventricular arrhythmias: as irregular repolarization sequences facilitate the formation of functional barriers, an adversely timed extra stimulus may initiate a re-entry arrhythmia [5]. Furthermore, most electrocardiographic repolarization indices are related to the QRS duration, which in turn is related to RVEDV. This interdependency can be seen as a limitation towards the additional value of repolarization analysis. However, mechanical factors, depolarization and repolarization may all play a role in the process of arrhythmogenesis. A previous study in Fallot patients after total surgical correction registered body surface maps that showed a high similarity between de- and repolarization patterns [38]. Repolarization differences influenced by a smoothly progressing depolarization wave front do not necessarily increase the susceptibility to arrhythmias. However, in volume overloaded

ventricles, fibrosis and mechanically induced changes in conduction velocity may cause patchy, irregular repolarization sequences.

Conclusions

Normal repolarization indices may be associated with the absence of severe ventricular arrhythmias. Pulmonary valve replacement in Fallot patients with dilated right ventricles has a beneficial effect on electrocardiographic indices of repolarization heterogeneity.

References

1. Carvalho JS, Shinebourne EA, Busst C, Rigby ML and Redington AN. Exercise capacity after complete repair of tetralogy of Fallot: deleterious effects of residual pulmonary regurgitation. Br Heart J 1992;67:470-473.

2. Gatzoulis MA, Balaji S, Webber SA, Siu SC, Hokanson JS, Poile C, Rosenthal M, Nakazawa M, Moller JH, Gillette PC, Webb GD and Redington AN. Risk factors for arrhythmia and sudden cardiac death late after repair of tetralogy of Fallot: a multicentre study. Lancet 2000;356:975-981.

3. Gatzoulis MA, Till JA, Somerville J and Redington AN. Mechanoelectrical interaction in tetralogy of Fallot. QRS prolongation relates to right ventricular size and predicts malignant ventricular arrhythmias and sudden death. Circulation 1995;92:231-237.

4. Han J and Moe GK. Nonuniform recovery of excitability in ventricular muscle. Circ Res 1964;14:44-60.

5. Kuo CS, Munakata K, Reddy CP and Surawicz B. Characteristics and possible mechanism of ventricular arrhythmia dependent on the dispersion of action potential durations. Circulation 1983;67:1356-1367.

6. Gatzoulis MA, Till JA and Redington AN. Depolarization-repolarization inhomogeneity after repair of tetralogy of Fallot. The substrate for malignant ventricular tachycardia? Circulation 1997;95:401-404.

7. Kardys I, Kors JA, van der Meer I, Hofman A, van der Kuip DA and Witteman JC. Spatial QRS-T angle predicts cardiac death in a general population. Eur Heart J 2003;24:1357-1364.

8. Zabel M, Acar B, Klingenheben T, Franz MR, Hohnloser SH and Malik M. Analysis of 12-lead T-wave morphology for risk stratification after myocardial infarction. Circulation 2000;102:1252-1257.

9. de Torbal A, Kors JA, van Herpen G, Meij S, Nelwan S, Simoons ML and Boersma E. The electrical T-axis and the spatial QRS-T angle are independent predictors of long-term mortality in patients admitted with acute ischemic chest pain. Cardiology 2004;101:199-207.

10. Priori SG, Mortara DW, Napolitano C, Diehl L, Paganini V, Cantu F, Cantu G and Schwartz PJ. Evaluation of the spatial aspects of T-wave complexity in the long-QT syndrome. Circulation 1997;96:3006-3012.

11. van Huysduynen BH, Swenne CA, Draisma HH, Antoni ML, Van de Vooren H, van der Wall EE and Schalij MJ. Validation of ECG indices of ventricular repolarization heterogeneity: a computer simulation study. J Cardiovasc Electrophysiol 2005;16:1097-1103.

12. van Opstal JM, Verduyn SC, Winckels SK, Leerssen HM, Leunissen JD, Wellens HJ and Vos MA. The JT-area indicates dispersion of repolarization in dogs with atrioventricular block. J Interv Card Electrophysiol 2002;6:113-120.

13. van Huysduynen BH, van Straten A, Swenne CA, Maan AC, van Eck HJ, Schalij MJ, van der Wall EE, de Roos A, Hazekamp MG and Vliegen HW. Reduction of QRS duration after pulmonary valve replacement in adult Fallot patients is related to reduction of right ventricular volume. Eur Heart J 2005;26:928-932.

14. Vliegen HW, van Straten A, de Roos A, Roest AA, Schoof PH, Zwinderman AH, Ottenkamp J, van der Wall EE and Hazekamp MG. Magnetic resonance imaging to assess the hemodynamic effects of pulmonary valve replacement in adults late after repair of tetralogy of fallot. Circulation 2002;106:1703-1707.

15. Draisma HH, Swenne CA and Van de Vooren H. LEADS: an interactive research oriented ECG/VCG analysis system. Computers in Cardiology 2005;32:515-518.

16. Edenbrandt L and Pahlm O. Vectorcardiogram synthesized from a 12-lead ECG: superiority of the inverse Dower matrix. J Electrocardiol 1988;21:361-367.

17. Prineas RJ, Crow RS and Blacburn RS. The Minnesota code manual of electrocardiographic findings: standards and procedures for measurement and classification. In: Intraventricular conduction defects, Boston, MA: Wright, 1982, p. 111-130.

18. Mirvis DM and Goldberger AL. Electrocardiography. In: Braunwald's Heart Disease, edited by Zipes DP, Libby P, Bonow RO and Braunwald E. Philadelphia, PA: Saunders, 2004, p. 120-125.

19. Lay DC. Linear algebra and its applications. In: Symmetric matrices and quadratic forms, edited by Lay DC. Reading, MA: Addison-Wesley, 2003, p. 441-486.

20. Benjamini Y and Hochberg Y. Controlling the false discovery rate - a practical and powerful approach to multiple testing. J R Stat Soc Ser 1995;289-300.

21. Berul CI, Hill SL, Geggel RL, Hijazi ZM, Marx GR, Rhodes J, Walsh KA and Fulton DR. Electrocardiographic markers of late sudden death risk in postoperative tetralogy of Fallot children. J Cardiovasc Electrophysiol 1997;8:1349-1356.

22. Sarubbi B, Pacileo G, Ducceschi V, Russo MG, Iacono C, Pisacane C, Iacono A and Calabro R. Arrhythmogenic substrate in young patients with repaired tetralogy of Fallot: role of an abnormal ventricular repolarization. Int J Cardiol 1999;72:73-82.

23. Kors JA, de Bruyne MC, Hoes AW, van HG, Hofman A, van Bemmel JH and Grobbee DE. T axis as an indicator of risk of cardiac events in elderly people. Lancet 1998;352:601-605.

24. Rautaharju PM, Nelson JC, Kronmal RA, Zhang ZM, Robbins J, Gottdiener JS, Furberg CD, Manolio T and Fried L. Usefulness of T-axis deviation as an independent risk indicator for incident cardiac events in older men and women free from coronary heart disease (the Cardiovascular Health Study). Am J Cardiol 2001;88:118-123.

25. Dean JW and Lab MJ. Arrhythmia in heart failure: role of mechanically induced changes in electrophysiology. Lancet 1989;1:1309-1312.

26. Vos MA, de Groot SH, Verduyn SC, van der ZJ, Leunissen HD, Cleutjens JP, van BM, Daemen MJ, Schreuder JJ, Allessie MA and Wellens HJ. Enhanced susceptibility for acquired torsade de pointes arrhythmias in the dog with chronic, complete AV block is related to cardiac hypertrophy and electrical remodeling. Circulation 1998;98:1125-1135.

27. Draper HW, Peffer CJ, Stallmann FW, Littmann D and Pipberger HV. The corrected orthogonal electrocardiogram and vectorcardiogram in 510 normal men (Frank lead system). Circulation 1964;30:853-864.

28. Helbing WA, Roest AA, Niezen RA, Vliegen HW, Hazekamp MG, Ottenkamp J, de Roos A and van der Wall EE. ECG predictors of ventricular arrhythmias and biventricular size and wall mass in tetralogy of Fallot with pulmonary regurgitation. Heart 2002;88:515-519.

29. Day CP, McComb JM and Campbell RW. QT dispersion: an indication of arrhythmia risk in patients with long QT intervals. Br Heart J 1990;63:342-344.

30. Kors JA, van HG and van Bemmel JH. QT dispersion as an attribute of T-loop morphology. Circulation 1999;99:1458-1463.

31. Zabel M, Malik M, Hnatkova K, Papademetriou V, Pittaras A, Fletcher RD and Franz MR. Analysis of T-wave morphology from the 12-lead electrocardiogram for prediction of long-term prognosis in male US veterans. Circulation 2002;105:1066-1070.

32. De Ambroggi L, Aime E, Ceriotti C, Rovida M and Negroni S. Mapping of ventricular repolarization potentials in patients with arrhythmogenic right ventricular dysplasia: principal component analysis of the ST-T waves. Circulation 1997;96:4314-4318.

33. Zabel M, Portnoy S and Franz MR. Electrocardiographic indexes of dispersion of ventricular repolarization: an isolated heart validation study. J Am Coll Cardiol 1995;25:746-752.

34. Shimizu W and Antzelevitch C. Cellular basis for the ECG features of the LQT1 form of the long-QT syndrome: effects of beta-adrenergic agonists and antagonists and sodium channel blockers on transmural dispersion of repolarization and torsade de pointes. Circulation 1998;98:2314-2322.

35. di Bernardo D and Murray A. Explaining the T-wave shape in the ECG. Nature 2000;403:40.

36. Shimizu W, Aiba T, Kurita T and Kamakura S. Paradoxic abbreviation of repolarization in epicardium of the right ventricular outflow tract during augmentation of Brugada-type ST segment elevation. J Cardiovasc Electrophysiol 2001;12:1418-1421.

37. Blomstrom-Lundqvist C, Hirsch I, Olsson SB and Edvardsson N. Quantitative analysis of the signal-averaged QRS in patients with arrhythmogenic right ventricular dysplasia. Eur Heart J 1988;9:301-312.

38. Liebman J, Rudy Y, Diaz P, Thomas CW and Plonsey R. The spectrum of right bundle branch block as manifested in electrocardiographic body surface potential maps. J Electrocardiol 1984;17:329-346.

V

Early changes in rat hearts with developing pulmonary arterial hypertension can be detected with three-dimensional electrocardiography

Ivo R. Henkens

Koen T.B. Mouchaers

Hubert W. Vliegen

Willem J. van der Laarse

Cees A. Swenne

Arie C. Maan

Harmen H.M. Draisma

Ingrid Schalij

Ernst E van der Wall

Martin J. Schalij

Anton Vonk Noordegraaf

Am J Physiol Heart Circ Physiol 2007;293:H1300-7

Abstract

Background

The study aim was to assess three-dimensional electrocardiogram (ECG) changes during development of pulmonary arterial hypertension (PAH).

Methods

PAH was induced in male Wistar rats (n=23) using monocrotaline (MCT; 40 mg·kg^{-1} sc). Untreated healthy rats served as controls (n=5). ECGs were recorded with an orthogonal three-lead system on days 0, 14, and 25 and analyzed with dedicated computer software. In addition, left ventricular (LV)-to-right ventricular (RV) fractional shortening ratio was determined using echocardiography.

Results

Invasively measured RV systolic pressure was 49 ± 10 mmHg on day 14 and 64 ± 10 mmHg on day 25 vs. 25 ± 2 mmHg in controls (both $P<0.001$). Baseline ECGs of controls and MCT rats were similar, and ECGs of controls did not change over time. In MCT rats, ECG changes were already present on day 14 but more explicit on day 25: increased RV electromotive forces decreased mean QRS-vector magnitude and changed QRS-axis orientation. Important changes in action potential duration distribution and repolarization sequence were reflected by a decreased spatial ventricular gradient magnitude and increased QRS-T spatial angle. On day 25, LV-to-RV fractional shortening ratio was increased, and RV hypertrophy was found, but not on day 14.

Conclusions

Developing PAH is characterized by early ECG changes preceding RV hypertrophy, whereas severe PAH is marked by profound ECG changes associated with anatomical and functional changes in the RV. Three-dimensional ECG analysis appears to be very sensitive to early changes in RV afterload.

Introduction

Pulmonary arterial hypertension (PAH) is a rare and severe disease of the afferent pulmonary vasculature, characterized by a progressive increase in pulmonary vascular resistance and overloading of the right side of the heart [1]. In patients with developing PAH, there is generally a considerable delay between the onset of pulmonary vasculature loss and the onset of PAH-related symptoms [2-5]. Diagnosis of PAH is therefore often delayed [6]. Hence, a simple noninvasive diagnostic test for PAH is warranted to allow earlier detection of the disease [6]. The routine electrocardiogram (ECG) is a very simple test but has proven to be of limited value in the evaluation of patients with suspected PAH [6, 7]. In rats it has been demonstrated that pulmonary hypertension precedes right ventricular hypertrophy, where the latter can be detected with sequentially recorded ECGs [8]. The vectorcardiogram (VCG) has been considered of additional value to ECG analysis, since it renders different information and allows calculation of parameters that cannot be computed from separate ECG leads [9-11]. However, the potential value of sequentially recorded VCGs for detection of changes in developing pulmonary hypertension has not been studied. Information recorded by three orthogonally oriented bipolar leads can be readily reconstructed into a three-dimensional VCG with the help of dedicated software. Since the right ventricle (RV) has a lower mass than the left ventricle (LV) in both rats [8, 12] and humans [13], RV electrical activity is largely masked by the LV electrical activity under normal conditions [14]. We hypothesized that an increasing RV workload, elicited by progressive loss of pulmonary vasculature in PAH, would trigger a corresponding degree of RV hypertrophy, inducing three-dimensional body surface ECG changes [15]. We chose to investigate the evolution of three-dimensional body surface ECG abnormalities in a rat model of pulmonary hypertension. In addition, we evaluated RV and LV contractility using echocardiography and determined RV hypertrophy by measuring mean cross-sectional area of RV cardiomyocytes. We investigated whether ECG abnormalities precede echocardiographic abnormalities and RV hypertrophy. Invasively measured RV systolic pressure served as the gold standard for presence of PAH.

Methods

Experimental setup

This study was performed in accordance with the national guidelines and with the permission of our institutional animal ethics and welfare committee. Male Wistar rats (Harlan Laboratories, Horst, The Netherlands) weighing 180–200 g were used in this study (n=28).

PAH was induced by a single subcutaneous injection of monocrotaline (MCT; 40 mg·kg^{-1}, n=23; Sigma-Aldrich, Steinheim, Germany) dissolved in 0.9% NaCl (8 mg·mL^{-1}) at pH 7.4. Untreated healthy rats received an equal volume of saline alone and served as controls (n=5). The local animal ethics and welfare committee ruled that an experiment involving rats exposed to 40 mg·kg^{-1} MCT should not be extended beyond 25 days, since comparable doses had led to end-stage heart failure and premature death in other experimental setups [16]. Animals were housed two per cage with a 12:12 h light-dark cycle. Food and water were available ad libitum. This study protocol was performed parallel to an ongoing project aimed at elucidating changes in pulmonary vasculature in PAH and the effects of medication on these changes. As such, this protocol was designed as a reversal study in which rats injected with MCT received either placebo (n=10) or one of three drugs: the dual endothelin receptor antagonist bosentan (100 mg·kg^{-1}·day^{-1}, n=4), the phosphodiesterase-5 inhibitor sildenafil (1 mg·kg^{-1}·day^{-1}, n=4), or the ρ-kinase inhibitor fasudil (30 mg·kg^{-1}·day^{-1}, n=5). Drugs were dissolved in 2 mL of commercially available vanilla pudding, which served as vehicle. Drugs were administered orally from day 14 onward. Untreated healthy and MCT rats received vehicle alone. On day 0 (before MCT injection), on day 14, and on day 25, a body surface ECG and echocardiogram were recorded. We chose to perform measurements on day 14, since elevated pulmonary arterial pressures were reportedly present at this time after administration of similar doses of MCT [17]. Before ECG recording and echocardiography, rats were anesthetized by inhalation of 4% isoflurane. Anesthesia was maintained under 2% isoflurane administration. All rats breathed spontaneously throughout this procedure.

RV pressure measurements

After completion of ECG and echo recordings, right ventricular systolic pressure (RVSP) was measured in 8 MCT rats on day 14 and in 15 MCT rats and 5 controls on day 25. Before the procedure, rats were intubated with a 16-gauge plastic venflon that was inserted directly into the trachea. Animals were subsequently attached to a mechanical micro ventilator (UNO, Zevenaar, The Netherlands), ensuring a breathing frequency of 75 breaths·min^{-1} with an intermittent positive pressure ventilation/positive end-expiratory plateau (IPPV/PEEP) of 15 - 5 mbar (control) or 8 - 2 mbar (MCT). PEEP was kept lower in MCT rats to avoid ventilator-induced lung injury. Pressure measurements were performed using a Millar pressure catheter (Millar, Houston, TX) that was directly inserted through the apical RV free wall after right lateral thoracotomy through the fifth intercostal space. RVSP was measured for 10 s and averaged. Data were obtained using a PowerLab setup (AD Instruments, Castle Hill, NSW, Australia). After RV pressure measurement, rats were killed. Before animal death, isoflurane administration was increased again to 4% and

the absence of reactivity to external stimuli was verified. During the entire procedure, body temperature was monitored and maintained at 37°C with a controlled heating pad.

RV hypertrophy

Hematoxylin and eosin staining was performed on cross sections of each heart as described by des Tombe et al. [18] to determine the degree of cardiomyocyte hypertrophy in both ventricles. The cross-sectional area (CSA) of 40 randomly chosen cardiomyocytes in the RV was measured. In addition, sarcomere length was randomly determined in five areas of each ventricle, where cardiomyocytes were cut along their longitudinal axis. CSA was then normalized on a sarcomere length of 2 μm to correct for variation between sarcomere lengths, which makes comparison between different hearts feasible. In addition, the occurrence of endured ischemia was determined by staining for cytosolic cytochrome c release [19].

Electrocardiography

Body surface ECGs were made with rats in the supine position. ECGs were recorded using five subcutaneously placed needle electrodes: one on each limb and one chest electrode centrally placed over the fourth intercostal space (Figure 1). A resistance network was used to derive three ECG leads, equivalent to Einthoven's lead I, lead aVF, and the inverted average of leads V1 and V2. In the following, these three leads are treated as vectorcardiographic leads X (right to left), Y (craniocaudal direction), and Z (anteroposterior direction). Orientation of the X-, Y-, Z-axis is according to the American Heart Association recommendations [20]. The fifth electrode on the right hind limb functioned as a reference electrode. The three orthogonal ECG signals were recorded with a 2,000-Hz sampling rate. The registration setup (PowerLab) was optimized with respect to grounding and shielding to keep background noise to a minimum. Registrations were performed with a minimum duration of 1 min to allow for beat selection and subsequent averaging, further improving the signal-to-noise ratio. All ECGs were recorded without electronic filters and were processed off-line.

Electrocardiographic analysis

ECGs were analyzed using LEADS, our dedicated electrocardiography analysis program [9]. In short, LEADS automatically selects beats for averaging on the basis of signal quality criteria (baseline, noise). This selection of beats is then reviewed and edited by the investigator. The beats are then averaged by LEADS. After the onset and end of QRS complex and the end of T-wave in the averaged beat are manually reviewed and edited, vectorcardiographic calculations are automatically performed.

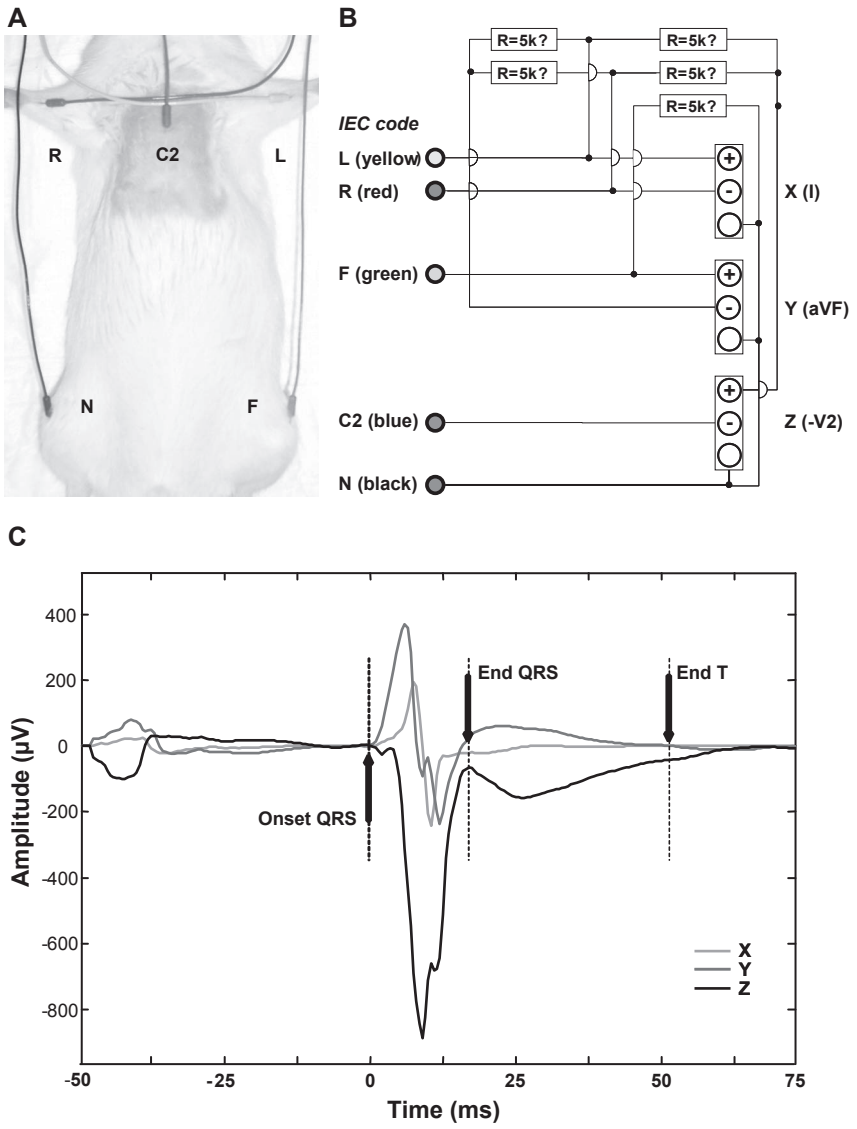

Figure 1

A) Rat in the supine position with the 5 ECG electrodes in place: red (right front limb), yellow (left front limb), green (left hind limb), blue (central over 4th intercostal space), and black (right hind limb).

B) Resistor network to derive ECG leads I, aVF, and the inverted mean of leads V1 and V2, taken as substitutes for vectorcardiographic X,Y, and Z leads.

C) Averaged beat from a healthy rat, generated by LEADS.

Electrocardiographic parameters

Depolarization was characterized by QRS duration, the orientation of the QRS-axis, and the mean QRS vector magnitude. QRS-axis orientation with unit radius was decomposed in its X, Y, and Z components for comparison of orientation over time. Concordance/discordance of depolarization and repolarization on the ECG was characterized by the spatial QRS-T angle (the angle between the spatial orientation of the QRS- and T-axes) [21]. Action potential duration heterogeneity was characterized by the spatial ventricular gradient (VG) magnitude [22]. All parameters were derived from the averaged beat, using information from the three orthogonal leads.

Echocardiography

The average heart rate of a rat is approximately five times higher than that of humans, precluding real-time appreciation of cardiac function with echocardiography. We chose to perform echocardiography with a straightforward, easily reproducible approach, capturing both LV and RV during the cardiac cycle. RV and LV short-axis images were made in B-mode and M-mode, using a ProSound SSD-4000 PureHD echo machine (Aloka, Tokyo, Japan). End-diastolic and end-systolic diameters (EDD and ESD, respectively) for both RV and LV were measured perpendicularly to the interventricular septum at midseptal level. EDD and ESD were used to calculate fractional shortening with the following formula: fractional shortening=[(EDD - ESD)/EDD]·100%. Since comparison of individual RV and LV fractional shortening over time is sensitive to changes in echo probe positioning along the longitudinal cardiac axis, we used the ratio of LV fractional shortening to RV fractional shortening (LV/RV fractional shortening) to describe changes in cardiac function.

Statistical analysis

All data sets were randomized before analysis by observers (I.R. Henkens and K.T.B. Mouchaers) who were blinded to treatment groups. SPSS for Windows software (version 12.0.1; SPSS, Chicago, IL) was used for data analysis. Normally distributed values are presented as means ± standard deviation. Values not normally distributed are presented as medians and their minimum and maximum values in parentheses. Independent t-tests were used for comparison of controls and MCT rats. Sequential measurements within groups of similarly treated rats were compared with paired t-tests. A value of $P < 0.05$ was considered to be statistically significant.

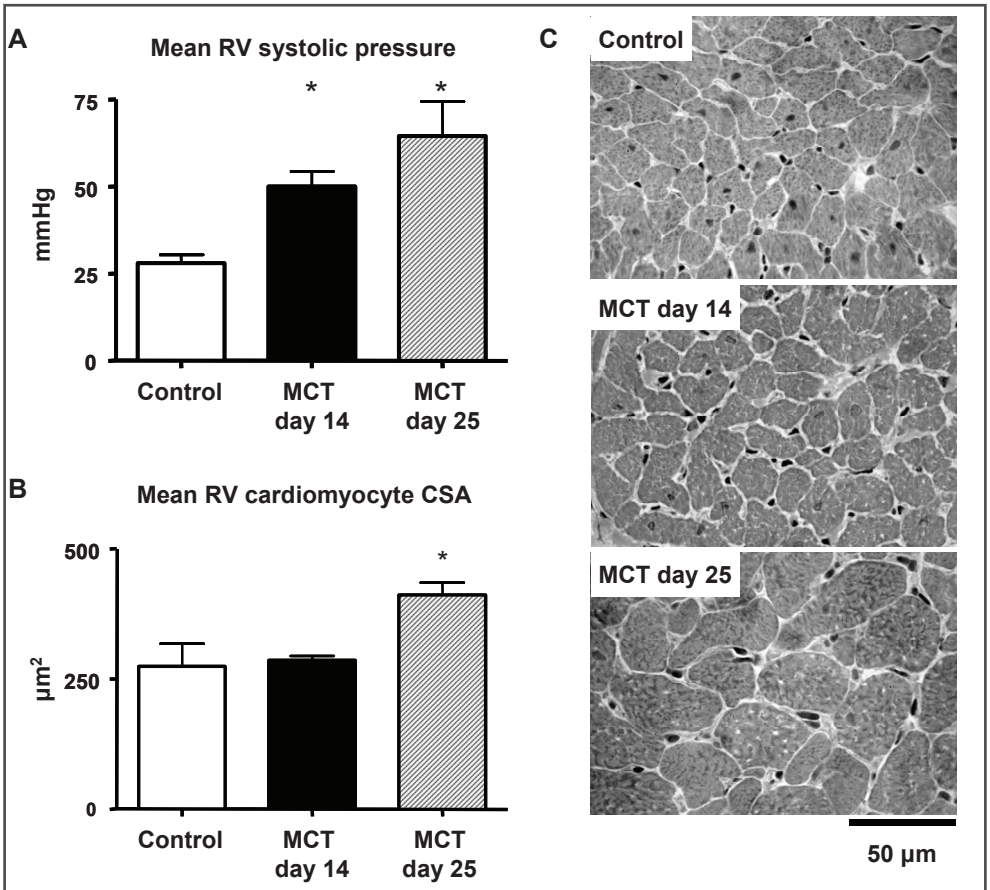

Figure 2

A. Mean RV systolic pressure was 25±2 mmHg in controls vs. 49±10 mmHg in MCT rats on day 14, and 64 ± 10 mmHg on day 25;

B. Mean Cross sectional area of RV myocytes was 274±44 µm2 in controls vs. 286±23 µm2 in MCT rats on day 14 and 476±65 µm2 on day 25,

C. RV myocytes in a control rat (magnification 40x);
RV myocytes in a MCT rat on day 14 (magnification 40x);
RV myocytes in a MCT rat on day 25 (magnification 40x).

**: P<0.001, MCT = Monocrotaline, CSA = Mean cross sectional area, normalized on sarcomere length, RVSP = Mean right ventricular systolic pressur*

Results

RV systolic pressure and hypertrophy

On day 14 all MCT rats already had elevated RVSP compared with controls (Figure 2A). However, RV hypertrophy was not yet present at this time, as demonstrated by a mean cross-sectional cardiomyocytes area of 286 ± 23 μm^2, which was not different from 274 ± 44 μm^2 in controls (P=0.52) (Figure 2B and C). On day 25, all MCT rats, regardless of therapy, had severe PAH (Figure 2A). At this time MCT rats showed marked RV hypertrophy, with a considerably higher mean CSA of RV cardiomyocytes of 476 ± 65 μm^2 compared with both controls and MCT rats on day 14 (both P<0.001) (Figure 2B and C). LV cardiomyocyte dimensions were not different between MCT rats and controls. MCT rats were negative for cytochrome c release, indicating that myocardial perfusion was adequate despite marked hypertrophy in MCT rats.

Body surface ECGs and echocardiograms

Of the 76 recorded body surface ECGs, 2 (2.6%) were not interpretable because of 50-Hz background noise. Suitable for analysis were 28 registrations on day 0, 28 registrations on day 14, and 18 registrations on day 25. Out of 76 echocardiographic registrations performed, 72 (94.7%) were suitable for interpretation of RV and LV fractional shortening.

ECGs at baseline

There was no difference at baseline between rats receiving saline and rats receiving MCT with respect to heart rate, QRS duration, QRS-axis orientation, mean QRS vector magnitude, QRS-T spatial angle, or VG magnitude. There were no rats with a bundle branch block configuration in the ECG.

ECGs after 14 and 25 days

Controls did not show ECG changes on day 14 or day 25. MCT rats, however, showed marked changes in ECG characteristics on day 14 compared with baseline, which had further evolved on day 25 (Table 1). ECG changes were not different for MCT rats receiving treatment compared with MCT rats receiving placebo. In addition, ECG changes were also not different between rats receiving different medications (bosentan, sildenafil, or fasudil). New onset bundle branch block was not observed. On day 14, heart rate was lower in MCT rats than on day 0. Furthermore, depolarization changes were present

in MCT rats, as well as changes in concordance of depolarization and repolarization and changes in action potential duration heterogeneity. The increased RV contribution to the electromotive forces was demonstrated by an important decrease in mean QRS vector magnitude. Furthermore, there was a change in three-dimensional QRS-axis orientation, most notably in the Z direction. The suggested evolutionary mechanism for the observed changes on day 14 and day 25 is presented in the Discussion. Of note, VG magnitude declined, whereas QRS-T spatial angle increased, signifying an alteration in both action potential duration heterogeneity and repolarization sequence. On day 25, ongoing development of PAH had resulted in marked changes in both depolarization

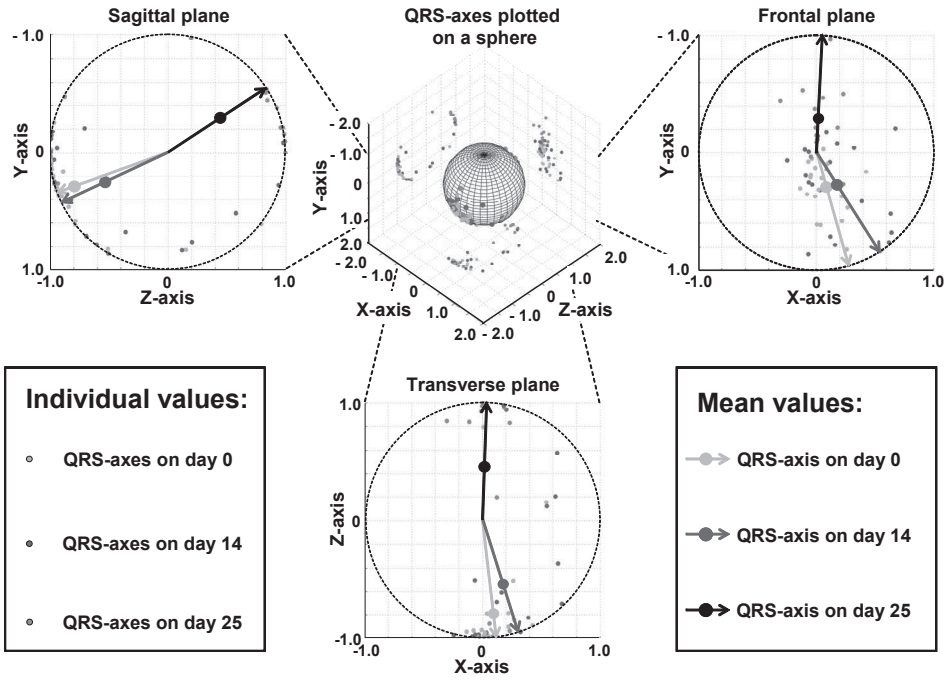

Figure 3

Individual QRS-axes orientations (small dots) on day 0, day 14, and day 25 are plotted on a sphere with unit radius (varying between -1 and +1) and projected on the horizontal, transverse and sagittal planes. Mean values (large dots) are projected on the orthogonal planes only. Mean QRS-axis orientation shifted along the X-axis and Z-axis from day 0 to day 14 and along both Y-axis and Z-axis from day 14 to day 25. The 3-dimensional plot and its projections allow appreciation of the virtual inversion in QRS-axis orientation due to development of severe PAH. Quantitative results are presented in Table 1.

and repolarization characteristics in MCT rats, compared with both baseline and day 14 (Table 1). The sphere plot of QRS-axes (orientation and projections on the transverse, frontal, and sagittal plane) illustrates the changes in spatial orientation 14 and 25 days after administration of MCT compared with baseline (Figure 3).

TABLE 1: 3-DIMENSIONAL ELECTROCARDIOGRAPHIC ANALYSIS DERIVED VARIABLES FOR MONOCROTALIN RATS ON DAY 0 (N=23), DAY 14 (N=23), AND DAY 25 (N=13) ILLUSTRATING EVOLUTIONARY CHANGES DURING THE DEVELOPMENT OF PULMONARY ARTERIAL HYPERTENSION

	Day 0	Day 14	Day 25	Day 0 vs. day 14	Day 0 vs. day 25	Day 14 vs. day 25
3-D ECG variables	Mean	Mean	Mean	*P*	*P*	*P*
Heart Rate (bpm)	419 ± 25	400 ± 24	328 ± 27	<0.001	<0.001	<0.001
QRS duration (ms)	15.6 ± 2.3	16.5 ± 2.2	17.9 ± 3.1	0.19	0.066	0.085
QRS X component	0.08 ± 0.17	0.18 ± 0.28	0.03 ± 0.15	0.01	0.521	0.052
QRS Y component	0.29 ± 0.27	0.27 ± 0.36	-0.28 ± 0.32	0.689	<0.001	<0.001
QRS Z component	-0.78 ± 0.49	-0.55 ± 0.56	0.44 ± 0.81	0.01	<0.001	0.002
QRS vector magnitude (μV)	318 ± 169	175 ± 98	274 ± 170	<0.001	0.247	0.167
QRS-T spatial angle (°)	32 ± 30	49 ± 46	146 ± 45	0.01	<0.001	<0.001
VG magnitude (mV·ms)	12.2 ± 4.3	9.8 ± 3.6	4.4 ± 2.0	0.02	<0.001	<0.001

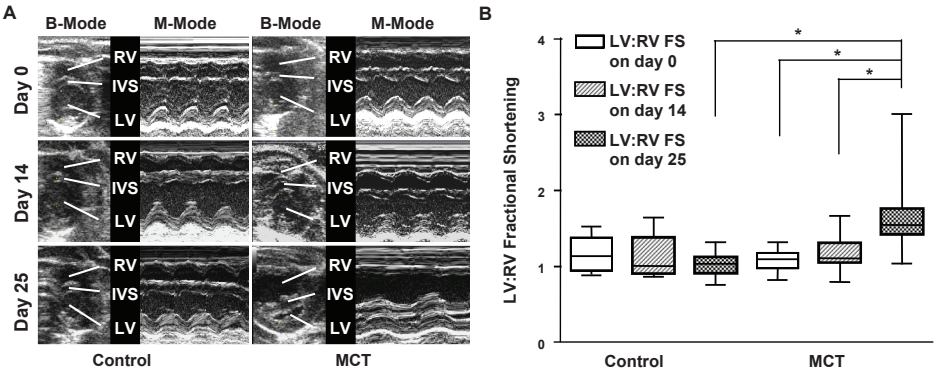

Figure 4

A) Echocardiography in B-Mode and M-Mode in controls and MCT rats on day 0, day 14, and day 25. There were no changes in controls. MCT rats were still unchanged on day 14, whereas there is marked RV dilatation and a decreased LV lumen in MCT rats on day 25.

B) LV:RV fractional shortening ratio in controls and MCT rats on day 0, day 14, and day 25.

**: P < 0.001, LV = left ventricular, RV = right ventricular, IVS = interventricular septum, FS = fractional shortening, MCT = monocrotaline.*

Echocardiography

A typical illustration of echocardiographic images obtained at baseline, on day 14, and on day 25 is shown in Figure 4A. LV/RV fractional shortening was un-changed in MCT rats on day 14 but was significantly increased on day 25 (Figure 4B).

Discussion

The key finding of this study is that the development of PAH in rats is associated with a distinct evolution of ECG abnormalities. These ECG abnormalities were already present early in the development of PAH and preceded the onset of both RV hypertrophy and echocardiographic abnormalities. To our knowledge, this is the first report of serial three-dimensional electrocardiography detecting changes early in the development of PAH in animals with the use of a three-lead body surface ECG.

Right heart catheterization, echocardiography, and electrocardiography

We used right heart catheterization as the gold standard for diagnosis of PAH in rats, similar to the guidelines for patient evaluation [23]. Measuring mean CSA of RV cardiomyocytes served to determine RV hypertrophy. Since echocardiography is regarded as the most important noninvasive diagnostic tool in the initial evaluation of PAH [6], we performed a limited, reliable echocardiographic evaluation of all rats for comparison with ECG recordings. Although echocardiography did not detect changes in MCT rats on day 14, there were important changes in LV/RV fractional shortening on day 25. This confirms that the echocardiographic measurements used offer a fair appreciation of the rat heart and changes in RV afterload. The three-lead body surface ECG used in this study is an orthogonal lead system in its most simple form. Our longitudinal three-dimensional ECG analysis rendered variables unique to vectorcardiography, enhancing understanding of RV evolutionary changes during the development of PAH.

Early electrocardiographic abnormalities in developing pulmonary arterial hypertension

On day 14, initial changes in both depolarization and repolarization characteristics were already apparent. The decrease in QRS vector magnitude and the change in three-dimensional QRS-axis orientation imply a change in depolarization characteristics. The change in VG magnitude signifies a change in action potential duration heterogeneity in the ventricles, and the increased QRS-T spatial angle signifies a change in repolarization sequence. In the absence of ventricular conduction delays, these changes are most likely the result of increased cancellation of LV electromotive forces by an augmented RV contribution (Figure 5) [24, 25].

Late electrocardiographic abnormalities in end-stage pulmonary arterial hypertension

On day 25, there were marked ECG changes in MCT rats, indicated by depolarization abnormalities, discordance of depolarization and repolarization, and decreased action potential duration heterogeneity. Heart rate was lowered further, and QRS-axis orientation changed dramatically. At the same time, mean QRS vector magnitude "normalized." Changes in both QRS-axis orientation and "normalization" of mean QRS vector magnitude can be explained by an increased RV contribution to the resultant ventricular depolarization activity (Figure 5). The further decrease in VG magnitude in MCT rats, despite a normalized mean QRS vector magnitude, can be understood by taking a closer look at the significant increase in QRS-T spatial angle. The mean QRS-T spatial angle of 146° ± 45° in MCT rats on day 25 implies that direction of the T-axis is partially opposite to the QRS-axis, thereby decreasing ventricular gradient magnitude [22]. These more pronounced late ECG changes are consistent with the observed abnormalities in LV/RV fractional shortening and the elevated RVSP values that were also present in the late stage of the experiment. In advanced PAH, moderate to severe RV hypertrophy is observed, often with RV dilatation and paradoxical septal movement [26, 27].

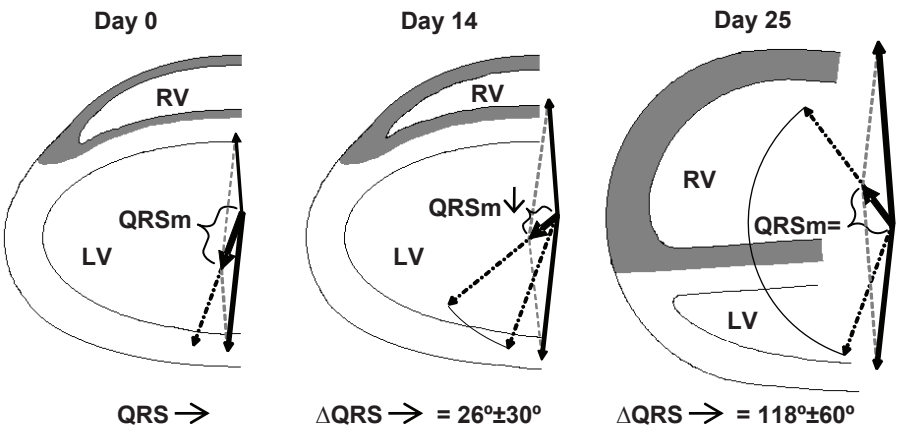

Figure 5

Changes in mean QRS vector magnitude and QRS-axis in MCT rats. Day 0: LV contribution to QRS vector magnitude is dominant over RV contribution. Day 14: an increased RV contribution initially decreases QRS vector magnitude while slightly shifting QRS-axis. Day 25: due to presence of severe PAH RV contribution is markedly increased, returning QRS vector magnitude to baseline level while shifting QRS-axis in the opposite direction.

LV = left ventricle, RV = right ventricle, QRSm = QRS vector magnitude, QRS→ = QRS-axis

Together, these anatomical and functional changes may have induced the impressive change in QRS-axis orientation on day 25 in MCT rats (Figure 5). MCT administration does not affect LV remodeling or LV afterload [17]. Hence, ECG changes reflect RV adaptation to the increased pulmonary vascular resistance.

The idea that sequential electrocardiography could detect cardiac changes in developing pulmonary hypertension was put forward by Bruner et al. [8], who observed a rightward shift in the frontal plane of the mean QRS-axis in rats 14 days after direct administration of MCT pyrrole (the active metabolite of MCT). Although the QRS-axis shift was in correspondence with the level of RV hypertrophy, elevated pulmonary artery pressures had been present for 7 days [8]. However, two important differences should be noted between the study of Bruner et al. [8] and the current study. First, instead of using MCT pyrrole, we used MCT, causing a significant delay in development of pulmonary hypertension [8]. Electrocardiographic changes observed in this study on day 14 are therefore not comparable to the changes observed by Bruner et al. [8] on day 14. Second, the three-dimensional QRS-axis orientation is the basis for QRS-axis orientation in any plane. Therefore, any change in QRS-axis orientation in a plane of choice (e.g., the frontal plane as used by Bruner et al.) can be a meaningful approximation of the true change in three-dimensional QRS-axis orientation when the QRS-axis is oriented in or close to this frontal plane at the time of each measurement. However, when the three-dimensional QRS-axis is oriented more perpendicularly to the plane of choice, a change in three-dimensional orientation may either be largely underestimated or overestimated by the change in QRS-axis orientation in this particular plane. A change in three-dimensional QRS-axis orientation is therefore more accurate and reliable than a change in two-dimensional QRS-axis orientation. With the advent of state-of-the-art techniques such as continuous invasive telemetry, future research will likely unravel the true relationship between ECG changes and the onset of elevated pulmonary pressures. Our observation that elevated pulmonary artery pressures precede RV hypertrophy confirms prior reports that RV hypertrophy is a relatively insensitive marker of pulmonary hypertension [8]. Lee et al. [12] established the presence of "compensated" RV hypertrophy after 14 days, using 5-wk-old male Wistar rats exposed to a 60 $mg \cdot kg^{-1}$ dose of MCT. Others demonstrated that RV hypertrophy precedes neurohumoral activation and β-adrenoceptor down regulation [17]. In our study, MCT rats showed a progressive decrease in heart rate under anesthesia during development of PAH. This may reflect the increased cardiodepressive effect of anesthesia in the presence of early neurohumoral changes.

Monocrotaline-induced pulmonary arterial hypertension

MCT-induced PAH is broadly recognized as an experimental model for studying RV hypertrophy as well as treatment effects of PAH-attenuating medication. Although MCT has been shown to primarily affect the RV, with no known effects on LV remodeling or changes in potassium channel expression, a direct effect of MCT on myocardial electrical properties cannot be fully excluded [28-30]. Although the presence of discordance between depolarization and repolarization is a global and rather aspecific marker of ventricular pathology, it is associated with an adverse long-term prognosis [31]. Since this particular model only affects RV afterload, such discordance between depolarization and repolarization is most likely a direct consequence of resultant RV hypertrophy in the absence of RV ischemia. Ventricular repolarization sequence becomes abnormal in rats with PAH, given the high spatial angle (Table 1). In fact, changes in RV action potential duration and/or action potential duration heterogeneity are necessary to elicit such changes. However, these changes are by no means indicative of spatial differences in action potential duration distribution or repolarization within the RV. The exact mechanism underlying this phenomenon is beyond the scope of the current study. A RV load-dependent down regulation of voltage-gated potassium channels is likely involved [12, 28]. Further research is necessary to appreciate changes in RV myocardium elicited by PAH.

Limitations

A limitation in our study, which was essentially designed as a reversal protocol, is that the limited time of therapy as well as the relatively low dosages may have precluded a beneficial effect of bosentan, sildenafil, and fasudil on RV pressure overload [32-34].

Conclusions

Developing pulmonary arterial hypertension is characterized by early ECG changes preceding RV hypertrophy, whereas severe pulmonary arterial hypertension is marked by profound ECG changes, associated with anatomical and functional changes in the RV. Three-dimensional ECG analysis appears to be very sensitive to early changes in RV afterload. Having established that developing pulmonary arterial hypertension in the rat is associated with distinct evolutionary ECG changes, this finding must now meet its clinical use by serial ECG analysis in a select group of patients at risk for developing pulmonary arterial hypertension.

References

1. Chin KM, Kim NH and Rubin LJ. The right ventricle in pulmonary hypertension. Coron Artery Dis 2005;16:13-18.

2. Eddahibi S, Morrell N, d'Ortho MP, Naeije R and Adnot S. Pathobiology of pulmonary arterial hypertension. Eur Respir J 2002;20:1559-1572.

3. Humbert M, Morrell NW, Archer SL, Stenmark KR, MacLean MR, Lang IM, Christman BW, Weir EK, Eickelberg O, Voelkel NF and Rabinovitch M. Cellular and molecular pathobiology of pulmonary arterial hypertension. J Am Coll Cardiol 2004;43:13S-24S.

4. Rich S, Dantzker DR, Ayres SM, Bergofsky EH, Brundage BH, Detre KM, Fishman AP, Goldring RM, Groves BM and Koerner SK. Primary pulmonary hypertension. A national prospective study. Ann Intern Med 1987;107:216-223.

5. Yuan JX and Rubin LJ. Pathogenesis of pulmonary arterial hypertension: the need for multiple hits. Circulation 2005;111:534-538.

6. McGoon M, Gutterman D, Steen V, Barst R, McCrory DC, Fortin TA and Loyd JE. Screening, early detection, and diagnosis of pulmonary arterial hypertension: ACCP evidence-based clinical practice guidelines. Chest 2004;126:14S-34S.

7. Ahearn GS, Tapson VF, Rebeiz A and Greenfield JC, Jr. Electrocardiography to define clinical status in primary pulmonary hypertension and pulmonary arterial hypertension secondary to collagen vascular disease. Chest 2002;122:524-527.

8. Bruner LH, Hilliker KS and Roth RA. Pulmonary hypertension and ECG changes from monocrotaline pyrrole in the rat. Am J Physiol 1983;245:H300-H306.

9. Draisma HH, Swenne CA and Van de Vooren H. LEADS: an interactive research oriented ECG/VCG analysis system. Computers in Cardiology 2005;32:515-518.

10. Frank E. An accurate, clinically practical system for spatial vectorcardiography. Circulation 1956;13:737-749.

11. Frank E and Seiden GE. Comparison of limb and precordial vectorcardiographic systems. Circulation 1956;14:83-89.

12. Lee JK, Nishiyama A, Kambe F, Seo H, Takeuchi S, Kamiya K, Kodama I and Toyama J. Downregulation of voltage-gated K(+) channels in rat heart with right ventricular hypertrophy. Am J Physiol 1999;277:H1725-H1731.

13. Lehtonen J, Sutinen S, Ikaheimo M and Paakko P. Electrocardiographic criteria for the diagnosis of right ventricular hypertrophy verified at autopsy. Chest 1988;93:839-842.

14. Ritsema van Eck HJ, Kors JA and van Herpen G. Dispersion of repolarization, myocardial isosource maps, and the electrocardiographic T and U waves. J Electrocardiol 2006;39:S96-100.

15. Chou TC. When is the vectorcardiogram superior to the scalar electrocardiogram? J Am Coll Cardiol 1986;8:791-799.

16. Cowan KN, Heilbut A, Humpl T, Lam C, Ito S and Rabinovitch M. Complete reversal of fatal pulmonary hypertension in rats by a serine elastase inhibitor. Nat Med 2000;6:698-702.

17. Leineweber K, Brandt K, Wludyka B, Beilfuss A, Ponicke K, Heinroth-Hoffmann I and Brodde OE. Ventricular hypertrophy plus neurohumoral activation is necessary to alter the cardiac beta-adrenoceptor system in experimental heart failure. Circ Res 2002;91:1056-1062.

18. Des Tombe AL, Van Beek-Harmsen BJ, Lee-De Groot MB and van der Laarse WJ. Calibrated histochemistry applied to oxygen supply and demand in hypertrophied rat myocardium. Microsc Res Tech 2002;58:412-420.

19. Van Beek-Harmsen BJ and van der Laarse WJ. Immunohistochemical determination of cytosolic cytochrome C concentration in cardiomyocytes. J Histochem Cytochem 2005;53:803-807.

20. Kossmann CE, Brody DA, Burch GE, Hecht HE, Johnston FD, Kay C, Lepeschkin E, Pipberger HV, Baule G, Berson AS, Briller SA, Geselowitz DB, Horan LG and Schmitt OH. Report of committee on electrocardiography, American Heart Association. Recommendations for standardization of leads and of specifications for instruments in electrocardiography and vectorcardiography. Circulation 1967;35:583-602.

21. Okin PM and Kligfield P. Solid-angle theory and heart rate adjustment of ST-segment depression for the identification and quantification of coronary artery disease. Am Heart J 1994;127:658-667.

22. Draisma HH, Schalij MJ, van der Wall EE and Swenne CA. Elucidation of the spatial ventricular gradient and its link with dispersion of repolarization. Heart Rhythm 2006;3:1092-1099.

23. Barst RJ, McGoon M, Torbicki A, Sitbon O, Krowka MJ, Olschewski H and Gaine S. Diagnosis and differential assessment of pulmonary arterial hypertension. J Am Coll Cardiol 2004;43:40S-47S.

24. Helm RA. Electrocardiographic cancellation: mathematical basis. Am Heart J 1960;60:251-265.

25. Helm RA and Chou TC. Electrocardiographic cancellation. A study of a single dipole at variable locations. Am Heart J 1966;72:218-237.

26. Roeleveld RJ, Marcus JT, Faes TJ, Gan TJ, Boonstra A, Postmus PE and Vonk Noordegraaf A. Interventricular septal configuration at mr imaging and pulmonary arterial pressure in pulmonary hypertension. Radiology 2005;234:710-717.

27. Vonk Noordegraaf A, Marcus JT, Gan CT, Boonstra A and Postmus PE. Interventricular mechanical asynchrony due to right ventricular pressure overload in pulmonary hypertension plays an important role in impaired left ventricular filling. Chest 2005;128:628S-630S.

28. Kogler H, Hartmann O, Leineweber K, Nguyen van P, Schott P, Brodde OE and Hasenfuss G. Mechanical load-dependent regulation of gene expression in monocrotaline-induced right ventricular hypertrophy in the rat. Circ Res 2003;93:230-237.

29. Lourenco AP, Roncon-Albuquerque R, Jr., Bras-Silva C, Faria B, Wieland J, Henriques-Coelho T, Correia-Pinto J and Leite-Moreira AF. Myocardial dysfunction and neurohumoral activation without remodeling in left ventricle of monocrotaline-induced pulmonary hypertensive rats. Am J Physiol Heart Circ Physiol 2006;291:H1587-H1594.

30. Zhang TT, Cui B and Dai DZ. Downregulation of Kv4.2 and Kv4.3 channel gene expression in right ventricular hypertrophy induced by monocrotaline in rat. Acta Pharmacol Sin 2004;25:226-230.

31. Zabel M, Malik M, Hnatkova K, Papademetriou V, Pittaras A, Fletcher RD and Franz MR. Analysis of T-wave morphology from the 12-lead electrocardiogram for prediction of long-term prognosis in male US veterans. Circulation 2002;105:1066-1070.

32. Abe K, Shimokawa H, Morikawa K, Uwatoku T, Oi K, Matsumoto Y, Hattori T, Nakashima Y, Kaibuchi K, Sueishi K and Takeshit A. Long-term treatment with a Rho-kinase inhibitor improves monocrotaline-induced fatal pulmonary hypertension in rats. Circ Res 2004;94:385-393.

33. Hill NS, Warburton RR, Pietras L and Klinger JR. Nonspecific endothelin-receptor antagonist blunts monocrotaline-induced pulmonary hypertension in rats. J Appl Physiol 1997;83:1209-1215.

34. Schermuly RT, Kreisselmeier KP, Ghofrani HA, Yilmaz H, Butrous G, Ermert L, Ermert M, Weissmann N, Rose F, Guenther A, Walmrath D, Seeger W and Grimminger F. Chronic sildenafil treatment inhibits monocrotaline-induced pulmonary hypertension in rats. Am J Respir Crit Care Med 2004;169:39-45.

VI

Improved ECG detection of presence and severity of right ventricular pressure load validated with cardiac magnetic resonance imaging

Ivo R. Henkens

Koen T.B. Mouchaers

Anton Vonk Noordegraaf

Anco Boonstra

Cees A. Swenne

A.C. Maan

Sum-Che Man

Jos W.R. Twisk

Ernst E. van der Wall

Martin J. Schalij

Hubert W. Vliegen

Am J Physiol Heart Circ Physiol 2008;294:H2150-7

Abstract

Background

The study aimed to assess whether the 12-lead electrocardiogram (ECG) derived ventricular gradient, a vectorial representation of ventricular action potential duration heterogeneity directed towards the area of shortest action potential duration, can improve ECG diagnosis of chronic right ventricular (RV) pressure load.

Methods

We compared ECGs from 72 pulmonary arterial hypertension patients recorded <30 days before onset of therapy with ECGs from matched healthy controls subjects (n=144). We compared conventional ECG criteria for increased RV pressure load with the ventricular gradient.

Results

In 38 patients a cardiac magnetic resonance (CMR) study had been performed within 24 hours of the ECG. By multivariable analysis, combined use of conventional ECG parameters (rsr'or rsR' in V1, R/S>1 with R>0.5 mV in V1, and QRS axis >90º) had a sensitivity of 89%, and a specificity of 93% for presence of chronic RV pressure load. However, the ventricular gradient not only had a higher diagnostic accuracy for chronic RV pressure load by ROC analysis (AUC=0.993, SE 0.004 vs. AUC=0.945, SE 0.021, $P<0.05$), but also discriminated between mild to moderate and severe RV pressure load. CMR identified an inverse relation between the ventricular gradient and RV mass, and a trend to a similar relation with RV volume.

Conclusions

Chronically increased RV pressure load is electrocardiographically reflected by an altered ventricular gradient associated with RV remodeling related changes in ventricular action potential duration heterogeneity. Using the ventricular gradient allows ECG detection of even mildly increased RV pressure load.

Introduction

Moderately increased chronic right ventricular (RV) pressure load is hard to detect non-invasively due to the position and mass of the RV [1-3]. Conventional 12-lead electrocardiographic (ECG) parameters of increased RV pressure load lack diagnostic accuracy, precluding their use for screening purposes [4-8]. Partly because the chest electrodes predominantly overly the left ventricle, partly because the 12-lead ECG renders 12 separate one-dimensional projections of the three-dimensional (3D) cardiac vector in time [9], but not in the least because the RV mass is relatively low compared to the left ventricular (LV) mass. This scalar ECG representation hampers the direct appreciation of the ECG as a recording of a 3D process. However, a synthesized vectorcardiogram can be easily derived mathematically from the ECG allowing the calculation of electrocardiographic 3D parameters. One of these parameters is the ventricular gradient (VG), a 3D measure of ventricular action potential duration (APD) heterogeneity oriented from the area with the longest APD towards the area with the shortest APD [10, 11]. The VG (mV·ms) is the sum of the 3D integrals of both the QRS complex and the T-wave (net area subtended by the heart vector over the QRS complex and the T-wave) [10, 11]. A change in magnitude and/or orientation of the VG signifies a change in APD heterogeneity [10, 12]. APD changes due to chronic RV pressure load must therefore change the VG [12]. In a rat model we recently demonstrated that the VG changes markedly during the development of pulmonary arterial hypertension (PAH), a model of chronic RV pressure load [13]. We therefore decided to study the use of the VG in diagnosing chronic RV pressure load. In humans however, comparison of ECGs at the time of diagnosis of PAH with ECGs from a disease-free state is in general not feasible, since PAH remains undetected for a long time [14]. ECGs from PAH patients were therefore compared with ECGs from healthy controls. To further appreciate the diagnostic potential of the VG in chronic RV pressure load, all ECGs were also evaluated for the conventional criteria of increased right heart load [15].

Methods

Patients

The study complies with the Declaration of Helsinki. Patient data were gathered as part of routine clinical care in the VU University Medical Center and analyzed retrospectively. Healthy control subjects gave written informed consent for this study that was approved by the institutional ethical review board of the Leiden University Medical Center.

Between December 1999 and December 2005, 565 consecutive patients were evaluated

with a right heart catheterization because of suspected PAH, defined as a mean pulmonary artery pressure >25 mmHg and pulmonary capillary wedge pressure <15 mmHg. PAH was considered to be idiopathic when identifiable causes for pulmonary hypertension (i.e. congenital heart disease, portal hypertension, collagen vascular disease, HIV infection, left heart disease, hypoxic pulmonary disease or chronic thrombo-embolic disease) were excluded [8, 16]. One hundred and ten patients were identified with idiopathic PAH. A digitally stored ECG recorded within 30 days prior to diagnostic right heart catheterization was available in 72 patients (15 male).

Right heart catheterization

All PAH patients underwent right heart catheterization, during which right atrial pressure, pulmonary artery pressure, pulmonary capillary wedge pressure, and mixed venous oxygen saturation were measured. Cardiac output was calculated using Fick's principle. Oxygen consumption was measured during right heart catheterization. Pulmonary vascular resistance ($mmHg \cdot L^{-1} \cdot min^{-1}$) was calculated by dividing the transpulmonary gradient (pressure difference between mean pulmonary artery pressure and pulmonary capillary wedge pressure) by cardiac output.

ECG analysis

Conventional 10-second ECGs were recorded by certified ECG technicians with patients in supine position using the standard 12-lead electrode configuration. ECGs were recorded on commercially available electrocardiographs (MAC VU and MAC 5000, GE Healthcare, The Netherlands, and Megacart, Siemens, Germany, respectively), at a paper speed of 25 $mm \cdot s^{-1}$; sensitivity 1mV=10mm; sample frequency of 500 Hz. All ECGs were assessed for the presence of conventional 12-lead ECG criteria of RV hypertrophy [15]. ECGs were also analyzed with LEADS, our non-commercial, research oriented ECG analysis program which automatically renders amplitudes, areas and vector directions [17]. In short, LEADS automatically selects beats for averaging based on signal quality criteria (baseline, noise). This selection of beats is then reviewed and edited by the investigator. The thus selected beats are then averaged by LEADS. After manually reviewing and editing the onset and end of the QRS-complex, a synthesized vectorcardiogram is generated with the inverse Dower matrix [17, 18]. Parameters derived from this vectorcardiogram, such as the VG magnitude (mV·ms) and spatial orientation (azimuth°, orientation in the transversal plane, and elevation°, deviation from the transversal plane), are then calculated. The VG is defined as: $\int H(t) \cdot dt$ in which H(t) is the heart vector, as represented in the X,Y, and Z leads of the vectorcardiogram [19]. This integral, taken over the

QRST interval, is non-zero due to action potential morphologic differences in the ventricles, most often thought of as APD differences [10]. Orientation of the axes is in accordance with the American Heart Association recommendations: X axis positive from right to left, Y axis positive in cranio-caudal direction, and Z axis positive in antero-posterior direction [20]. Control ECGs were selected from a large database of healthy students of the Leiden University Medical Faculty. All ECGs were scrutinized for normality according to the Minnesota criteria by an experienced cardiologist [21]. Prior to the use of the selected ECGs for comparison in this study, all ECGs were anonymized. All ECGs were analyzed twice by the first author (IRH), and a third time by the second author (KTBM) to determine the intra-observer and inter-observer variability for calculating the VG. As the VG depends on heart rate [22] and gender, but not on age (unpublished data), we matched each patient ECG for heart rate and gender with two ECGs from healthy subjects.

Cardiac magnetic resonance imaging

In 38 patients CMR imaging had been performed on a Siemens 1.5 T Sonata scanner (Siemens Medical Solutions, Erlangen, Germany) within 24 hours of the ECG recording, as previously described [23]. Cardiac short-axis cine images of both RV and left ventricle (LV) were acquired from base to apex at 10 mm slice distance. A blinded observer delineated RV and LV endocardial and epicardial contours manually, and MASS software (Dept. of Radiology, Leiden University Medical Center, Leiden, the Netherlands) was used to obtain RV and LV mass ratios and RV and LV end-diastolic volume ratios.

Statistical analysis

The SPSS for Windows Software package (version 12.0.1, SPSS Inc, Chicago Illinois) was used for data analysis. Normally distributed values are presented as means ± standard deviations. Independent t-tests were used for comparison of PAH patients and healthy controls. Comparison of three categories was performed with one-way analysis of variance with post-hoc Bonferroni correction. To determine the discriminative power of dichotomous variables for diagnosing PAH, cross tabulations were used for determination of sensitivity and specificity. To determine the diagnostic value of vectorcardiogram-derived parameters compared to conventional electrocardiographic parameters we used a receiver operating characteristic (ROC) analysis. Areas under the curve (AUC) were compared using the method proposed by Hanley and McNeil [24], which corrects for existing correlations between ROC curves derived from the same cases. Binary logistic regression analysis was used to determine the optimal model for classification of increased RV afterload for both ECG-derived variables and vectorcardiogram-

derived variables. Subsequently the optimal model was used in a bootstrapping analysis to determine the accuracy of the odds ratio (OR) in this classification model. Pearson correlation analysis was used for analysis of intra-observer and inter-observer variability, as well as for comparison of the VG with CMR derived variables of RV mass, and volume. A value of $P<0.05$ was considered to be statistically significant.

Results

Patient characteristics at the time of the diagnostic right heart catheterization are presented in Table 1. Controls (n=144, 30 male) were younger than patients (mean age: 19.7 ± 1.3 years vs. 43.7 ± 22.8 years, $P<0.001$). Mean heart rate was 82·min^{-1} ± 17·min^{-1} in PAH patients vs. 80·min^{-1} ± 14·min^{-1} in controls ($P=0.47$). Calculation of the VG proved to be highly reproducible, with both excellent intra-observer (r=0.994, $P<0.001$) and inter-observer agreement (r=0.992, $P<0.001$).

Typical examples of RV and pulmonary artery pressures (PAP) with the corresponding ECG and vectorcardiogram findings are presented in Figure 1 for a healthy subject (catheterized for exclusion of familial PAH after inconclusive transthoracic contrast echocardiography), a patient with moderate PAH, and a patient with severe PAH. It can be appreciated from leads I and aVF that an intermediate frontal plane QRS axis is present in the subject without PAH as well as in the patient with moderate PAH, whereas a right axis deviation is present in the patient with severe PAH. Furthermore, lead V1 is within normal limits for both the subject without PAH and the patient with moderate PAH, whereas lead V1 qualifies for RV hypertrophy in the patient with severe PAH: R>S and R>5 mm, initial P wave>1mm high and wide, and the T wave is discordant with the QRS, reflecting RV strain. A closer look at the projection of the VG on the X, Y, and Z axes reveals that the VG projection on the X axis (net QRST area in the X lead) becomes smaller proportional to the degree of chronic RV pressure load. The lower

Table 1: PAH patient characteristics (n=72, 15 male)

Characteristic	Mean
RAP (mmHg)	9 ± 6
Mean PAP (mmHg)	56 ± 14
PCWP (mmHg)	7 ± 4
PVR (mmHg·L^{-1}·min^{-1})	13.4 ± 7.2
Mixed venous SpO_2 (%)	63 ± 10
Cardiac index (L·m^{-2}·min^{-1})	2.3 ± 0.9

RAP = right atrial pressure, Mean PAP = mean pulmonary artery pressure, PCWP = pulmonary capillary wedge pressure, PVR = pulmonary vascular resistance, SpO_2 = oxygen saturation in blood.

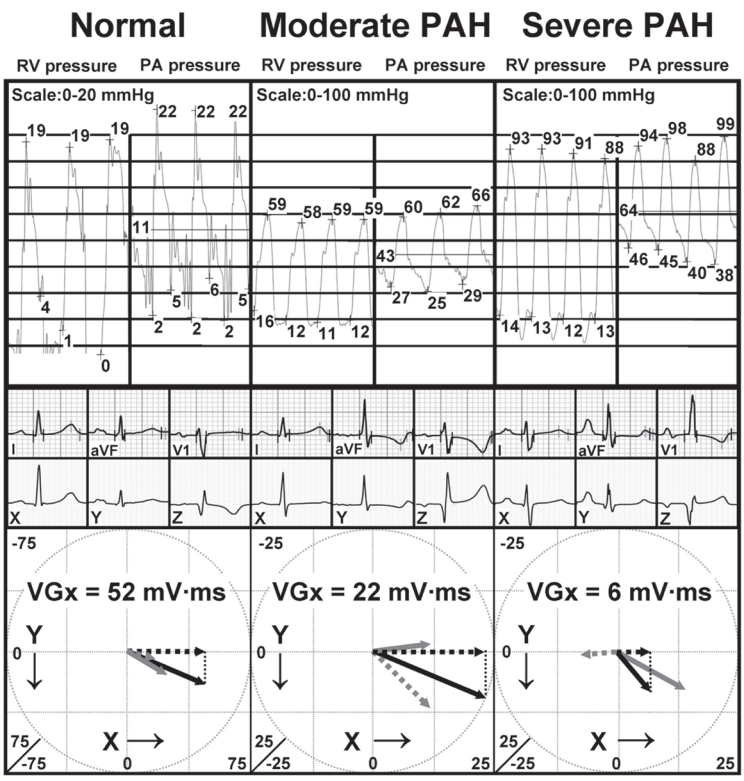

Figure 1

The effect of different levels of chronic RV pressure load on the ECG and vectorcardiogram is illustrated in a patient without PAH (catheterized for exclusion of familial PAH after inconclusive transthoracic contrast echocardiography; left), a patient with moderate PAH (middle), and a patient with severe PAH (right), respectively. Top panels: RV and pulmonary artery pressures (PAP). Horizontal lines: mean PAP; mean PAP=11 mmHg in the patient without PAH, mean PAP=43 mmHg in the patient with moderate PAH, and mean PAP=64 mmHg in the patient with severe PAH. Of note: the pressure scale is set at 0 - 20 mmHg in the control subject with normal RV pressure load, whereas the pressure scale is set at 0 - 100 mmHg in the patients with moderate and severe PAH. Second row panels: corresponding ECG leads I, aVF, and V1; no ECG abnormalities are present in the patient with moderate PAH, despite a chronically elevated RV pressure load. Third row panels: the VG projections (QRST integral) on the X, Y, and Z axis, revealing that the VG projection on the X axis gradually becomes smaller, proportionate to the degree of chronic RV pressure load. The relation between the QRS integral, the T wave integral and the VG is illustrated in the bottom row for the VG projection on the X axis (VGx) in the frontal plane. The VG (solid black line) is the vectorial sum of the QRS (dashed grey line) and T (solid grey line) integrals. VGx is the projection of the VG on the X axis (dashed black line). Of note: all numbers in the bottom panels are expressed in mV·ms, with a scale of 0 - 75 mV·ms for the control subject with normal RV pressure load, and a scale of 0 - 25 mV·ms for the patients with moderate and severe PAH.

Table 2: Difference in ECG derived variables between controls and patients with moderate or severe PAH

	Controls (n=144)	Mild to Moderate PAH (n=16)	Severe PAH (n=56)	Controls vs. Mild to Moderate PAH	Controls vs. Severe PAH	Mild to Moderate PAH vs. Severe PAH
ECG variables	Mean ± SD	Mean ± SD	Mean ± SD	*P*	*P*	*P*
QRS	38.5 ± 13.8	24.3 ± 10.9	28.6 ± 16.2	0.001	<0.001	NS
T	68.4 ± 25.2	31.2 ± 13.3	37.4 ± 19.3	<0.001	<0.001	NS
VG	85.9 ± 27.6	34.1 ± 17.1	35.0 ± 17.8	0.001	<0.001	NS
QRS-X	22.4 ± 10.1	4.4 ± 9.6	-2.9 ± 11.1	<0.001	<0.001	0.040
QRS-Y	21.2 ± 10.5	15.3 ± 9.3	14.4 ± 13.3	NS	<0.001	NS
QRS-Z	18.8 ± 12.5	12.1 ± 12.0	-2.7 ± 23.9	NS	<0.001	0.005
T-X	46.6 ± 19.2	15.0 ± 12.9	6.9 ± 18.5	<0.001	<0.001	NS
T-Y	21.6 ± 12.6	5.9 ± 16.5	-0.5 ± 22.3	0.001	<0.001	NS
T-Z	-40.9 ± 21.8	1.6 ± 22.2	18.9 ± 23.4	<0.001	<0.001	0.020
VG-X	68.1 ± 22.0	17.5 ± 15.0	2.8 ± 16.1	<0.001	<0.001	0.033
VG-Y	42.7 ± 17.8	21.2 ± 12.5	14.7 ± 20.6	<0.001	<0.001	NS
VG-Z	-20.4 ± 21.9	12.9 ± 13.0	13.8 ± 21.4	<0.001	<0.001	NS
QRS-T(º)	71.5 ± 23.5	97.5 ± 45.9	105.2 ± 38.6	0.004	<0.001	NS

QRS, T, and QRST integrals (the latter denoted as ventricular gradient, VG). "-X", "-Y", "-Z": projections on the X, Y, and Z axis, respectively (all in mV·ms). QRS-T(º): spatial angle between the QRS and T integrals.

panels illustrate also that chronic RV pressure load leads to a proportionate decrease in QRS and T integral vectors, and to an increase in QRS-T spatial angle (Table 2), together resulting in a smaller and differently oriented VG.

In general, conventional ECG criteria had low diagnostic accuracy for presence of increased RV afterload (Table 3). With a sensitivity of 84% and a specificity of 96%, a QRS axis >90º in the frontal plane was the conventional ECG parameter with the highest individual diagnostic accuracy for chronically increased RV pressure load (Table 3). Multivariable binary logistic regression analysis performed in a backward stepwise fashion (removal if $P>0.10$, inclusion if $P<0.05$, a priori chance of PAH=0.33) rendered the following formula for optimal prediction of presence of PAH: y = 2.204 · (presence of rSr' or rSR' in lead V1) + 3.079 · (presence of R:S>1 in lead V1 with R>0.5mV) + 4.542 · (presence of QRS axis >90º) - 6.679 (sensitivity=89%, specificity=94%, $P<0.001$). Although sensitivity and specificity did not differ importantly between the prediction based on a multivariable analysis compared to the single prediction of the presence of QRS axis>90º, the multivariable prediction showed

Table 3: Diagnosis of chronically increased RV pressure load with conventional ECG criteria

ECG criterion	Sensitivity (%)	Specificity (%)	Correct diagnosis in all 216 subjects (%)
P>0.25 mV in lead II	30	91	71
qR pattern in lead V1	36	100	79
rSR' pattern in lead V1	18	96	70
R in lead aVR>0.5 mV	14	100	71
R:S>1 in lead V1 with R>0.5 mV	51	98	82
R in lead V1 + S in lead V5>1 mV	53	94	80
R:S<1 in lead V5 or V6	24	99	74
R≤0.4 mV in lead V5 or V6 with S=<0.2mV in lead V1	13	100	71
S in lead I and Q in lead III	49	70	63
S wave in leads I, II, and III	28	74	59
S in lead V5 or V6=>0.7 mV	31	98	76
Inverted T wave in lead V1	69	62	64
QRS axis >90°	84	96	92

The "P" denotes the deflection caused by atrial depolarization. The "Q" denotes an initial negative deflection, the "R" is the first positive wave, and the first negative wave after a positive wave is the S wave. A second upright wave following an S wave is an R' wave. Tall waves (>0.5 mV) are denoted by capital letters and smaller ones by lowercase letters. Together, the QRS complex reflects ventricular depolarization. The T wave denotes the deflection caused by ventricular repolarization.

a larger AUC than QRS axis>90º alone (Figure 2).

Significant differences in the VG were observed, however, between PAH patients and healthy controls. In general, in PAH patients the VG assumed a different orientation from healthy controls and was also considerably smaller: 34.8 ± 17.5 mV·ms vs. 85.9 ± 27.6 mV·ms (P<0.001) (Figure 3). It is easily appreciated from the right lower panel that VG magnitude alone can not accurately separate PAH patients and healthy controls. Multivariable analysis showed that a combination of VG magnitude and orientation had superior discriminating power to either variable alone, especially the VG projection on the X axis. Multivariable analysis in a stepwise forward fashion (inclusion if P<0.01, removal if P>0.05) including the respective orthogonal projections of the mean QRS integrals, mean T-wave integrals, and the mean VGs, illustrated that of all the significantly related single variables the VG projection on the X axis was the variable with the highest discriminating power (Table 2). PAH patients and controls were therefore compared for the VG projection on the X axis. Receiver-operating-curve analyses for diagnosis of increased RV pressure load are presented in Figure 3. The VG magnitude

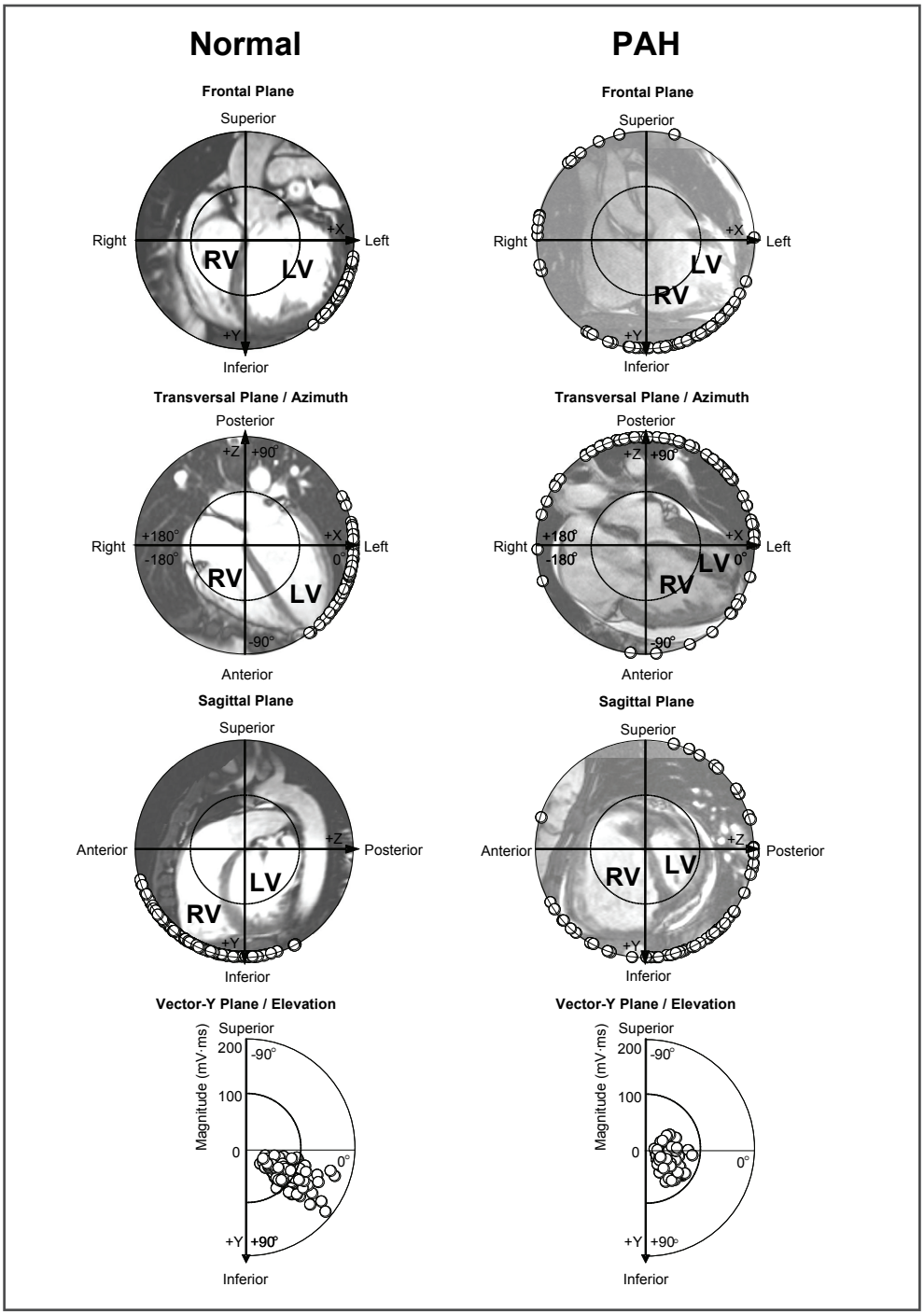
Normal
PAH
Frontal Plane
Superior
Right
Left
Inferior
RV
LV
+X
+Y
Transversal Plane / Azimuth
Posterior
Anterior
+Z
+90°
+180°
-180°
0°
-90°
Sagittal Plane
Vector-Y Plane / Elevation
Magnitude (mV·ms)
200
100
0

◄ **Figure 2**

Superimposed representations of the spatial orientation of all individual VG vectors in the frontal, transversal and sagittal planes, and of the VG vector magnitude in the Vector-Y plane. Left-side plots: normal subjects; right-side plots: PAH patients. Insets are frontal, transversal and sagittal MRI slices of one arbitrarily chosen normal subject (left) and PAH patient (right). The MRI insets are chosen in such a way that the AV-node area is in the origin, which parallels the usual vectorial representation of the electrical heart activity. VG azimuths can be directly appreciated in the transversal plane, while the VG magnitudes and elevations can be directly appreciated in the Vector-Y plane. Of note, this Vector-Y plane is a different plane for each vector; therefore, there is no representative MRI slice that can serve as an inset for the Vector-Y plane. All VG-Y planes have been superimposed to allow comparison of all VG magnitudes and elevations. These images illustrate that although in normals there is considerable heterogeneity in both VG orientation and magnitude, the VG orientation is quite different in PAH patients and VG magnitude is generally lower. Due to the heterogeneity of disease severity among PAH patients the VG orientation and VG magnitude varies considerably among PAH patients.
'O'=an individual VG

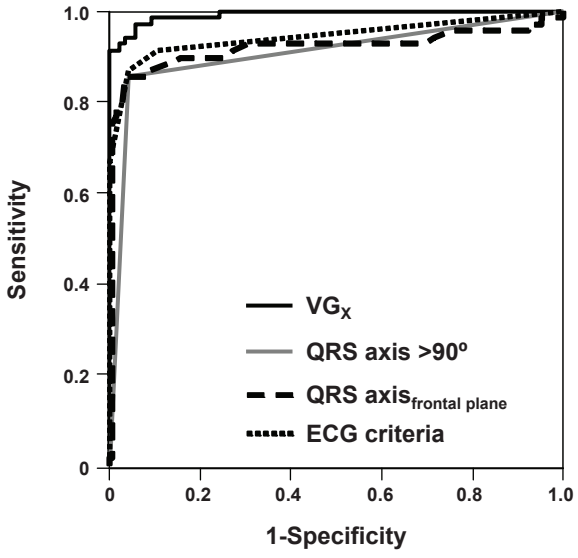

Figure 3

Receiver operating characteristics (ROC) curves for diagnosis of increased RV pressure load. Solid black line: ROC of the VG projection on the X axis (continuous variable; AUC=0.993). Solid grey line: ROC of the presence of a QRS axis >90º in the frontal plane (dichotomous variable; AUC=0.900). Coarse dashed line: ROC of the QRS axis in the frontal plane (continuous variable; AUC=0.904). Fine dashed line: ROC of the composite model of conventional ECG criteria: y=2.204·(presence of rSr' or rSR' in lead V1) + 3.079·(presence of R:S>1 in lead V1 with R>0.5mV) + 4.542·(presence of QRS axis >90º) - 6.679 (AUC=0.945).

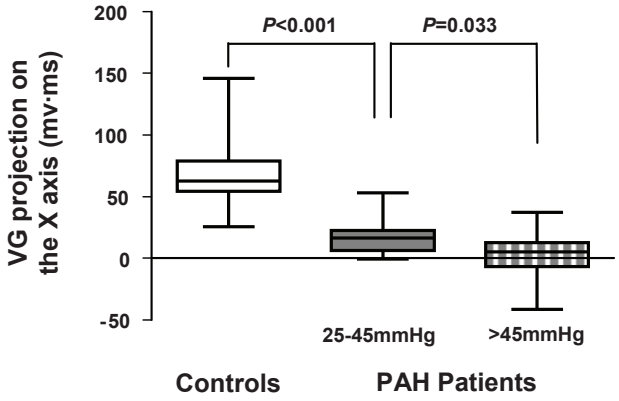

Figure 4

In healthy controls (assumed mean PAP<25 mmHg, n=144) the VG projection on the X axis is much larger than in patients with a chronically increased RV pressure load (mean PAP>25 mmHg, n=72). Furthermore, the VG projection on the X axis allows distinction between a mildly to moderately elevated RV pressure load (mean PAP=25-45 mmHg) and a severely elevated RV pressure load (mean PAP>45 mmHg, n=56).

projection on the X axis (AUC=0.993) had a significantly larger AUC than presence of a QRS axis >90º (dichotomous variable; AUC=0.900, z-score=3.36, $P<0.01$), QRS axis in the frontal plane (continuous variable; AUC=0.904, z-score=2.89, $P<0.01$), and the composite model of conventional ECG parameters (AUC=0.945, z-score=2.27, $P<0.05$). Binary logistic regression analysis rendered the following formula for prediction of presence of increased RV pressure load by the X component of the VG: $y = -0.195 \cdot VGx + 6.195$ (OR=0.82 for each unit increase in VG projection on the X axis) with a sensitivity of 97% and a specificity of 94%. Bootstrapping analysis validated the adequacy of this model, rendering a 95% confidence interval for the OR of 0.74-0.91 ($P<0.001$) based on a normal distribution of the regression coefficients over the bootstrap samples. To assess whether the VG projection on the X axis could differentiate between mild to moderate and severe PAH, patients were stratified in two categories according to mean pulmonary artery pressure (mean PAP) level: mean PAP=25-45 mmHg (n=16), and mean PAP>45 mmHg (n=56). Figure 4 illustrates that the VG projection on the X axis was already markedly decreased in patients with mildly to moderately increased RV pressure load (mean PAP=25-45 mmHg), and even more in patients with a severely increased RV pressure load (mean PAP>45 mmHg). One-way analysis of variance showed that PAH patients with a mean PAP=25-45 mmHg had a VG projection on the X axis that was significantly lower than in controls (17.5 ± 15.0 mV·ms vs. 68.1 ± 22.0

mV·ms, $P<0.001$), but still higher than in PAH patients with a mean PAP>45 mmHg (17.5 ± 15.0 mV·ms vs. 2.8 ± 16.1 mV·ms, $P=0.033$). Here too, the projection of the VG on the X axis was best discriminating, since the VG magnitude alone did not differentiate between patients with a mean PAP=25-45 mmHg and patients with a mean PAP>45 mmHg, although VG magnitude in both groups of PAH patients was lower than in controls (Table 2.) Since the VG is the vectorial sum of the QRS and T integrals, projections of QRS and T integrals as well as the QRS-T spatial angle were also calculated. Mean QRS integral and mean T-wave integral magnitudes and projections on the X, Y, and Z axes were generally different between controls and PAH patients, although the distinction between mild to moderate PAH and severe PAH could only be made by QRS integral projections on the X and Z axis, the T-wave integral projection on the Z axis, and again the VG projection on the X axis (Table 2). Overall the QRS-T spatial angle was higher in patients with a chronically increased RV afterload than in controls, signifying that there is a higher degree of discordance between depolarization and repolarization in PAH patients (Table 2).

CMR showed that RV mass was related to the VG projection on the X axis (Figure 5A), and a trend was observed towards a relation between a higher RV volume and a smaller VG projection on the X axis (Figure 5B).

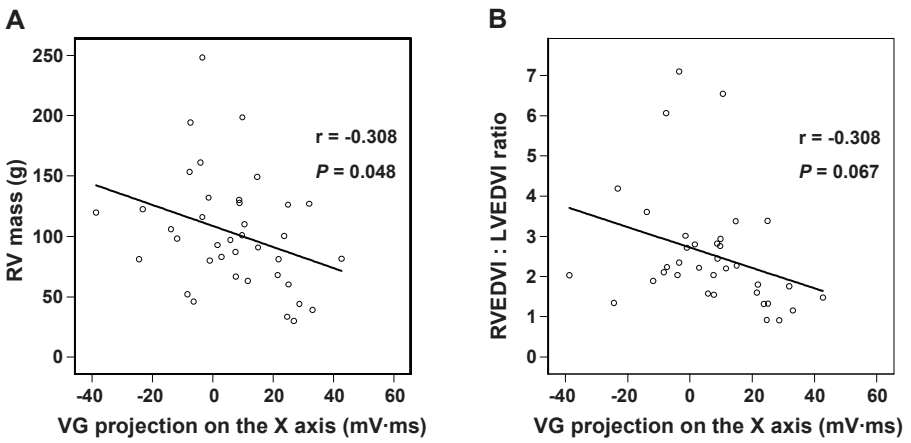

Figure 5

A. RV mass showed an inverse relation with the VG projection on the X axis (r=-0.323, P=0.048)

B. There was a trend toward a similar inverse relation between a higher RV end-diastolic volume and the VG projection on the X axis (r=-0.308, P=0.067). RVEDVI=RV end-diastolic volume indexed for body surface area. LVEDVI=LV end-diastolic volume indexed for body surface area.

Discussion

The key finding of this study is that it proves that the ECG-derived VG is highly accurate in detecting chronic increase in RV pressure load, and as such can be used to distinguish between normal RV pressure load, mildly to moderately increased RV pressure load, and severely increased chronic RV pressure load. Furthermore, the ECG-derived VG proved to be of higher diagnostic accuracy for chronically increased RV pressure load than conventional ECG parameters. Available CMR data suggest that VG changes in PAH patients reflect changes in APD heterogeneity related to RV remodeling as a result of an increased RV pressure load.

Vectorcardiography vs. electrocardiography

The general approach towards ECG interpretation is one directed at individual leads overlying cardiac regions of interest, whereas each lead is derived from the same heart vector. Although a projection of the VG in a direction of interest is essentially a similar simplification of assessing a 3D process in time, this projection nevertheless holds all information derived from the two limb leads and six chest leads [9]. The vectorcardiogram takes into account that ECG leads have a different sensitivity (amongst others because of the variation in proximity to the heart) and does not suffer from the problem that onset QRS, end QRS, and end T instants may differ per lead [9]. The ECG-derived VG therefore renders robust results. Since calculation of the VG requires only straightforward integration over the QRST complex of the instantaneous heart vector (that can be synthesized from the ECG leads by a simple matrix multiplication) [18], this algorithm can easily be implemented in existing ECG analysis software, like we did in our LEADS program.

Despite the recognition of certain ECG characteristics in newborns and patients with an increased RV afterload, the diagnostic potential of conventional 12-lead ECG parameters for increased RV afterload has been reported as insufficient for clinical use or screening purposes [7, 25-27]. The results of our study support this view, yet underline the importance of using the full potential of an electrocardiogram. Contemporary software now renders (synthesized) vectorcardiogram-derived calculations with such ease that clinical application of this information is certainly feasible [17].

Rationale for using the VG

The VG is oriented towards the left and slightly antero-inferior in healthy human beings (Figure 2) within a smaller range than the mean QRS axis orientation in the frontal plane

[22]. The VG is the integrated ventricular APD heterogeneity, which is the 3D sum of the integrated ventricular depolarization and repolarization heterogeneities [10]. As such, the VG has a strong physiological link to the way in which the ventricular APD distribution is affected by chronic RV pressure load. Any intra-individual change in the VG magnitude and orientation signifies an alteration in APD heterogeneity in the ventricles, and hence a change in myocardial electrophysiological properties [10, 12]. Chou et al. evaluated the use of QRS loop area for diagnosis of RV hypertrophy [28]. As discussed by the authors, the QRS loop area is the sum of all depolarization vectors, allowing appreciation of the resultant spatial orientation and the ratio of leftward and rightward oriented forces, rendering evaluation of quantitative conventional ECG parameters of RV hypertrophy superfluous [28]. Cowdery et al. recognized the importance of the QRS loop area, and further improved diagnostic accuracy for RV hypertrophy by interpreting QRS amplitude in the transversal plane (60% sensitivity and 96% specificity) [29]. Kawaguchi et al. further concluded that repolarization characteristics should not be overlooked, since in their diagnostic model for RV hypertrophy combined T loop area and direction rendered the best result [30]. The high diagnostic accuracy for presence of chronic RV pressure load of the 3D VG (Figure 3), which is the sum of QRS and T integrals, is in accordance with these reports regarding changes in QRS complex and T wave morphology in patients with an increased RV pressure load [28-30].

There is a distinct evolution of ECG characteristics with developing PAH [13]. Changes in VG with increasing RV pressure load are best assessed in 3D, although single lead assessment is theoretically possible [11, 12]. Much like we observed in rats [13], a higher RV pressure load effectively cancels out the net LV contribution to the VG (Figure 1, lower panel) [13, 31, 32]. Obviously, this cancellation effect occurs because RV pressure load induced RV hypertrophy introduces APD heterogeneity substantially opposing the net LV APD heterogeneity. Thus, mild to moderate elevation of RV pressure load decreases VG magnitude, while VG orientation is largely maintained (Table 2, Figure 4). Further elevation of RV pressure load does not necessarily lead to a further decrease of VG magnitude, although it may drastically affect VG orientation (Figure 1, Figure 4, Table 2) [10]. A comparison with CMR studies in a subgroup of patients showed that RV pressure load induced changes in APD heterogeneity were related to changes in RV to LV mass ratio rather than to changes in RV to LV volume ratio. In steadily developing PAH, hypertrophy occurs already with mildly elevated pulmonary artery pressure, before dilatation of the RV is seen [13, 33]. This may explain the closer association of the VG projection on the X axis with RV hypertrophy rather than with RV dilatation.

Limitations

In the absence of available ECGs from the time before development of PAH we compared the ECGs of patients with a mildly to moderately elevated RV afterload as well as the ECGs of patients with a severely elevated RV afterload to the ECGs of healthy control subjects. Since we may assume that idiopathic PAH patients once had a normal RV afterload, comparison with ECGs from healthy individuals seems to be the most obvious alternative [34, 35]. This cross-sectional approach allows appreciation of the supposed evolution of changes in the VG in response to an increasing RV pressure load. The selection of patients with idiopathic PAH precludes application of our findings to patients with important lung disease or left-sided heart disease. However, since even a mildly to moderately elevated RV pressure load was associated with marked differences in the VG, the ECG seems a suitable screening tool for increased RV pressure load in selected groups of patients, such as relatives of patients with familial PAH, patients with HIV, systemic sclerosis, portal hypertension, or other diseases associated with development of PAH [7, 26]. Despite the obvious advantages of simply projecting the VG in the direction of interest (the X axis), a potential downside of this approach is the observed non-linear relation between PAH severity and the degree of chronic RV pressure load (Figure 4) which precludes classification of chronic RV pressure load beyond the categories of normal, mild to moderate, and severe RV pressure load. The size of our study group did not permit use of a learning set and test set. However, bootstrapping analysis confirmed the validity of the proposed predictive model of increased RV pressure load. The uneven sample sizes of mild to moderate PAH patients and severe PAH groups is suboptimal, yet a representative reflection of the high number of PAH patients with a mean PAP > 45mmHg at the time of diagnosis. The limited sample size of patients with mild to moderate PAH in our study may have affected the ability of the other ECG variables to discriminate between mild to moderate PAH and severe PAH.

Clinical implications

In patients with a genetic profile or disease known to predispose to PAH, serial ECG recording may prove a feasible concept for early detection of an increasing RV afterload. Apart from incorporation of calculations based on the VG into software for electrocardiographs, another way of indirectly assessing presence of chronic RV pressure load may be to calculate QRST areas in a lead with a lead vector that assumes about the direction of the X axis, such as lead I or V6. Whether such an individual lead-based VG approximation will prove to be of similar diagnostic accuracy deserves further study. Screening for PAH among patients at risk is still subject to debate, but is generally regarded as very costly due to the high rate of false

negative diagnoses with the available tools for non-invasive detection [36, 37]. The improved ECG detection of right ventricular pressure load using the VG may dramatically cut cost of screening. Whether sequential ECG recording allows for early distinction of 'responders' from 'non-responders' to PAH attenuating therapy by detection of VG changes, a distinction currently made by repetitive 6-minute walking tests, cardiac magnetic resonance imaging or right heart catheterization deserves further study [23, 38]. In patients without congenital or acquired left-sided heart disease and/or pulmonary disease the VG may prove to be an important tool for screening purposes and follow-up.

Conclusion

Chronically increased right ventricular pressure load induces changes in ventricular APD heterogeneity, which are reflected by distinct changes in the ventricular gradient. The ECG-derived ventricular gradient can be used with high accuracy for detection of chronically increased right ventricular pressure load, and is a potentially useful tool for follow-up in selected groups of patients. VG changes in PAH patients likely reflect changes in ventricular APD heterogeneity related to RV remodeling as a result of an increased RV pressure load.

References

1. Kosiborod M and Wackers FJ. Assessment of right ventricular morphology and function. Semin Respir Crit Care Med 2003;24:245-262.

2. Farb A, Burke AP and Virmani R. Anatomy and pathology of the right ventricle (including acquired tricuspid and pulmonic valve disease). Cardiol Clin 1992;10:1-21.

3. Chemla D, Castelain V, Herve P, Lecarpentier Y and Brimioulle S. Haemodynamic evaluation of pulmonary hypertension. Eur Respir J 2002;20:1314-1331.

4. Harrigan RA and Jones K. ABC of clinical electrocardiography. Conditions affecting the right side of the heart. BMJ 2002;324:1201-1204.

5. Sukhija R, Aronow WS, Ahn C and Kakar P. Electrocardiographic abnormalities in patients with right ventricular dilation due to acute pulmonary embolism. Cardiology 2006;105:57-60.

6. Punukollu G, Gowda RM, Vasavada BC and Khan IA. Role of electrocardiography in identifying right ventricular dysfunction in acute pulmonary embolism. Am J Cardiol 2005;96:450-452.

7. McGoon M, Gutterman D, Steen V, Barst R, McCrory DC, Fortin TA and Loyd JE. Screening, early detection, and diagnosis of pulmonary arterial hypertension: ACCP evidence-based clinical practice guidelines. Chest 2004;126:14S-34S.

8. Barst RJ, McGoon M, Torbicki A, Sitbon O, Krowka MJ, Olschewski H and Gaine S. Diagnosis and differential assessment of pulmonary arterial hypertension. J Am Coll Cardiol 2004;43:40S-47S.

9. MacFarlane PW, Edenbrandt L and Pahlm O. 12 Lead Vectorcardiography. Oxford: Butterworth-Heinemann, 1995.

10. Draisma HH, Schalij MJ, van der Wall EE and Swenne CA. Elucidation of the spatial ventricular gradient and its link with dispersion of repolarization. Heart Rhythm 2006;3:1092-1099.

11. Hurst JW. Thoughts about the ventricular gradient and its current clinical use (Part I of II). Clin Cardiol 2005;28:175-180.

12. Hurst JW. Thoughts about the ventricular gradient and its current clinical use (part II of II). Clin Cardiol 2005;28:219-224.

13. Henkens IR, Mouchaers K, Vliegen HW, van der Laarse WJ, Swenne CA, Maan AC, Draisma HH, Schalij I, van der Wall EE, Schalij MJ and Vonk Noordegraaf A. Early changes in rat hearts with developing pulmonary arterial hypertension can be detected with 3-dimensional electrocardiography. Am J Physiol Heart Circ Physiol 2007;

14. Kim NH. Diagnosis and evaluation of the patient with pulmonary hypertension. Cardiol Clin 2004;22:367-3vi.

15. Mirvis DM and Goldberger AL. Electrocardiography. In: Braunwald's Heart Disease, edited by Zipes DP, Libby P, Bonow RO and Braunwald E. Saunders, 2004, p. 120-125.

16. Galie N, Torbicki A, Barst R, Dartevelle P, Haworth S, Higenbottam T, Olschewski H, Peacock A, Pietra G, Rubin LJ, Simonneau G, Priori SG, Garcia MA, Blanc JJ, Budaj A, Cowie M, Dean V, Deckers J, Burgos EF, Lekakis J, Lindahl B, Mazzotta G, McGregor K, Morais J, Oto A, Smiseth OA, Barbera JA, Gibbs S, Hoeper M, Humbert M, Naeije R and Pepke-Zaba J. Guidelines on diagnosis and treatment of pulmonary arterial hypertension. The Task Force on Diagnosis and Treatment of Pulmonary Arterial Hypertension of the European Society of Cardiology. Eur Heart J 2004;25:2243-2278.

17. Draisma HH, Swenne CA and Van de Vooren H. LEADS: an interactive research oriented ECG/VCG. Computers in Cardiology 2005;32:515-518.

18. Edenbrandt L and Pahlm O. Vectorcardiogram synthesized from a 12-lead ECG: superiority of the inverse Dower matrix. J Electrocardiol 1988;21:361-367.

19. Burger HC. A theoretical elucidation of the notion ventricular gradient. Am Heart J 1957;53:240-246.

20. Kossmann CE, Brody DA, Burch GE, Hecht HE, Johnston FD, Kay C, Lepeschkin E, Pipberger HV, Baule G, Berson AS, Briller SA, Geselowitz DB, Horan LG and Schmitt OH. Report of committee on electrocardiography, American Heart Association. Recommendations for standardization of leads and of specifications for instruments in electrocardiography and vectorcardiography. Circulation 1967;35:583-602.

21. Blackburn H. Electrocardiographic classification for population comparisons. The Minnesota code. J Electrocardiol 1969;2:5-9.

22. Yano K and Pipberger HV. Spatial magnitude, orientation, and velocity of the normal and abnormal QRS complex. Circulation 1964;29:107-117.

23. van Wolferen SA, Marcus JT, Boonstra A, Marques KM, Bronzwaer JG, Spreeuwenberg MD, Postmus PE and Vonk Noordegraaf A. Prognostic value of right ventricular mass, volume, and function in idiopathic pulmonary arterial hypertension. Eur Heart J 2007;28:1250-1257.

24. Hanley JA and McNeil BJ. A method of comparing the areas under receiver operating characteristic curves derived from the same cases. Radiology 1983;148:839-843.

25. Rich S, Dantzker DR, Ayres SM, Bergofsky EH, Brundage BH, Detre KM, Fishman AP, Goldring RM, Groves BM and Koerner SK. Primary pulmonary hypertension. A national prospective study. Ann Intern Med 1987;107:216-223.

26. Ahearn GS, Tapson VF, Rebeiz A and Greenfield JC, Jr. Electrocardiography to define clinical status in primary pulmonary hypertension and pulmonary arterial hypertension secondary to collagen vascular disease. Chest 2002;122:524-527.

27. Penaloza D and Arias-Stella J. The heart and pulmonary circulation at high altitudes: healthy highlanders and chronic mountain sickness. Circulation 2007;115:1132-1146.

28. Chou TC, Masangkay MP, Young R, Conway GF and Helm RA. Simple quantitative vectorcardiographic criteria for the diagnosis of right ventricular hypertrophy. Circulation 1973;48:1262-1267.

29. Cowdery CD, Wagner GS, Starr JW, Rogers G and Greenfield JC, Jr. New vectorcardiographic criteria for diagnosing right ventricular hypertrophy in mitral stenosis: comparison with electrocardiographic criteria. Circulation 1980;62:1026-1032.

30. Kawaguchi Y. Studies on deflection area vectors of QRS and T and ventricular gradient in right ventricular hypertrophy. Jpn Circ J 1985;49:395-405.

31. Abildskov JA, Burgess MJ, Millar K, Wyatt R and Baule G. The primary T wave a new electrocardiographic waveform. Am Heart J 1971;81:242-249.

32. Burgess MJ, Millar K and Abildskov JA. Cancellation of electrocardiographic effects during ventricular recovery. J Electrocardiol 1969;2:101-107.

33. Vonk Noordegraaf A, Marcus JT, Holverda S, Roseboom B and Postmus PE. Early changes of cardiac structure and function in COPD patients with mild hypoxemia. Chest 2005;127:1898-1903.

34. Rubin LJ. Pathology and pathophysiology of primary pulmonary hypertension. Am J Cardiol 1995;75:51A-54A.

35. Perros F, Dorfmuller P and Humbert M. Current insights on the pathogenesis of pulmonary arterial hypertension. Semin Respir Crit Care Med 2005;26:355-364.

36. Mukerjee D, St GD, Knight C, Davar J, Wells AU, Du Bois RM, Black CM and Coghlan JG. Echocardiography and pulmonary function as screening tests for pulmonary arterial hypertension in systemic sclerosis. Rheumatology (Oxford) 2004;43:461-466.

37. Williams MH, Handler CE, Akram R, Smith CJ, Das C, Smee J, Nair D, Denton CP, Black CM and Coghlan JG. Role of N-terminal brain natriuretic peptide (N-TproBNP) in scleroderma-associated pulmonary arterial hypertension. Eur Heart J 2006;27:1485-1494.

38. Kawut SM and Palevsky HI. Surrogate end points for pulmonary arterial hypertension. Am Heart J 2004;148:559-565.

VII

Pulmonary hypertension: the role of the electrocardiogram

Ivo R. Henkens

Roderick W.C. Scherptong

Klaas W. van Kralingen

Salah A.M. Said

Hubert W. Vliegen

Neth Heart J 2008;16:250-4

Abstract

A 54-year-old female was referred to our center for further evaluation of recently established severe pulmonary hypertension. Six months prior to presentation to the cardiologist from the referring center the patient had first experienced exertional dyspnea. At the time of presentation to the referring cardiologist the patient's ECG showed signs of an increased right heart load. Interestingly, this patient had undergone a thorough cardiac evaluation in the referring center seven years before when she suffered from severe hyperthyroidism. At that time there were no symptoms or signs of pulmonary hypertension on ECG, echocardiography, or at heart catheterization. Thorough evaluation in cooperation with the referring center demonstrated that this patient suffered from idiopathic pulmonary arterial hypertension, a rare form of pulmonary hypertension. We conclude this report with a discussion on the potential use of the ECG for diagnosis of increased right heart load.

In August 2005, a 54-year-old female was referred to our center for additional evaluation into the etiology of recently established severe pulmonary arterial hypertension (PAH). The patient had first experienced exertional dyspnea six months prior to presentation to the referring cardiologist. There was no history of cardiac or pulmonary disease, but this patient had undergone an extensive cardiac evaluation seven years before, after a one-time syncope. At that time, the ECG showed a sinus rhythm, a QRS axis of 36º, normal P waves, conduction intervals within normal limits, and an inverted T wave in leads aVF and V4-V6 (Figure 1A). Because of the observed repolarization abnormalities, a series of additional test was performed. Apart from severe hyperthyroidism, there were no cardiac or pulmonary

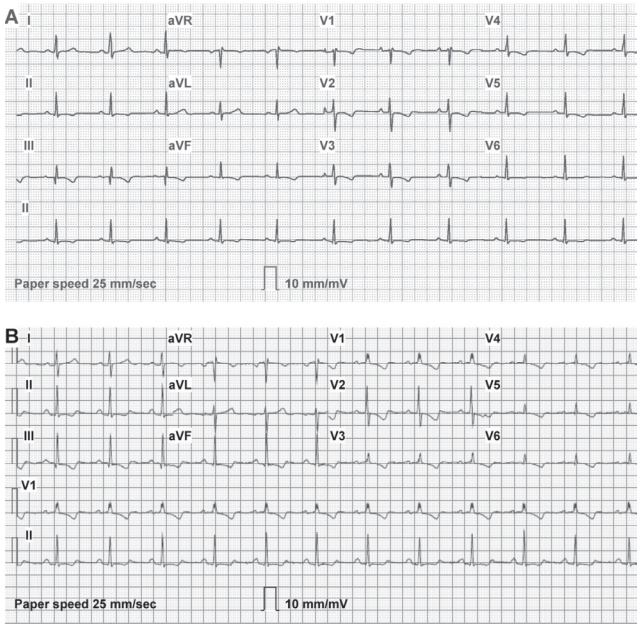

Figure 1

A) ECG of the patient at first presentation, seven years before the diagnosis of pulmonary arterial hypertension, demonstrated a regular sinus rhythm of 65 bpm, a QRS axis of 36º, normal P waves, conduction intervals within normal limits, and an inverted T wave in leads aVF and V4-V6. In short, there were no reasons to suspect an increased right heart load at the time, based on this ECG.

B) ECG recorded at the time of renewed presentation showed a regular sinus rhythm of 84/min, a QRS axis of 90º, the R-wave in lead V1 measured 6 mm in the absence of an S wave, and there were diffuse repolarization abnormalities, all in agreement with an increased right heart load. Given this second ECG, especially with an available ECG from several years before, further investigation regarding an increased right heart load is warranted.

abnormalities found at echocardiography (tricuspid and pulmonary valve regurgitation gradient were within normal limits, there was no right atrial or ventricular dilatation, right ventricular hypertrophy, or paradoxical septal bowing), left heart and coronary catheterization, or pulmonary function tests. At renewed presentation, the ECG now showed a QRS axis of 90º, the R-wave in lead V1 measured 6 mm in the absence of an S wave, and there were diffuse repolarization abnormalities, all in agreement with an increased right heart load (Figure 1B). At bicycle ergometry the patient performed 120W (88% of predicted), without evidence of exercise-induced ischemia. A pulmonary perfusion scan showed no signs of pulmonary embolism. Coronary angiography again revealed normal coronary arteries. The patient (height: 170 cm, weight: 90 kg) now had a normal thyroid function, and used no medication. Hemodynamics at right heart catheterization are presented in Figure 2. Pulmonary pressures and pulmonary vascular resistance approached systemic values, signifying the degree of right heart load was severely elevated in this patient. According to the guidelines [1] the patient was further evaluated, eliminating possible etiologic factors in a stepwise fashion. Our patient denied past use of anorexigens or intravenous drugs. There were no relatives with similar symptoms or established pulmonary hypertension. There was a history of alcohol abuse, but our patient had managed to refrain from drinking alcohol for several years, and

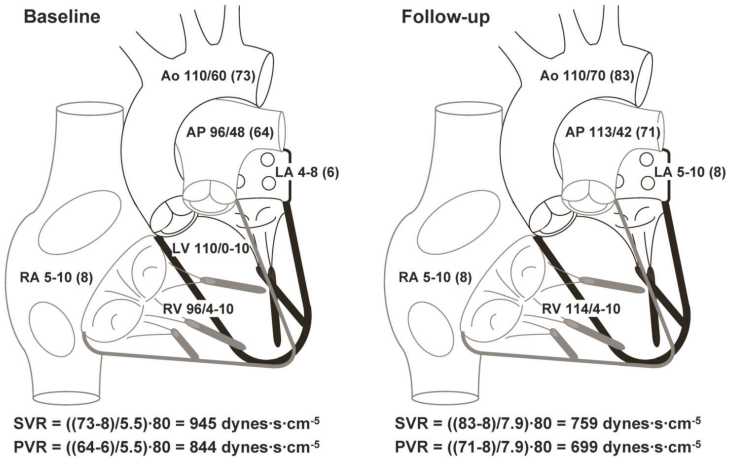

Figure 2

Hemodynamics recorded at baseline and at follow-up. Despite the fact that the systolic pulmonary artery pressure is increased after one year of treatment, PVR has decreased due to an improved cardiac output. Essentially, right ventricular function seems improved, generating higher pulmonary artery pulse pressures and an increased cardiac output.

an abdominal echo showed normal hepatopetal flow in the portal vein, essentially excluding presence of portal hypertension. The patient consented to a HIV test, which was negative. The echocardiogram showed no signs of left ventricular dysfunction or incompetence of the aortic and mitral valve, hence there was no indication that the pulmonary hypertension was secondary to left-sided heart disease. Pulmonary function tests showed a mild obstruction pattern with a diffusion capacity of 68%, corrected for alveolar volume. Arterial blood gas analysis rendered the following values: O2 saturation 97% (94-99%), pH 7.47 (7.35-7.45), pCO2 4.2 kPa (4.5-6.0 kPa), pO2 10.9 kPa (10.6-13.3 kPa), Base excess -0.4 mmol/L (-2 – 2mmol/L), Bicarbonate concentration 22 mmol/L (22-29 mmol/L). Nocturnal oximetry showed no signs of desaturation or sleep apnea. Additional CT imaging of the lungs and

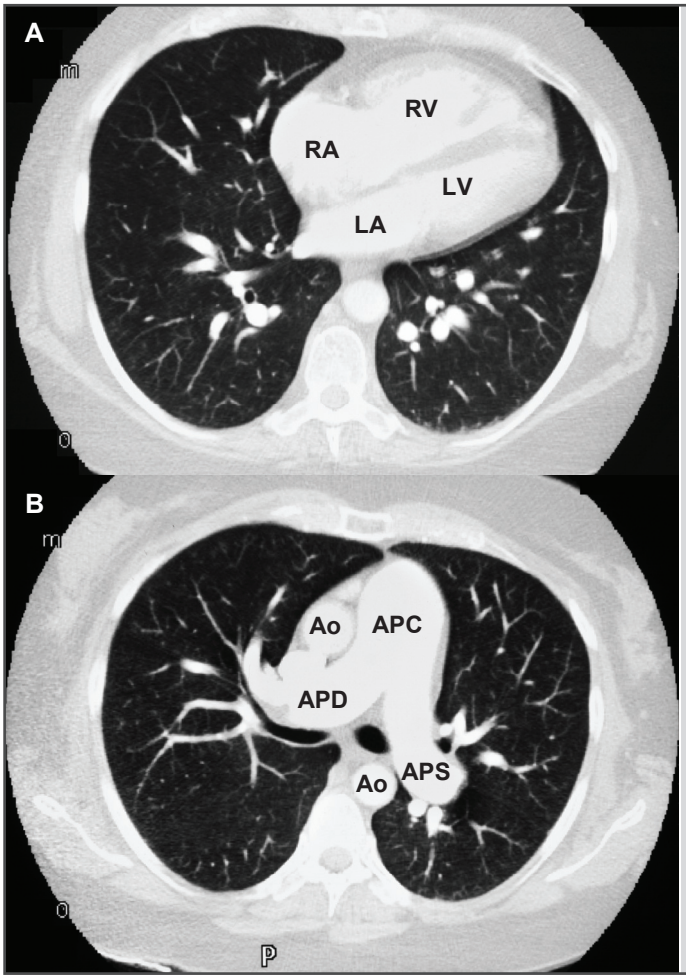

Figure 3

A) CT image which clearly shows the marked dilation of the right atrium and right ventricle, whereas the left atrium and left ventricle are considerably smaller.

B) CT image of the aorta, and pulmonary arteries. The diameter of the common pulmonary artery is almost twice that of the ascending aorta, and the right and left pulmonary arteries are also dilated. The severe dilatation of the pulmonary arteries indicates that the pulmonary arterial hypertension is not of recent onset, yet a chronic condition.

RA=right atrium,
RV=right ventricle,
LA=left atrium,
LV=left ventricle,
Ao=aorta,
APC=common pulmonary artery,
APD=right pulmonary artery,
APS=left pulmonary artery.

pulmonary arteries showed no signs of interstitial lung disease or thromboembolic disease, but dilatation of the right atrium, right ventricle, and central pulmonary arteries was striking (Figure 3). Since no satisfactory explanation for the pulmonary arterial hypertension could be found, the patient was classified as having idiopathic PAH. Despite the impressive level of PAH, treatment would not be reimbursed, given the relatively mild symptoms of the patient (NYHA functional class II). Since the severity of the disease led to believe that refraining from treatment would lead to worsening in the near future, the patient was suggested to partake in a clinical trial evaluating the benefit of an endothelin antagonist. The patient gave informed consent, and reported an improvement in her overall well-being during the first months of treatment. After one year of treatment pulmonary artery pressures were virtually unchanged. However, systemic venous oxygen saturation had dramatically improved from 65% to 75%. Cardiac output calculated with the Fick method had increased from 5.5 $L \cdot m^{-2}$ to 7.9 $L \cdot m^{-2}$, meaning that PVR had dropped to approximately 600 $dynes \cdot s \cdot cm^{-5}$. The ECG was unchanged compared to a year before. Since this pulmonary vascular resistance is still much higher than the upper limit of normal (≈240 $dynes \cdot s \cdot cm^{-5}$), the patient received additional treatment with a phosphodiesterase-inhibitor.

PAH is a rare disease, with an estimated incidence of 2-16 per million [2]. PAH often remains undetected until there are already advanced pulmonary vascular abnormalities [1, 3]. In recent years, however, awareness for this orphan disease has increased, mainly due to the advent of new drug therapies [4]. Historically, the time interval from symptoms to diagnosis has been substantial for PAH patients, rendering most patients in NYHA class III or IV before treatment initiation [3]. Although in the majority of PAH patients ECG abnormalities corresponding with right heart overload are present at diagnosis, [3, 5] the scalar ECG has been considered inadequate for screening [1]. Recent studies in rats and humans have illustrated, however, that even a mildly increased right ventricular pressure load is associated with substantial changes in myocardial electrical properties, detectable in a standard 12-lead ECG recording [6, 7]. A possible explanation for the reportedly lower sensitivity for right ventricular pressure overload of the ECG by conventional assessment is the wide range of normal ECG values, i.e. the 'normal' heart axis ranges from -30º to +90º or even to + 100º, depending on the criteria used [8]. In contrast to the wide inter-individual heterogeneity in ECG characteristics, the ECG is a very reliable tool to detect intra-individual changes over time. In this particular patient, there had been an extensive cardiac evaluation several years before. In the meantime, the patient developed PAH and the ECG changed markedly: QRS axis turned rightward, changing from 36º to 90º, the R in lead V1 became >0.5mV and was more pronounced than the S, and there were diffuse repolarization abnormalities (Figure 1). Together, these

abnormalities correspond with increased right heart load and right ventricular hypertrophy [8]. This particular patient had relatively mild symptoms, given the severity of the PAH. The fairly stable cardiac situation was reflected by a sinus rhythm of 84 bpm, indicating that stroke volume is adequate at rest [9]. The absence of a 'P Pulmonale' (P wave>0.25 mV in lead II) signifies that PAH has not yet induced a significant retrograde atrial overload, which is otherwise an ominous sign of poor prognosis [10, 11]. More specifically, P amplitude in lead II increases as a result of progressive RV hypertrophy-associated diastolic dysfunction, and RV dilatation-associated tricuspid regurgitation in PAH patients [12]. Karliner et al. documented an increase in P amplitude in lead II in healthy men who ascended from sea level to a height of 6300 meters above sea level on Mount Everest, and suffered from hypoxia-induced PAH [12]. Furthermore, QRS axis turned in a more rightward direction with increasing pulmonary vascular resistance at high altitude, a phenomenon also observed in our patient. Lastly, as QRS duration is related to ventricular size, function, and prognosis, there was no reason to believe that the right ventricle was performing poorly with a QRS duration of only 76 msec in this patient [13]

There is fairly extensive knowledge on the ECG changes that can be observed with regression of right ventricular hypertrophy in developing newborns, as well as on the ECG abnormalities that remain present in people living at high altitudes [10]. Similarly, patients with a thorough effect of PAH attenuating treatment – such as the rare patients that respond to calcium channel blockers – have shown dramatic ECG changes from a pattern corresponding with right ventricular hypertrophy to a (near)-normal pattern [14].

Being able to assess evolutionary ECG changes due to the development of PAH is exceptionally rare. This is understandable, since PAH is an uncommon disease. Futhermore, PAH often presents relatively early in life, meaning patients lack cardiopulmonary comorbidity, and therefore prior ECG recordings [2]. Nevertheless, recording ECGs in patients at risk for developing PAH might be a cost-effective way of screening or longitudinal case-finding. Screening for PAH in patients at risk, such as patients with a genetic predisposition, HIV infection, portal hypertension, or systemic sclerosis, has been subject to debate for some time [1]. While results of clinical trials regarding earlier onset of treatment are awaited, critics claim that such screening is impracticable without properly validated tools. However, the results of improved ECG detection of increased right ventricular pressure load may well bring screening within reach [7]. Of course, pre-selecting patients at risk for pulmonary arterial hypertension will remain necessary, given the rarity of the disease. Now that the groups of patients at risk have been well identified [1, 2, 15], there is ample opportunity to evaluate the diagnostic value of longitudinal ECG recordings in a clinical setting.

References

1. McGoon M, Gutterman D, Steen V, Barst R, McCrory DC, Fortin TA and Loyd JE. Screening, early detection, and diagnosis of pulmonary arterial hypertension: ACCP evidence-based clinical practice guidelines. Chest 2004;126:14S-34S.

2. Peacock AJ, Murphy NF, McMurray JJ, Caballero L and Stewart S. An epidemiological study of pulmonary arterial hypertension. Eur Respir J 2007;30:104-109.

3. Rich S, Dantzker DR, Ayres SM, Bergofsky EH, Brundage BH, Detre KM, Fishman AP, Goldring RM, Groves BM and Koerner SK. Primary pulmonary hypertension. A national prospective study. Ann Intern Med 1987;107:216-223.

4. Badesch DB, Abman SH, Simonneau G, Rubin LJ and McLaughlin VV. Medical therapy for pulmonary arterial hypertension: updated ACCP evidence-based clinical practice guidelines. Chest 2007;131:1917-1928.

5. Ahearn GS, Tapson VF, Rebeiz A and Greenfield JC, Jr. Electrocardiography to define clinical status in primary pulmonary hypertension and pulmonary arterial hypertension secondary to collagen vascular disease. Chest 2002;122:524-527.

6. Henkens IR, Mouchaers KT, Vliegen HW, van der Laarse WJ, Swenne CA, Maan AC, Draisma HH, Schalij I, van der Wall EE, Schalij MJ and Vonk Noordegraaf A. Early changes in rat hearts with developing pulmonary arterial hypertension can be detected with three-dimensional electrocardiography. Am J Physiol Heart Circ Physiol 2007;293:H1300-H1307.

7. Henkens IR, Mouchaers KT, Vonk Noordegraaf A, Boonstra A, Swenne CA, Maan AC, Man SC, Twisk JW, van der Wall EE, Schalij MJ and Vliegen HW. Improved ECG detection of presence and severity of right ventricular pressure load validated with cardiac magnetic resonance imaging. Am J Physiol Heart Circ Physiol 2008;294:H2150-H2157.

8. Zipes DP, Libby P, Bonow RO and Braunwald E. Heart Disease. Saunders, 2004.

9. Holverda S, Gan CT, Marcus JT, Postmus PE, Boonstra A and Vonk Noordegraaf A. Impaired stroke volume response to exercise in pulmonary arterial hypertension. J Am Coll Cardiol 2006;47:1732-1733.

10. Penaloza D and Arias-Stella J. The heart and pulmonary circulation at high altitudes: healthy highlanders and chronic mountain sickness. Circulation 2007;115:1132-1146.

11. Bossone E, Paciocco G, Iarussi D, Agretto A, Iacono A, Gillespie BW and Rubenfire M. The prognostic role of the ECG in primary pulmonary hypertension. Chest 2002;121:513-518.

12. Karliner JS, Sarnquist FF, Graber DJ, Peters RM, Jr. and West JB. The electrocardiogram at extreme altitude: experience on Mt. Everest. *Am Heart J* 1985;109:505-513.

13. Gatzoulis MA, Till JA, Somerville J and Redington AN. Mechanoelectrical interaction in tetralogy of Fallot. QRS prolongation relates to right ventricular size and predicts malignant ventricular arrhythmias and sudden death. *Circulation* 1995;92:231-237.

14. Rich S and Brundage BH. High-dose calcium channel-blocking therapy for primary pulmonary hypertension: evidence for long-term reduction in pulmonary arterial pressure and regression of right ventricular hypertrophy. *Circulation* 1987;76:135-141.

15. Humbert M, Sitbon O, Chaouat A, Bertocchi M, Habib G, Gressin V, Yaici A, Weitzenblum E, Cordier JF, Chabot F, Dromer C, Pison C, Reynaud-Gaubert M, Haloun A, Laurent M, Hachulla E and Simonneau G. Pulmonary arterial hypertension in France: results from a national registry. *Am J Respir Crit Care Med* 2006;173:1023-1030.

VIII

Electrocardiographic monitoring of treatment response in pulmonary arterial hypertension patients

Ivo R. Henkens

C. Tji-Joong Gan

Serge A. van Wolferen

Miki Hew

Anco Boonstra

Jos W.R. Twisk

Otto Kamp

Ernst E. van der Wall

Martin J. Schalij

Anton Vonk Noordegraaf

Hubert W. Vliegen

Chest 2008: Jul 18. [Epub ahead of print]

Abstract

Background

The potential use of the electrocardiogram for monitoring treatment effect in patients with pulmonary arterial hypertension (PAH) has not been investigated. We evaluated whether the ECG is useful for monitoring treatment response based on changes in pulmonary vascular resistance (PVR).

Methods

An ECG was recorded in 81 PAH patients at the time of diagnostic right heart catheterization, and after one year of treatment. Patients were treated according to the guidelines. Patients were divided into two groups based on PVR (<500 dynes·s·cm^{-5} or >500 dynes·s·cm^{-5}). A positive treatment response was defined as >25% decrease in PVR to an absolute PVR<500 dynes·s·cm^{-5}.

Results

At baseline, the 19 patients with a PVR<500 dynes·s·cm^{-5} had a significantly lower P amplitude in lead II, a less rightward oriented QRS axis, and a more rightward T axis than the 62 patients with a PVR>500 dynes·s·cm^{-5}. Overall (n=81), mean change in PVR was -143±360 dynes·s·cm^{-5} after one year of treatment (P<0.001). Twelve patients (19%) with a baseline PVR>500 dynes·s·cm^{-5} classified as responders. Receiver operating characteristics analysis determined that P amplitude in lead II (AUC=0.80, 95% CI, 0.67 - 0.94, P<0.01), QRS axis (AUC=0.70, 95% CI, 0.52 - 0.89, P=0.03), and T axis (AUC=0.90, 95% CI, 0.82 - 0.97, P<0.001) were important determinants of treatment response. Presence of P amplitude in lead II<0.175mV, and T axis≥25º combined, had a positive and negative predictive value for treatment response of 0.81(CI, 0.37 - 0.96) and 0.94 (CI, 0.86 - 0.99), respectively.

Conclusions

Routine ECG evaluation can be an important contribution in the assessment of treatment response in PAH patients.

Introduction

Pulmonary arterial hypertension (PAH) is a disease with intrinsic dismal prognosis [1], despite the advent of new PAH attenuating drugs [2-5]. Since treatment effect varies considerably among PAH patients, discriminating between 'responders' and 'non-responders' is often difficult [6-8]. Although considered of limited use for the diagnosis of PAH [1, 9, 10], an electrocardiogram (ECG) is routinely recorded in PAH patients and may be of use in the evaluation of treatment response after the diagnosis of PAH has been established. We therefore studied to what extent ECG variables might contribute in the repeated evaluation of PAH patients regarding treatment response.

Methods

The study procedures were in accordance with the Declaration of Helsinki. The local institutional review board did not require full approval, since this retrospective study included only patients familiar to the VU University Medical Center, and patient data were treated confidentially.

Patients

Between October 1999 and October 2007, 856 patients were evaluated for pulmonary hypertension. Patients were included in this study if concomitant resting ECGs before diagnostic right heart catheterization and before repeated right heart catheterization at follow-up were available. A mean pulmonary artery pressure (PAP)>25 mmHg with a pulmonary capillary wedge pressure≤15 mmHg was considered PAH [11, 12]. PAH was considered to be idiopathic when identifiable causes for pulmonary hypertension were excluded [11, 12]. Idiopathic PAH was identified in 109 patients, of whom 13 died before follow-up, and 15 did not have a repeated ECG or right heart catheterization at follow-up. Consequently, 81 patients were included in the study.

Electrocardiography

Standard 12-lead ECGs were recorded by certified ECG technicians with patients in supine position. Commercially available electrocardiographs (MAC VU and MAC 5000; GE Healthcare; The Netherlands), were used for ECG recording (paper speed=25 $mm \cdot s^{-1}$; sensitivity 1 mV=10 mm; sample frequency = 500 Hz). Heart rate, P axis, QRS axis, QRS duration, and T axis were directly derived from standard electrocardiographic calculations. P

amplitude in lead II was assessed from digitally stored ECGs, measured with the isoelectric PR-interval as reference point in steps of 0.025 mV (=0.25 mm on paper). ECGs were examined by an experienced cardiologist (HWV), blinded to the data.

Treatment

All patients underwent a vasoreactivity test [11, 13]. Patients with a positive response were started on calcium antagonists [11]. Before 2002, prostacyclin (epoprostenol) was prescribed to all patients in WHO class III and IV. From 2002 onward, patients in WHO class III received endothelin receptor antagonists (bosentan or sitaxsentan) or a phosphodiesterase-inhibitor (sildenafil), whereas patients in WHO class IV received prostacyclin (epoprostenol, treprostinil or iloprost).

Classification of responders

Based on recent studies, we assumed that compensatory right ventricular hypertrophy would be reflected by ECG changes over a limited range of PVR only [9, 14]. To allow categorization of patients based on ECG variables we first defined a cut-off point in pulmonary vascular resistance (PVR). Since a PVR of 240 dynes·s·cm^{-5} is considered the upper limit of normal [13], a PVR<500 dynes·s·cm^{-5} was considered a reasonable treatment goal for PAH patients. We hypothesized that a PVR<500 dynes·s·cm^{-5} (mild-to-moderate PAH) would be associated with less ECG abnormalities than a PVR>500 dynes·s·cm^{-5} (severe PAH), since the standard ECG lacks sensitivity for mild PAH [9, 10, 15]. At baseline, patients were compared for ECG variables based on a PVR above or below 500 dynes·s·cm^{-5}. Subsequently, in patients with mild–to-moderate PAH we evaluated differences in ECG characteristics at follow-up between patients with stable disease and patients who experienced a >25% increase in PVR to a PVR>500 dynes·s·cm^{-5}. Similarly, in patients with severe PAH at baseline we evaluated differences in ECG characteristics at follow-up between patients who experienced a >25% decrease in PVR to a PVR<500 dynes·s·cm^{-5} and patients without such a positive treatment response.

Statistical analyses

Normally distributed data are expressed as mean ± standard deviation or otherwise as median (interquartile range). The SPSS for Windows Software (version 12.0.1; SPSS Inc; Chicago, Ill) was used for data analysis. Correlation analyses (Pearson and Spearman) were used to determine relations between ECG variables, and catheterization variables. Paired t-tests were used for comparison of ECG variables over time. Receiver operating characteristics

(ROC) analyses were used to determine whether ECG variables could accurately classify patients as responders or non-responders. Comparison of the area under the curve (AUC) was performed according to the method described by Hanley and McNeil [16]. Binary logistic stepwise regression analysis (inclusion if $P<0.05$, removal if $P>0.10$) was used to construct an optimal model for classification of patients according to treatment response. A 95% confidence interval (CI) is provided for all estimates. A value of $P<0.05$ was considered to be statistically significant.

Results

Baseline PVR in patients surviving to follow-up (n=81) was considerably lower (891±466 vs.1612±753 dynes·s·cm^{-5}, $P<0.01$) than in patients who died before follow-up (n=13). Baseline characteristics for patients with mild-to-moderate PAH, patients with severe PAH, and deceased patients are presented in Table 1. Baseline ECG characteristics are presented in Table 2. The hemodynamic differences between patients with a PVR<500 dynes·s·cm^{-5} and patients with a PVR>500 dynes·s·cm^{-5} were predominantly reflected by P amplitude in lead II, and T axis, and to a lesser extent by QRS axis. Correlation analyses between the selected ECG variables and hemodynamic variables for both baseline and follow-up are described

Table 1

	PVR<500 (n=19)	PVR>500 (n=62)	Deceased (n=13)*	Between Groups	PVR<500 vs. PVR>500	PVR<500 vs. Deceased	PVR>500 vs. Deceased
Patient characteristics	Mean ± SD	Mean ± SD	Mean ± SD	*P*	*P*†	*P*†	*P*†
Age (years)	45 ± 12	43 ± 14	39 ± 16	0.72	1.00	0.74	1.00
Gender (male/female)	4/15	12/50	6/7	0.87	1.00	0.37	0.12
Body surface area (m²)	1.8 ± 0.2	1.8 ± 0.2	1.8 ± 0.2	0.86	1.00	1.00	1.00
RAP (mmHg)	5 ± 3	9 ± 5	16 ± 4	<0.01	0.01	<0.001	<0.001
mean PAP(mmHg)	37 ± 8	58 ± 11	67 ± 14	<0.001	<0.001	<0.001	0.07
Cardiac index (L·min^{-1}·m^{-2})	3.6 ± 0.7	2.3 ± 0.6	1.5 ± 0.3	<0.001	<0.001	<0.001	<0.01

*Baseline characteristics for patients with a PVR<500 dynes·s·cm^{-5}, a PVR>500 dynes·s·cm^{-5}, and patients who died before follow-up. RAP = right atrial pressure. PAP = pulmonary artery pressure. * PVR in the deceased patients was 1612 ± 753 dynes·s·cm^{-5}. † Post-Hoc Bonferroni correction for the significance of the observed differences between the groups.*

TABLE 2

	PVR<500 (n=19)	PVR>500 (n=62)	Deceased (n=13)	Between Groups	PVR<500 vs. PVR>500	PVR<500 vs. Deceased	PVR>500 vs. Deceased
ECG variables	mean ± SD or median (IQR)	mean ± SD or median (IQR)	mean ± SD or median (IQR)	*P*	*P**	*P**	*P**
Heart rate (bpm)	75 ± 18	81 ± 16	94 ± 19	<0.01	0.53	<0.01	0.04
P amplitude in lead II (mV)	0.17 ± 0.07	0.22 ± 0.08	0.26 ± 0.07	0.01	0.04	<0.01	0.44
P axis (º)	65 (55 - 74)	65 (55 - 76)	69 (56 - 76)	0.75	1.00	1.00	1.00
QRS axis (º)	96 (65 - 115)	114 (97 - 128)	118 (99 - 133)	0.10	0.10	0.43	1.00
QRS duration (ms)	95 ± 21	92 ± 12	95 ± 15	0.67	1.00	1.00	1.00
T axis (º)	48 (29 - 70)	-9 (-40 - 38)	-23 (-39 - 57)	0.02	0.03	0.10	1.00

Baseline differences in ECG variables between PAH patients with a PVR<500 dynes·s·cm-5, a PVR>500 dynes·s·cm-5, and PAH patients who died before follow-up.
** Post-Hoc Bonferroni correction for the significance of the observed differences between the groups.*

TABLE 3

		RAP (mmHg)		mean PAP (mmHg)		Cardiac index ($L \cdot min^{-1} \cdot m^{-2}$)		PVR ($dynes \cdot s \cdot cm^{-5}$)	
ECG variables		1st	2nd	1st	2nd	1st	2nd	1st	2nd
Heart rate (bpm)	r	0.18	0.28*	0.23*	0.25*	-0.24*	-0.17	0.32†	0.31†
P amplitude in lead II (mV)	r	0.15	0.24*	0.43‡	0.45‡	-0.27†	-0.34†	0.45‡	0.52‡
P axis (º)	r	-0.08	-0.16	0.08	0.10	-0.02	-0.08	0.14	0.12
QRS duration (ms)	r	0.24*	-0.18	-0.02	-0.37‡	0.16	0.11	-0.11	-0.31†
QRS axis (º)	r	0.22	0.46‡	0.34†	0.53‡	-0.19	0.39‡	0.28*	0.48‡
T axis (º)	r	-0.30†	-0.21	-0.32†	-0.47‡	0.16	0.37†	-0.29*	-0.52‡

*Correlations between ECG-derived variables and hemodynamic parameters at baseline (1st) and at follow-up (2nd). Heart rate, P amplitude in lead II, and QRS duration were assessed in linear correlation analysis (Pearson) with hemodynamic parameters. P axis, QRS axis, and T axis were assessed in nonlinear correlation analysis (Spearman) with hemodynamic parameters. RAP = right atrial pressure. PAP = pulmonary artery pressure. PVR = pulmonary vascular resistance. * P<0.05, † P<0.01, ‡P<0.001*

in Table 3. The strongest linear relation was found between P amplitude and PVR (r=0.45, *P*<0.001 at baseline, and r=0.52, *P*<0.001 at follow-up, respectively, Figure 1). After 13.1 months of treatment (11.8-17.1 months) mean change in PVR was -143±360 dynes·s·cm^{-5} for all 81 patients (*P*<0.001).

Three of the 19 patients with a baseline PVR <500 dynes·s·cm^{-5} experienced a >25% increase in PVR to a PVR>500 dynes·s·cm^{-5}; eleven remained stable, and five patients experienced a >25% decrease in PVR. An example of ECG leads I, II, and aVF derived from a patient in whom PAH progressed is depicted in Figure 2 (A+B). Patients who deteriorated had a more rightward oriented QRS axis at follow-up compared to the other patients with a baseline PVR<500 dynes·s·cm^{-5} (129±16º vs. 79±29º, *P*=0.01). ROC analysis defined a QRS axis>116º to have 100% sensitivity and 100% specificity (CI, 1.00 - 1.00 for both) for patients with >25% increase in PVR to a PVR>500 dynes·s·cm^{-5} (*P*<0.01). Other ECG variables, medication use or gender distribution were not statistically different between patient groups with an initial PVR <500 dynes·s·cm^{-5}.

Twelve (19%) out of 62 patients with severe PAH at baseline demonstrated a positive treatment response. Responders had a significantly lower PVR than non-responders both at baseline

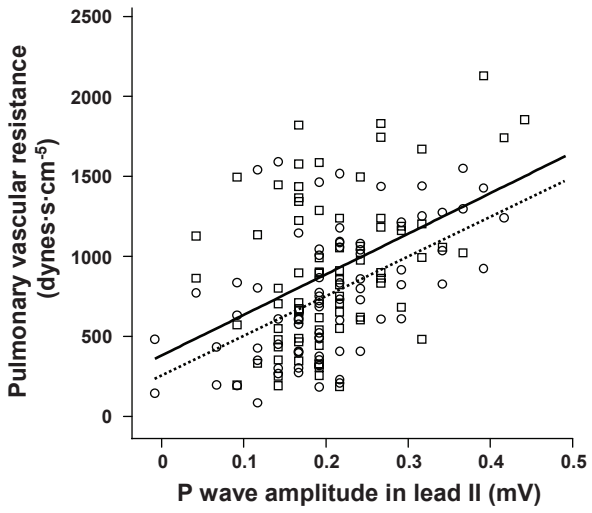

Figure 1

ECG data and hemodynamic data from all 81 patients from baseline (open squares, solid line) and follow-up (open circles, dotted line) combined. There was a linear relation between P amplitude in lead II and PVR both at baseline and at follow-up: r=0.45, P<0.001 and r=0.52, P<0.001, respectively).

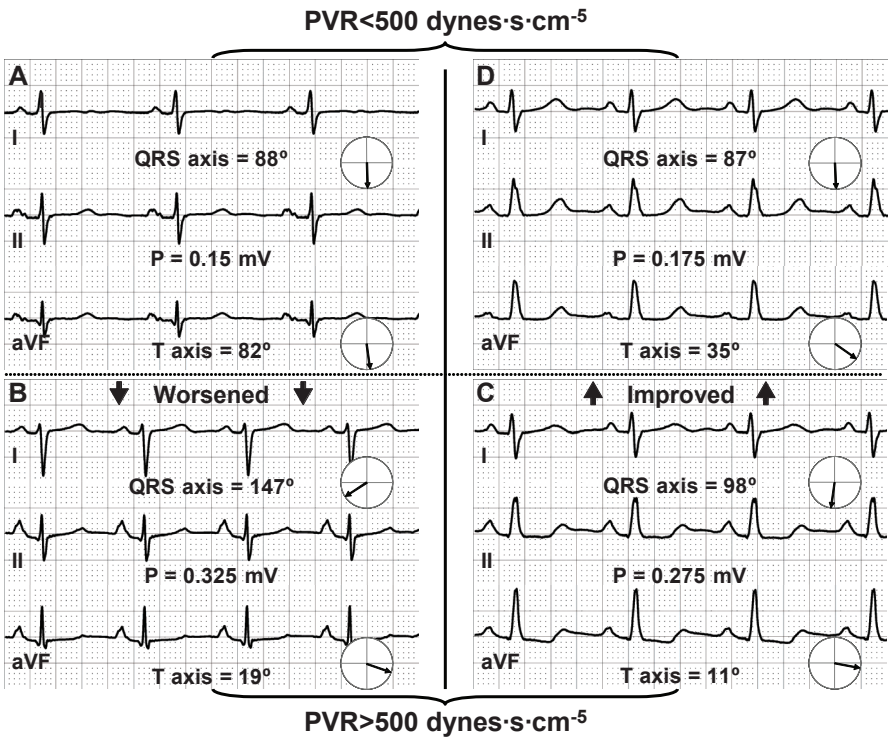

Figure 2

Left: representative example of leads I, II, and aVF of standard 12-lead ECGs from a patient with a PVR of 330 dynes·s·cm^{-5} before treatment (A), and a PVR of 600 dynes·s·cm^{-5} at follow-up (B) demonstrating an increase in P amplitude in lead II (0.15 mV to 0.325 mV), a more rightward QRS axis orientation (88º to 147º), and a less rightward T axis orientation (82º to 19º). Right: representative example of leads I, II, and aVF of standard 12-lead ECGs from a patient with a PVR of 540 dynes·s·cm^{-5} before treatment (C), and a PVR of 300 dynes·s·cm^{-5} at follow-up (D) demonstrating a decrease in P amplitude in lead II (0.275 mV to 0.175 mV), a less rightward QRS axis orientation (98º to 87º), and a more rightward T axis orientation (11º to 35º). The initial strain pattern, most evident in lead aVF (C) was no longer present (D).

(762±240 dynes·s·cm^{-5} vs. 1120±406 dynes·s·cm^{-5}, P<0.01) and at follow-up (370±100 dynes·s·cm^{-5} vs. 976±307 dynes·s·cm^{-5}, P<0.001). Responders did not differ from non-responders with respect to age (44±13 vs. 43±15, P=0.81), gender distribution (3:9 vs. 9:41, male:female, P=0.59), treatment with calcium-channel blockers (n=1:11 vs. n=3:47, P=0.77), endothelin receptor antagonists (n=7:5 vs. n=23:27, P=0.45), phosphodiesterase-5 inhibitors (n=2:10 vs. n=8:42, P=0.96), or prostacyclin (n=4:8 vs. n=23:27, P=0.44). In responders,

mean PAP decreased by 14±8 mmHg to 39±6 mmHg (P<0.001), whereas in non-responders mean PAP changed by 1±11 mmHg to 57±10 mmHg (P=0.48). In responders, cardiac index increased by 1.1±1.2 L·min^{-1}·m^{-2} to 3.9±1.4 L·min^{-1}·m^{-2} (P=0.02). In non-responders, cardiac index also increased by 0.3±0.6 L·min^{-1}·m^{-2} to 2.5±0.7 L·min^{-1}·m^{-2} (P<0.01). An example of ECG leads I, II, and aVF from a responder is depicted in Figure 2 (C+D).

Hemodynamic differences between responders and non-responders were again best reflected by P amplitude in lead II, QRS axis, and T axis (Table 4). Results of ROC analysis for these ECG variables for discrimination between responders and non-responders are depicted in Figure 3. Given the observed a priori chance of 0.19 (12/62 patients) for a positive treatment

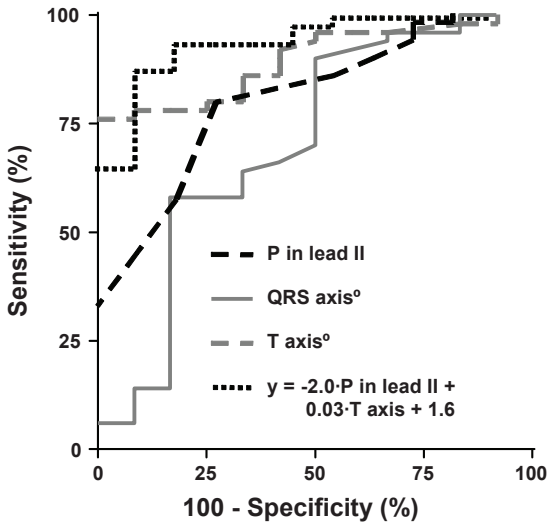

Figure 3

Receiver operating characteristics analysis for determination of treatment response in PAH patients. P amplitude had a sensitivity and specificity of 73% (CI, 39 - 94%) and 80% (CI, 66 - 90%) respectively for a cut-off point of 0.175 mV (AUC=0.80, CI, 0.67 - 0.94, P<0.01), QRS axis had a sensitivity and specificity of 42% (CI, 15 - 72%) and 92% (CI, 81 - 98%) respectively for a cut-off point of 90° (AUC= 0.70, CI, 0.52 - 0.89, P=0.03), and T axis had a sensitivity and specificity of 100% (CI, 74 - 100%) and 76% (CI, 62 - 87%) respectively for a cut-off point of 25° (AUC= 0.90, CI, 0.82 - 0.97, P<0.001). Binary logistic regression analysis rendered the following formula for prediction of a positive treatment response: y=-2.0·P amplitude in lead II + 0.03·T axis + 1.6 (AUC=0.94, CI, 0.87 - 1.01, P<0.001). Although according to binary logistic regression analysis the latter formula performed better than assessment of T axis alone, the AUC was not significantly larger than that of T axis alone (P=0.12), according to the method described by Hanley and McNeil [16]. By the same method, however, the regression formula was better than using either P amplitude (P=0.01) or QRS axis (P<0.01).

response, the respective positive and negative predictive values for a positive treatment response were 0.46 (CI, 0.21 - 0.69) and 0.93 (CI, 0.82 - 0.98) for P amplitude >0.175mV, 0.55 (CI, 0.16 - 0.89) and 0.87 (CI, 0.80 - 0.94) for QRS axis >90º, and 0.48 (CI, 0.31 - 0.64) and 1.00 (CI, 0.91 - 1.00) for T axis<25º. Binary logistic regression analysis determined that only P amplitude in lead II had additional value after assessing T axis (Figure 3). A stepwise prediction model was constructed with sequential assessment of T axis and P amplitude in lead II. Since a T axis <25º had a negative predictive value of 1.00 (CI, 0.91 - 1.00) for a PVR<500 dynes·s·cm^{-5} all patients with a T axis <25º were classified as non-responders. Patients with a T axis ≥25º and a P amplitude in lead II ≤0.175 mV were classified as responders. This algorithm had a sensitivity and specificity of 75% (CI, 43 - 95%) and 96% (CI 83 - 99%), respectively, for detection of a positive treatment response. Positive and negative predictive values of this two-step treatment response assessment were 0.81 (CI, 0.37 - 0.96) and 0.94 (CI, 0.86 - 0.99), respectively.

Discussion

Key finding of this study is that there is a robust correlation between PVR and the ECG-derived P amplitude, QRS axis, and T axis. Repeated ECG analysis may therefore be of use in both early and late evaluation of treatment response, and hence facilitate targeted treatment adjustment in patients not reaching their treatment goal.

We detected a linear relation between P amplitude in lead II and PVR. For P amplitude in lead II 0.175 mV was defined as the best cut-off point in ROC analysis for discrimination between responders and non-responders. This cut-off point is still below the 0.25mV threshold for a 'P pulmonale' which has good specificity, yet poor sensitivity for mild-to-moderate RV hypertrophy [17]. The prognostic value of P amplitude in PAH reportedly increases with its amplitude [18], stressing its clinical value in singling out PAH patients with advanced disease and a dismal prognosis. PAH-induced RV hypertrophy and RV dilation associated tricuspid regurgitation are considered causative factors of increased systolic and diastolic atrial load responsible for the increased P amplitude in lead II [19]. In healthy men, Karliner et al. observed an increase in P amplitude in lead II from sea level to a few months later at a height of 6300 meters above sea level on Mount Everest.[19] This report concurs with the recent overview on the heart and pulmonary circulation in highlanders by Penaloza and Aries-Stella who link an elevated P amplitude, a rightward oriented QRS axis, and inverted T waves to increased pulmonary pressures [20]. They elegantly demonstrate that QRS axis reflects RV hypertrophy in individuals with a hypoxia-induced

elevation of pulmonary vascular resistance at high altitude, and that QRS axis increases over time in accordance with increases in pulmonary vascular resistance or vice versa. For different populations, different cut-off values have been proposed for QRS axis for optimal diagnosis of RV hypertrophy [17]. Although the relatively wide normal range for QRS axis hampers diagnostic accuracy for RV hypertrophy in a cross-sectional study of the general population [21], QRS axis is a useful tool for follow-up of patients with established PAH, as was shown in our population. Rich and Brundage demonstrated a reduction in rightward QRS axis orientation in PAH patients with a long-term positive response to high-dose calcium channel blockers [22]. A more recent study reported a QRS axis>100º to be highly predictive of a PVR>400 dynes·s·cm^{-5} [10]. This cut-off point for QRS axis lies in between the QRS axis>116º we found for PAH patients with a baseline PVR<500 dynes·s·cm^{-5} yet progressive disease, and the QRS axis>90º we found for PAH patients with a baseline PVR>500 dynes·s·cm^{-5} with a positive treatment response. The observed importance of the T axis in our population concurs with T wave abnormalities registered in patients with RV hypertrophy due to residence at high altitudes [20]. Furthermore, Kawaguchi et al. found the T wave to discriminate best between patients with and without RV hypertrophy [23]. In selected PAH patients the T axis is therefore a valuable indicator of disease burden.

Our definition of treatment response was based on PVR, a robust measure of interplay between cardiac output and RV afterload [13]. Using PVR secures unambiguous results, whereas sequential measurement of mean PAP or cardiac output alone might underestimate or overestimate treatment effect [11, 13]. The PVR cut-off point of <500 dynes·s·cm^{-5} and the >25% decrease in PVR may be considered 'aiming high' given our results and those of others [6, 24]. Given the suboptimal sensitivity of the standard ECG [10], we considered such an important change in disease burden necessary for any effect in the

Table 4

ECG variables	PVR<500 dynes·s·cm^{-5} (n=12)	PVR>500 dynes·s·cm^{-5} (n=50)	*P*
Heart rate (bpm)	77 ± 12	84 ± 17	0.07
P amplitude in lead II (mV)	0.14 ± 0.08	0.24 ± 0.08	<0.001
P axis (º)	61 (23 - 74)	64 (15 - 73)	0.20
QRS axis (º)	98 (62 - 108)	114 (101 - 121)	<0.01
QRS duration (ms)	95 ± 10	95 ± 12	0.87
T axis (º)	60 (34 - 76)	-5 (-33 - 25)	<0.001

Differences in ECG variables at follow-up between responders and non-responders in pulmonary arterial hypertension patients with a baseline PVR>500 dynes·s·cm^{-5}

ECG to be observed. Because the range of normal ECG values is relatively wide [25], we categorized PAH patients as having mild–to-moderate PAH or severe PAH. ECG variables in patients with mild-to-moderate PAH approximated normal values in the majority of patients. Similarly, ECGs variables of patients with severe PAH and a positive treatment response regressed to a (near-)normal situation, whereas the opposite was true for PAH patients with mild-to-moderate PAH with progressive disease (Table 4, Figure 2).

Since PAH is essentially a hemodynamic diagnosis, right heart catheterization remains the gold standard for diagnosis of PAH [11, 15]. Although the inherent risk of this invasive procedure is low [26], clinicians are exploring and validating other ways of patient monitoring.

Ubiquitous use of the 6-minute walk test [27], biomarkers [28, 29], and non-invasive imaging [30, 31] for evaluation of PAH has greatly improved understanding prognosis, yet clear cut-off values for timely detection of treatment response are lacking. This is likely explained by the considerable inter-individual variation in PAH-related variables as well as their intrinsic optimal discrimination range of PAH severity; e.g. the ECG was only useful for discrimination between mild-to-moderate PAH and severe PAH (Table 2), whereas the 6-minute walk distance becomes increasingly important in end-stage disease. Importantly, the ECG correctly classified the majority of PAH patients that worsened from a favorable baseline situation or improved from an unfavorable baseline situation.

Clinical implications

Randomized clinical trials have demonstrated that after 12-16 weeks of treatment, there is generally a modest, though overall significant beneficial effect of PAH attenuating drugs [2, 4, 5, 32-35]. However, the individual treatment effect is difficult to evaluate non-invasively, and patients generally require treatment indefinitely. Currently, patients with a suboptimal effect of monotherapy would receive additional PAH attenuating therapy [36, 37]. Evaluation of treatment effect could therefore ascertain earlier initiation of tailored combination therapy in these patients. Assessing the ECG at follow-up for disease progression and treatment response in PAH patients is simple, and requires merely an additional evaluation of the P amplitude in lead II, QRS axis, and T axis. The robustness and reproducibility of ECG recordings as well as the ease of interpretation render the ECG an excellent tool for longitudinal evaluation of treatment effect by any clinician familiar with PAH. Implementation of routine ECG evaluation in all PAH patients may therefore be an important contribution to clinical assessment of these patients.

Limitations

Although the choice for a cut-off point of <500 dynes·s·cm^{-5} for PVR was based on recent studies regarding diagnostic accuracy of the ECG [9], and consequences of an increasing PVR [14], it remains arbitrary. Furthermore, it resulted in an unequal distribution of patients with mild-to-moderate PAH and patients with severe PAH. However, this resembles the common clinical situation where most PAH patients already have advanced disease at the time of diagnosis. A certain caution in interpretation of these data is therefore warranted, especially in the smaller group with a baseline PVR<500 dynes·s·cm^{-5}.

Conclusion

Routine ECG evaluation can be an important contribution in the assessment of treatment response in PAH patients.

References

1. Rich S, Dantzker DR, Ayres SM, Bergofsky EH, Brundage BH, Detre KM, Fishman AP, Goldring RM, Groves BM and Koerner SK. Primary pulmonary hypertension. A national prospective study. Ann Intern Med 1987;107:216-223.

2. Barst RJ, Rubin LJ, Long WA, McGoon MD, Rich S, Badesch DB, Groves BM, Tapson VF, Bourge RC, Brundage BH and . A comparison of continuous intravenous epoprostenol (prostacyclin) with conventional therapy for primary pulmonary hypertension. The Primary Pulmonary Hypertension Study Group. N Engl J Med 1996;334:296-302.

3. Sitbon O, Humbert M, Jais X, Ioos V, Hamid AM, Provencher S, Garcia G, Parent F, Herve P and Simonneau G. Long-term response to calcium channel blockers in idiopathic pulmonary arterial hypertension. Circulation 2005;111:3105-3111.

4. Galie N, Ghofrani HA, Torbicki A, Barst RJ, Rubin LJ, Badesch D, Fleming T, Parpia T, Burgess G, Branzi A, Grimminger F, Kurzyna M and Simonneau G. Sildenafil citrate therapy for pulmonary arterial hypertension. N Engl J Med 2005;353:2148-2157.

5. Rubin LJ, Badesch DB, Barst RJ, Galie N, Black CM, Keogh A, Pulido T, Frost A, Roux S, Leconte I, Landzberg M and Simonneau G. Bosentan therapy for pulmonary arterial hypertension. N Engl J Med 2002;346:896-903.

6. Hoeper MM, Markevych I, Spiekerkoetter E, Welte T and Niedermeyer J. Goal-oriented treatment and combination therapy for pulmonary arterial hypertension. Eur Respir J 2005;26:858-863.

7. Peacock A, Naeije R, Galie N and Reeves JT. End points in pulmonary arterial hypertension: the way forward. Eur Respir J 2004;23:947-953.

8. Hoeper MM, Oudiz RJ, Peacock A, Tapson VF, Haworth SG, Frost AE and Torbicki A. End points and clinical trial designs in pulmonary arterial hypertension: clinical and regulatory perspectives. J Am Coll Cardiol 2004;43:48S-55S.

9. Henkens IR, Mouchaers KT, Vonk Noordegraaf A, Boonstra A, Swenne CA, Maan AC, Man SC, Twisk JW, van der Wall EE, Schalij MJ and Vliegen HW. Improved ECG detection of presence and severity of right ventricular pressure load validated with cardiac magnetic resonance imaging. Am J Physiol Heart Circ Physiol 2008;

10. Ahearn GS, Tapson VF, Rebeiz A and Greenfield JC, Jr. Electrocardiography to define clinical status in primary pulmonary hypertension and pulmonary arterial hypertension secondary to collagen vascular disease. Chest 2002;122:524-527.

11. Galie N, Torbicki A, Barst R, Dartevelle P, Haworth S, Higenbottam T, Olschewski H, Peacock A, Pietra G, Rubin LJ, Simonneau G, Priori SG, Garcia MA, Blanc JJ, Budaj A, Cowie M, Dean V, Deckers J, Burgos EF, Lekakis J, Lindahl B, Mazzotta G, McGregor K, Morais J, Oto A, Smiseth OA, Barbera JA, Gibbs S, Hoeper M, Humbert M, Naeije R and Pepke-Zaba J. Guidelines on diagnosis and treatment of pulmonary arterial hypertension. The Task Force on Diagnosis and Treatment of Pulmonary Arterial Hypertension of the European Society of Cardiology. Eur Heart J 2004;25:2243-2278.

12. Barst RJ, McGoon M, Torbicki A, Sitbon O, Krowka MJ, Olschewski H and Gaine S. Diagnosis and differential assessment of pulmonary arterial hypertension. J Am Coll Cardiol 2004;43:40S-47S.

13. Chemla D, Castelain V, Herve P, Lecarpentier Y and Brimioulle S. Haemodynamic evaluation of pulmonary hypertension. Eur Respir J 2002;20:1314-1331.

14. Lankhaar JW, Westerhof N, Faes TJ, Gan CT, Marques KM, Boonstra A, van den Berg FG, Postmus PE and Vonk Noordegraaf A. Pulmonary vascular resistance and compliance stay inversely related during treatment of pulmonary hypertension. Eur Heart J 2008;

15. McGoon M, Gutterman D, Steen V, Barst R, McCrory DC, Fortin TA and Loyd JE. Screening, early detection, and diagnosis of pulmonary arterial hypertension: ACCP evidence-based clinical practice guidelines. Chest 2004;126:14S-34S.

16. Hanley JA and McNeil BJ. A method of comparing the areas under receiver operating characteristic curves derived from the same cases. Radiology 1983;148:839-843.

17. Lehtonen J, Sutinen S, Ikaheimo M and Paakko P. Electrocardiographic criteria for the diagnosis of right ventricular hypertrophy verified at autopsy. Chest 1988;93:839-842.

18. Bossone E, Paciocco G, Iarussi D, Agretto A, Iacono A, Gillespie BW and Rubenfire M. The prognostic role of the ECG in primary pulmonary hypertension. Chest 2002;121:513-518.

19. Karliner JS, Sarnquist FF, Graber DJ, Peters RM, Jr. and West JB. The electrocardiogram at extreme altitude: experience on Mt. Everest. Am Heart J 1985;109:505-513.

20. Penaloza D and Arias-Stella J. The heart and pulmonary circulation at high altitudes: healthy highlanders and chronic mountain sickness. Circulation 2007;115:1132-1146.

21. Pipberger HV, Goldman MJ, Littmann D, Murphy GP, Cosma J and Snyder JR. Correlations of the orthogonal electrocardiogram and vectorcardiogram with consitutional variables in 518 normal men. Circulation 1967;35:536-551.

22. Rich S and Brundage BH. High-dose calcium channel-blocking therapy for primary pulmonary hypertension: evidence for long-term reduction in pulmonary arterial pressure and regression of right ventricular hypertrophy. Circulation 1987;76:135-141.

23. Kawaguchi Y. Studies on deflection area vectors of QRS and T and ventricular gradient in right ventricular hypertrophy. Jpn Circ J 1985;49:395-405.

24. Sitbon O, McLaughlin VV, Badesch DB, Barst RJ, Black C, Galie N, Humbert M, Rainisio M, Rubin LJ and Simonneau G. Survival in patients with class III idiopathic pulmonary arterial hypertension treated with first line oral bosentan compared with an historical cohort of patients started on intravenous epoprostenol. Thorax 2005;60:1025-1030.

25. MacFarlane PW and Lawrie TDV. Comprehensive Electrocardiology. Oxford: Pergamon Press, 1989.

26. Hoeper MM, Lee SH, Voswinckel R, Palazzini M, Jais X, Marinelli A, Barst RJ, Ghofrani HA, Jing ZC, Opitz C, Seyfarth HJ, Halank M, McLaughlin V, Oudiz RJ, Ewert R, Wilkens H, Kluge S, Bremer HC, Baroke E and Rubin LJ. Complications of right heart catheterization procedures in patients with pulmonary hypertension in experienced centers. J Am Coll Cardiol 2006;48:2546-2552.

27. Miyamoto S, Nagaya N, Satoh T, Kyotani S, Sakamaki F, Fujita M, Nakanishi N and Miyatake K. Clinical correlates and prognostic significance of six-minute walk test in patients with primary pulmonary hypertension. Comparison with cardiopulmonary exercise testing. Am J Respir Crit Care Med 2000;161:487-492.

28. Gan CT, McCann GP, Marcus JT, van Wolferen SA, Twisk JW, Boonstra A, Postmus PE and Vonk Noordegraaf A. NT-proBNP reflects right ventricular structure and function in pulmonary hypertension. Eur Respir J 2006;28:1190-1194.

29. Torbicki A, Kurzyna M, Kuca P, Fijalkowska A, Sikora J, Florczyk M, Pruszczyk P, Burakowski J and Wawrzynska L. Detectable serum cardiac troponin T as a marker of poor prognosis among patients with chronic precapillary pulmonary hypertension. Circulation 2003;108:844-848.

30. Mahapatra S, Nishimura RA, Sorajja P, Cha S and McGoon MD. Relationship of pulmonary arterial capacitance and mortality in idiopathic pulmonary arterial hypertension. J Am Coll Cardiol 2006;47:799-803.

31. van Wolferen SA, Marcus JT, Boonstra A, Marques KM, Bronzwaer JG, Spreeuwenberg MD, Postmus PE and Vonk Noordegraaf A. Prognostic value of right ventricular mass, volume, and function in idiopathic pulmonary arterial hypertension. Eur Heart J 2007;28:1250-1257.

32. Channick RN, Simonneau G, Sitbon O, Robbins IM, Frost A, Tapson VF, Badesch DB, Roux S, Rainisio M, Bodin F and Rubin LJ. Effects of the dual endothelin-receptor antagonist bosentan in patients with pulmonary hypertension: a randomised placebo-controlled study. Lancet 2001;358:1119-1123.

33. Barst RJ, Langleben D, Badesch D, Frost A, Lawrence EC, Shapiro S, Naeije R and Galie N. Treatment of pulmonary arterial hypertension with the selective endothelin-A receptor antagonist sitaxsentan. J Am Coll Cardiol 2006;47:2049-2056.

34. Olschewski H, Simonneau G, Galie N, Higenbottam T, Naeije R, Rubin LJ, Nikkho S, Speich R, Hoeper MM, Behr J, Winkler J, Sitbon O, Popov W, Ghofrani HA, Manes A, Kiely DG, Ewert R, Meyer A, Corris PA, Delcroix M, Gomez-Sanchez M, Siedentop H and Seeger W. Inhaled iloprost for severe pulmonary hypertension. N Engl J Med 2002;347:322-329.

35. Simonneau G, Barst RJ, Galie N, Naeije R, Rich S, Bourge RC, Keogh A, Oudiz R, Frost A, Blackburn SD, Crow JW and Rubin LJ. Continuous subcutaneous infusion of treprostinil, a prostacyclin analogue, in patients with pulmonary arterial hypertension: a double-blind, randomized, placebo-controlled trial. Am J Respir Crit Care Med 2002;165:800-804.

36. Rich S. The current treatment of pulmonary arterial hypertension: time to redefine success. Chest 2006;130:1198-1202.

37. Benza RL, Park MH, Keogh A and Girgis RE. Management of pulmonary arterial hypertension with a focus on combination therapies. J Heart Lung Transplant 2007;26:437-446.

IX

Resting heart rate reflects prognosis in patients with idiopathic pulmonary arterial hypertension

Ivo R. Henkens

Serge A. Van Wolferen

C. Tji-Joong Gan

Anco Boonstra

Cees A. Swenne

Jos W. Twisk

Otto Kamp

Ernst E. van der Wall

Martin J. Schalij

Anton Vonk Noordegraaf

Hubert W. Vliegen

Submitted

Abstract

Background

Resting heart rate is an important marker of prognosis in heart failure, but has not been addressed in pulmonary arterial hypertension.

Methods

To determine the prognostic value of resting heart rate in pulmonary arterial hypertension patients we retrospectively analyzed 140 consecutive patients with idiopathic pulmonary arterial hypertension. ECG-derived resting heart rate was evaluated as a potential predictor of adverse prognosis (death or lung transplantation), alongside WHO functional class, 6-minute walk distance, and hemodynamics, both before and approximately one and two years after initiation of pulmonary arterial hypertension treatment.

Results

Forty-nine patients (35%) died, and 5 patients (4%) underwent lung transplantation during follow-up. Both before treatment initiation, and after one and two years of treatment, respectively, a higher resting heart rate was an independent predictor of adverse prognosis (hazard ratio per 10 bpm increase, 1.76 [95% CI, 1.42 - 2.18], 2.31 [CI, 1.58 - 3.38], and 2.1 [CI, 1.39 - 3.19], respectively, $P<0.001$ for all). Change in heart rate between the first and last ECG also independently predicted prognosis (hazard ratio per 1 bpm increase, 1.03 [CI, 1.01 - 1.06].

Conclusions

Both a higher resting heart rate and an important increase in resting heart rate during follow-up signify a considerable risk of death in patients with pulmonary arterial hypertension. The ECG-derived resting heart rate is an important marker of prognosis, and should be assessed both before and at frequent intervals after initiation of treatment for pulmonary arterial hypertension.

Introduction

Pulmonary arterial hypertension is a condition with a poor prognosis. Nevertheless, life expectancy may vary widely among patients [1]. Assessment of patient prognosis has gradually shifted from evaluation of histopathology [2], and hemodynamics [1] towards evaluation of exercise capacity [3], non-invasive imaging [4, 5], and serum markers of disease severity [6, 7]; all important predictors of survival. In pulmonary arterial hypertension, despite its pulmonary-artery-pressure-based definition [8], not the degree of right ventricular afterload but rather cardiac index is considered important for estimation of prognosis [1, 9]. This is easily understood since exercise capacity, reflected by the oxygen uptake reserve, depends on both pulmonary artery driving pressure reserve and heart rate reserve [10, 11]. The increased right ventricular afterload is often associated with impaired right ventricular stroke volume and a compensatory increase in heart rate, most notably with exercise [12]. In advanced pulmonary arterial hypertension, heart rate increase is therefore the main compensatory mechanism, and reflects an increased sympathetic tone [13]. We therefore hypothesized that resting heart rate might be an equally important marker of prognosis in pulmonary arterial hypertension as it is known to be in left-sided heart failure [14, 15]. In order to test our hypothesis, we evaluated the prognostic value of the ECG-derived resting heart rate in parallel with established prognosticators in pulmonary arterial hypertension, related to clinical well-being, exercise capacity, and hemodynamics.

Methods

The study procedures were in accordance with the Declaration of Helsinki. National and institutional guidelines did not require Institutional Review Board approval since the study was retrospectively performed, patient data were anonymized and randomized, and solely included patients from the VU University Medical Center.

Study subjects and study design

Between January 1997 and July 2007, out of 868 consecutive patients referred to the VUMC for evaluation of pulmonary hypertension, 140 patients were found to have idiopathic pulmonary arterial hypertension (Figure 1). Pulmonary arterial hypertension was defined as a mean pulmonary artery pressure >25 mmHg with a pulmonary capillary wedge pressure <15 mmHg. Pulmonary arterial hypertension was considered to be idiopathic when identifiable causes for pulmonary hypertension (i.e. congenital heart disease, portal hypertension, collagen

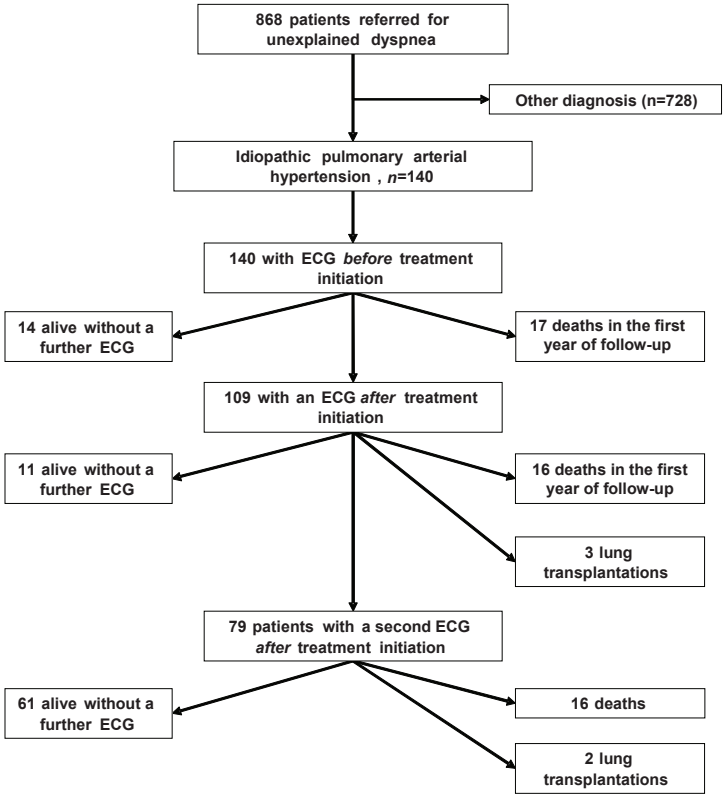

Figure 1: study outline

Death rates and follow-up with resting heart rate assessment in patients with idiopathic pulmonary arterial hypertension.

vascular disease, HIV infection, left heart disease, hypoxic pulmonary disease or chronic thromboembolic disease) were excluded [16]. According to routine clinical protocol all patients underwent a 6-minute walk test at regular outpatient visits, and a resting ECG approximately once yearly, at least. The majority of patients also underwent one or more subsequent right heart catheterizations during follow-up for evaluation of treatment effect. World Health Organization (WHO) functional class [17] was assessed at each patient visit. No patients were lost to follow-up, and follow-up was completed up to February 15th 2008. Available ECGs were matched in time with available catheterizations and 6-minute walk tests. If more than one ECG was available, the ECG with the lowest heart was selected for the study.

Treatment

Patients with a positive response to an acute vasodilator challenge were treated with calcium antagonists [16]. Before 2002, all patients in WHO class III or IV received intravenous prostacyclin (epoprostenol). After 2002 patients in WHO class III received oral monotherapy with an endothelin receptor antagonist (bosentan or sitaxsentan) or phosphodiesterase-5 inhibitor (sildenafil), whereas patients in WHO class IV received a prostacyclin-analog (epoprostenol, treprostinil or iloprost). All patients received oral anticoagulants.

6-minute walk distance

The 6-minute walk distance as well as the Borg dyspnea score was measured according to American Thoracic Society guidelines [18].

Electrocardiography

ECGs were recorded by certified ECG technicians with patients in supine position using the standard 12-lead configuration. ECGs were recorded on commercially available electrocardiographs (MAC VU and MAC 5000, GE Healthcare, The Netherlands), at a paper speed of 25 $mm \cdot s^{-1}$; sensitivity 1 mV = 10 mm; sample frequency of 500 Hz. Besides heart rate we also derived P amplitude in lead II, QRS axis, and QRS duration, directly from the standard electrocardiographic calculations, since these variables were of prognostic value [19] or correlated with clinical status [20] in pulmonary arterial hypertension patients. Measurements concerning P wave amplitude in lead II (mV), and presence of RV hypertrophy according to WHO criteria were performed on ECGs in digital format [21]. All ECGs were analyzed by an experienced cardiologist who was blinded to the data.

Right heart catheterization

The following measurements were performed: right atrial pressure, mean pulmonary artery pressure, pulmonary capillary wedge pressure, and mixed venous oxygen saturation. Cardiac output was measured using the Fick method. Oxygen consumption was also measured during right heart catheterization. Pulmonary vascular resistance was calculated by dividing the transpulmonary gradient (=mean pulmonary artery pressure - pulmonary capillary wedge pressure) by cardiac output. Pulmonary vascular resistance was expressed in $dynes \cdot s \cdot cm^{-5}$. All patients underwent vasodilatory testing with inhaled nitric oxide (20 ppm) [16].

Statistical analysis

We expressed all data as mean ± standard deviation or median (interquartile range). We used the SPSS for Windows Software (version 12.0.1, SPSS Inc, Chicago Illinois) for data analysis. For comparison of baseline variables between survivors and non-survivors we used independent t-tests or χ^2-tests. We performed Cox proportional hazards regression analyses to assess the predictive value of resting heart rate and other variables at the time of diagnosis (first ECG), and at follow-up (second and third ECG). We also evaluated the predictive value of changes in individual variables between the time of diagnosis and the last available moment of follow-up. We considered both death and lung transplantation as adverse events in these analyses. Death was of cardiopulmonary origin in all cases but one, which was treated as a censored case in the survival analyses. We entered variables with a univariable association with adverse prognosis (P<0.20) in multivariable Cox proportional hazards regression analyses. We used stepwise elimination to identify variables independently associated with adverse prognosis. We did not include catheterization data in the multivariable Cox proportional hazards analysis regarding the third ECG, since only 42 out of 79 patients underwent a catheterization. In additional analyses we investigated the predictive value of resting heart rate as a predictor of event-free survival more thoroughly. First, we created receiver operating characteristics curves (ROC) for all variables present in the final prediction models. Subsequently, we plotted Kaplan-Meier curves for resting heart rate as a predictor of adverse prognosis based on the ROC analysis-derived cut-off values at the time of the first, second, and third ECG, respectively. We compared the Kaplan-Meier curves by means of the log-rank test. Finally, to investigate the relationship between resting heart rate and adverse prognosis from a different point of view, we used Cox proportional hazards analysis for risk stratification in patients based on resting heart rate and changes in resting heart rate. We considered a value of P <0.05 to be statistically significant.

Results

During the follow-up period of 43 ± 28 months, 49 out of 140 patients (35%) died, and 5 patients (4%) underwent lung transplantation (Figure 1). During follow-up 13 patients (9%) had documented episodes of atrial fibrillation/flutter. Electrical cardioversion was applied successfully in all but four patients, who remained in atrial fibrillation, and received either amiodarone (n=1), digoxin (n=1), or no medication (n=2).

Baseline

Table 1 displays characteristics of survivors and non-survivors before treatment initiation. In general, non-survivors had less favorable hemodynamics. Medication use after these baseline measurements was similar in survivors and non-survivors with the exception of endothelin receptor antagonists (Table 1). Univariable Cox proportional hazards analysis of baseline variables as predictors of survival demonstrated that age, WHO functional class IV, 6-minute walk distance, mean right atrial pressure, pulmonary vascular resistance, and resting heart rate were all univariable predictors of adverse prognosis (Table 2).

TABLE 1: BASELINE DIFFERENCES BETWEEN SURVIVORS AND NON-SURVIVORS

	Survivors (n=86, 17 male)	Non-survivors (n=54, 13 male)	*P*
General			
Age, *years*	43 ± 14	48 ± 15	0.05
NYHA functional class			<0.001
NYHA class II, n	17	1	<0.001
NYHA class III, n	59	33	0.55
NYHA class IV, n	10	20	<0.01
Exercise			
6-minute walk distance, *m*	404 ± 132	326 ± 120	<0.001
Borg dyspnea index, *units (1-10)*	4 ± 2	4 ± 2	0.50
Right heart catheterization			
Mean RAP, *mmHg*	8 ± 5	11 ± 6	0.01
Mean PAP, *mmHg*	53 ± 13	53 ± 16	0.90
PVR, *dynes·s·cm^{-5}*	859 ± 455	1165 ± 610	0.01
ECG			
Heart rate, *bpm*	76 ± 13	90 ± 17	<0.001
P wave amplitude in lead II, *mm*	2.1 ± 0.9	2.3 ± 1.0	0.22
QRS axis, *°*	107 ± 41	113 ± 45	0.44
QRS duration, *ms*	96 ± 16	93 ± 19	0.22
WHO criteria for RVH, *n (%)*	42 (49%)	32 (58%)	0.23
Medication use*			
None	0	5	0.02
Calcium antagonist, n	4	1	0.07
Endothelin receptor antagonist, n	41	17	0.02
Phosphodiesterase-inhibitor, n	5	3	0.53
Prostacyclin, n	28	26	0.16
Combination therapy, n	8	2	0.17

*RAP=right atrial pressure. PCWP=pulmonary capillary wedge pressure. CI=cardiac index. PVR=pulmonary vascular resistance. *Medication use refers to the period after baseline measurements.*

TABLE 2: HAZARD RATIOS FOR ADVERSE PROGNOSIS BEFORE AND AFTER TREATMENT INITIATION

	First ECG			Second ECG			Third ECG			Δ first to last ECG		
Variables	HR	95% CI	*P*	HR	95% CI	*P*	HR	95% CI	*P*	HR	95% CI	*P*
Age, *years*	1.03	1.01-1.05	0.01	1.05	1.02-1.07	<0.001	1.04	1.00-1.08	0.06			
NYHA class IV*	19.5	2.7-146	0.004	16.8	5.3-53.5	<0.001	4.57	1.13-18.5	0.03	0.28	0.04-2.10	0.22
6-minute walk distance·10^{-1}, *m*	0.96	0.94-0.98	<0.001	0.95	0.92-0.98	<0.001	0.99	0.95-1.03	0.63	0.97	0.93-1.01	0.11
Mean RAP, *mmHg*	1.09	1.03-1.15	<0.01	1.06	0.99-1.15	0.11						
Mean PAP, *mmHg*	1.00	0.98-1.02	0.95	1.01	0.98-1.03	0.72						
PVR ·10^{-2}, *dynes·s·cm*$^{-5}$	1.10	1.04-1.17	<0.01	1.14	1.03-1.27	0.01						
Heart rate·10^{-1}, *bpm*	1.65	1.38-1.97	<0.001	2.02	1.62-2.53	<0.001	1.70	1.23-2.36	<0.01	1.02	1.00-1.04	0.07
P amplitude in lead II, *mm*	1.23	0.93-1.63	0.15	1.33	0.96-1.84	0.09	1.44	0.93-2.24	0.10	1.13	0.83-1.54	0.45
QRS axis, *°*	1.00	1.00-1.01	0.47	1.01	1.00-1.02	0.06	1.00	0.99-1.01	0.84	0.99	0.99-1.01	0.87
QRS duration, *ms*	0.99	0.97-1.00	0.13	1.00	0.97-1.02	0.60	1.00	0.97-1.03	0.82	1.04	1.0-1.09	0.05
WHO criteria for RVH†	1.19	0.69-2.01	0.53	1.21	0.62-2.38	0.58	1.52	0.57-4.04	0.41	0.49	0.50-4.23	0.49
Use of ERA, *yes/no*‡	0.66	0.37-1.17	0.16	0.81	0.40-1.61	0.54	0.45	0.17-1.12	0.11	0.83	0.50-1.39	0.48

*RAP=right atrial pressure, PAP=pulmonary artery pressure, PVR=pulmonary vascular resistance, RVH=right ventricular hypertrophy, ERA=endothelin receptor antagonist. *NYHA class II was used as reference category. †Patients were categorized as 'no longer RVH' (1), 'no change' (2), and 'new-onset RVH' (3) with category 1 as reference category. ‡Patients were categorized as 'no longer ERA' (1), 'no ERA-no change' (2), 'ERA-no change' (3), and 'initiation of ERA' with category 1 as reference category.*

Follow-up

The median interval between the first and second ECG was 389 days (310 - 515 days) for the 109 patients who survived to undergo a second ECG recording. The median interval between the second and third ECG was 440 days (308 - 686 days) for the 79 patients who survived to undergo a third ECG recording. Measured values for 6-minute walk

Table 3: Measurements of variables in patients at the first, second, and third ECG

Variables	ECG 1 n=140	ECG 2 n=109	ECG 3 n=79
General			
Age, *years*	45 ± 14	46 ± 14	47 ± 13
NYHA functional class, *I-IV*	3.1 ± 0.6	3.0 ± 0.6	2.9 ± 0.5
Exercise			
6-minute walk distance, *m*	374 ± 133	446 ± 125	452 ± 138
Borg dyspnea index, *1-10*	4 (3 - 6)	4 (3 - 5)	4 (3 - 5)
Right heart catheterization*			
Mean RAP, *mmHg*	8 (5 - 12)	7 (3 - 11)	6 (3 - 8)
Mean PAP, *mmHg*	53 ± 14	50 ± 14	51 ± 13
PVR·10^{-2}, *dynes·s·cm*$^{-5}$	8.6 (5.4 - 12.9)	7.3 (4.1 - 10.5)	5.9 (4.3 - 8.2)
ECG			
Heart rate, *bpm*	81 ± 16	81 ± 16	79 ± 15
P wave amplitude in lead II, *mm*	2.2 ± 0.9	2.0 ± 1.0	2.3 ± 1.0
QRS axis, *°*	110 (95 - 126)	107 (93 - 120)	104 (90 - 121)
QRS duration, *ms*	94 (83 - 104)	96 (84 - 104)	96 (86 - 108)
WHO criteria for RVH, *n (%)*	74 (53%)	60 (55%)	45 (57%)
Medication use†			
None, *n (%)*	5 (4%)	1 (1%)	-
Calcium antagonist, *n (%)*	5 (4%)	1 (1%)	1 (1%)
ERA, *n (%)*	58 (41%)	29 (27%)	17 (16)
PDE-5 inhibitor, *n (%)*	8 (6%)	8 (7%)	5 (6%)
ERA combined with PDE-5 inhibitor, *n (%)*	6 (4%)	23 (21%)	23 (29%)
Prostacyclin, *n (%)*	54 (39%)	31 (28%)	14 (18%)
Prostacyclin + ERA/PDE-5 inhibitor, *n (%)*	4 (3%)	16 (15%)	19 (24%)

RAP=right atrial pressure, PAP=pulmonary artery pressure, PVR=pulmonary vascular resistance, RVH=right ventricular hypertrophy, ERA=endothelin receptor antagonist, PDE-5=Phosphodiesterase-5. Values measured at the first ECG were all measured before treatment initiation.
**Right heart catheterization was performed in 86 patients at the time of the 2nd ECG, and in 42 patients at the time of the 3rd ECG. †Medication use as displayed was initiated after diagnosis of pulmonary arterial hypertension by right heart catheterization.*

distance, catheterization-derived variables, ECG-derived variables, and medication use at the time of the first, second and third ECG, respectively are displayed in Table 3. Of all variables assessed at the time of the second ECG, age, WHO class IV, 6-minute walk distance, pulmonary vascular resistance, and resting heart rate were predictors of adverse prognosis in univariable Cox proportional hazards analysis (Table 2). WHO class IV and resting heart rate were also predictors of adverse prognosis in univariable Cox proportional hazards analysis at the time of ECG 3. During the time interval between the first ECG and the last ECG only change in QRS duration was a predictor of adverse prognosis in univariable Cox proportional hazards analysis (Table 2).

Multivariable analysis of predictors of adverse prognosis

By multivariable analysis, in which we satisfied the proportional hazards assumption for all models, only resting heart rate and age were independent predictors of adverse prognosis at the time of the first ECG, before treatment initiation (Table 4). Resting heart rate and age were also independent predictors of adverse prognosis at the time of the first and second ECG after treatment initiation (Table 4). Between the first and last available ECG, change in resting heart rate and change in QRS duration were independent predictors of adverse prognosis by multivariable analysis (Table 4).

Table 4: Independent prognosticators by multivariable Cox proportional hazards analysis

Time	Variables	Hazard ratio	95% CI	*P*
ECG 1	Heart rate·10^{-1}, *bpm*	1.76	1.42 - 2.18	<0.001
	Age, *years*	1.04	1.01 - 1.07	0.01
	PVR, *dynes·s·cm^{-5}*	1.06	0.99 - 1.14	0.08
ECG 2	Heart rate·10^{-1}, *bpm*	2.31	1.58 - 3.38	<0.001
	Age, *years*	1.09	1.05 - 1.13	<0.001
ECG 3	Heart rate·10^{-1}, *bpm*	2.10	1.34 - 3.15	<0.001
	Age, *years*	1.10	1.01 - 1.10	<0.01
	WHO class IV, *yes/no**	3.94	0.82 - 18.8	0.09
	P amplitude in lead II	1.73	0.98 - 3.06	0.06
Δ first to last ECG	Δ Heart rate, *bpm*	1.03	1.00 - 1.06	0.04
	Δ QRS duration, *ms*	1.07	1.01 - 1.13	0.03
	Δ 6-minute walk distance, *m·10^{-1}*	0.96	0.92 - 1.01	0.09

PVR=Pulmonary vascular resistance
WHO=World Health Organization
**WHO class II as reference category in Cox proportional hazards regression analysis*

Table 5: Risk stratification of adverse events per year based on heart rate

	Events (rate/year)	Cut-off value	Hazard ratio (95% CI)	Event risk/year
ECG 1	17 (0.12)	Heart rate ≥ 82 bpm	4.2 (2.3 - 7.6)	0.10
		Heart rate < 82 bpm	0.24 (0.13 - 0.43)	0.02
ECG 2	16 (0.15)	Heart rate ≥ 91 bpm	10.7 (4.9 - 23.1)	0.14
		Heart rate < 91 bpm	0.09 (0.04 - 0.20)	0.01
ECG 3	9 (0.11)	Heart rate ≥ 92 bpm	5.7 (2.2 - 14.4)	0.09
		Heart rate < 92 bpm	0.18 (0.07 - 0.45)	0.02
Δ ECG	23 (0.21)	Δ Heart rate ≥ 19 bpm	2.8 (1.3 - 6.0)	0.15
		Δ Heart rate < 19 bpm	0.36 (0.17 - 0.76)	0.06

Δ ECG = change between first and last ECG
Δ Heart rate = change in heart rate between first and last ECG

Receiver Operating Characteristics

Receiver operating characteristics analysis rendered the optimal cut-off value for resting heart rate to be 82 bpm at the first ECG, and 91 bpm and 92 bpm at the second and third ECG, respectively. The optimal cut-off value for change in resting heart rate between the first and last ECG was 19 bpm.

Kaplan-Meier lifetime analysis

Kaplan-Meier analysis defined resting heart rate to be a strong marker of prognosis before treatment initiation (Log Rank = 26.6, $P<0.001$), and even more so after treatment initiation (Log Rank = 55.2, $P<0.001$, and Log Rank = 16.7, $P<0.001$, respectively) (Figure 2 A,B, and C). Similarly, an increased heart rate from the time between the first and the last ECG was associated with a worse prognosis (Log Rank = 7.7, $P<0.01$) (Figure 3D).

Risk of adverse events

We performed Cox proportional hazards analysis according to ROC analysis-derived cut-off values for resting heart rate at the time of the first, second and third ECG, as well as for the cut-off value for change in resting heart between the first and last ECG (Table 5).

With an adverse event rate of 0.12 in the year after the first ECG, based on hazards analysis the event-risk was calculated to be 0.10 for patients with a baseline resting heart rate ≥ 82 bpm, and 0.02 for patients with a baseline resting heart rate <82 bpm. Although the adverse event rate was slightly higher at 0.15 in the year after the second ECG, based on hazards analysis the event-risk was calculated to be 0.16 for patients with a resting heart rate ≥ 91 bpm, and only 0.01 for patients with a resting heart rate < 91 bpm (Table 5).

Discussion

Key finding of this study is that a high resting heart rate and/or an increase in resting heart rate is strongly associated with an adverse prognosis in patients with idiopathic pulmonary arterial hypertension. Since an elevated resting heart rate most likely reflects the degree of disease burden in idiopathic pulmonary arterial hypertension patients [13], we suggest that the easily

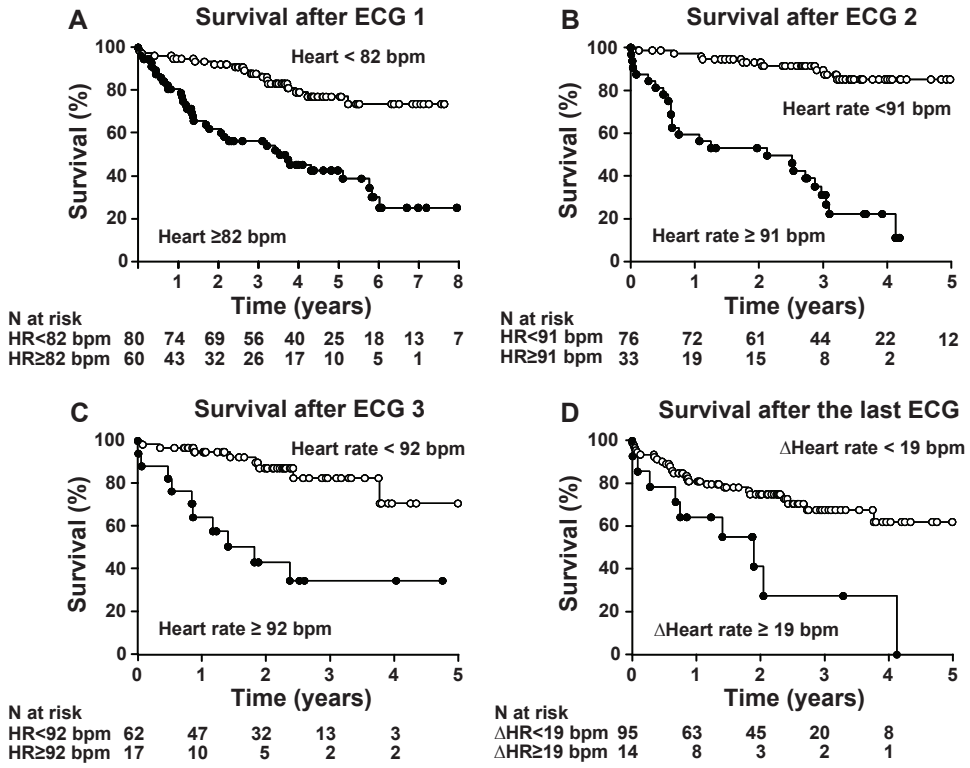

Figure 2: resting heart rate and event-free survival in pulmonary arterial hypertension

Kaplan-Meier survival analysis based on cut-off values for resting heart rate derived from receiver-operating-characteristics.

A. Survival analysis based on resting heart rate before treatment initiation.

B. Survival analysis based on resting heart rate derived from the first ECG approximately one year after treatment initiation.

C. Survival analysis based on resting heart rate derived from the second ECG after treatment initiation.

D. Survival analysis based on the change in resting heart rate between the first ECG before treatment initiation and the last ECG after treatment initiation.

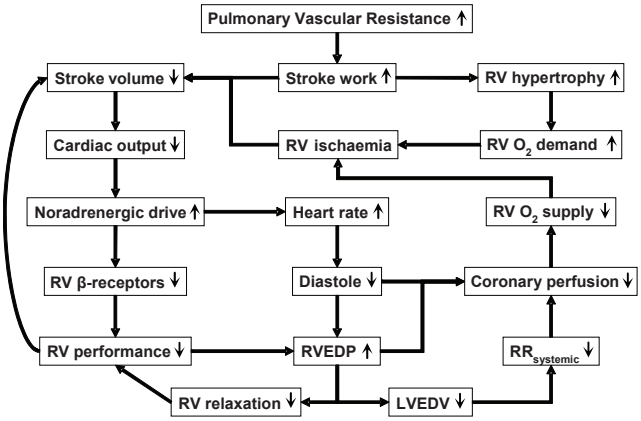

Figure 3: resting heart rate in idiopathic pulmonary arterial hypertension
An elevated pulmonary vascular resistance (PVR) induces increased right ventricular (RV) stroke work, as a result of which the right ventricle hypertrophies, and right ventricular oxygen (O_2) consumption rises. Stroke volume ultimately declines [12], rendering cardiac output dependent on a compensatory increase in heart rate [9, 12]. Heart rate increases as a result of right atrial stretch [30, 31], and an increased noradrenergic drive [13], the latter inducing a down regulation of right ventricular β-adrenergic receptors [23]. Chronic noradrenergic overdrive induces impairment of right ventricular function [23], in turn further decreasing stroke volume and increasing right ventricular end-diastolic pressure [9, 32]. The impaired right ventricular relaxation [33] induces a decreased left ventricular end-diastolic volume (LVEDV), and impaired left ventricular function [34]. Poor left ventricular filling and decreased stroke volume lead to systemic hypotension, most notably with exercise [3, 10, 12]. Both systemic hypotension and increased right ventricular pressures hamper right coronary artery flow [28], to the extent where the right ventricle is supplied with oxygen mainly in diastole, like the left ventricle. The both absolute and relative shorter diastolic filling time at higher heart rates [34] can further impair coronary perfusion, inducing right ventricular ischemia [29], which may lead to further deterioration of right ventricular function. Therefore, resting heart rate reflects right ventricular function. Pulmonary arterial hypertension attenuating treatments associated with a decrease in resting heart rate may therefore preserve or even improve right ventricular function.

acquired ECG-derived resting heart rate should be evaluated more frequently in assessment of these patients.

In comparison with variables related to clinical well-being, exercise capacity, and hemodynamics – all established determinants of prognosis [4, 10] – resting heart rate was the strongest prognosticator, both before and after treatment initiation (Figure 2). To a lesser extent, a change in resting heart rate between the first and last ECG recording also proved to be an important predictor of prognosis. Of note, it seems important to concomitantly assess baseline resting heart rate and the subsequent change in resting heart rate to be able to determine whether a change in

resting heart rate is indeed of clinical importance (Figure 2, Table 5).

Mean pulmonary artery pressure, stroke volume, and heart rate are intertwined around pulmonary vascular resistance at a given oxygen demand of the body [9, 12]. We suggest the following straightforward, partially overlapping chain of events in the evolution of pulmonary hypertension (Figure 3). Initially, at the early onset of afferent pulmonary vascular disease, the right ventricle will increase pulmonary artery pressure accordingly in order to maintain stroke volume [9]. Right ventricular hypertrophy ensues in response to increased wall stress [22]. As disease progresses to the point where the right ventricle can no longer sufficiently increase peak pressure to maintain stroke volume at rest or during exercise [12], a compensatory increase in heart rate emerges, most likely as a result of increased right atrial stretch and increased noradrenergic activation [13]. It has been shown that an increased noradrenergic activation is necessary in the presence of right ventricular hypertrophy for down regulation of β-adrenoceptors, often seen in heart failure [23]. The observed association between a decreasing stroke volume and poor survival supports our finding of the importance of assessing resting heart rate [4]. Cardiac reserve is highly impaired in patients with pulmonary arterial hypertension [10, 24], the degree of which predominantly depends on heart rate reserve, since the already impaired stroke volume does not increase with exercise [12]. In pulmonary arterial hypertension the hemodynamic profile at rest and during exercise therefore depends largely on the degree of right ventricular burden. Resting heart rate essentially reflects this burden, since heart rate is the net result of a complex mechanism of modifying reflex pathways aimed at preserving tissue oxygenation. Especially at rest, an increased heart rate is therefore an ominous sign of a compromised hemodynamic situation, associated with an adverse prognosis. Heart rate has been evaluated before as a possible predictor of adverse prognosis in pulmonary arterial hypertension, both at rest and during exercise [9, 10, 19, 25]. In general, heart rate was measured during right heart catheterization [1, 5, 10] or during echocardiography [26]. However, despite being a predictor in univariable analysis heart rate was not always included in multivariable analysis, or not assessed at follow-up [1]. In our study, ECG-derived resting heart rate was superior to pulmonary vascular resistance for prediction of event-free survival. This may well be because a routine clinical ECG recording is less stressful for patients and, hence, more reliable due to standardization of acquisition. Based on the observed prognostic value, we suggest that resting heart rate should always be assessed, since it outperforms many other diagnostic tools with respect to cost-effectiveness, patient burden, and ease of implementation.

Despite important differences between patients with pulmonary arterial hypertension and patients with congestive heart failure, morbidity and survival are quite similar. In congestive heart failure, clinical well-being and survival has improved substantially with ß-blockade[14]. So far, controlled studies investigating the potential benefit of ß-blockade or selective heart rate

reducing agents have not yet been performed in idiopathic pulmonary arterial hypertension patients. Whether a treatment strategy aimed at heart rate slowing might be of benefit in PAH patients with increased neurohumoral activation is therefore unclear. Theoretically, however, a reduction of resting heart rate could improve right ventricular function in at least two ways. Firstly, the impaired right ventricular diastolic function in pulmonary arterial hypertension [27] may improve by prolonging the relative duration of diastolic filling. Secondly, the extended diastolic filling time may allow right coronary artery perfusion to increase, thereby improving oxygen delivery to the hypertrophied, and often hypoperfused right ventricle [28, 29] and effectively improving right ventricular systolic function (Figure 3).

Bossone et al. [19] studied the prognostic value of ECG-derived variables in pulmonary arterial hypertension, and evaluated heart rate accordingly. However, they merely evaluated patients before initiation of treatment, and did not conduct a similar evaluation after treatment initiation, precluding the appreciation of prognostic value of heart rate and other ECG-derived variables [19]. As is evident from our data, resting heart rate is an even more important prognosticator after treatment initiation (Figure 2, and Table 5), most likely since it reflects the effect, or lack thereof, of the initiated treatment. Bossone et al. observed that P wave amplitude in lead II, a qR pattern in V1, and RV hypertrophy by WHO criteria were related to decreased survival [19]. We only found P wave amplitude in lead II to play a role in the final multivariable prognostic model at the time of the third ECG. Perhaps this discrepancy is related to the more advanced disease state of our patients, as can be deducted from the higher mean PVR, higher QRS axis, and higher mean P amplitude in lead II [19].

Limitations

The retrospective nature of our study precluded evaluation of the potential value of a more frequent assessment of resting heart rate. Nevertheless, we have meanwhile adopted the policy to acquire ECG recordings at each patient visit and at least once yearly. Despite the obvious advantages for both doctor and patient of assessing resting heart rate with an ECG recording, a 24-hour ECG recording has the potential advantage that the lowest heart rate as well as heart rate variability can be assessed more accurately.

Lastly, we solely assessed patients with idiopathic pulmonary arterial hypertension, which precludes straightforward extrapolation of our results to just any patient with pulmonary arterial hypertension, or pulmonary hypertension due to lung disease or left heart disease. Nevertheless, since resting heart rate is largely determined by the activity of the autonomic nervous system, it seems plausible that resting heart will also be of prognostic importance in other groups of pulmonary arterial hypertension patients[15].

Conclusions

Pulmonary arterial hypertension patients with a resting heart rate in the lower ranges have a favorable prognosis within the limits of their disease. In contrast, patients with a high resting heart rate or a substantially increasing resting heart rate during follow-up are at considerable risk of death, and should be considered for lung transplantation. Resting heart rate is most likely a reflection of the individual's coping with disease, and as such a reflection of prognosis. More frequent risk assessment based on resting heart rate may cost-effectively help to improve outcome in patients with pulmonary arterial hypertension.

References

1. D'Alonzo GE, Barst RJ, Ayres SM, Bergofsky EH, Brundage BH, Detre KM, Fishman AP, Goldring RM, Groves BM and Kernis JT. Survival in patients with primary pulmonary hypertension. Results from a national prospective registry. Ann Intern Med 1991;115:343-349.

2. Pietra GG, Edwards WD, Kay JM, Rich S, Kernis J, Schloo B, Ayres SM, Bergofsky EH, Brundage BH and Detre KM. Histopathology of primary pulmonary hypertension. A qualitative and quantitative study of pulmonary blood vessels from 58 patients in the National Heart, Lung, and Blood Institute, Primary Pulmonary Hypertension Registry. Circulation 1989;80:1198-1206.

3. Wensel R, Opitz CF, Anker SD, Winkler J, Hoffken G, Kleber FX, Sharma R, Hummel M, Hetzer R and Ewert R. Assessment of survival in patients with primary pulmonary hypertension: importance of cardiopulmonary exercise testing. Circulation 2002;106:319-324.

4. van Wolferen SA, Marcus JT, Boonstra A, Marques KM, Bronzwaer JG, Spreeuwenberg MD, Postmus PE and Vonk Noordegraaf A. Prognostic value of right ventricular mass, volume, and function in idiopathic pulmonary arterial hypertension. Eur Heart J 2007;28:1250-1257.

5. Mahapatra S, Nishimura RA, Sorajja P, Cha S and McGoon MD. Relationship of pulmonary arterial capacitance and mortality in idiopathic pulmonary arterial hypertension. J Am Coll Cardiol 2006;47:799-803.

6. Gan CT, McCann GP, Marcus JT, van Wolferen SA, Twisk JW, Boonstra A, Postmus PE and Vonk Noordegraaf A. NT-proBNP reflects right ventricular structure and function in pulmonary hypertension. Eur Respir J 2006;28:1190-1194.

7. Torbicki A, Kurzyna M, Kuca P, Fijalkowska A, Sikora J, Florczyk M, Pruszczyk P, Burakowski J and Wawrzynska L. Detectable serum cardiac troponin T as a marker of poor prognosis among patients with chronic precapillary pulmonary hypertension. Circulation 2003;108:844-848.

8. McGoon M, Gutterman D, Steen V, Barst R, McCrory DC, Fortin TA and Loyd JE. Screening, early detection, and diagnosis of pulmonary arterial hypertension: ACCP evidence-based clinical practice guidelines. Chest 2004;126:14S-34S.

9. Chemla D, Castelain V, Herve P, Lecarpentier Y and Brimioulle S. Haemodynamic evaluation of pulmonary hypertension. Eur Respir J 2002;20:1314-1331.

10. Provencher S, Chemla D, Herve P, Sitbon O, Humbert M and Simonneau G. Heart rate responses during the 6-minute walk test in pulmonary arterial hypertension. Eur Respir J 2006;27:114-120.

11. Miyamoto S, Nagaya N, Satoh T, Kyotani S, Sakamaki F, Fujita M, Nakanishi N and Miyatake K. Clinical correlates and prognostic significance of six-minute walk test in patients with primary pulmonary hypertension. Comparison with cardiopulmonary exercise testing. Am J Respir Crit Care Med 2000;161:487-492.

12. Holverda S, Gan CT, Marcus JT, Postmus PE, Boonstra A and Vonk Noordegraaf A. Impaired stroke volume response to exercise in pulmonary arterial hypertension. J Am Coll Cardiol 2006;47:1732-1733.

13. Velez-Roa S, Ciarka A, Najem B, Vachiery JL, Naeije R and Van de Borne P. Increased sympathetic nerve activity in pulmonary artery hypertension. Circulation 2004;110:1308-1312.

14. Hjalmarson A, Goldstein S, Fagerberg B, Wedel H, Waagstein F, Kjekshus J, Wikstrand J, El AD, Vitovec J, Aldershvile J, Halinen M, Dietz R, Neuhaus KL, Janosi A, Thorgeirsson G, Dunselman PH, Gullestad L, Kuch J, Herlitz J, Rickenbacher P, Ball S, Gottlieb S and Deedwania P. Effects of controlled-release metoprolol on total mortality, hospitalizations, and well-being in patients with heart failure: the Metoprolol CR/XL Randomized Intervention Trial in congestive heart failure (MERIT-HF). MERIT-HF Study Group. JAMA 2000;283:1295-1302.

15. Fox K, Borer JS, Camm AJ, Danchin N, Ferrari R, Lopez Sendon JL, Steg PG, Tardif JC, Tavazzi L and Tendera M. Resting heart rate in cardiovascular disease. J Am Coll Cardiol 2007;50:823-830.

16. Galie N, Torbicki A, Barst R, Dartevelle P, Haworth S, Higenbottam T, Olschewski H, Peacock A, Pietra G, Rubin LJ, Simonneau G, Priori SG, Garcia MA, Blanc JJ, Budaj A, Cowie M, Dean V, Deckers J, Burgos EF, Lekakis J, Lindahl B, Mazzotta G, McGregor K, Morais J, Oto A, Smiseth OA, Barbera JA, Gibbs S, Hoeper M, Humbert M, Naeije R and Pepke-Zaba J. Guidelines on diagnosis and treatment of pulmonary arterial hypertension. The Task Force on Diagnosis and Treatment of Pulmonary Arterial Hypertension of the European Society of Cardiology. Eur Heart J 2004;25:2243-2278.

17. Barst RJ, McGoon M, Torbicki A, Sitbon O, Krowka MJ, Olschewski H and Gaine S. Diagnosis and differential assessment of pulmonary arterial hypertension. J Am Coll Cardiol 2004;43:40S-47S.

18. ATS statement: guidelines for the six-minute walk test. Am J Respir Crit Care Med 2002;166:111-117.

19. Bossone E, Paciocco G, Iarussi D, Agretto A, Iacono A, Gillespie BW and Rubenfire M. The prognostic role of the ECG in primary pulmonary hypertension. Chest 2002;121:513-518.

20. Ahearn GS, Tapson VF, Rebeiz A and Greenfield JC, Jr. Electrocardiography to define clinical status in primary pulmonary hypertension and pulmonary arterial hypertension secondary to collagen vascular disease. Chest 2002;122:524-527.

21. Lehtonen J, Sutinen S, Ikaheimo M and Paakko P. Electrocardiographic criteria for the diagnosis of right ventricular hypertrophy verified at autopsy. Chest 1988;93:839-842.

22. Henkens IR, Mouchaers KT, Vliegen HW, van der Laarse WJ, Swenne CA, Maan AC, Draisma HH, Schalij I, van der Wall EE, Schalij MJ and Vonk Noordegraaf A. Early changes in rat hearts with developing pulmonary arterial hypertension can be detected with three-dimensional electrocardiography. Am J Physiol Heart Circ Physiol 2007;293:H1300-H1307.

23. Leineweber K, Brandt K, Wludyka B, Beilfuss A, Ponicke K, Heinroth-Hoffmann I and Brodde OE. Ventricular hypertrophy plus neurohumoral activation is necessary to alter the cardiac beta-adrenoceptor system in experimental heart failure. Circ Res 2002;91:1056-1062.

24. Sun XG, Hansen JE, Oudiz RJ and Wasserman K. Exercise pathophysiology in patients with primary pulmonary hypertension. Circulation 2001;104:429-435.

25. Sandoval J, Bauerle O, Palomar A, Gomez A, Martinez-Guerra ML, Beltran M and Guerrero ML. Survival in primary pulmonary hypertension. Validation of a prognostic equation. Circulation 1994;89:1733-1744.

26. Mahapatra S, Nishimura RA, Oh JK and McGoon MD. The prognostic value of pulmonary vascular capacitance determined by Doppler echocardiography in patients with pulmonary arterial hypertension. J Am Soc Echocardiogr 2006;19:1045-1050.

27. Marcus JT, Gan CT, Zwanenburg JJ, Boonstra A, Allaart CP, Gotte MJ and Vonk Noordegraaf A. Interventricular mechanical asynchrony in pulmonary arterial hypertension: left-to-right delay in peak shortening is related to right ventricular overload and left ventricular underfilling. J Am Coll Cardiol 2008;51:750-757.

28. van Wolferen SA, Marcus JT, Westerhof N, Spreeuwenberg MD, Marques KM, Bronzwaer JG, Henkens IR, Gan CT, Boonstra A, Postmus PE and Vonk Noordegraaf A. Right coronary artery flow impairment in patients with pulmonary hypertension. Eur Heart J 2008;29:120-127.

29. Gomez A, Bialostozky D, Zajarias A, Santos E, Palomar A, Martinez ML and Sandoval J. Right ventricular ischemia in patients with primary pulmonary hypertension. J Am Coll Cardiol 2001;38:1137-1142.

30. Horner SM, Murphy CF, Coen B, Dick DJ, Harrison FG, Vespalcova Z and Lab MJ. Contribution to heart rate variability by mechanoelectric feedback. Stretch of the sinoatrial node reduces heart rate variability. Circulation 1996;94:1762-1767.

31. Barbieri R, Triedman JK and Saul JP. Heart rate control and mechanical cardiopulmonary coupling to assess central volume: a systems analysis. Am J Physiol Regul Integr Comp Physiol 2002;283: R1210-R1220.

32. Yeo TC, Dujardin KS, Tei C, Mahoney DW, McGoon MD and Seward JB. Value of a Doppler-derived index combining systolic and diastolic time intervals in predicting outcome in primary pulmonary hypertension. Am J Cardiol 1998;81:1157-1161.

33. Castelain V, Chemla D, Humbert M, Sitbon O, Simonneau G, Lecarpentier Y and Herve P. Pulmonary artery pressure-flow relations after prostacyclin in primary pulmonary hypertension. Am J Respir Crit Care Med 2002;165:338-340.

34. Chang SM, Lin CC, Hsiao SH, Lee CY, Yang SH, Lin SK and Huang WC. Pulmonary hypertension and left heart function: insights from tissue Doppler imaging and myocardial performance index. Echocardiography 2007;24:366-373.

X

Summary, conclusions and future perspectives
Samenvatting, conclusies en blik op de toekomst

Summary

Right ventricular overload covers a spectrum ranging from volume overload to pressure overload, and often is a combination of these, compromising cardiac function. The general introduction describes the anatomy of the right ventricle and its role in normal hemodynamics, as well as in pathological hemodynamics due to right ventricular volume and/or pressure overload.

Part I focuses on right ventricular volume overload in adults in whom surgical correction for Fallot's tetralogy was performed in early childhood. Importantly, many adult Fallot patients will require repeated pulmonary valve replacement. We attempted to elucidate which patient characteristics are associated with a more prompt recovery time after surgical replacement. Furthermore, we analyzed what may be expected from pulmonary valve replacement with respect to right ventricular reverse remodeling. We also determined that pulmonary valve replacement has a positive effect on the repolarization characteristics in adult Fallot patients.

Part II goes into right ventricular pressure overload due to pulmonary arterial hypertension. In an animal experimental setup, induction of pulmonary arterial hypertension in rats led to characteristic evolutionary changes in right ventricular morphology and function. We used electrocardiography, echocardiography, and heart catheterization to monitor this chain of events. The documented evolutionary electrocardiographic changes due to right ventricular pressure overload in rats were similar to the abnormalities found in patients with varying degrees of pulmonary arterial hypertension. Based on the hemodynamic abnormalities associated with electrocardiographically detectable abnormalities, we defined electrocardiographic cut-off points for determination of treatment response in pulmonary arterial hypertension patients. Finally, we determined that resting heart rate, reflecting hemodynamics and neurohumoral activation, is a very important marker of prognosis in pulmonary arterial hypertension. Implementing the prognostic value of resting heart rate in clinical decision making may allow for earlier, more tailored additional therapy or (heart-)lung transplantation.

Chapter I is a general introduction to the topics of the thesis: right ventricular volume overload and right ventricular pressure overload are extensively discussed, offering the reader an insight into the normal right ventricular anatomy, pathophysiology of right ventricular volume and pressure overload, accompanying symptoms, diagnosis and follow-up.

Part I

In Chapter II we deal with the recovery time after pulmonary valve replacement in adult patients with a corrected tetralogy of Fallot. Surgical intervention in early childhood generally allows Fallot patients to grow up without major inhibitions. However, the malformed pulmonary valve will in time require replacement due to a combination of stenosis and insufficiency. Pulmonary valve replacement is a relatively straightforward surgical procedure with typically low mortality. We assessed recovery time – defined as the time between surgery and return to work or school – after mortality one of the most important aspects of this intervention for young patients. Importantly, we found that not New York Heart Association functional class or right ventricular function determined recovery time, but rather the patient's age.

In Chapter III we discuss the importance of pre-operative assessment of right ventricular function in adult tetralogy of Fallot patients. In many cases, surgical correction of the right ventricular outflow tract early in life does not allow for adequate long-term repair of the abnormal pulmonary valve. Since residual pulmonary valve stenosis is considered more deleterious to right ventricular function than residual pulmonary valve regurgitation, the surgeon will generally settle for a gradient-free right ventricular outflow tract with pulmonary valve regurgitation. Nevertheless, it is believed that decreased right ventricular function and increased right ventricular dimensions are a consequence of longstanding pulmonary valve regurgitation. However, we observed that the degree of pre-operative pulmonary valve regurgitation is not related to the effect of pulmonary valve replacement. Rather, pre-operative right ventricular dimensions and function predict reverse remodeling and functional improvement after pulmonary valve replacement.

In Chapter IV we explore the potentially beneficial effect of pulmonary valve replacement on myocardial repolarization characteristics in adult patients with tetralogy of Fallot. Cardiac arrhythmias and sudden death are important issues which need to be addressed by physicians caring for these patients. In adult Fallot patients with severely dilated right ventricles, conduction disorders as well as repolarization disorders are thought to predispose to severe ventricular arrhythmias. We found that, as a consequence of pulmonary valve replacement, right ventricular volumes decreased, average depolarization duration decreased, and repolarization characteristics changed towards a more normal pattern. Due to the relatively small number of patients our study was underpowered to

detect a clinically significant effect on the incidence of severe ventricular arrhythmias. Nevertheless, the observed changes suggest that pulmonary valve replacement has a beneficial effect on depolarization duration and repolarization heterogeneity, theoretically decreasing ventricular arrhythmia propensity.

Part II

In Chapter V we determine the evolutionary changes in the right ventricle as a consequence of developing pulmonary arterial hypertension, using an experimental animal setup. As pulmonary vascular resistance progressively rises in the face of ongoing pulmonary artery disease, the right ventricle is required to increase its stroke work order to maintain cardiac output. We studied rats before and 14 and 25 days after administration of monocrotaline, a substance that injures the pulmonary vasculature, inducing pulmonary arterial hypertension. Importantly, on day 14, even before pulmonary arterial hypertension induced right ventricular hypertrophy, the effect of an increased demand in right ventricular stroke work could be detected with a three-dimensional vectorcardiogram, reconstructed from a three-lead body surface ECG. Apparently, three-dimensional electrocardiography is very sensitive to early changes in right ventricular afterload. This finding is of potential use, since the ECG is ubiquitously utilized in everyday medical practice.

In Chapter VI we prove our hypothesis that using a three-dimensional vectorcardiogram, reconstructed from a standard 12-lead body surface ECG, improves detection of increased right ventricular pressure load. The three-dimensional vectorcardiogram renders additional parameters for analysis, among which the ventricular gradient, a mathematical representation of ventricular action potential duration heterogeneity which normally lies within a small range of magnitude and three-dimensional orientation. Using the ventricular gradient indeed improved ECG detection of right ventricular pressure overload significantly in our study population of 72 patients and 144 matched healthy controls. Importantly, much like in our prior experimental animal setup, the three-dimensional vectorcardiogram detected mild to moderate pulmonary arterial hypertension, otherwise misclassified by conventional ECG analysis. Additional MRI studies defined a fair association between the ventricular gradient and right ventricular mass and volume. Ventricular gradient changes in pulmonary arterial hypertension patients likely reflect changes in ventricular action potential duration heterogeneity related to right ventricular remodeling as a result of an increased right ventricular pressure load.

In Chapter VII we discuss the role of the ECG in diagnosis and follow-up of pulmonary arterial hypertension patients. Although inter-individual variation in ECG characteristics may vary widely, intra-individual variation in ECG characteristics over time is usually negligible except for situations in which intercurrent events trigger cardiac damage and/or adaptation. We describe two ECGs of the same patient, before and after development of idiopathic pulmonary arterial hypertension, which gave rise to suspicion of an increased right heart load. Furthermore, we discuss the available literature on specific electrocardiographic details associated with right heart overload. There is now ample evidence to redefine the role of the ECG as a tool for follow-up, as well as for diagnosis of increased right heart load in selected groups of patients at risk for developing pulmonary arterial hypertension.

In Chapter VIII we test our hypothesis that the ECG can be used for follow-up of pulmonary arterial hypertension patients, based on the severity of pulmonary vascular resistance. Although the conventional 12-lead ECG is less sensitive for increased right ventricular afterload than its derived three-dimensional vectorcardiogram, physicians are not equipped to reconstruct, let alone analyze the latter. We therefore focused on the conventional ECG for longitudinal individual monitoring of treatment response. Previous studies indicated that the conventional ECG often does not detect mild-to-moderate pulmonary arterial hypertension, whereas it almost always shows abnormalities in patients with severe pulmonary arterial hypertension. We classified a group of pulmonary arterial hypertension patients according to the presence of mild-to-moderate or severe pulmonary arterial hypertension – defined as a pulmonary vascular resistance below or above 500 dynes·s·cm^{-5} (double of the upper limit of normal) at the time of diagnosis. Subsequently, we determined which patients improved, worsened or maintained stable, according to pulmonary vascular resistance measured during repeated right heart catheterization. Importantly, no ECG changes were found in patients who remained stable. However, in patients with mild-to-moderate disease who deteriorated, as well as in patients with severe disease who improved, ECG changes were found consistently. Routine ECG evaluation in patients with established pulmonary arterial hypertension can therefore be an important contribution in the assessment of treatment response.

In Chapter IX we evaluate whether resting heart rate is as important a prognostic marker in pulmonary arterial hypertension as it is in left-sided heart failure. Resting heart rate, reflecting hemodynamics and noradrenergic drive, tends to be higher in patients with little cardiac reserve. We retrospectively analyzed resting ECGs from a cohort of 140 pulmonary arterial hypertension patients, recorded at the time of diagnosis, and after approximately one

and two years of follow-up, for prognostic value in predicting death or the need for (heart-)lung transplantation. Resting heart rate superseded hemodynamic data, and 6-minute walk distance – established prognosticators in pulmonary arterial hypertension patients – both at the time of diagnosis and at follow-up. Therefore, both a higher resting heart rate and an important increase in resting heart rate during follow-up signify a considerable risk of death in patients with pulmonary arterial hypertension. The ECG-derived resting heart rate is an important marker of prognosis, and should be assessed both before and at frequent intervals after initiation of treatment for pulmonary arterial hypertension.

Conclusions

- Pulmonary valve replacement is best reserved for adult Fallot patients who do not qualify for percutaneous valve implantation, and older patients should expect a more prolonged recovery time, regardless of pre-operative functional class or right ventricular function.

- Timing of pulmonary valve replacement should be based on right ventricular function rather than on the severity of pulmonary valve regurgitation.

- Pulmonary valve replacement in adult Fallot patients has a beneficial effect on electrocardiographic indices of repolarization heterogeneity.

- Early right ventricular changes in evolving pulmonary arterial hypertension can be detected with reconstructed three-dimensional ECG recordings.

- The ventricular gradient is very sensitive to right ventricular pressure overload, both in rats and humans, allowing for better electrocardiographic detection of pulmonary arterial hypertension.

- The role of the electrocardiogram in the diagnosis and follow-up of pulmonary arterial hypertension patients should not be underestimated: even standard 12-lead ECGs prove to be a useful contribution for monitoring treatment response.

- Resting heart rate is an important marker of prognosis in pulmonary arterial hypertension patients, and should be assessed before and at frequent intervals after treatment initiation: both a higher resting heart rate, and an increase in resting heart rate over time denote an adverse prognosis, requiring intensified treatment and/or lung transplantation.

Future perspectives

Non-invasive diagnosis in and the follow-up of patients with right ventricular overload was long based on physical examination, chest X-rays, and time-consuming electrocardiographical analyses [1-4]. Nowadays – much like in patients with left ventricular overload – we use biomarkers [5-8], validated exercise tests [9-13], advanced echocardiography [14-24], and cardiac MRI [25-31]. Although right ventricular myocardial viability and function associated with (relative) ischemia has not yet been investigated extensively enough, currently available data show that a lack of oxygen is important in the evolution of right ventricular failure from a situation of right ventricular overload [5, 32-34]. This signifies that ischemia-modulating therapy may have an important role in the treatment of right ventricular overload. Similarly, non-invasive diagnosis will likely be aimed more at the diagnosis of (episodes of) ischemia. Despite the fact that right heart catheterization will probably remain in use for diagnosis of pulmonary hypertension [35], there is an increasing demand for important markers of disease and prognosis, relevant to the individual patient [6, 36]. Despite the sound physiological principles one can distill from measuring right ventricular afterload, stroke volume, and heart rate [37-39], these do not explain why there is such a large heterogeneity in clinical presentation between patients. It will therefore become important to clarify the consequences of right ventricular overload for individual patients, in order to administer a specific therapy. One should think of the consequences for action potential conduction [40, 41], similar to left ventricular failure, where a certain degree of electromechanical dissociation in the myocardium should be considered highly unfavorable [42-44]. It is unlikely that pacing the right ventricle in one specific area will solve this problem [45]. Nevertheless, a substantial portion of patients with heart failure benefit from such an intervention [46].However, when there is a more diffuse electromechanical dissociation in the myocardium, rather than an electrically inactive area [47], the expected result of pacing may be next to nothing. Electrocardiography can provide insight into the degree of concordance of depolarization and repolarization [48, 49], whereas echocardiography can measure the degree of heterogeneity in myocardial contraction [24]. In future, the relevance of electromechanical dissociation for the occurrence of (fatal) arrhythmias will likely be investigated, and implemented more broadly in clinical care [50-53].

An interesting part of this research will be whether there is an important difference between patients with right ventricular overload from birth and patients who developed right ventricular overload at a later age. As discussed in the introduction, the role of the endothelium will presumably become more important for the follow-up of patients with

pulmonary hypertension associated right ventricular overload. Studies already demonstrated that endothelial progenitor cell levels are markedly decreased in patients with pulmonary arterial hypertension [54]. Perhaps the level of these cells may be used as a marker of the effect of pulmonary arterial hypertension attenuating treatment. So far, however, it is fair to say that the development and fine-tuning' of techniques for diagnosis and follow-up of right ventricular overload is suboptimal, compared to the field of left ventricular overload. The right ventricle is not wrongfully called the 'forgotten ventricle' [55]. On the one hand this may be a result of the smaller 'market' with less resultant scientific interest, on the other hand the same 'market' is probably limiting development and validation of new measurement utilities by its small size. Important for the further development is therefore the knowledge regarding the prevalence of right ventricular overload [56-61]. At the same time it is important to have a fair estimate of the number of people at risk for development of right ventricular overload, for instance after a pulmonary embolism [62, 63]. Once risk groups are identified, targeted screening of patients with a high risk profile becomes feasible [2]. Affordable and easily applicable modalities such as biomarkers and electrocardiography could be of good use in this setting.

Samenvatting

Rechter ventrikel overbelasting bestrijkt een breed spectrum tussen volume overbelasting en druk overbelasting. Vaak is er sprake van een combinatie van druk en volume overbelasting, waardoor het hart niet optimaal kan functioneren. In de algemene introductie wordt de anatomie van de rechter ventrikel beschreven, evenals de rol van de rechter kamer in de situatie van normale hemodynamiek en de situatie van pathologische hemodynamiek ten gevolge van rechter kamer druk en/of volume overbelasting.

Deel I gaat in op rechter ventrikel volume overbelasting in volwassenen bij wie een chirurgische correctie voor een tetralogie van Fallot in de eerste jaren na geboorte werd uitgevoerd. Veel volwassen patiënten met een tetralogie van Fallot zullen bij herhaling een pulmonaalklep vervanging moeten ondergaan. Wij hebben getracht te verhelderen welke patiënt eigenschappen zijn geassocieerd met een sneller functioneel herstel na chirurgische pulmonaalklep vervanging. Daarnaast hebben wij geanalyseerd wat het te verwachten effect is van pulmonaalklep vervanging ten aanzien van positieve remodellering van de rechter ventrikel. Tot slot hebben we laten zien dat pulmonaalklep vervanging een positief effect heeft op de repolarisatie karakteristieken van het myocard bij volwassen Fallot patiënten.

Deel II behandelt rechter ventrikel druk overbelasting ten gevolge van pulmonale arteriële hypertensie. In een dierexperimentele proef leidde inductie van pulmonale arteriële hypertensie bij ratten tot karakteristieke veranderingen in rechter ventrikel morfologie en functie. Wij pasten elektrocardiografie, echocardiografie en hartkatheterisatie toe om het beloop van de ontstane veranderingen in kaart te brengen. De in ratten met elektrocardiografie geobserveerde veranderingen ten gevolge van rechter ventrikel hypertrofie waren vergelijkbaar met de afwijkingen die werden gevonden in patiënten met een verschillende mate van pulmonale arteriële hypertensie. Op basis van de ernst van de hemodynamische afwijkingen die gepaard gingen met op het ECG detecteerbare afwijkingen, hebben we vervolgens duidelijke afkapwaarden voor het ECG gedefinieerd, waarmee het succes van behandeling in patiënten met pulmonale arteriële hypertensie kan worden bepaald. Tot slot hebben we bepaald dat de hartfrequentie in rust, als een weerspiegeling van hemodynamiek en neurohumorale activiteit, een belangrijke prognostische marker is bij patiënten met pulmonale arteriële hypertensie.

Hoofdstuk I is een algemene introductie over de onderwerpen van het proefschrift: rechter ventrikel druk en volume overbelasting worden uitgebreid besproken, waarmee de lezer

een goed beeld wordt geschetst van de normale anatomie van de rechter ventrikel, de pathofysiologie van rechter ventrikel druk en volume overbelasting, begeleidende symptomen, behandelopties, en follow-up.

Deel I

In Hoofdstuk II bespreken we de duur van het herstel na pulmonaalklep vervanging bij volwassen patiënten met een gecorrigeerde tetralogie van Fallot. Chirurgische behandeling kort na de geboorte heeft er voor gezorgd dat Fallot patiënten tegenwoordig doorgaans de volwassen leeftijd kunnen bereiken zonder groeivertraging of ernstige conditionele beperkingen. Niettemin vereist de in aanleg abnormale pulmonaalklep na initiële chirurgische correctie van de rechter ventrikel uitstroombaan op termijn een re-interventie; er is dan meestal sprake van een combinatie van stenose en lekkage van de pulmonaalklep. Pulmonaalklep vervanging is een relatief eenvoudige chirurgische procedure en kent een lage mortaliteit. Wij analyseerden hoe lang de patiënten nodig hadden voor hun herstel – gedefinieerd als de tijdsduur tussen operatie en het weer aan het werk of naar school gaan – omdat dit een van de belangrijkste gegevens is voor een jonge patiënt. Hierbij vonden we niet dat de herstelduur werd bepaald door het functioneren volgens de New York Heart Association classificatie of door rechter ventrikel functie, maar juist door de leeftijd van de patiënt.

In Hoofdstuk III behandelen we het belang van preoperatieve beoordeling van rechter ventrikel functie in volwassen Fallot patiënten. Chirurgische correctie van de rechter ventrikel uitstroombaan op zeer jonge leeftijd stelt de chirurg in veel gevallen niet in staat de pathologische pulmonaalklep zodanig te repareren, dat deze geen nieuwe interventie meer vereist. Omdat residuele pulmonaalklep stenose op lange termijn schadelijker wordt geacht voor de rechter ventrikel functie dan pulmonaalklep lekkage, zal de chirurg in de meeste gevallen kiezen voor een rechter ventrikel uitstroombaan met een minimale gradiënt en pulmonaalklep regurgitatie hierbij accepteren. Desondanks worden de op langere termijn verminderde rechter ventrikel functie en rechter ventrikel dilatatie wel geweten aan het langdurige bestaan van aanzienlijke pulmonaalklep lekkage. Wij observeerden echter dat de ernst van de preoperatieve pulmonaalklep lekkage niet gerelateerd is aan het effect van pulmonaalklep vervanging. In plaats daarvan zijn het de preoperatief gemeten rechter ventrikel dimensies en functie die de mate van postoperatieve positieve remodellering en verbetering van functie van de rechter ventrikel voorspellen.

In Hoofdstuk IV bestuderen we de potentieel gunstige effecten van pulmonaalklep vervanging op het repolarisatie patroon van het myocard van volwassen patiënten met een tetralogie van Fallot. Cardiale aritmieën en plotse dood zijn belangrijke problemen voor artsen die zorgen voor deze patiënten. Bij volwassen Fallot patiënten met ernstig verwijde rechter ventrikels worden geleidingsproblemen en repolarisatie afwijkingen geacht een hoger risico te geven op ernstige ventriculaire ritmestoornissen. Wij vonden dat als gevolg van pulmonaalklep vervanging rechter ventrikel dimensies afnamen, de gemiddelde depolarisatie duur afnam en het repolarisatie patroon minder afwijkend werd. Door het relatief kleine aantal patiënten in onze studie was het niet mogelijk om een klinisch significant effect te detecteren op de incidentie van ernstige ventriculaire ritmestoornissen. Dit neemt echter niet weg dat de geobjectiveerde veranderingen suggereren dat pulmonaalklep vervanging een positief effect heeft op zowel de depolarisatie duur als de repolarisatie heterogeniteit, waarmee in theorie de kans op het ontstaan van ventriculaire aritmieën zou moeten afnemen.

Deel II

In Hoofdstuk V bepalen we het beloop van het ontstaan van veranderingen in de rechter ventrikel als gevolg van een zich ontwikkelende pulmonale arteriële hypertensie, daarbij gebruik makend van dierexperimenteel onderzoek. Met een progressief toenemende pulmonale vaatweerstand als gevolg van voortgaande pulmonaal arteriële vaatziekte, wordt van de rechter ventrikel verlangd dat deze zijn arbeid per hartslag verhoogt teneinde het hartminuutvolume te garanderen. Wij hebben ratten bestudeerd voor en respectievelijk 14 en 25 dagen na toediening van monocrotaline, een stof die de longvaten beschadigt. Opvallend hierbij was dat al na 14 dagen, nog voor er sprake was van rechter ventrikel hypertrofie ten gevolge van pulmonale arteriële hypertensie, de gevolgen van noodzakelijke toename van de arbeid van de rechter ventrikel konden worden gedetecteerd met een 3-dimensionaal vectorcardiogram, gereconstrueerd uit een 3-afleidingen lichaamsoppervlak ECG. Het lijkt er dus op dat 3-dimensionale elektrocardiografie zeer gevoelig is voor vroege veranderingen in rechter kamer afterload. Dit is van belang, omdat het ECG binnen de medische praktijk zeer veel wordt gebruikt.

In Hoofdstuk VI leveren wij het bewijs voor onze hypothese dat het gebruik van een 3-dimensionaal vectorcardiogram, gereconstrueerd uit een standaard 12-afleidingen lichaamsoppervlakte ECG, de detectie van rechter ventrikel druk overbelasting kan verbeteren. Dit 3-dimensionale vectorcardiogram levert namelijk additionele parameters

voor analyse, waaronder de ventriculaire gradiënt, een mathematische weergave van de heterogeniteit van de duur van de verschillende ventriculaire actiepotentialen in het myocard. De ventriculaire gradiënt ligt normaliter binnen nauwe grenzen van grootte en oriëntatie. Het toepassen van de ventriculaire gradiënt verbeterde de diagnostische accuratesse van het ECG voor rechter ventrikel druk overbelasting significant in onze studie populatie van 72 patiënten gematched met 144 gezonde controles. Van belang hierbij was, dat net als in ons eerdere experiment bij ratten, het 3-dimensionale vectorcardiogram ook milde tot matige pulmonale arteriële hypertensie detecteerde, iets wat doorgaans wordt gemist bij conventionele ECG analyse. Aanvullend MRI onderzoek liet zien dat er een redelijke correlatie bestaat tussen de ventriculaire gradiënt en rechter ventrikel massa en volume. De veranderingen in de ventriculaire gradiënt bij patiënten met pulmonale arteriële hypertensie zijn waarschijnlijk een afspiegeling van de veranderingen in actiepotentiaal duur heterogeniteit, gerelateerd aan remodellering van de rechter ventrikel als gevolg van een toegenomen rechter ventrikel druk belasting.

In Hoofdstuk VII bespreken we de rol van het ECG voor diagnostiek en follow-up van patiënten met pulmonale arteriële hypertensie. Hoewel er een brede inter-individuele variatie bestaat in de algemene populatie, is een intra-individuele variatie in ECG karakteristieken doorgaans gering, behalve wanneer tussentijdse gebeurtenissen leiden tot myocardiale schade en/of adaptatie. Wij beschrijven twee ECGs van een patiënt, vóór en na ontwikkeling van idiopathische pulmonale arteriële hypertensie, welke aanleiding gaven tot het vermoeden van de aanwezigheid van een rechter ventrikel druk overbelasting. Daarnaast bespreken we de beschikbare literatuur over specifieke elektrocardiografische details, die geassocieerd zijn met rechter ventrikel druk overbelasting. Er is nu voldoende bewijs om de rol van het ECG te herdefiniëren: het is niet alleen een adequaat instrument voor follow-up, maar ook voor de diagnose van rechter ventrikel druk overbelasting in geselecteerde groepen patiënten die het risico lopen op het ontwikkelen van pulmonale arteriële hypertensie.

In Hoofdstuk VIII testen we onze hypothese dat het ECG kan worden gebruikt voor de follow-up van patiënten met pulmonale arteriële hypertensie, op basis van de ernst van de pulmonale vaatweerstand. Hoewel het 12-afleidingen ECG minder gevoelig is voor een verhoogde rechter ventrikel druk dan het 3-dimensionale vectorcardiogram, zijn artsen doorgaans niet in staat het laatstgenoemde te reconstrueren, laat staan te analyseren. We hebben onze aandacht daarom gericht op het conventionele ECG voor het longitudinaal monitoren van het effect van behandeling. Eerdere studies wezen uit dat het conventionele

ECG vaak milde tot matige pulmonale arteriële hypertensie niet detecteert, terwijl het ECG doorgaans wel afwijkend is bij patiënten met ernstige pulmonale arteriële hypertensie. We hebben daarom een groep patiënten met pulmonale arteriële hypertensie verdeeld in twee groepen op basis van de aanwezigheid van milde tot matige, dan wel ernstige pulmonale arteriële hypertensie – gedefinieerd als een pulmonale vaatweerstand kleiner of groter dan 500 dynes·s·cm^{-5} (twee keer het maximum van de normaalwaarde) ten tijde van diagnose. Vervolgens hebben we bepaald welke patiënten verbeterden, verslechterden of stabiel bleven, op basis van de gemeten pulmonale vaatweerstand tijdens een tweede hart catheterisatie. Er werden geen ECG veranderingen gevonden bij patiënten die stabiel bleven. Echter, in patiënten met milde tot matige pulmonale arteriële hypertensie die verslechterden, alsook in patiënten met ernstige pulmonale arteriële hypertensie die verbeterden, werden consequent ECG veranderingen gezien. Routinematige ECG opname in patiënten met aangetoonde pulmonale arteriële hypertensie kan daarom een belangrijke bijdrage leveren aan beoordeling van het effect van therapie.

In Hoofdstuk IX evalueren we of de hartfrequentie in rust een net zo belangrijke prognostische marker is bij patiënten met pulmonale arteriële hypertensie als bij patiënten met linkszijdig hartfalen. De hartfrequentie in rust, een weerspiegeling van de hemodynamiek en noradrenerge activiteit, is doorgaans hoger in patiënten met een krappe cardiale reserve. We hebben van een cohort van 140 patiënten met pulmonale arteriële hypertensie de ECGs geanalyseerd, gemaakt ten tijde van diagnose en na respectievelijk een en twee jaar follow-up. Hierbij keken we naar de prognostische waarde ten aanzien van het optreden van dood of (hart-) longtransplantatie. De hartfrequentie in rust bleek een betere prognostische parameter dan hemodynamische data of de afgelegde afstand tijdens de 6-minuten looptest – beiden geaccepteerde prognostische markers in patiënten met pulmonale arteriële hypertensie – zowel op het moment van diagnose als tijdens follow-up. Een hogere hartfrequentie in rust en een belangrijke toename van de hartfrequentie tijdens follow-up zijn daarom een teken van een verhoogd risico op overlijden in patiënten met pulmonale arteriële hypertensie. De van het ECG afgeleide hartfrequentie in rust is daarmee een belangrijke prognostische marker die dient te worden bepaald vóór start van therapie voor pulmonale arteriële hypertensie en regelmatig gedurende follow-up. Er kan dan vroegtijdig worden ingeschat of patiënten intensievere therapie nodig hebben of wellicht kandidaat zijn voor een (hart-)longtransplantatie.

Conclusies

- Pulmonaalklep vervanging is het meest geschikt voor volwassen Fallot patiënten die niet in aanmerking komen voor percutane klepvervanging en oudere patiënten moeten rekenen op een langer herstelduur na operatie, ongeacht hun pre-operatief functioneren of rechter ventrikel functie.

- Het tijdstip waarop pulmonaalklep vervanging wordt uitgevoerd, dient te worden gebaseerd op de rechter ventrikel functie en niet op de ernst van de pulmonaalklep lekkage.

- Pulmonaalklep vervanging heeft bij volwassen Fallot patiënten een gunstig effect op elektrocardiografische parameters van repolarisatie heterogeniteit.

- Vroege veranderingen in de rechter ventrikel bij zich ontwikkelende pulmonale arteriële hypertensie kunnen worden gedetecteerd met gereconstrueerde 3-dimensionale ECG opnames.

- De ventriculaire gradiënt is zeer gevoelig voor rechter ventrikel druk overbelasting, zowel in ratten als in mensen. Gebruik van deze parameter maakt een betere elektrocardiografische detectie van pulmonale arteriële hypertensie mogelijk.

- De rol van het elektrocardiogram ten tijde van diagnose en follow-up moet niet worden onderschat bij patiënten met pulmonale arteriële hypertensie: zelfs standaard 12-afleidingen ECGs blijken een belangrijke bijdrage te kunnen leveren aan het monitoren van het therapie effect.

- De hartfrequentie in rust is een belangrijke prognostische marker bij patiënten met pulmonale arteriële hypertensie. Idealiter zou de hartfrequentie in rust vóór en regelmatig ná het starten van therapie moeten worden bepaald, aangezien zowel een hogere hartfrequentie in rust, als een toename van de hartfrequentie in rust in het beloop der tijd een slechte prognose aangeeft, wat intensievere behandeling en/of long transplantatie vereist.

Toekomstperspectieven

Niet-invasieve diagnostiek bij en het vervolgen van patiënten met rechter ventrikel overbelasting heeft lange tijd geleund op lichamelijk onderzoek, thoraxfoto's en tijdrovende elektrocardiografische analyses [1-4]. Tegenwoordig kan men echter steeds meer – net als bij linker ventrikel overbelasting – gebruik maken van biomarkers [5-8], gevalideerde inspanningstesten [9-13], geavanceerde echocardiografie [14-24] en cardiale MRI [25-31]. Viabiliteit en functie van het myocard van de rechter ventrikel in relatie tot (relatieve) ischemie is weliswaar nog onvoldoende onderzocht, maar voorlopige resultaten laten zien dat zuurstof gebrek wel degelijk een rol speelt bij het gaan falen van een overbelaste rechter ventrikel [5, 32-34]. Daarmee zal ischemie-modulerende therapie een belangrijke rol kunnen gaan krijgen in de behandeling van rechter ventrikel overbelasting. Op dezelfde wijze zal niet-invasieve diagnostiek zich waarschijnlijk meer gaan richten op het aantonen dan wel uitsluiten van (episoden van) ischemie. Want hoewel de rechtszijdige hartkatheterisatie als gouden standaard voor het aantonen van pulmonale hypertensie waarschijnlijk gebruikt zal blijven worden [35], lijkt er steeds meer vraag te bestaan naar voor de individuele patiënt belangrijke markers van ziekte en prognose [6, 36]. Er zijn namelijk wel fysiologische principes te distilleren uit metingen van rechter ventrikel afterload, slagvolume en hartfrequentie [37-39], maar deze verklaren niet waarom er tussen patiënten een dergelijk grote variatie bestaat in klinische presentatie. Het zal daarbij dan ook belangrijk worden om de individuele gevolgen van rechter ventrikel overbelasting in kaart te brengen, teneinde een passende therapie in te stellen. Men moet hierbij denken aan gevolgen voor prikkelgeleiding [40, 41], waarbij analoog aan de situatie bij linker ventrikel falen, een zekere mate van elektromechanische ontkoppeling in het myocard als buitengewoon ongunstig moet worden beschouwd [42-44]. Dat het uniloculair pacen van de rechter ventrikel, teneinde een geleidingsvertraging ten dele teniet te doen, dit probleem zal oplossen, lijkt onwaarschijnlijk [45]. Niettemin lijkt een significant deel van patiënten met hartfalen wel baat bij te hebben bij een dergelijke interventie [46]. Wanneer er echter sprake is van een diffusie elektromechanische ontkoppeling, meer dan van een elektrisch inactief gebied [47], zal het resultaat van pacing geringer zijn. Elektrocardiografie kan inzicht geven in de mate van concordantie van depolarisatie en repolarisatie [48, 49], terwijl echocardiografie de mate van heterogeniteit van contractie kan weergeven [24]. In de toekomst zal waarschijnlijk ook het belang van elektromechanische ontkoppeling voor het optreden van (fatale) ritmestoornissen nader worden onderzocht en breder worden geïmplementeerd [50-53]. Interessant hierbij zal zijn of er een belangrijk verschil bestaat tussen patiënten met rechter ventrikel overbelasting vanaf de geboorte en patiënten die dit op

latere leeftijd ontwikkelden. Zoals besproken in de introductie, zal ook de rol van het endotheel belangrijker worden voor de follow-up van patiënten met rechter ventrikel drukoverbelasting t.g.v. pulmonale hypertensie. Studies laten reeds zien dat endotheel-progenitor-cellen in belangrijke mate minder aanwezig zijn bij patiënten met pulmonale arteriële hypertensie [54]. Wellicht dat de aanwezige hoeveelheid van deze cellen in het bloed in de toekomst zal worden gebruikt om het effect van pulmonale arteriële hypertensie modulerende therapie te beoordelen. Tot op heden mag men echter zeggen dat de ontwikkelingen op het gebied van diagnostiek aanzienlijk achter lopen op die in het veld van linkszijdig hartfalen. De rechter ventrikel wordt daarom niet ten onrechte wel de 'vergeten kamer' genoemd [55]. Enerzijds lijkt dit te wijten aan een kleinere 'markt' waardoor er minder wetenschappelijke interesse bestaat, anderzijds is diezelfde kleine 'markt' waarschijnlijk debet aan de trage ontwikkeling en validatie van nieuwe meetmethoden. Belangrijk voor de verdere ontwikkeling is dan ook de kennis aangaande het aantal patiënten dat reeds bekend is met een overbelaste rechter ventrikel [56-61]. Tegelijkertijd is het ook belangrijk een concreet idee te hebben hoeveel en welke personen er risico lopen op het ontwikkelen van een overbelaste rechter ventrikel, bijvoorbeeld na het doormaken van een longembolie [62, 63]. Er bestaat dan namelijk de mogelijkheid tot het gericht screenen van patiënten met een hoog risicoprofiel [2]. Hier zouden goedkope en gemakkelijk toepasbare technieken als elektrocardiografie en controle van biomarkers hun diensten kunnen bewijzen.

References

1. Perloff JK. Auscultatory and phonocardiographic manifestations of pulmonary hypertension. *Prog Cardiovasc Dis* 1967;9:303-340.

2. McGoon M, Gutterman D, Steen V, Barst R, McCrory DC, Fortin TA and Loyd JE. Screening, early detection, and diagnosis of pulmonary arterial hypertension: ACCP evidence-based clinical practice guidelines. *Chest* 2004;126:14S-34S.

3. Butler PM, Leggett SI, Howe CM, Freye CJ, Hindman NB and Wagner GS. Identification of electrocardiographic criteria for diagnosis of right ventricular hypertrophy due to mitral stenosis. *Am J Cardiol* 1986;57:639-643.

4. Kawaguchi Y. Studies on deflection area vectors of QRS and T and ventricular gradient in right ventricular hypertrophy. *Jpn Circ J* 1985;49:395-405.

5. Torbicki A, Kurzyna M, Kuca P, Fijalkowska A, Sikora J, Florczyk M, Pruszczyk P, Burakowski J and Wawrzynska L. Detectable serum cardiac troponin T as a marker of poor prognosis among patients with chronic precapillary pulmonary hypertension. *Circulation* 2003;108:844-848.

6. Hoeper MM, Oudiz RJ, Peacock A, Tapson VF, Haworth SG, Frost AE and Torbicki A. End points and clinical trial designs in pulmonary arterial hypertension: clinical and regulatory perspectives. *J Am Coll Cardiol* 2004;43:48S-55S.

7. Blyth KG, Groenning BA, Mark PB, Martin TN, Foster JE, Steedman T, Morton JJ, Dargie HJ and Peacock AJ. NT-proBNP can be used to detect right ventricular systolic dysfunction in pulmonary hypertension. *Eur Respir J* 2007;29:737-744.

8. Gan CT, McCann GP, Marcus JT, van Wolferen SA, Twisk JW, Boonstra A, Postmus PE and Vonk-Noordegraaf A. NT-proBNP reflects right ventricular structure and function in pulmonary hypertension. *Eur Respir J* 2006;28:1190-1194.

9. ATS statement: guidelines for the six-minute walk test. *Am J Respir Crit Care Med* 2002;166:111-117.

10. Miyamoto S, Nagaya N, Satoh T, Kyotani S, Sakamaki F, Fujita M, Nakanishi N and Miyatake K. Clinical correlates and prognostic significance of six-minute walk test in patients with primary pulmonary hypertension. Comparison with cardiopulmonary exercise testing. *Am J Respir Crit Care Med* 2000;161:487-492.

11. Provencher S, Chemla D, Herve P, Sitbon O, Humbert M and Simonneau G. Heart rate responses during the 6-minute walk test in pulmonary arterial hypertension. *Eur Respir J* 2006;27:114-120.

12. Paciocco G, Martinez FJ, Bossone E, Pielsticker E, Gillespie B and Rubenfire M. Oxygen desaturation on the six-minute walk test and mortality in untreated primary pulmonary hypertension. *Eur Respir J* 2001;17:647-652.

13. Sun XG, Hansen JE, Oudiz RJ and Wasserman K. Exercise pathophysiology in patients with primary pulmonary hypertension. *Circulation* 2001;104:429-435.

14. Lopez-Candales A, Rajagopalan N, Dohi K, Gulyasy B, Edelman K and Bazaz R. Abnormal right ventricular myocardial strain generation in mild pulmonary hypertension. *Echocardiography* 2007;24:615-622.

15. Borges AC, Knebel F, Eddicks S, Panda A, Schattke S, Witt C and Baumann G. Right ventricular function assessed by two-dimensional strain and tissue Doppler echocardiography in patients with pulmonary arterial hypertension and effect of vasodilator therapy. *Am J Cardiol* 2006;98:530-534.

16. Rajdev S, Nanda NC, Patel V, Singh A, Mehmood F, Vengala S, Fang L, Dasan V, Benza RL and Bourge RC. Tissue Doppler assessment of longitudinal right and left ventricular strain and strain rate in pulmonary artery hypertension. *Echocardiography* 2006;23:872-879.

17. Niemann PS, Pinho L, Balbach T, Galuschky C, Blankenhagen M, Silberbach M, Broberg C, Jerosch-Herold M and Sahn DJ. Anatomically oriented right ventricular volume measurements with dynamic three-dimensional echocardiography validated by 3-Tesla magnetic resonance imaging. *J Am Coll Cardiol* 2007;50:1668-1676.

18. Wang J, Prakasa K, Bomma C, Tandri H, Dalal D, James C, Tichnell C, Corretti M, Bluemke D, Calkins H and Abraham TP. Comparison of novel echocardiographic parameters of right ventricular function with ejection fraction by cardiac magnetic resonance. *J Am Soc Echocardiogr* 2007;20:1058-1064.

19. Raymond RJ, Hinderliter AL, Willis PW, Ralph D, Caldwell EJ, Williams W, Ettinger NA, Hill NS, Summer WR, de BB, Schwartz T, Koch G, Clayton LM, Jobsis MM, Crow JW and Long W. Echocardiographic predictors of adverse outcomes in primary pulmonary hypertension. *J Am Coll Cardiol* 2002;39:1214-1219.

20. Silversides CK, Veldtman GR, Crossin J, Merchant N, Webb GD, McCrindle BW, Siu SC and Therrien J. Pressure half-time predicts hemodynamically significant pulmonary regurgitation in adult patients with repaired tetralogy of fallot. *J Am Soc Echocardiogr* 2003;16:1057-1062.

21. Mahapatra S, Nishimura RA, Oh JK and McGoon MD. The prognostic value of pulmonary vascular capacitance determined by Doppler echocardiography in patients with pulmonary arterial hypertension. *J Am Soc Echocardiogr* 2006;19:1045-1050.

22. Dambrauskaite V, Delcroix M, Claus P, Herbots L, D'hooge J, Bijnens B, Rademakers F and Sutherland GR. Regional right ventricular dysfunction in chronic pulmonary hypertension. *J Am Soc Echocardiogr* 2007;20:1172-1180.

23. Huez S, Vachiery JL, Unger P, Brimioulle S and Naeije R. Tissue Doppler imaging evaluation of cardiac adaptation to severe pulmonary hypertension. *Am J Cardiol* 2007;100:1473-1478.

24. Yeo TC, Dujardin KS, Tei C, Mahoney DW, McGoon MD and Seward JB. Value of a Doppler-derived index combining systolic and diastolic time intervals in predicting outcome in primary pulmonary hypertension. *Am J Cardiol* 1998;81:1157-1161.

25. Oosterhof T, Mulder BJ, Vliegen HW and de Roos A. Cardiovascular magnetic resonance in the follow-up of patients with corrected tetralogy of Fallot: a review. *Am Heart J* 2006;151:265-272.

26. Pettersen E, Helle-Valle T, Edvardsen T, Lindberg H, Smith HJ, Smevik B, Smiseth OA and Andersen K. Contraction pattern of the systemic right ventricle shift from longitudinal to circumferential shortening and absent global ventricular torsion. *J Am Coll Cardiol* 2007;49:2450-2456.

27. Oosterhof T, Mulder BJ, Vliegen HW and de Roos A. Corrected tetralogy of Fallot: delayed enhancement in right ventricular outflow tract. *Radiology* 2005;237:868-871.

28. McCann GP, Beek AM, Vonk-Noordegraaf A and van Rossum AC. Delayed contrast-enhanced magnetic resonance imaging in pulmonary arterial hypertension. *Circulation* 2005;112:e268.

29. Roest AA, Helbing WA, Kunz P, van den Aardweg JG, Lamb HJ, Vliegen HW, van der Wall EE and de Roos A. Exercise MR imaging in the assessment of pulmonary regurgitation and biventricular function in patients after tetralogy of fallot repair. *Radiology* 2002;223:204-211.

30. McCann GP, Gan CT, Beek AM, Niessen HW, Vonk Noordegraaf A and van Rossum AC. Extent of MRI delayed enhancement of myocardial mass is related to right ventricular dysfunction in pulmonary artery hypertension. *AJR Am J Roentgenol* 2007;188:349-355.

31. Vliegen HW, van Straten A, de Roos A, Roest AA, Schoof PH, Zwinderman AH, Ottenkamp J, van der Wall EE and Hazekamp MG. Magnetic resonance imaging to assess the hemodynamic effects of pulmonary valve replacement in adults late after repair of tetralogy of fallot. *Circulation* 2002;106:1703-1707.

32. Kluge R, Barthel H, Pankau H, Seese A, Schauer J, Wirtz H, Seyfarth HJ, Steinbach J, Sabri O and Winkler J. Different mechanisms for changes in glucose uptake of the right and left ventricular myocardium in pulmonary hypertension. *J Nucl Med* 2005;46:25-31.

33. Gomez A, Bialostozky D, Zajarias A, Santos E, Palomar A, Martinez ML and Sandoval J. Right ventricular ischemia in patients with primary pulmonary hypertension. *J Am Coll Cardiol* 2001;38:1137-1142.

34. Oikawa M, Kagaya Y, Otani H, Sakuma M, Demachi J, Suzuki J, Takahashi T, Nawata J, Ido T, Watanabe J and Shirato K. Increased [18F]fluorodeoxyglucose accumulation in right ventricular free wall in patients with pulmonary hypertension and the effect of epoprostenol. *J Am Coll Cardiol* 2005;45:1849-1855.

35. Galie N, Torbicki A, Barst R, Dartevelle P, Haworth S, Higenbottam T, Olschewski H, Peacock A, Pietra G, Rubin LJ, Simonneau G, Priori SG, Garcia MA, Blanc JJ, Budaj A, Cowie M, Dean V, Deckers J, Burgos EF, Lekakis J, Lindahl B, Mazzotta G, McGregor K, Morais J, Oto A, Smiseth OA, Barbera JA, Gibbs S, Hoeper M, Humbert M, Naeije R and Pepke-Zaba J. Guidelines on diagnosis and treatment of pulmonary arterial hypertension. The Task Force on Diagnosis and Treatment of Pulmonary Arterial Hypertension of the European Society of Cardiology. *Eur Heart J* 2004;25:2243-2278.

36. Peacock A, Naeije R, Galie N and Reeves JT. End points in pulmonary arterial hypertension: the way forward. *Eur Respir J* 2004;23:947-953.

37. Lankhaar JW, Westerhof N, Faes TJ, Gan CT, Marques KM, Boonstra A, van den Berg FG, Postmus PE and Vonk-Noordegraaf A. Pulmonary vascular resistance and compliance stay inversely related during treatment of pulmonary hypertension. *Eur Heart J* 2008;

38. Holverda S, Gan CT, Marcus JT, Postmus PE, Boonstra A and Vonk-Noordegraaf A. Impaired stroke volume response to exercise in pulmonary arterial hypertension. *J Am Coll Cardiol* 2006;47:1732-1733.

39. Fox K, Borer JS, Camm AJ, Danchin N, Ferrari R, Lopez Sendon JL, Steg PG, Tardif JC, Tavazzi L and Tendera M. Resting heart rate in cardiovascular disease. *J Am Coll Cardiol* 2007;50:823-830.

40. Chinushi M, Aizawa Y, Kitazawa H, Takahashi K, Washizuka T and Shibata A. Clockwise and counter-clockwise circulation of wavefronts around an anatomical obstacle as one mechanism of two morphologies of sustained ventricular tachycardia in patients after a corrective operation of tetralogy of Fallot. *Pacing Clin Electrophysiol* 1997;20:2279-2281.

41. Walsh EP. Interventional electrophysiology in patients with congenital heart disease. *Circulation* 2007;115:3224-3234.

42. Dhingra R, Ho NB, Benjamin EJ, Wang TJ, Larson MG, D'Agostino RB, Sr., Levy D and Vasan RS. Cross-sectional relations of electrocardiographic QRS duration to left ventricular dimensions: the Framingham Heart Study. *J Am Coll Cardiol* 2005;45:685-689.

43. Gatzoulis MA, Till JA, Somerville J and Redington AN. Mechanoelectrical interaction in tetralogy of Fallot. QRS prolongation relates to right ventricular size and predicts malignant ventricular arrhythmias and sudden death. *Circulation* 1995;92:231-237.

44. Kashani A and Barold SS. Significance of QRS complex duration in patients with heart failure. *J Am Coll Cardiol* 2005;46:2183-2192.

45. Diller GP, Okonko D, Uebing A, Ho SY and Gatzoulis MA. Cardiac resynchronization therapy for adult congenital heart disease patients with a systemic right ventricle: analysis of feasibility and review of early experience. *Europace* 2006;8:267-272.

46. Abraham WT, Fisher WG, Smith AL, Delurgio DB, Leon AR, Loh E, Kocovic DZ, Packer M, Clavell AL, Hayes DL, Ellestad M, Trupp RJ, Underwood J, Pickering F, Truex C, McAtee P and Messenger J. Cardiac resynchronization in chronic heart failure. *N Engl J Med* 2002;346:1845-1853.

47. Uebing A, Gibson DG, Babu-Narayan SV, Diller GP, Dimopoulos K, Goktekin O, Spence MS, Andersen K, Henein MY, Gatzoulis MA and Li W. Right ventricular mechanics and QRS duration in patients with repaired tetralogy of Fallot: implications of infundibular disease. *Circulation* 2007;116:1532-1539.

48. Draisma HH, Schalij MJ, van der Wall EE and Swenne CA. Elucidation of the spatial ventricular gradient and its link with dispersion of repolarization. *Heart Rhythm* 2006;3:1092-1099.

49. Scherptong RW, Henkens IR, Man SC, Le CS, Vliegen HW, Draisma HH, Maan AC, Schalij MJ and Swenne CA. Normal limits of the spatial QRS-T angle and ventricular gradient in 12-lead electrocardiograms of young adults: dependence on sex and heart rate. *J Electrocardiol* 2008;

50. DiMarco JP. Implantable cardioverter-defibrillators. *N Engl J Med* 2003;349:1836-1847.

51. Gatzoulis MA, Balaji S, Webber SA, Siu SC, Hokanson JS, Poile C, Rosenthal M, Nakazawa M, Moller JH, Gillette PC, Webb GD and Redington AN. Risk factors for arrhythmia and sudden cardiac death late after repair of tetralogy of Fallot: a multicentre study. *Lancet* 2000;356:975-981.

52. Khairy P, Landzberg MJ, Gatzoulis MA, Lucron H, Lambert J, Marcon F, Alexander ME and Walsh EP. Value of programmed ventricular stimulation after tetralogy of fallot repair: a multicenter study. *Circulation* 2004;109:1994-2000.

53. Hoeper MM, Galie N, Murali S, Olschewski H, Rubenfire M, Robbins IM, Farber HW, McLaughlin V, Shapiro S, Pepke-Zaba J, Winkler J, Ewert R, Opitz C, Westerkamp V, Vachiery JL, Torbicki A, Behr J and Barst RJ. Outcome after cardiopulmonary resuscitation in patients with pulmonary arterial hypertension. *Am J Respir Crit Care Med* 2002;165:341-344.

54. Diller GP, van ES, Okonko DO, Howard LS, Ali O, Thum T, Wort SJ, Bedard E, Gibbs JS, Bauersachs J, Hobbs AJ, Wilkins MR, Gatzoulis MA and Wharton J. Circulating endothelial progenitor cells in patients with Eisenmenger syndrome and idiopathic pulmonary arterial hypertension. *Circulation* 2008;117:3020-3030.

55. Rigolin VH, Robiolio PA, Wilson JS, Harrison JK and Bashore TM. The forgotten chamber: the importance of the right ventricle. *Cathet Cardiovasc Diagn* 1995;35:18-28.

56. Engelfriet PM, Duffels MG, Moller T, Boersma E, Tijssen JG, Thaulow E, Gatzoulis MA and Mulder BJ. Pulmonary arterial hypertension in adults born with a heart septal defect: the Euro Heart Survey on adult congenital heart disease. *Heart* 2007;93:682-687.

57. Duffels MG, Engelfriet PM, Berger RM, van Loon RL, Hoendermis E, Vriend JW, van der Velde ET, Bresser P and Mulder BJ. Pulmonary arterial hypertension in congenital heart disease: an epidemiologic perspective from a Dutch registry. *Int J Cardiol* 2007;120:198-204.

58. Mukerjee D, St George D, Coleiro B, Knight C, Denton CP, Davar J, Black CM and Coghlan JG. Prevalence and outcome in systemic sclerosis associated pulmonary arterial hypertension: application of a registry approach. *Ann Rheum Dis* 2003;62:1088-1093.

59. Sitbon O, Lascoux-Combe C, Delfraissy JF, Yeni PG, Raffi F, De ZD, Gressin V, Clerson P, Sereni D and Simonneau G. Prevalence of HIV-related pulmonary arterial hypertension in the current antiretroviral therapy era. *Am J Respir Crit Care Med* 2008;177:108-113.

60. Humbert M, Sitbon O, Chaouat A, Bertocchi M, Habib G, Gressin V, Yaici A, Weitzenblum E, Cordier JF, Chabot F, Dromer C, Pison C, Reynaud-Gaubert M, Haloun A, Laurent M, Hachulla E and Simonneau G. Pulmonary arterial hypertension in France: results from a national registry. *Am J Respir Crit Care Med* 2006;173:1023-1030.

61. Jais X, Ioos V, Jardim C, Sitbon O, Parent F, Hamid A, Fadel E, Dartevelle P, Simonneau G and Humbert M. Splenectomy and chronic thromboembolic pulmonary hypertension. *Thorax* 2005;60:1031-1034.

62. Pengo V, Lensing AW, Prins MH, Marchiori A, Davidson BL, Tiozzo F, Albanese P, Biasiolo A, Pegoraro C, Iliceto S and Prandoni P. Incidence of chronic thromboembolic pulmonary hypertension after pulmonary embolism. *N Engl J Med* 2004;350:2257-2264.

63. Sanchez O, Trinquart L, Colombet I, Durieux P, Huisman MV, Chatellier G and Meyer G. Prognostic value of right ventricular dysfunction in patients with haemodynamically stable pulmonary embolism: a systematic review. *Eur Heart J* 2008;29:1569-1577.

Publicatielijst

Publicaties

Pulmonary arterial hypertension associated with congenital heart disease: the efficacy of drug treatment in symptomatic patients
Ivo R. Henkens, Hubert W. Vliegen
Neth Heart J. 2006;14(6):207-8.

Predicting Outcome of Pulmonary Valve Replacement in Adult Tetralogy of Fallot Patients
Ivo R. Henkens, Alexander Van Straten, Martin J. Schalij, Mark G. Hazekamp, Albert de Roos, Ernst E. Van der Wall, Hubert W. Vliegen
Ann Thorac Surg. 2007 Mar;83(3):907-11.

Preoperative determinants of recovery time in adult Fallot patients after late Pulmonary Valve Replacement
Ivo R. Henkens, Alexander van Straten, Mark G. Hazekamp, Martin J. Schalij, Albert de Roos, Ernst E. van der Wall, Hubert W. Vliegen
Int J Cardiol. 2007 Sep 14;121(1):123-4.

Early changes in rat hearts with developing pulmonary arterial hypertension can be detected with 3-dimensional electrocardiography.
Ivo R. Henkens, Koen T.B. Mouchaers, Hubert W. Vliegen, Willem J. van der Laarse, Cees A. Swenne, Arie C. Maan, Harmen H.M. Draisma, Ingrid Schalij, Ernst E. van der Wall, Martin J. Schalij, Anton Vonk Noordegraaf
Am J Physiol Heart Circ Physiol. 2007 Aug;293(2):H1300-7.

Right coronary artery flow impairment in patients with pulmonary hypertension.
Serge A. van Wolferen, J Tim Marcus, Nico Westerhof, MD Spreeuwenberg, Koen M. Marques, Jean G. Bronzwaer, Ivo R. Henkens, C. Tji-Joong Gan, Anco Boonstra, Piet E Postmus, Anton Vonk Noordegraaf.
Eur Heart J. 2008 Jan;29(1):120-7.

Pulmonary valve replacement improves the repolarization in tetralogy of Fallot.
Bart Hooft van Huysduynen, Ivo R. Henkens, Cees A. Swenne, Martin J. Schalij, Ernst E. van der Wall, Hubert W. Vliegen.
Int J Cardiol. 2008 Mar 14;124(3):301-6.

Improved ECG detection of chronic right ventricular pressure overload validated with cardiac magnetic resonance imaging.
Ivo R. Henkens, Koen T.B. Mouchaers, Anton Vonk Noordegraaf, Anco Boonstra, Cees A. Swenne, Arie C. Maan, Sum-Che Man, Jos W.R. Twisk, Ernst E. van der Wall, Martin J. Schalij, Hubert W. Vliegen
Am J Physiol Heart Circ Physiol. 2008 May;294:H2150-7.

Electrocardiographic monitoring of treatment response in pulmonary arterial hypertension patients
Ivo R. Henkens, C. Tji-Joong Gan, Serge A. van Wolferen, M. Hew, Anco Boonstra, Jos W.R. Twisk, Otto Kamp, Ernst E. van der Wall, Martin J. Schalij, Anton Vonk Noordegraaf, Hubert W. Vliegen
Accepted for publication in Chest (June 2008)

Pulmonary hypertension: the role of the electrocardiogram
Ivo R. Henkens, Roderick W.C. Scherptong, Klaas W. van Kralingen, Salah A.M. Said, Hubert W. Vliegen
Neth Heart J. 2008;16(8):250-4.

Normal limits of the spatial QRS-T angle and ventricular gradient in 12-lead electrocardiograms of young adults: dependence on sex and heart rate
Roderick W.C. Scherptong, Ivo R. Henkens, Sum-Che Man, Saskia Le Cessie, Hubert W. Vliegen, Harmen H.M. Draisma, Arie C. Maan, Martin J. Schalij, Cees A. Swenne
J Electrocardiol 2008. Sep 23 [Epub ahead of print].

Book chapter: "**hepatopulmonary syndrome and portopulmonary hypertension"** related to "clinical hepatology course", June 2006, Leiden

Book chapter: "**Pulmonale hypertensie: classificatie, diagnostiek en behandeling**"
Henkens IR, Vliegen HW
Verpleeghuisgeneeskunde in de praktijk 2006

Behandeling van hoge druk in de longslagaders bij ongeopereerde patiënten met een aangeboren hartafwijking bij het syndroom van Down
Ivo R. Henkens, Hubert W. Vliegen
Down + Up June 2007

Behandeling van pulmonale hypertensie.
Ivo R. Henkens, Hubert W. Vliegen
Patient Care Oktober 2007

Pulmonale hypertensie en het belang van de transpulmonale gradiënt
Ivo R. Henkens, Klaas W. van Kralingen, Arend de Weger, Menno Huisman, Jaap van Laar en Hubert W. Vliegen
Hart Bulletin 2008;39(3):56.

Dankwoord

Dankwoord

Dit proefschrift had niet tot stand kunnen komen zonder de bereidwilligheid van velen om samen te werken aan disciplineoverstijgend wetenschappelijk onderzoek in klinische en preklinische setting. Onze samenwerking, die altijd op basis van goed vertrouwen heeft bestaan, heb ik als zeer positief ervaren en ik hoop ook in de toekomst actief deel te kunnen blijven nemen in wetenschappelijk onderzoek.

Klaas, Jaap, Menno, Arend, Bart, Annemie, Trudeke, Luc, Roderick, dank voor jullie geduld, vertrouwen en medewerking bij het opstarten van een multidisciplinaire werkgroep voor analyse en behandeling van pulmonale hypertensie. Kwestan, Bea, dank voor jullie inzet bij het realiseren van doelmatige en patiëntvriendelijke logistiek. Eduard, jouw inzicht en uitleg is vreselijk belangrijk geweest voor de diagnostiek en behandeling van patiënten met pulmonale hypertensie als gevolg van een aangeboren hartafwijking.

Koen, bedankt voor de gezellige lunches en de introductie in het basale onderzoek. Serge en Tji, mijn onderzoek is zeer gebaat geweest bij jullie medewerking. Martha, Frank en Iris, mijn dank voor jullie inzet bij het verzamelen van data.

Arie en Kees, voor de vele nuttige discussies en jullie tomeloze inzet bij de vaak ingewikkelde en frustrerende ECG analyse, alsmede de vervaardiging van originele figuren ben ik jullie zeer dankbaar.

Tuincollegae, jullie waren onmisbaar door jullie praktische hulp, steun en gezelligheid. De kalender zal nog lang blijven hangen!

Annette en Jurgen, dank voor jullie hulp bij de lay-out van dit proefschrift.

Jurgen, Tom, Aernout, Jelle, Jurriaan en Godard, er gaat niets boven de briljante woensdagavonden, behalve wanneer ze op vrijdag zouden zijn.

Lieve ouders, dank voor het luisterend oor en bemoedigend commentaar ten aanzien van jullie eigen ervaring met promoveren.

Alexandra, dank je wel voor je begrip, steun en aanmoediging. Dat was het belangrijkste van alles.

Curriculum vitae

Curriculum vitae

Ivo Henkens was born April 29th 1977 in Leiderdorp, the Netherlands. Shortly after he moved to Werkhoven, a small village in the province of Utrecht, where he lived until he was eighteen years old. After his Gymnasium diploma from the St. Bonifatius College in Utrecht in 1995, he traded Dutch soil for a horizon-broadening year of undergraduate study at Wittenberg University, in Springfield, Ohio, USA. He was inspired to study Biomedical Science, and enrolled in 1996 at the Leiden University. In the same year he joined the Leiden Student Union Minerva. However, the idea of interaction with patients appealed to him so much, that after finishing his freshmen year he started studying Medicine. After a successful first year, he joined the "Joshua's", a group of students, involved in post-operative patient care at the thoracic intensive care unit of the Leiden University Hospital. His first scientific research project was a spin-off of this work, and inspired him to persevere in research in parallel to his clinical work. He finished his clinical studies with an internship at the department of Cardiology at the Leiden University Medical Center. After his medical degree in 2004 he started his PhD-research in January 2005 at this same department under supervision of Dr. H.W. Vliegen, Professor M.J. Schalij and Professor E.E. van der Wall. During the following three years and three months, of which this thesis is the result, he has worked hard to setup the multidisciplinary Leiden University Medical Center "pulmonary hypertension working group". Regarding the pulmonary hypertension research he has worked in close cooperation with Dr. A. Vonk Noordegraaf, Dr. A. Boonstra, and K.T.B. Mouchaers of the VU University Medical Center. As of April 1st 2008 he is active as a Cardiology trainee, currently in the pre-cardiology phase of Internal Medicine at the HAGA hospital in The Hague.

Curriculum vitae

Ivo Henkens werd geboren op 29 april 1977 te Leiderdorp. Kort nadien is hij verhuisd naar Werkhoven, in de provincie Utrecht, alwaar hij tot en met zijn achttiende jaar heeft gewoond. Na het behalen van het Gymnasium eindexamen in 1995 aan het St. Bonifatius College te Utrecht, verliet hij de Nederlandse bodem voor een jaar blikverruimende studie aan Wittenberg University in Springfield, Ohio, in de Verenigde Staten. De hier opgedane ervaring leidde er toe om in 1996 te beginnen met Biomedische Wetenschappen in Leiden. In datzelfde jaar werd hij lid van de Leidse Studenten Vereniging Minerva. Al snel bleek echter dat Geneeskunde meer aansloot bij zijn interesse en na het behalen van de propedeuse Biomedische Wetenschappen kon hij instromen in de studie Geneeskunde. Vanaf het behalen van de propedeuse Geneeskunde in 1998, heeft hij – verbonden aan de "Joshua's" – gewerkt op de thorax-IC van het Leids Universitair Medisch Centrum, waar hij ook zijn wetenschapsstage heeft gedaan. De co-schappen rondde hij af met een stage bij de afdeling Hartziekten van het Leids Universitair Medisch Centrum. Na het behalen van het artsexamen in 2004 is hij per 1 januari 2005 begonnen met zijn promotieonderzoek onder begeleiding van Dr. H.W. Vliegen, professor M.J. Schalij en professor E.E. van der Wall. Tijdens het drie jaar en drie maanden durende traject, waarvan dit proefschrift het resultaat is, heeft hij zich mede ingezet om de multidisciplinaire "werkgroep pulmonale hypertensie" binnen het Leids Universitair Medisch Centrum gestalte te geven. Voor zijn onderzoek betreffende pulmonale hypertensie heeft hij nauw samen gewerkt met o.a. Dr. A. Vonk Noordegraaf, Dr. A. Boonstra, en Drs. K.T.B. Mouchaers, verbonden aan het VU Medisch Centrum.
Per 1 april 2008 is hij begonnen met de opleiding cardiologie, in welk kader hij momenteel de vooropleiding interne geneeskunde volgt binnen het HAGA ziekenhuis te 's Gravenhage.

Notes

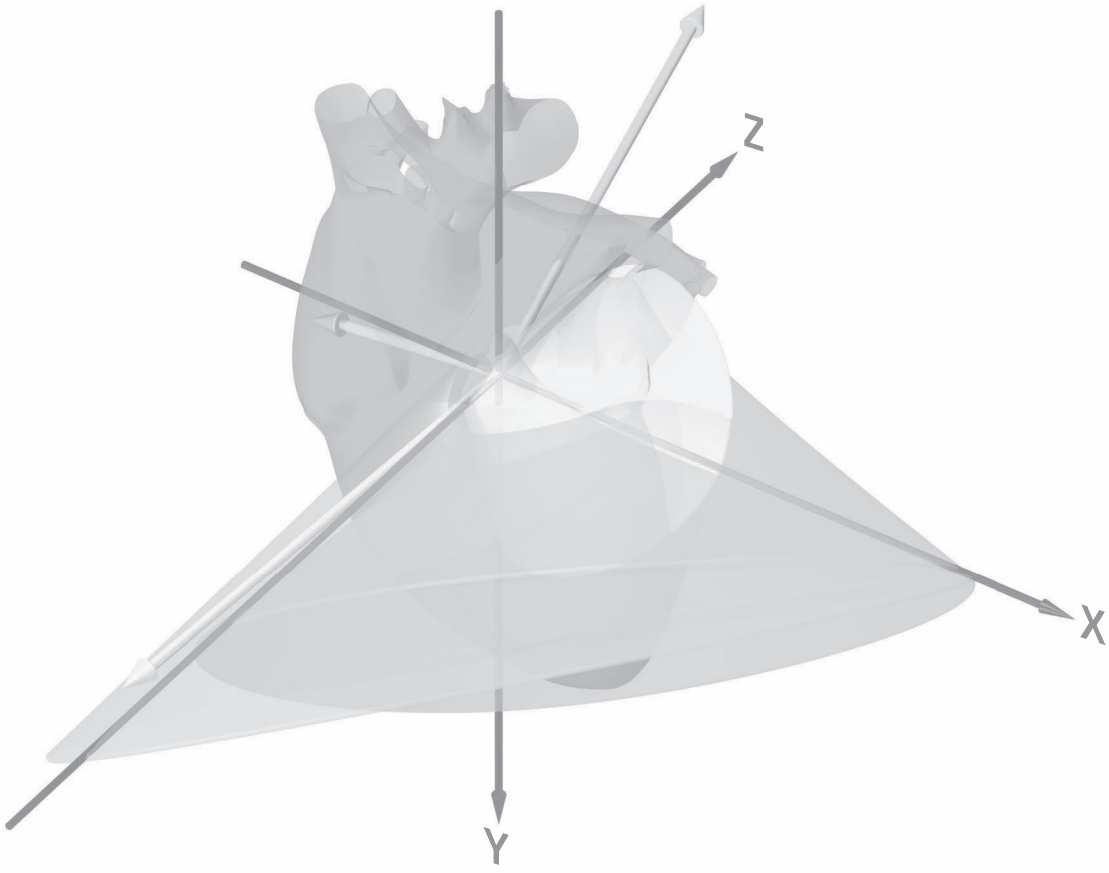

Notes

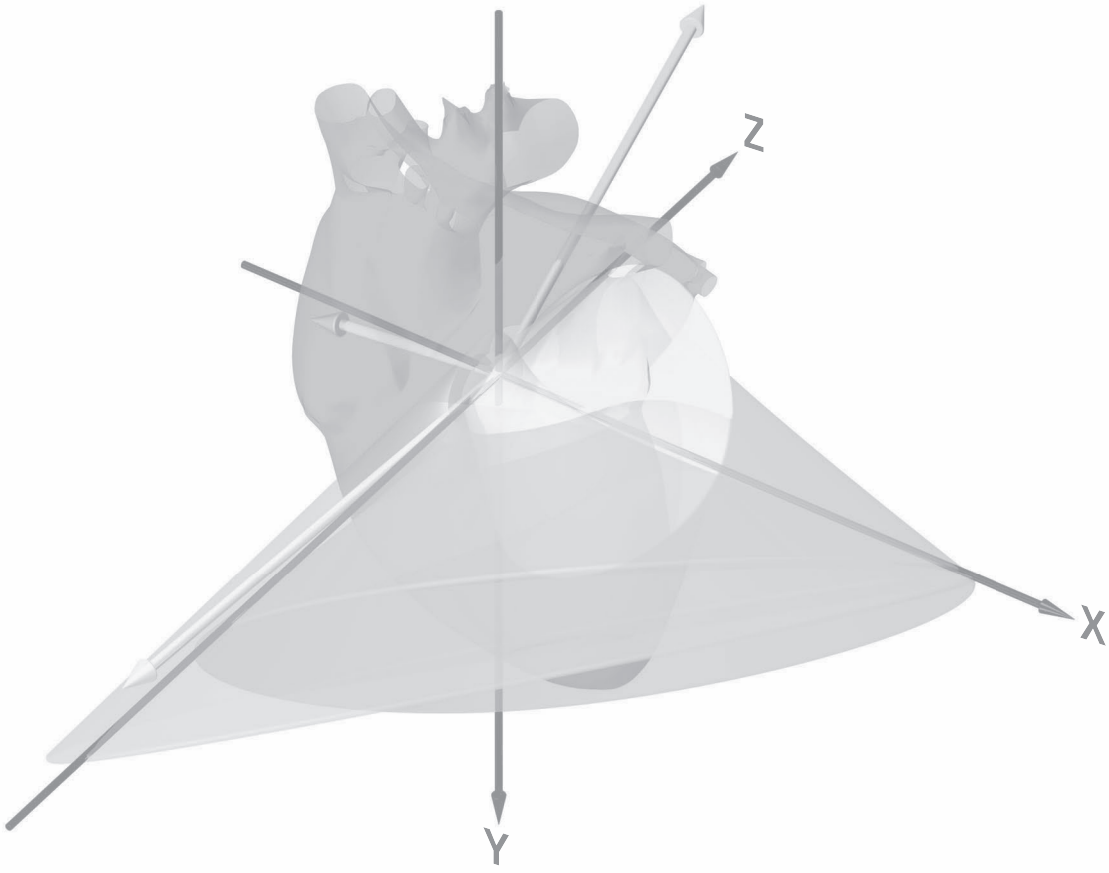

Notes

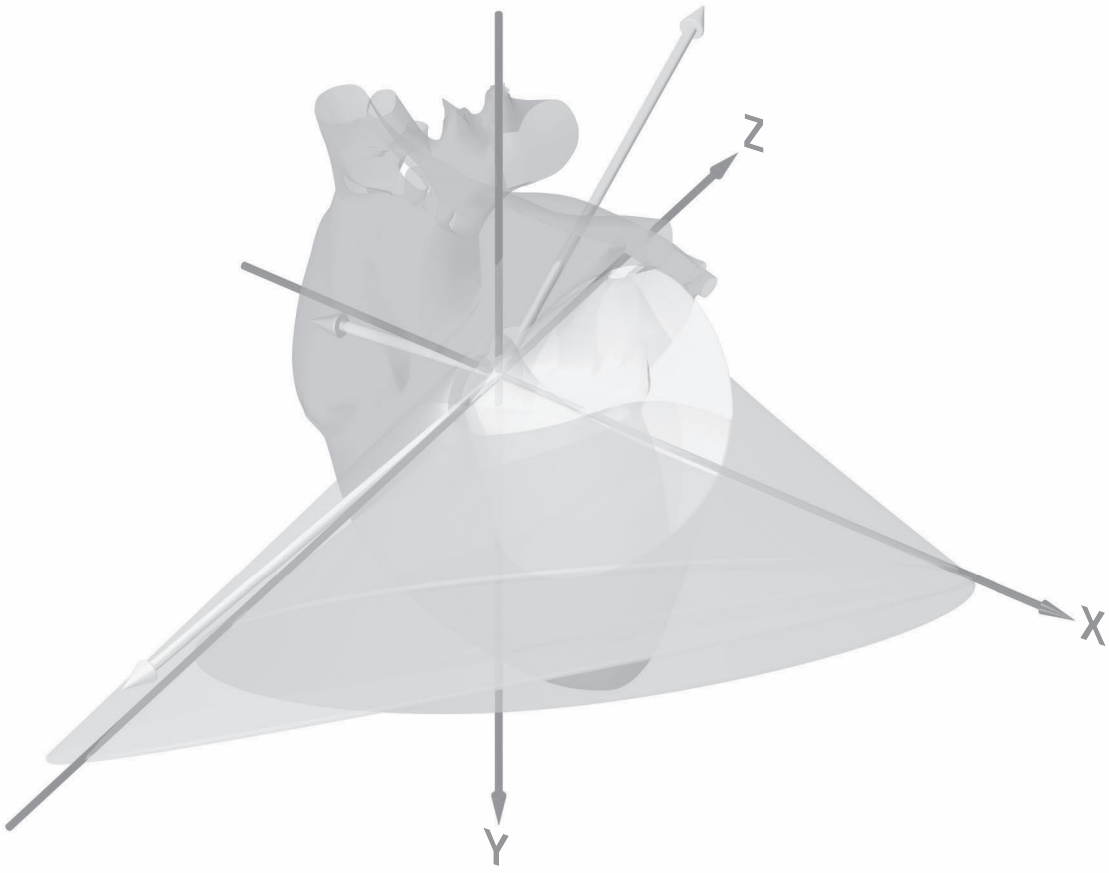

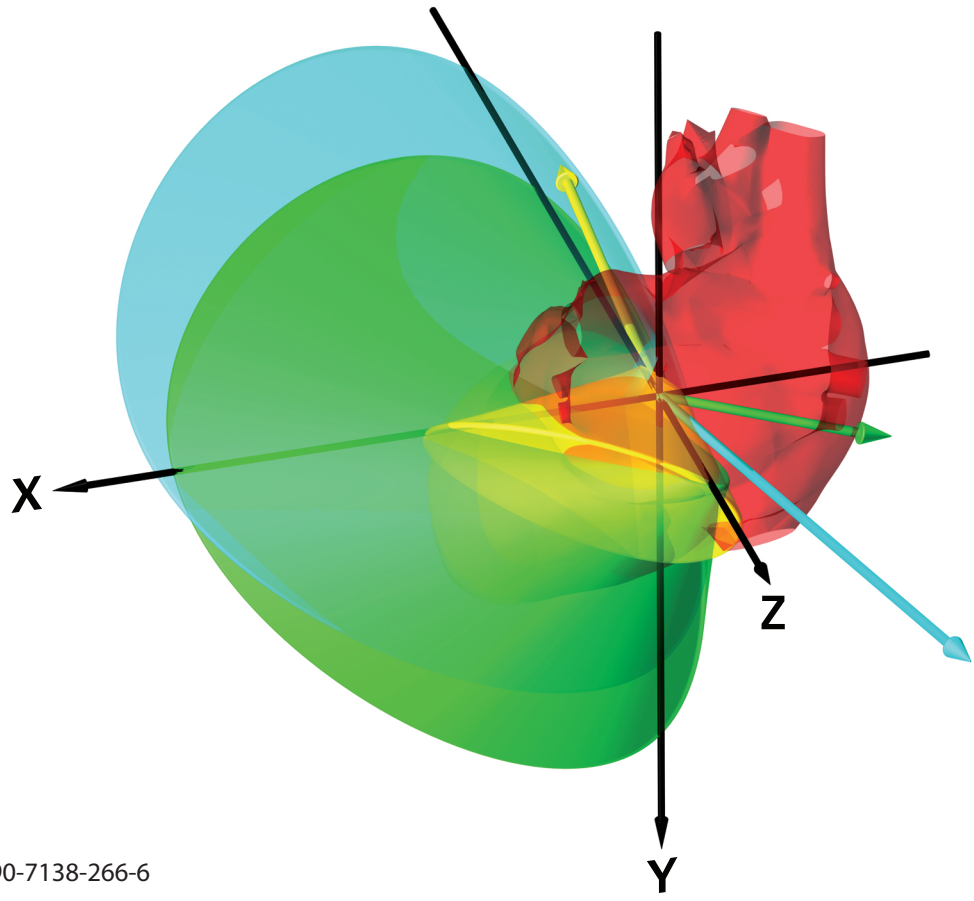

ISBN 978-90-7138-266-6